Technische Universität München
TUM School of Engineering and Design

Methodical Coupling of Multidisciplinary Structural Design and Flight Control Systems

Daniel Frank Nussbächer

Vollständiger Abdruck der von der TUM School of Engineering and Design der Technischen Universität München zur Erlangung eines

Doktors der Ingenieurwissenschaften (Dr.-Ing.)

genehmigten Dissertation.

Vorsitz: Prof. Dr.-Ing. Fernaß Daoud

Prüfende der Dissertation:

1. Prof. Dr.-Ing. Mirko Hornung
2. Prof. Dr.-Ing. Wolf R. Krüger

Die Dissertation wurde am 20.01.2025 bei der Technischen Universität München eingereicht und durch die TUM School of Engineering and Design am 15.08.2025 angenommen.

Für meine Familie

Abstract

During the process of designing a modern aircraft, engineering methods are applied which were well established over decades. Especially in laying out the airframe, the loads it will experience are numerically estimated from mostly passive means. However, considering the interaction of aircraft structure and an active control system is not as well established. This dissertation develops a framework for the optimisation of structural components, focusing on aeroelastic and flight control system analysis. In order to support engineering decisions in the early phases of aircraft design, where great design freedom is given, fast low- and medium-fidelity methods of structural, aerodynamic and control system design come into use. The methods are coupled in multidisciplinary design optimisation loops, relying on gradient based algorithms, to enable a sensible treatment of large scale problems. Structural analysis and optimisation is performed with the help of unreduced finite element method models, coupled with a transient response solver for structural dynamic problems. To efficiently evaluate pressure, force and moment distributions, aerodynamic influence coefficient matrices are used. Discrete time controllers contribute to the overall process through a computational interface. The application of the developed framework allows to spotlight the topic of "controlled loads" in sizing optimisation problems. This answers the question of how to extend the inherently multidisciplinary process of airframe design through a flight control system and how this benefits the final product. While the integration of controllers and the resulting methodical description are of primary interest for this work, sensible studies which can support the control-design itself are presented, as well. The resulting approach, to size an aircraft with controlled loads, is demonstrated in different studies using the model of an unmanned aerial vehicle of industrial scale and complexity.

Keywords: Aeroelasticity, Aeroservoelasticity, Optimisation, Airframe design

Kurzfassung

Während der Entwicklung eines modernen Flugzeugs kommen Auslegungsmethoden zum Einsatz, welche sich über Jahrzehnte hinweg etabliert haben. Besonders beim Auslegen der mechanischen Struktur werden die Lasten, welche diese tragen wird, basierend auf meist passiven Maßnahmen numerisch abgeschätzt. Die Berücksichtigung der Wechselwirkung zwischen Flugzeugstruktur und einem aktiven Regelungssystem hat sich hingegen noch nicht etabliert. Diese Doktorarbeit entwickelt den Rahmen für die Optimierung struktureller Bauteile, unter den Schwerpunkten der Analysen von Aeroelastik und Flugregelungssystem. Um technische Entscheidungen in der frühen Phase der Flugzeugentwicklung, in welcher ein hohes Maß an Entwurfsfreiheit vorhanden ist, zu unterstützen, kommen schnelle Methoden der strukturellen, der aerodynamischen und der regelungstechnischen Auslegung mit niedriger und mittlerer Genauigkeit zum Einsatz. Die Methodiken werden in multidisziplinären Optimierungskreisläufen, welche auf gradientenbasierte Algorithmen setzen, verknüpft, um einen sinnvollen Umgang mit großskaligen Problemen zu ermöglichen. Die strukturmechanische Berechnung und Optimierung wird mit Hilfe vollständiger Modelle der Finite-Elemente-Methode, welche mit einem Lösungsalgorithmus für strukturdynamische Problemstellungen gekoppelt wird, durchgeführt. Um Druck-, Kraft- und Momentenverteilungen effizient auswerten zu können, werden aerodynamische Einflusskoeffizienten verwendet. Regler, die im diskreten Zeitraum arbeiten, tragen zum Gesamtprozess über eine numerische Schnittstelle bei. Die Anwendung der entwickelten Werkzeuge erlaubt die Beleuchtung des Themas „kontrollierte Lasten“ in Optimierungsproblemen. Dadurch wird die Frage beantwortet wie man die Flugregelung in dem von Natur aus multidisziplinären Prozess der Flugzeugstrukturauslegung berücksichtigen, und welchen Nutzen man daraus für das Endprodukt ziehen kann. Die Integration von Reglern und die entsprechende Beschreibung der Methodik sind das Hauptinteresse dieser Arbeit. Daneben werden aber auch sinnvolle Studien, welche den Reglerentwurf selbst unterstützen, vorgestellt. Der sich ergebende Ansatz, ein Flugzeug mit geregelten Lasten zu dimensionieren, wird in verschiedenen Untersuchungen an einem unbemannten Luftfahrzeug mit industrieller Größe und Komplexität demonstriert.

Schlagwörter: Aeroelastizität, Aeroservoelastizität, Optimierung, Flugzeugstrukturauslegung

Danksagung

Die vorliegende Arbeit entstand während meiner Zeit als Doktorand bei der Airbus Defence and Space GmbH in Manching, Deutschland. Ohne die Unterstützung folgender Personen wäre sie nicht zustande gekommen.

Zuerst möchte ich mich bei meinem Doktorvater Prof. Dr.-Ing. Mirko Hornung bedanken. Sein Rat und seine Führung haben der Arbeit durch wertvolle Diskussionen und Gespräche die richtige Richtung gewiesen.

Des Weiteren bedanke ich mich bei Prof. Dr.-Ing. Wolf Krüger für seine zahlreichen Anmerkungen sowie die Erstellung seines Gutachtens.

Prof. Dr.-Ing. Fernaß Daoud danke ich dafür, dass ich die Forschungstätigkeiten in Manching ausüben durfte.

Besonderer Dank gebührt Ögmundur Petersson, der mir stets mit wertvollem, fachlichen Rat zur Seite stand und oft zündende Ideen auf den Weg brachte. Durch seine Erfahrung, Hinweise und Anmerkungen zu allen Themenfeldern dieser Arbeit konnten zahllose Probleme gelöst werden.

Bei den Kollegen Dr.-Ing. Sebastian Deinert, Reinhold Maierl, Dr.-Ing. Stephan Rechtik, Alessandro Gastaldi und Paul Bronny möchte ich mich für die fachlichen Diskussionen und die Untersützung bei der programmiertechnischen Umsetzung bedanken, welche für diese Arbeit nötig waren.

Meinen Eltern Andrea und Werner Nussbächer danke ich für all die Unterstützung, die sie mir schon immer bedingungslos zukommen ließen.

Ich danke meinem Bruder Thomas Nussbächer für seine positive Einstellung und die aufbauenden Worte, welche in stressigen Zeiten zum Fortschritt der Arbeit beitrugen.

Abschließend bedanke ich mich bei meiner Frau Margit Nussbächer, die während der gesamten Dauer der Arbeit tiefes Verständnis und Rückhalt für mich aufbrachte.

Ingolstadt, im September 2024

Daniel Nussbächer

Table of contents

List of figures

List of tables

List of symbols

A	State matrix
B	Input matrix
C	Output matrix
C_p	Dimensionless pressure coefficient
$C_{m\alpha}$	Pitch stability
$C_{m\eta}$	Pitch moment derivative w.r.t. elevator
C_{mq}	Pitch damping
C_m	Pitch moment coefficient
D	Feedthrough matrix
D_{jk}	Matrix entries of the aerodynamic differentiation matrix
D_{jx}	Matrix entries of the aerodynamic differentiation matrix for extra points
G	Transfer function
I_{yy}	Moment of inertia
N	Shape function
S_{ref}	Wing reference area
T	Sample time
Γ	Structural boundary
Γ_σ	Stress boundary
Γ_u	Displacement boundary
Ω	Structural domain
Θ	Pitch angle
$\ddot{u}$	Acceleration
$\dot{u}$	Velocity
ϵ	Mechanical strain
η_c	Elevator controller command
γ	Climb angle
ω_m	Angular eigenfrequency of mode m
σ	Mechanical stress
τ	Time constant
$\vec{\Phi}_m$	Eigenvector of mode m
ξ_c	Aileron controller command

ζ_c	Rudder controller command
b_i	Body force
c_{ref}	Reference chord length
d	Nodal displacement
dx_i	Thickness of the infinitesimal body
e	Control error
f	Objective function
f	Sample frequency
g	Constraint function
$g(C_{m\alpha})$	Stability derivative constraint
$k^{(e)}$	Element stiffness matrix
k_d	Gain factor of differentiator element
k_i	Gain factor of integrator element
k_p	Gain factor of proportional element
$k_{\eta q}$	Gain of pitch damper
$k_{\kappa\xi}$	Gain from ξ to κ
$k_{\zeta\xi}$	Gain from ξ to ζ
s	State variable
u	Displacement
u	System input
u_c	Controller command
u_g	Structural displacement
u_k	Aerodynamic displacement of a VLM box
w	Control system set point, nominal value
w	Weighting/Testing function
w_j	Downwash (normal wash) of a VLM box j at 75% relative chord
x	Control system state
x	Design variable
x_0	Initial design/Initial value of design variable
x_{opt}	Optimal design/Final value of design variable
y	System output
C_D	Drag coefficient

C_L	Lift coefficient
$C_{L\alpha}$	Lift slope
D	Damping matrix
D	Drag force
F	Force
G	Spline matrix
IAE	Integrated absolute error
IE	Integrated error
K^a	Aeroelastic stiffness matrix
K	Structural stiffness matrix
L	Lift force
M_α	Equivalent value for pitching moment due to incidence
M_η	Pitching moment due to elevator
M_q	Equivalent value for pitching moment due to pitch rate
M	Mass matrix
M	Moment, pitch moment
P	Load (force or moment)
Q	Aerodynamic stiffness matrix
R	Residual of governing equation
Γ	Circulation (vortex strength)
Λ	Wing aspect ratio
Φ	Bank angle
α_1	Mass coefficient of Rayleigh damping matrix
α_2	Stiffness coefficient of Rayleigh damping matrix
α	Angle of attack
η	Elevator deflection
κ_c	Roll spoiler controller command
κ	Roll spoiler deflection
λ	Ratio between roll spoiler and aileron deflection
μ	Viscosity
ρ	Fluid density
$\vec{\omega}$	Rotation of the fluid velocity field (vorticity)
$\vec{v}^{(\Phi)}$	Fluid velocity field without vorticity

$\vec{v}^{(\omega)}$	Fluid velocity field without divergence
$\vec{v}$	Fluid velocity field
ξ_m	Damping ratio of mode m
ξ	Aileron deflection
ζ	Rudder deflection
b	Wing span
c_m	Modal damping of mode m
c	Wing chord
l	Lift per unit span
m	Mass
p_0	Reference pressure
p_∞	Free stream pressure
p_{dyn}	Dynamic pressure
p	Pressure
q	Pitch rate
rf	Reserve factor
u_x	Extra point displacements
v	Fluid velocity

List of acronyms

AC	Aircraft
AFC	Aerodynamic Force Coefficients
AIC	Aerodynamic Influence Coefficients
ALAF	Active Load Alleviation Functionality
AoA	Angle of Attack
API	Application Programming Interface
ASE	Aeroservoelasticity
BE	Balance Equation
CE	Constitutive Equation
CFD	Computational Fluid Dynamics
CoC	Centre of Competence
CoG	Centre of Gravity
CPACS	Common Parametric Aircraft Configuration Schema
DBC	Dirichlet Boundary Condition
DLM	Doublet Lattice Method
DLR	Deutsches Zentrum für Luft und Raumfahrt
DNS	Direct Numerical Simulation
DoF	Degree of Freedom
EoM	Equations of Motion
FCS	Flight Control System
FE	Finite Element
FEM	Finite Element Method
GFEM	Global Finite Element Model
GLA	Gust Load Alleviation
HALE	High Altitude Long Endurance
HTP	Horizontal Tail Plane
IC	Initial Condition
IPS	Infinite Plate Spline
KE	Kinematic Equation
LAF	Load Alleviation Functionality
LAS	Load Alleviation System
LES	Large Eddy Simulation

LQR	Linear Quadratic Regulator
MALE	Medium Altitude Long Endurance
MDO	Multidisciplinary Design Optimisation
MIMO	Multiple Input Multiple Output
MLA	Manoeuvre Load Alleviation
MMA	Method of Moving Asymptotes
MONA	ModGen and MSC Nastran
MTOW	Maximum Takeoff Weight
NBC	Newman Boundary Condition
NDI	Non-linear Dynamic Inversion
NLPQL	Non-Linear Programming with Quadratic Line Search
PLAF	Passive Load Alleviation Functionality
PvW	Principle of Virtual Works
RANS	Reynolds Averaged Navier-Stokes
RBA	Rigid Body Approximation
RCE	Remote Component Environment
RFA	Rational Function Approximation
RSM	Response Surface Modelling
SAS	Stability Augmentation System
SISO	Single Input Single Output
SLP	Sequential Linear Programming
TF	Transfer Function
UAV	Unmanned Aerial Vehicle
VLM	Vortex Lattice Method

1 Introduction

Aircraft (AC) engineering uses light weight structures as core components of its modern designs. The main structures that withstand the extraordinary forces and moments experienced in flight can be grouped into wings, empennage, landing gear and fuselage. These components are commonly referred to as the airframe, its design is task of airframe engineering. In this context, more and more approaches from Multidisciplinary Design Optimisation (MDO) were applied during the last decades. MDO aims to find better designs for a given start design, respecting demands from multiple disciplines through the application of numerical optimisation and computational automation. Finding valid, "feasible" designs (by means of respective technical requirements) from given invalid, "infeasible" designs is a common task of optimisation, as well. The three main methods applied in AC engineering are sizing optimisation (varying the inner shape of a design), shape optimisation (varying the outer shape of a design) and topology optimisation (varying material distribution of a design). Aeroservoelasticity (ASE) and aeroelasticity, which will be explained in detail in this thesis, are common examples for engineering fields that are handled in a multidisciplinary way.

According to Raymer (2018) the development process of an aircraft can be split in the three phases of conceptual, preliminary and detail design. With the level of detail increasing from one phase to the next, the fidelity of the applied methods and tools increases, as well. As within this process, the numerical models get more complex, related studies get more time-consuming. Costs for late changes in an AC program, increase more dramatically, the later these changes become necessary. This raises the claim to reduce the number of necessary design iteration loops over AC programs (compare Brockhaus et al. (2011)) in the first place. The integrated airframe design philosophy is an approach to meet this requirement.

The terms MDO, integrated airframe design and aeroservoelasticity are of main importance for the present work. In academic research, they have a variety of meanings. In the scope of this thesis, MDO can be seen as a general design philosophy, using the engineering discipline of aeroservoelasticity to practically enable integrated airframe design.

Figure 1.1: Central technical terms of this thesis

The meaning of these terms for the work at hand shall be explained in more detail through a summary of recent and ongoing activities in aeronautical science. But not only does an overview on available capabilities in these fields help to understand the core technical terms of this thesis, it also exposes gaps in today's research, especially w.r.t. industrial applicability. These gaps need to be closed, when the challenging demands of future products shall be met.

1.1 State of the Art

The present work implements a multidisciplinary design optimisation approach which extends the methods currently used for sizing airframe structures in consideration of flight control systems in an integrated way. In this chapter an overview on the most important research in the fields of aeroservoelasticity and its consideration in integrated design is given. Further, it is highlighted for each work which aspects of aeroservoelastic optimisation are approached and how this is done. As a result, Table 1.1 summarises the modelling approaches. This gives an overview on the state of the art of and helps to identify weaknesses in the respective methodical workflows.

Aeroservoelasticity is an engineering field, mainly of interest in aircraft design, which combines the three disciplines aerodynamics, structural mechanics and flight control system (see e.g. Tewari (2015)). It aims to study effects from all three subfields simultaneously and gained importance over the last decades. Integrated design refers to a philosophy of AC design, which is able to assess interdisciplinary phenomena and find critical aspects, that can be detected only when demands and effects of all disciplines are evaluated simultaneously in a thus "integrated" way. The approach has been followed for decades and brought up various frameworks and tool-chains (see e.g. Seywald (2016), Kuchar (2012), Liersch & Hepperle (2011), Kier & Hofstee (2004), Zotemantel (1992)). A core characteristic of integrated designing is an interdisciplinary way of working. In the scope of this work, this means designing in the fields of aeroelasticity and aeroservoelasticity.

A great overview on the current state of the art in the field of aeroservoelasticity is given in Livne (2018). Although focus is laid on the technology of active flutter suppression, research activities of all fields connected to this work are summarised and highlighted. It is shown that active means, i.e. means with a Flight Control System (FCS) in the design loop, enable effective solutions for design problems, when they occur in later phases of the AC development process. Further, it is stated that integrating active controllers in a MDO process is necessary to allow integrated AC optimisation from the early design stages. The overview on the modelling methods applied in ASE shows that unsteady aerodynamic loads are still very challenging. The paper gives two especially important statements for this work. First, it is summarised that high-fidelity airframe models are considered as still too large for AC design studies considering ASE, even when massive parallel computation is applied. Second, the Equations of Motion (EoM) of the elastic aircraft were derived from two historically different fields, which resulted in strongly differing mathematical models and methods. This difference in modelling still continues to have a negative effect on the consistency of today's aeroservoelastic research.

Haghighat et al. (2012) uses a low-fidelity aerodynamic Vortex Lattice Method (VLM) in com-

bination with a simplified structural beam modelling approach and simultaneously considers a Load Alleviation System (LAS) as a controller for a gust response and an altitude change manoeuvre. The application of a gradient-free optimisation algorithm is demonstrated at a High Altitude Long Endurance (HALE)-Unmanned Aerial Vehicle (UAV) and proofs that sizing aircraft structures in consideration of a FCS must be seen as superior over optimising without it.

When it comes to process-design, the following works use similar approaches to solve the technical problems adressed by the thesis at hand. Klimmek et al. (2019) describes the Common Parametric Aircraft Configuration Schema (CPACS) and a process for aeroelastic structural design called "ModGen and MSC Nastran (MONA)" and brings it together in the parameterized aeroelastic structural design process CPACS-MONA. CPACS-MONA makes use of preliminary mass and loads estimations and delivers simulation models and an optimisation model. It is mentioned that the approach of quasi-static loads resulting from the process can be extended by taking into account flight control laws for closed loop manoeuvres through the VarLoads framework. Optimisations of composite wing structures using gradient based methods are performed in Dillinger et al. (2019). The results obtained from a Doublet Lattice Method (DLM) are corrected using a higher order aerodynamic method. The paper highlights the limit of applicability w.r.t. increasing Angle of Attack (AoA) values. In Handojo (2021) the author proves that consideration of manoeuvre and gust load alleviation in early design stages is a promising concept to reduce wing bending moments, structural mass and extend the fatigue life. Voss & Klimmek (2022) adresses manoeuvre loads analysis of fighter design, taking into account aeroelasticity using the ModGen framework. Results from lower order aerodynamic methods are compared with those from higher order methods. The paper finds a good agreement of the overall pressure distribution between panel aerodynamics and higher fidelity results obtained from CFD for the studied cases. Zimmer et al. (2022) wants to prepare a framework for high-fidelity geometrically nonlinear loads. A comparison of geometrical linear and nonlinear approaches can be found. Assessments of structural componentes by means of the von Mises strain evaluated with both, linear and nonlinear methods are given.

In Deinert (2016), the VLM is used together with a detailed structural Finite Element Method (FEM) model to realise combined sizing and shape optimisation through the application of deterministic, gradient-based algorithms. Induced drag and Breguet range are main quantities, studied through variations of the internal structural and the external aerodynamic shape. The integrated and automated design process is applied onto a commercial Airbus A320 class aircraft model.

As a representative of research papers on aeroservoelasticity and integrated designing, the work in Davies et al. (2012) can be named. It discusses the application of MDO processes w.r.t. specific conceptual fighter/strike design problems and technologies. Higher fidelity anal-

ysis capabilities are brought forward, as both strength and aeroelastic criteria for structural sizing with an industrial standard process and respective software are applied for various load cases in an integrated way. To deal with high-fidelity results, Response Surface Modelling (RSM) is used.

In Petersson, Leitner & Stroscher (2010) a non-linear rigid body flight dynamics model is combined with linear aeroelastic dynamics in an automated process. The usage of a full, structural finite element model without static condensation step enables proper sizing of structural elements like skins, ribs, spars or caps by an optimisation algorithm. It is shown that a minimum mass design can be reached in only few iterations. Both, an aerodynamic DLM model and a flight control system along with a state space model of a flexible, blended wing body aircraft are considered in an integrated way in the overall numerical model. This integrated design approach enables to assess the effect of structural changes on manoeuvre responses with realistic AC loads.

In Becker et al. (1999) decoupling elastic modes and flight mechanic modes is addressed from a modelling side. Especially as modern AC gain in elasticity, the resulting elastic modes tend to lower frequencies, which can interfere with the flight mechanical ones. An integrated design process for notch filters during FCS design is discussed. Therefore, unsteady aerodynamics based on linear potential theory are applied together with a reduced FEM model. The FCS is described as being composed out of individual transfer functions covering gain and phase stabilisation. It is emphasized that the structural FEM model poses major limitations for dynamic modelling.

The problem of the separate treatment of flight mechanics and aeroelasticity in flight control design for modern AC is discussed in Ferreira et al. (2010). The gap between the maximum rigid body frequency and the minimum structural mode frequency for conventional AC structures is the base of classical notch filter design for FCS applications. The assumption of these frequencies being sufficiently separated is violated through modern, elastic airframe designs. Control laws for altitude hold, stability augmentation using a Stability Augmentation System (SAS) and structural mode damping are highlighted. Optimisation of only the FCS is carried out in the frequency domain, in consideration of generalised aerodynamic forces and moments resulting from VLM /DLM and elastic properties from FEM models. Generalised damping coefficients, based on mass and stiffness parameters are applied in the equations of structural dynamics. The fact of structural modes interfering with rigid body modes suggests an integrated design approach that does not rely on the separation of frequencies.

A modelling approach of an integrated loads analysis is presented in Kier (2011). Both gust and manoeuvre loads can be calculated in the time domain making use of DLM aerodynamics in combination with Rational Function Approximation (RFA). The paper points out that gust

induced loads can often be calculated beforehand. However, it further emphasizes that with temporally changing aerodynamic conditions, as is the case for aeroservoelastic studies, their influence has to be included in time domain simulations.

The work presented in Kier (2018), describes an integrated modelling approach, which is suitable for both flight loads analyses and flight dynamics investigations. It shows how more advanced 3D panel methods might replace the lower fidelity state of the art vortex and doublet lattice based aerodynamic methods in integrated airframe design. Especially for MDO applications, which demand repeated simulations and require multiple design evaluations, such fast, loop capable approaches need to be further developed. The paper further demonstrates how time simulations (which are necessary when an active flight control system influences the aircraft dynamics and are therefore a must for aeroservoelastic studies) can be realised in the scope of integrated airframe design.

Further examples for industrially driven research of integrated airframe design is given by Daoud et al. (2012), Daoud et al. (2015), Deinert et al. (2013*a*), Deinert et al. (2013*b*) and Schuhmacher et al. (2012). They all use a gradient based optimisation approach, a main focus on structural design and the respective design process in common. It is pointed out that the traditional airframe design process addresses the various disciplines sequentially and that this must be changed resulting in a more integrated way. Automation is another key driver, especially when it comes to making the potentials of integrated designing accessible to early stages like conceptual and preliminary design. Particular attention is paid to a parametric airframe representation, which helps for structural shape optimisation and performance assessment studies. These are especially valuable to determine an initial AC layout.

Although not focussing on an integrated way of designing or the airframe design process itself, Karpel et al. (2005) explains how ASE studies must be approached. It depicts both frequency and time domain methods to enable dynamic response analyses for atmospheric gust excitations in consideration of aeroservoelastic systems. State space formulations for the EoM and control system design are explained and both a Single Input Single Output (SISO) and a h_∞-controller are applied to a structural stick model of a generic transport aircraft. The control systems aim to reduce the wing tip acceleration resulting from atmospheric gusts, which are simulated through both Fourier transformation and time domain simulations. Unsteady aerodynamic modelling is realised with the ZAERO software and is based on oscillatory, frequency-dependent Aerodynamic Force Coefficients (AFC) matrices, calculated through DLM or panel methods.

The papers of Shearer & Cesnik (2006), Shearer & Cesnik (2007) and Shearer & Cesnik (2008) deal with flight dynamics of flexible aircraft. Time integration of non-linear EoM for flexible AC is developed and applied to HALE configurations. These works bring together

the governing equations, as classically used in aeroelastic studies, and the six-degree-of freedom EoM in an aircraft reference point, as applied in flight mechanical analyses. Geometrically non-linear structural beam models are solved with implicit modified Newmark methods. Demonstrations highlight the importance of non-linear structural modelling when comparing with linearised structural analyses and rigid-body approaches. Shearer & Cesnik (2008) specifically presents a control architecture for very flexible aircraft. It uses an unsteady finite state potential flow aerodynamics model and a low-order strain-based non-linear structural analysis. Longitudinal and lateral motion are handled by separate control systems: A Linear Quadratic Regulator (LQR) formulation is used for the lateral motion, a Non-linear Dynamic Inversion (NDI) approach is applied for the longitudinal motion. A highly flexible AC model, where elastic modes are not separated by an order of magnitude from the rigid body modes, serves as a demonstrator for the proposed evaluation methods of aeroservoelasticity.

The work in Luber (2012) explains the influence of aeroservoelasticity to the strategy of the digital FCS development, rather than on the structural layout of an aircraft. It is outlined that FEM models, representing airframe structures together with data of ground resonance tests, serve as the base for notch filters applied in modern digital flight controllers. Interdisciplinary designing of control laws is identified as an important step to minimise aeroservoelastic effects in a modern AC.

Wildschek et al. (2015) proves, that an active control system can be used as a mean to enable the equipment of an aircraft with large winglets for load alleviation without the necessity to strengthen the outer wing structure. A feed-forward gust LAS and a simplified beam model are optimised, simultaneously. It has highlighted that modelling the wing box through beam elements is very generic and that higher fidelity FEM is necessary to compute mass savings more exactly. Therefore, an equivalent skin thickness is derived analytically and used in an aeroelastic re-assessment applying a doublet lattice panel method.

Table 1.1 gives a summary on the methods and approaches applied in the selected scientific studies dealing with multidisciplinary aircraft design and optimisation.

Reference	Aerodynamic model	Control system model/tasks	Structural model	Optimisation
Becker et al. (1999)	Unsteady, linear potential	Notch filter	Reduced FEM	Gradient-based (FCS)
Daoud et al. (2012), Daoud et al. (2015), Deinert et al. (2013*a*), Deinert et al. (2013*b*), Schuhmacher et al. (2012)	VLM/DLM	-	Full FEM	Gradient-based (structural sizing and shape)
Davies et al. (2012)	Low and high fidelity methods	Control surface scheduling	FEM and RSM	Not specified
Deinert (2016)	VLM	-	Full FEM	Gradient-based (structural sizing and shape)
Dillinger et al. (2019)	Low and high fidelity methods	-	FEM plus stacking sequence for composites	Gradient-based
Ferreira et al. (2010)	VLM/DLM	SAS, structural mode damping	Reduced FEM	Frequency domain (FCS)
Haghighat et al. (2012)	VLM	LAS controller	FEM beam model	Gradient-free
Handojo (2021)	DLM	Load alleviation concept	FEM plus fatigue demands	(Nastran SOL200)
Karpel et al. (2005)	DLM/panel method	gust-controller (SISO/h_∞)	Stick FEM	-
Kier (2011)	DLM with RFA	-	Reduced FEM	-
Kier (2018)	VLM/DLM panel method	-	Reduced FEM	-
Petersson, Leitner & Stroscher (2010)	DLM	Not specified (state space model based)	Full FEM	Not specified (Nastran SOL200)
Shearer & Cesnik (2008)	Unsteady potential flow	NDI and LQR (longitudinal and lateral motion)	Non-linear, beam modelling	-
Voss & Klimmek (2022)	Low and high fidelity methods	-	FEM	Not specified
Wildschek et al. (2015)	DLM	gust LAS	FEM (beam and shell)	Convex optimisation (FCS and structure)

Table 1.1: Contributions to airframe structural sizing through integrated design with aeroservoelastic approaches

1.2 Motivation

The number of disciplines, which provide main contributions to an airframe layout, increases with every new AC project. While over the last decades aeroelasticity became one of the main design changers, especially for high aspect ratio configurations, it is today not enough to only encounter for aeroelastic effects. Demands from system, engine, and even special airport conditions can have major influences to the final aircraft design. As all modern AC use fly by wire control systems, which are mainly responsible for the control surface deflections that induce desired movements, and as the FCS is not really considered in early development phases yet, it is identified as a component promising a lot of potential when it comes to enlarging the design space for future airplanes. Therefore, consideration of the FCS in the conceptual and preliminary design phase of aircraft projects resulting in aeroservoelasticity must be enabled.

Strongly connected to the demand of respecting the FCS in multidisciplinary airframe design optimisation applications is the desire to account for controlled loads. The fact that structural reserves are not exploited due to overly conservative methods results in too heavy and expensive designs. A stronger and explicit call for controlled forces and moments must follow a concrete implementation in a respective tool framework.

The more an aircraft project advances, the smaller is the remaining design flexibility. As big changes in late development phases are especially expensive, various design freezes are applied in specific project stages. As a detailed layout of flight controllers is usually initiated in later phases, the remaining freedom is rather small. To overcome this limitation is another motivating aspect of considering FCS aspects as early as possible and through means of MDO.

Thinking further into the direction of FCS integration shows that dynamic effects in general are not considered enough in early design stages. Conceptual AC-design studies mainly focus on steady loading conditions. Although flutter and gust analyses may be performed, the meaning of transient phenomena for the final structural layout is still underestimated. Carrying out more dynamic studies in early development phases promises another extension of the valid design space in AC projects. While the topic of realising more dynamic evaluations in conceptual stages can not be fully adressed in this thesis, methods and approaches which support this target shall still be described. Therefore, this work uses static aeroelasticity and handles transient effects with the assumption of quasi-steadiness, which is generally valid to evaluate slow manoeuvres. The aerostructural methods are based on the same theory as implemented in the commercial program MSC Nastran.

Various possibilities, for simplifying the way to solve more complex engineering problems of aviation, arise when pushing the limits of current aircraft development processes. Load Alle-

viation Functionality (LAF) may serve as one example, here. It is a key technology, applied in modern aircraft systems. Its development, however, does not follow a pre-defined scientific or industrial process, yet. Application of MDO in combination with the consideration of FCS can massively support the design of such systems and therefore help in meeting respective requirements. The lessons learned during establishing a process for new technologies can lay the ground for introducing further technologies.

This work originated from a practical, industrial background, which demanded a scientific way of approaching its topics. Therefore, the need for practical applicability of the tools to be developed and the processes to be designed is a strong motivational driver for the efforts to be made. The transfer of theoretical, university knowledge to a practical, application level motivates an attempt which directly implements the gathered know-how in industrial codes. Tool frameworks and collections of specific numerical programs are a common outcome of most academic studies, that deal with multidisciplinarity. Usually, they are generated to meet specific project or program requirements and do not account for a more general applicability. Therefore, they can be used only to a limited extend in productive aircraft development. It is necessary to enlarge the capabilities of available MDO tools such that they meet both academic and industrial demands, especially w.r.t. aeroservoelasticity.

An integrated design process targets to capture all physical effects, relevant for a given engineering problem in a global, overall way, rather than solving subtasks separately in the respective Centre of Competence (CoC). The underlying philosophy does not raise the claim to capture all details in the behaviour of the studied system. It rather tends to highlight aspects that stem from the interdisciplinary character of modern products, which can not be determined with a way of working that counts on decentralised solutions, where solver steps can only be performed successively. However, integrated design still demands a high level of knowledge in various disciplines, which is often not available in one source but needs to be gathered in a cumbersome way. A collection which describes all aspects necessary for solving problems of airframe design in an integrated way must be provided.

With computational engineering, more and more theoretical knowledge is included in modern, numerical tools. This offers a still growing number of possibilities through automation. Various examples for automation activities in AC design, as e.g. the development and application of CPACS or the Remote Component Environment (RCE) can be named. In this scope MDO is not only a design methodology but is the implementation of automation in the way of working of modern engineers. Like FEM or Computational Fluid Dynamics (CFD) methods extended the AC design process and laid the foundations for the success of today's products, multidisciplinary optimisation is the logical next step for further improvements. The underlying way of thinking is promoted further, if solving more technical problems in an easier way with it is enabled.

The open issues, which have to be solved and which motivate this work, can be summarised as follows:

- The FCS is not addressed in early phases of AC design
- Controlled loads are not used for conceptual sizing of an AC layout
- Unnecessary small design freedom is left to FCS designer in later phases of AC design
- Transient phenomena are respected only late in AC design
- Potentials of LAF technologies are not exploited as they are considered too late in the design process
- Most process descriptions are too academic for practical application in designing AC structures
- State of the art in structural design is not integrated as long as the FCS is not respected
- Numerical optimisation and automation is not yet well established as way of working in AC design

1.3 Objective of Thesis

The motivation presented in Chapter 1.2 allows to derive targets of this thesis. While not all open issues from the state of the art and all aspects from the motivational thoughts can be solved here, a main goal can be formulated:

> The primary target of this work is to extend the current, integrated design process by a FCS and to thus enable airframe sizing with controlled loads making use of optimisation and automation.

The technical realisation of necessary methodical enhancements is the main focus. The necessity to respect arbitrary transient behaviour and effects shall be addressed in a tool framework. It will enable a maximum of design flexibility through allowing variable fidelity in structural, aerodynamic and controller modelling.

A main outcome of the research and development activities will be given through the fact that the airframe can be designed with controlled loads. With this possibility, a spotlight is put on the detection and handling of structurally critical loads. The implementation will enable industrial applicability for large scale numerical models.

Further, it is aimed to extend the available design flexibility for the FCS. The capability of being able to handle generic, arbitrary FCS layouts independently of specific programs and tools will be realised. The resulting enhancement of the valid design space supports the process of solving more complex engineering problems. LAS-layout can be named as an example.

This work respects the facts that computational optimisation gains attraction in engineering and that the possibilities of automation are recognised for AC development projects. It con-

tributes through the description and implementation of a modern way of inter- and cross-disciplinary working. Both, integration of core aspects from one discipline into another, and clear separation of competences between the disciplines involved must be respected, therefore.

1.4 Thesis Structure and Nomenclature

Each of the following chapters starts with a brief outline on its content. A general explanation of the whole work shall be given here.

Chapter 2 gives an overview on the necessary, physical basics of all disciplines involved with the topic of aeroservoelastic airframe design optimisation. Mathematical descriptions of aeroelasticity, structural dynamics, control theory and MDO will be provided. This gives an idea of the parameters and variables, which are relevant in the respective discipline and explains which data must be interchanged accordingly.

The transition from pure theories to more practical applications is made in Chapter 3. While it structurally follows the setup of its predecessor, it concentrates on the description of how to model the physical effects that are described through the respective mathematical equations. It targets to give an overview on both methods and tools used in numerical modelling and on their possibilities and limitations for practical usage. Further, input and output quantities of the various disciplines and computational tools, which are especially important when it comes to formulating interfaces in a next step, are highlighted.

Creating and handling numerical interfaces is topic of Chapter 4. It brings theoretical and practical ingredients together. A detailed explanation on how to methodically realise data exchange and on model updates from automated optimisation is given. Further, aspects interesting for a computational implementation are emphasized. The description of how to correctly set up an interdisciplinary analysis is followed by an explanation of how it needs to be embedded into a numerical optimisation process.

The derived, integrated airframe design and sizing process is applied for different engineering problems in Chapter 5. Structural optimisation studies for classical use cases, longitudinal and lateral AC flight manoeuvres and analyses with low-fidelity load alleviation approaches are demonstrated for a Medium Altitude Long Endurance (MALE) UAV configuration. Technical quantities like reserve factors, mechanical displacements, strains and stresses are discussed and compared for both initial and optimised designs, to show which improvements were achieved through the application of MDO methods.

The thesis finishes with a summary of its contributions to state of the art airframe sizing in Chapter 6. A discussion on next steps to be performed in integrated AC design is given.

The fact that multiple disciplines need to be covered poses a challenge concerning the nomen-

clature used in the following chapters. Different notational conventions for mathematical symbols and physical variables were established in the three core fields of structural mechanics, aerodynamics and control theory. While structures are often described through tensors, aerodynamic formulations usually apply matrix-vector notations and control equations are often formulated in other mathematical domains like the Laplace domain. This thesis does not try to construct a generic mathematical representation covering all disciplines at once, but formulates equations in a way as they are used in the respective discipline.

Parameters and variables used in this thesis are used to explain physical effects. Basic interrelations are explained with the help of scalar quantities. When it comes to more complex relationships, i.e. when a multidimensional character must be described, index-, matrix- or vector-notation comes into use. All three are perfectly equal and are capable of describing the underlying physical effects with the same level of accuracy. To support a possible computational implementation, index notation can be favoured. The vector of a quantity x is denoted as $\vec{x}$ and consists of the components $x_1, ...x_n$ according to the respective vectorial basis (only Euclidean coordinate systems are assumed, which means that vectors are formulated with Euclidean bases). The index notation, representing the same quantity, is x_i, where i indexes x. In proper tensorial notation, working on an n-dimensional Euclidean vector space with the basis vectors $\mathbf{e_1}, ..., \mathbf{e_n}$, the vector components occur as well:

$$\vec{x} = \begin{pmatrix} x_1 \\ \vdots \\ x_n \end{pmatrix} \quad \longleftrightarrow \quad x_i \; \forall i \in [1, n] \quad \longleftrightarrow \quad \mathbf{x} = \sum_{i=1}^{n} x^i \mathbf{e_i}$$

Side note: The notations x^i and x_i for vector components incorporate the concept of covariance and contravariance of vectors (compare e.g. Itskov (2007)).

The Einstein summation convention is applied for structure mechanical formulations, exclusively. The scalar product of two vectors $\vec{a}, \vec{b}$ results in a scalar according to

$$\vec{a} \cdot \vec{b} = \sum_{i=1}^{n} a_i \cdot b_i = a_1 \cdot b_1 + ... + a_n \cdot b_n \tag{1.1}$$

The Nabla operator describes gradient information according to partial derivatives. Applied to a scalar c deriving w.r.t. spatial coordinates $x_1, ..., x_n$ it provides

$$\nabla c = \begin{pmatrix} \frac{\partial c}{\partial x_1} \\ \vdots \\ \frac{\partial c}{\partial x_n} \end{pmatrix} \tag{1.2}$$

2 Fundamentals of Aeroservoelastic Airframe Design Optimisation

Respecting the influence of multiple disciplines at the same time rather than considering them as isolated components, is a mean to meet the challenge of modern aircraft becoming more and more complex. This multidisciplinary approach helps to fulfil technical requirements in an integrated way of designing. Interdisciplinary knowledge of different areas of expertise is merged and approaches of the respective disciplines are brought together into comprehensive models. The practical realisation of this design methodology lies in the numerical modelling, which aims to couple suitable computational tools and programs (see Chapters 3 and 4). The theoretical base for this integrated designing must always be the proper formulation of the system equations of all involved disciplines. With regard to aeroservoelasticity, this chapter therefore explains fundamentals of aeroelasticity, control systems, structural dynamics and multidisciplinary design optimisation.

With the target of this work of developing an integrated airframe design process considering flight control system demands in mind, Chapter 2 formulates the therefore necessary physical basics. They are needed to understand the modelling components, which are highlighted in Chapter 3 and merged into a final process in Chapter 4.

2.1 Static Aeroelasticity

A main component of an aeroservoelastic design process is the field of aeroelasticity. It describes the interaction between elastic deformations of structures and externally acting, aerodynamic loads. In this chapter, the governing equations of the thus contributing disciplines aerodynamics and structural mechanics are derived in such a way that they can be applied in an integrated airframe design process.

Forces and moments applied to a given structure lead to a displacement field. The pressure distribution resulting from the aerodynamic flow and the external loading, accordingly changes due to this deformation (see Figure 2.1). The circular dependency can be solved only with methods that evaluate both disciplines and respect the mutual, physical effects between them.

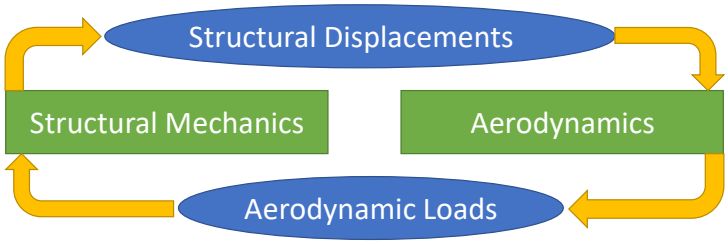

Figure 2.1: The interconnections of static aeroelasticity

In aircraft design, aeroelasticity is of main importance for flexible structures. The wing aspect ratio Λ is a basic, purely geometric characteristic, which is well known from aircraft design fundamentals. The dimensionless Λ is often defined as in equation (2.1) with the wing span b and the wing reference area S_{ref}. For a wing without kink, it can be expressed through its chord length c and span b, as well.

$$\Lambda = \frac{b^2}{S_{ref}} \tag{2.1}$$

When introducing the topic of aeroelasticity an important side note must be made, concerning the orientation of aeroelastic quantities. In structural aircraft design, the main coordinate system is usually oriented with the x-axis pointing from nose to tail and the y-axis pointing from fuselage to starboard. As a result, the z-axis orients upwards which is different from the common definitions in e.g. flight mechanics.

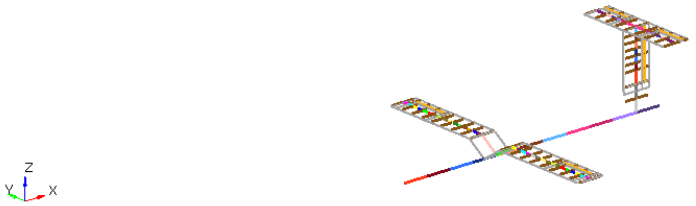

Figure 2.2: Coordinate system applied in aeroelastic modelling

Respecting the influence of aerodynamically induced elastification helps to find improved aircraft designs and to detect dangerous physical effects, which can even lead to a loss of the AC. Various dynamic phenomena as flutter, gust, buffeting or control surface reversal can cause serious damage and even lead to a loss of the aircraft. Therefore they need to be assessed in an integrated design approach, best with higher fidelity methods like presented e.g. in Rozov et al. (2019), Breitsamter (2001), Breitsamter (2005), Wildschek et al. (2010).

2.1.1 Aerodynamics

One of the two pillars of aeroelasticity as part of an aeroservoelastic analysis is the field of aerodynamics. Its physical basics, the governing equations and their mathematical implementation are described here.

An important dimensionless parameter in aerodynamics is the pressure coefficient C_p. It is formulated with the pressure p, a reference pressure p_0 (e.g. the free stream pressure p_∞), the density ρ and the velocity v of the respective fluid (compare e.g. Katz & Plotkin (2010)).

$$C_p = \frac{p - p_0}{\frac{1}{2}\rho v^2} \tag{2.2}$$

The denominator of C_p is the dynamic pressure p_{dyn}.

$$p_{dyn} = \frac{1}{2}\rho v^2 \tag{2.3}$$

With respective C_p, the pressure difference Δp between two points, e.g. the lower and the upper side of a surface, is then given as

$$\Delta p = p_{dyn}\Delta C_p \tag{2.4}$$

The spatial distribution of Δp, enables the calculation of forces F and moments M, which are used to load a mechanical structure. The main question in the field of aircraft aeroelasticity is therefore, how to determine the resulting pressure distribution for certain environmental conditions, given by respective flight states.

The mathematical closed form of the system equations, describing the flow of the Newtonion fluids handled in aircraft design, is usually formulated by the Navier-Stokes equations (compare Katz & Plotkin (2010)):

$$\rho(\frac{\partial v_i}{\partial t} + \vec{v}\cdot\nabla v_i) = \rho f_i - \frac{\partial}{\partial x_i}(p + \frac{2}{3}\mu\nabla\cdot\vec{v}) + \frac{\partial}{\partial x_j}\mu(\frac{\partial v_i}{\partial x_j} + \frac{\partial v_j}{\partial x_i}) \tag{2.5}$$

They result from the differential forms of the conservation of mass and conservation of momentum given in index notation ($i, j = 1, 2, 3$). Here f are mass specific forces externally applied to the fluid, x represents a generic spatial orientation and μ is a viscosity coefficient.

According to the given problem, sensible assumptions are made, simplifying the equations. Common assumptions are made for the viscosity coefficient, the compressibility of the flow, transient effects or boundary conditions of the respective, physical problem. The resulting differential equations are then solved for the velocity field with an appropriate numerical solver, in general. A method solving the transient Navier-Stokes equations directly is the Direct Numerical Simulation (DNS), where no turbulence model or specific boundary conditions through wall models are needed. The Large Eddy Simulation (LES) is solving (2.5) as well, however uses a turbulence model reducing the numerical effort. Reynolds Averaged Navier-Stokes (RANS) is treating a time-averaged form of the Navier-Stokes equations. Euler methods mainly assume a non-viscous fluid but still need to solve a second order differential equation system. All of the previously named methods demand volumetric discretisation, bringing high computational effort, which is an inevitable nuisance that must be accepted for respective aerodynamic problems.

Especially with regard to an application in optimisation frameworks, where many evaluations of the governing equations are necessary, the volume based discretisation is a huge disad-

vantage, however. The methodical coupling of such high-fidelity solvers in an integrated way within optimisation is still topic of current research activities. Therefore DNS, LES, RANS or even Euler-approaches are not yet suited to serve as subcomponents, in the scope of a framework aiming to handle a wider range of disciplinary fields. (It shall still be noted that recent works in the field of aerodynamics like e.g. Weigold et al. (2017) see a shift of panel methods to more advanced CFD-methods in the near future, which MDO-processes have to adapt to sooner or later, as well. An example successfully applying higher fidelity methods in the background of conceptual design is Hermanutz & Hornung (2017).)

Less numerical effort is required by panel and lattice approaches, which discretise surfaces rather than volumes. Due to the demand for low computational cost in MDO applications, a decision between the possibilities of a two-dimensional panel method and the one-dimensional VLM and DLM had thus to be taken, for this work.

Panel methods are capable of respecting effects of air displacement as a result of volumetric components. Lift distributions obtained from lattice approaches are accurate for many, especially conceptual aircraft studies. The engineering issues, to be demonstrated in the following, are dealing with incompressible, low-speed flows. Respecting compressible and transonic or supersonic effects would not bring methodical changes to the derived processes, but bring additional problems, which need to be solved. A key problem lies within respecting transient system responses, necessitated through the targeted integration of control systems into the structural design loop. For this purpose an unsteady vortex lattice method, which demands the consideration of aerodynamic wakes could be used. To get an idea of how this can be achieved, Binder et al. (2018) shall be recommended. However, assuring that the studied manoeuvres are carried out slow enough, enables neglecting transient aerodynamic effects with the assumption of quasi-steadiness (compare e.g. Kier (2005), Kier (2011)).

Obviously, this assumption reduces the number of engineering tasks, that can be accurately described. In the scope of this thesis, this limitation is acceptable. Therefore steady VLM is selected as the primary aerodynamic method. Its governing equations must be described from a theoretical point of view, briefly, to better understand practical details of the modelling aspects. As based on potential theory, most of the following equations can be found in basic courses on aerodynamics. Katz & Plotkin (2010) contains an excellent description of all necessary aspects of the potential theory. Kier & Looye (2009) contains very valuable details on the VLM. An early description of the DLM is given in Albano & Rodden (1969).

Lattice methods are mathematically motivated from potential theory. The velocity field $\vec{v}$ is assumed to arise of a component without vorticity $\vec{v}^{(\Phi)}$ and a divergence-free component (without sinks or sources) $\vec{v}^{(\omega)}$. The vorticity $\vec{\omega}$ is the mathematical rotation of the field. The

irrotational part $\vec{v}^{(\Phi)}$ can be derived as gradient of a scalar potential Φ.

$$\vec{v} = \vec{v}^{(\Phi)} + \vec{v}^{(\omega)} \tag{2.6}$$

$$\nabla \times \vec{v}^{(\Phi)} = \vec{0} \tag{2.7}$$

$$\nabla \cdot \vec{v}^{(\omega)} = 0 \tag{2.8}$$

$$\vec{v}^{(\Phi)} = \nabla\Phi \tag{2.9}$$

$$\vec{\omega} = rot(\vec{v}) = \nabla \times \vec{v} \tag{2.10}$$

A VLM now calculates the rotation-free velocity field $\vec{v}^{(\Phi)}$. Planforms of lifting surfaces are discretised in panels through horse-shoe vortices, concentrating a finite circulation Γ_j at their 25% relative panel chord lengths.

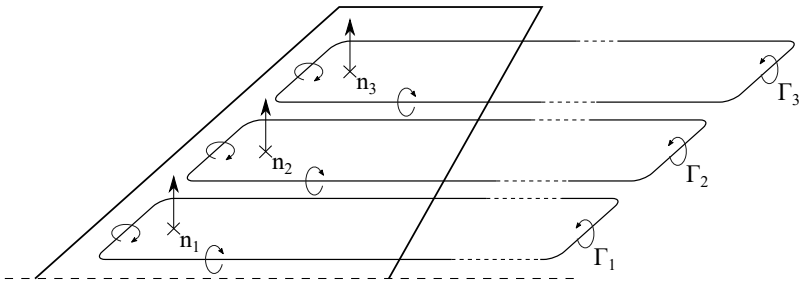

Figure 2.3: Discretisation of aerodynamic surfaces with vortex lattice

The circulation Γ of a velocity field $\vec{v}$ with respect to a given contour S which encloses an area A is defined as the line integral of the tangential velocity alongside of S. Γ is connected with the vorticity through the theorem of Stokes.

$$\Gamma(S) = \oint_S \vec{v} \cdot \, d\vec{s} = \int_A \vec{\omega} \cdot \vec{n} \, dA \tag{2.11}$$

$\vec{n}$ is the normal vector to the area A. Following the Kutta–Joukowski theorem, which states

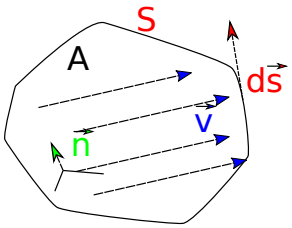

Figure 2.4: Velocity field and path for line integration

that lift per unit span l on a lifting airfoil is proportional to the respective Γ, each horse-shoe j

generates an amount of lift l_j according to its Γ_j (represented in vector notation by $\vec{\Gamma}$).

$$l_j = \rho v_\infty \Gamma_j \tag{2.12}$$

Thus, the spatial distribution of the finite Γ_j enables the calculation of the aerodynamic lift distribution. The unknown Γ_j are determined by the flow conditions describing the aerodynamic problem. A linear equation system formulates the dependency between the Γ_j and the up to this point undefined flow v_j, that is to be evaluated on a respective panel. The matrix describing this relationship mainly depends on the problem geometry, i.e. the distances resulting from the spatial discretisation of the lifting surface through the horse-shoe vortices and is referred to as Aerodynamic Influence Coefficients (AIC) matrix.

$$AIC \cdot \vec{\Gamma} = \vec{v} \tag{2.13}$$

The Biot-Savart law describes how the rotational part of a vector field $\vec{v}^{(\omega)}$ geometrically results from its vorticity $\vec{\omega}$ and is thus used to calculate the entries of the AIC matrix. The exact numerical procedure shall not be highlighted here in detail, as it can be found in corresponding literature and works (e.g. Katz & Plotkin (2010)). To solve the mathematical equation system (2.13), a physically sensible right hand side v_j has to be defined. Respective constraints are given by flow conditions, known at certain points through the problem to be solved. It was possible to introduce pre-defined Γ_j using a Dirichlet Boundary Condition (DBC), directly. However, it is more common to formulate the demand as a Newman Boundary Condition (NBC), evaluated at a location of 75% relative chord length of each panel ("collocation/Pistolesi point"). The fact of a common airfoil being impermeable for the flow is used to formulate appropriate, mathematical boundary conditions for equation (2.13), by means of defining the zero normal flow.

The demand of the panel being impermeable induces a normal component to the velocity field of the flow. The normalised form of this component shall be referred to as downwash, or normal wash, and is given for each box as w_j. It results of the time derivative $\dot{u}_j$ of the aerodynamic displacement field with the box component u_j, evaluated at 75% relative chord, which is identical with the respective velocity v_j:

$$w_j = \frac{\dot{u}_j}{v_\infty} = \frac{v_j}{v_\infty} \tag{2.14}$$

For the sake of generality, the possibility to evaluate the aerodynamic displacement of the discrete field u_k is maintained through the index k, rather than staying with the box index j. From a purely methodical point of view, it makes no difference, where the aerodynamic

displacement of the respective box is evaluated. In any case, the lever arm between the aerodynamic evaluation points indexed with j or k must be respected properly. Commonly the evaluation of the aerodynamic displacements is performed either at the mid point or at 75% relative panel chord position.

From a computational side, equation (2.13) is reformulated as the connection of dimensionless downwash and pressures through the matrix A_{jj} correlating to the AIC:

$$w_j = \frac{1}{p_{dyn}} A_{jj} f_j \tag{2.15}$$

$$f_j = p_{dyn} A_{jj}^{-1} w_j \tag{2.16}$$

The steady rotational displacement Θ_k of a 6-Degree of Freedom (DoF), local, aerodynamic displacement u_k can be seen as a local pitch angle Θ and directly contributes to the downwash w_j. To numerically handle this, a differentiation matrix consisting of the entries D_{jk} is introduced. It mainly selects rotations from the displacement vector:

$$w_j = D_{jk} u_k \tag{2.17}$$

$$D_{jk} = [0\ 0\ 0\ 0\ 1\ 0] \tag{2.18}$$

With the boundary conditions being described at 75% relative panel chord position over the downwash, equation (2.16) can be reformulated as

$$Q_{jj} w_j = \Delta C_{p_j} \tag{2.19}$$

The matrix entries Q_{jj} correspond to those of the inverted AIC matrix A_{jj}^{-1}. With a known downwash distribution it enabled the calculation of discrete pressure coefficients ΔC_{p_j} over the aerodynamic mesh, directly.

Integrating the box pressure using the cross section area leads to the load P, generated by the box. The mathematical proper equation

$$\vec{P} = \int_A p \cdot \vec{n}\, dA \tag{2.20}$$

writes in a discrete, numerical form as

$$P_k = S_{kj} p_j \tag{2.21}$$

P_k shall be the force acting at 25% relative chord of the box (where the finite circulation Γ_i is located as well), p_j is the pressure difference between lower and upper side of the

box and S_{kj} represents an integration matrix mainly multiplying p_j with the cross section areas of the respective boxes. A connection between aerodynamic loads and displacements can be reformulated after inserting the dependencies considering the box pressure and the downwash, which ends in

$$P_k = p_{dyn} S_{kj} A_{jj}^{-1} D_{jk} u_k \tag{2.22}$$

$$Q_{kk} = S_{kj} A_{jj}^{-1} D_{jk} \tag{2.23}$$

With regard to a further usage in an aeroelastic formulation, the important coefficients of aerodynamic matrices summarise as

- A_{jj}, relating box pressures with downwash (equation (2.13) or equation (2.16))
- D_{jk}, selecting downwash components from local, aerodynamic displacements (equation (2.17))
- S_{kj}, integrating pressures to forces (equation (2.21))

To round up the description of pure aerodynamics, the necessary, most critical assumptions, for the results obtained with the VLM to be valid, shall be recapped:

- Quasi-steadiness: $\frac{\partial}{\partial t} \approx 0$
- Constant viscosity: $\mu = const$
- Incompressible flow: $\rho = const$
- No drag respected

2.1.2 Structural Mechanics

The second pillar of aeroelasticity is the field of structural mechanics. Its basic quantities, their interrelations and mathematical representations of the governing equations are described in this chapter.

To determine the elastic behaviour of airframe structures in consideration of aeroelasticity, static structural analyses must be performed. Key responses of such analyses are displacements u, strains ϵ and stresses σ. Based on the results of a structural analysis, sizing decisions can be taken. The solver responses are used by both, an actual stress engineer, to e.g. evaluate overall airframe integrity, and by a numerical optimiser, which provides design suggestions on an algorithmic base.

Depending on the design, materials and given boundary conditions, it may be necessary to consider non-linear effects. This work assumes linear structural behaviour. With respect to static aeroelasticity, time dependencies are not considered yet. The following basics on elasticity are valid for small, time-invariant deformations and shall therefore be used in the

scope of linear, static, structural analyses.

A proper description of the elastic state of a design under given loads demands a mathematical formulation of governing equations, which is valid in every point of the structure. Such a description is called the local or strong form of the mechanical problem. It consists of a set of equations, which completely describe the mechanical situation through u, ϵ and σ at all material points. The displacement u is defined by the current geometric position w.r.t. a central, basic coordinate system. It consists of both translational and rotational parts. Strains ϵ and stresses σ, however, can be defined in various ways. Common strain formulations are given by the Green-Lagrange strain tensor, the Euler-Almansi strain tensor, or the linear, engineering strain like used in Jones (1998) or Bathe (1996). Components of the strain tensor shall be noted by ϵ_{ij}. Stress tensor formulations usually are based on Cauchy or Kirchhoff (see Bathe (1996)). Their tensorial components are σ_{ij}. Per definition ϵ_{ij} and σ_{ij} are symmetric. The first index i denotes the normal direction, the second index j denotes the orientation of ϵ or σ, respectively (compare Figure 2.5, left).

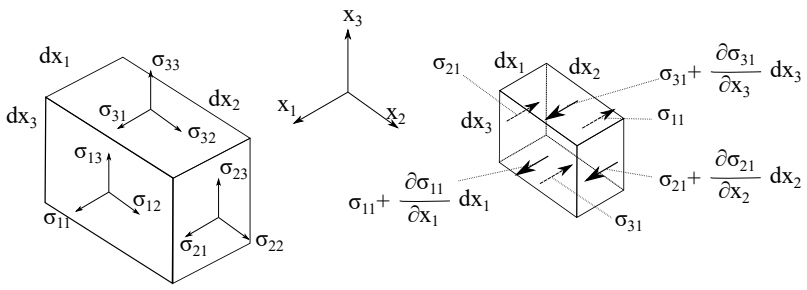

Figure 2.5: Index notation used for tensorial quantities in structural mechanics

Structural mechanics aims to evaluate displacements, strains and stresses in every point of the structural domain Ω. The equations coupling these three quantities are known as the Balance Equation (BE), Kinematic Equation (KE) and the Constitutive Equation (CE).

The balance equation follows from a mechanical equilibrium at the infinitesimal body with thickness dx_i (compare Figure 2.5, right).

$$\begin{aligned} \sigma_{ji,j} + \hat{b_i} &= 0 \text{ in } \Omega, \forall\ i,j = 1,2,3 \\ \frac{\partial \sigma_{11}}{\partial x_1} + \frac{\partial \sigma_{21}}{\partial x_2} + \frac{\partial \sigma_{31}}{\partial x_3} + \hat{b_1} &= 0 \text{ in } \Omega \\ \frac{\partial \sigma_{12}}{\partial x_1} + \frac{\partial \sigma_{22}}{\partial x_2} + \frac{\partial \sigma_{32}}{\partial x_3} + \hat{b_2} &= 0 \text{ in } \Omega \\ \frac{\partial \sigma_{13}}{\partial x_1} + \frac{\partial \sigma_{23}}{\partial x_2} + \frac{\partial \sigma_{33}}{\partial x_3} + \hat{b_3} &= 0 \text{ in } \Omega \end{aligned} \tag{2.24}$$

Body forces b_i are referred to a unit volume. The (spatial) kinematic equations give the geo-

metric relation between the displacement and the strain field.

$$\epsilon_{ij} = \frac{1}{2}(u_{i,j} + u_{j,i}) \text{ in } \Omega, \forall\, i,j = 1,2,3 \tag{2.25}$$

The constitutive equation directly relates the stresses to the strains. The discussion here shall be restricted to materials where this relation is linear (Hooke's law).

$$\begin{aligned} \sigma_{ij} =& C_{ijkl}\epsilon_{kl} \text{ in } \Omega, \forall\, i,j,k,l = 1,2,3 \\ \sigma_{ij} =& C_{ij11}\epsilon_{11} + C_{ij12}\epsilon_{12} + C_{ij13}\epsilon_{13} + \\ & C_{ij21}\epsilon_{21} + C_{ij22}\epsilon_{22} + C_{ij23}\epsilon_{23} + \\ & C_{ij31}\epsilon_{31} + C_{ij32}\epsilon_{32} + C_{ij33}\epsilon_{33} \end{aligned} \tag{2.26}$$

The fourth order tensor C_{ijkl} mainly carries the elastic moduli. Boundary conditions are necessary for a mathematical complete solution of the equations. The geometric boundary of the structural domain Ω, which u, ϵ and σ shall be evaluated on, is denoted as structural boundary Γ. Commonly, a boundary is given as mechanical DBC for pre-known displacements $\hat{u_i}$ on the displacement boundary Γ_u or mechanical NBC for implicitly defined stresses on the stress boundary Γ_σ. The latter can be determined directly from the explicitly defined constraint-forces, also known as traction forces $\hat{t_i}$. In the well known example of a one-side clamped cantilever beam, Γ_u is given by the clamped end, as the displacement result is pre-known there, and Γ_σ is given by the free end, as the stress result is pre-known there.

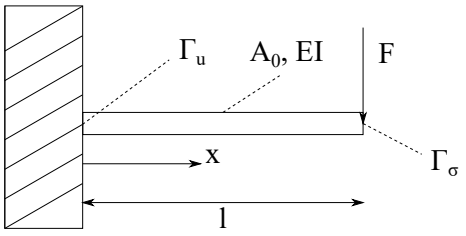

Figure 2.6: The cantilever

$$u_i = \hat{u_i} \text{ on } \Gamma_u, \forall\, i = 1,2,3 \tag{2.27}$$

$$\begin{aligned} \sigma_{ij}n_i = \hat{t_j} \text{ on } \Gamma_\sigma, \forall\, i = 1,2,3 \\ \sigma_{11}n_1 + \sigma_{21}n_2 + \sigma_{31}n_3 = \hat{t_1} \\ \sigma_{12}n_1 + \sigma_{22}n_2 + \sigma_{32}n_3 = \hat{t_2} \\ \sigma_{13}n_1 + \sigma_{23}n_2 + \sigma_{33}n_3 = \hat{t_3} \end{aligned} \tag{2.28}$$

Putting all equations together leads to the strong form of the governing equations of structural mechanics. They are often depicted in a Tonti diagram.

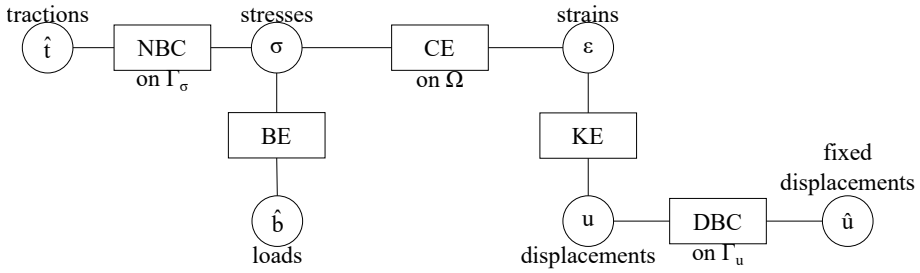

Figure 2.7: Tonti diagram of the strong form

BE: $\sigma_{ji,j} + \hat{b_i} = 0$	in Ω, $\forall\, i,j = 1,2,3$
KE: $\epsilon_{ij} = \frac{1}{2}(u_{i,j} + u_{j,i})$	in Ω, $\forall\, i,j = 1,2,3$
CE: $\sigma_{ij} = C_{ijkl}\epsilon_{kl}$	in Ω, $\forall\, i,j,k,l = 1,2,3$
DBC: $u_i = \hat{u_i}$	on Γ_u, $\forall\, i = 1,2,3$
NBC: $\sigma_{ij} n_i = \hat{t_j}$	on Γ_σ, $\forall\, i = 1,2,3$

The strong form is a complete representation of the continuum mechanical states in a given structural system. Ideally it is solved locally for every point. The residual R at every position x would vanish for each of the governing equations:

$$R(x) = 0$$

Usually such a solution is analytically possible for academic examples under various assumptions, only. This is rarely of use for large scale applications. A weaker demand can be formulated, when asking that the residual shall vanish globally, rather than locally. Thus it is not demanded that the equations are fulfilled in every point of the domain Ω, but it is sufficient that the respective governing equation is valid globally, in an integrated way:

$$\int R(x)dx = 0 \tag{2.29}$$

Obviously, this equation is fulfilled by the actual solution of the strong form of the governing equations. However, other functions may be allowed in equation (2.29) as well. Therefore a

set of weighting/testing functions w is introduced to test the residual R at specific points:

$$\int R(x)w(x)dx = 0$$

This approach is referred to as the method of weighted residuals like described in Bathe (1996) or Zienkiewicz et al. (2013). In structural applications, the weighted residuals of the balance equation and the Neumann boundary condition are summed up as follows:

$$\begin{aligned} R_{BE} &= \sigma_{ji,j} + \hat{b_i} \text{ in } \Omega, \forall\, i,j = 1,2,3 \\ R_{NBC} &= \hat{t_j} - \sigma_{ij} n_i \text{ on } \Gamma_\sigma, \forall\, i = 1,2,3 \\ \int_\Omega R_{BE}\, w\, d\Omega &+ \int_{\Gamma_\sigma} R_{NBC}\, w\, d\Omega = 0 \end{aligned} \tag{2.30}$$

The choice of the test functions w is arbitrary. Using mathematical theorems and selecting virtual displacements δu for w enables to identify different parts in equation (2.30) as mechanical components and finally leads to the Principle of Virtual Works (PvW), stated as follows:

$$\int_\Omega (C_{ijkl}\frac{1}{2}(u_{k,l} + u_{l,k}))\delta u_{i,j} d\Omega = \int_\Omega \hat{b_i}\delta u_i d\Omega + \int_{\Gamma_\sigma} \hat{t_i}\delta u_i d\Gamma \tag{2.31}$$

Equation (2.31) is now a weak form of the governing equations in structural mechanics. It describes the structural state in a global, an integrated way. It has the be noted that still no mathematical simplifications were made, the governing equations are valid in an analytical form. At this point a discretisation must, however, be introduced to enable the application of numerical computation. The domain Ω is discretised through a mesh of structural nodes in finite elements $\Omega^{(e)}$, as can be seen in Figure 2.8.

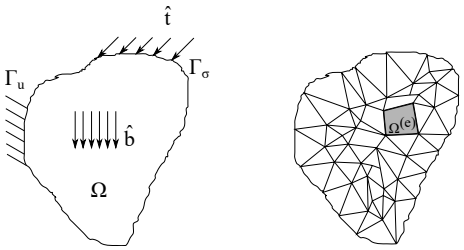

Figure 2.8: Finite element discretisation

It must be emphasized that equation (2.31) is not only valid on the overall domain Ω, but on each element $\Omega^{(e)}$, as well. The discretisation in finite elements gives name to the numerical method (FEM). The displacement field u and the variational displacement field δu are

approximated through discrete nodal displacements d using specific shape functions N:

$$\begin{aligned} \vec{u} &= N \cdot \vec{d} \\ \delta\vec{u} &= N \cdot \delta\vec{d} \end{aligned} \tag{2.32}$$

The nodal displacements d act at the nodes of the structural mesh represented in Figure 2.8. The shape functions N depend purely on geometrical properties. They are selected such that a nodal displacement contributes to the displacement field at the corresponding structural node, only.

One problem in the weak form (2.31) is given with the fact that not only the virtual displacement δu_i, but the virtual strain $\delta u_{i,j}$ is needed, as well. Therefore (2.32) must be differentiated. The differentiation is denoted by the differentiation operator L, which leads to vectorial strains

$$\begin{aligned} \vec{\epsilon} &= L \cdot \vec{u} \\ \vec{\epsilon} &= L \cdot N \cdot \vec{d} \\ \vec{\epsilon} &= B \cdot \vec{d} \end{aligned} \tag{2.33}$$

Equation (2.33) shows the B-operator, which basically represents the geometric differentiation of the shape functions. It connects the strains ϵ with the discrete, nodal displacements d.

The variational displacement field δu was introduced for the weight functions w, above. Therefore it was sensible to select the same shape functions N for the displacement field and the actual weight functions $w = \delta u$. This approach is the common "Bubnov-Galerkin" approach, which is not the only way to handle the weak form, however.

With given nodal displacements d, both the displacement and the strain field u and ϵ are approximated through (2.32) and (2.33). To determine d, the latter equations are substituted in the weak form (2.31) for each element $\Omega^{(e)}$. From the resulting equation, element stiffness matrices $k^{(e)}$ can be identified, which connect nodal displacements on the element with respective nodal loads. The global stiffness matrix K is assembled from the local, element stiffness matrices $k^{(e)}$. The same applies for the global vector of discrete displacements, the global vector of discrete loads and the global mass matrix M.

$$K = \bigA_{e=1}^{n_{ele}} (k^{(e)}) \tag{2.34}$$

The assembly process over all the n_{ele} elements is indicated by the assembly operator A. As a result of the discretisation and the assembly process, the governing equation can be written

in form of a matrix vector equation

$$K \cdot \vec{d} = \vec{P} \tag{2.35}$$

$$\begin{bmatrix} K_{11} & K_{12} & K_{13} & \dots & K_{1n_{dof}} \\ K_{21} & K_{22} & K_{23} & \dots & K_{2n_{dof}} \\ K_{31} & K_{32} & K_{33} & \dots & K_{3n_{dof}} \\ \vdots & \vdots & \vdots & \ddots & \vdots \\ K_{n_{dof}1} & K_{n_{dof}2} & K_{n_{dof}3} & \dots & K_{n_{dof}n_{dof}} \end{bmatrix} \cdot \begin{Bmatrix} d_1 \\ d_2 \\ d_3 \\ \vdots \\ d_{n_{dof}} \end{Bmatrix} = \begin{Bmatrix} P_1 \\ P_2 \\ P_3 \\ \vdots \\ P_{n_{dof}} \end{Bmatrix} \tag{2.36}$$

Care must be taken concerning the fact that the assembly of the element stiffness matrices is carried out over all n_{ele} elements, whereas the resulting matrices and vectors in equation (2.36) are formulated for the n_{dof} structural degrees of freedom. As the degrees of freedom are not exclusively bound to single elements, during the assembly process the element stiffness matrices are not only positioned in the global stiffness matrix, but its components need to be summed up for those degrees of freedom which are shared by multiple elements.

The resulting, actually continuous displacement field u is interpolated over the elements via the discrete, nodal displacements d. The vector of discrete, nodal displacements d is often not properly differentiated from the continuous displacement field u. Equation (2.35) is then noted with u being the vector of discrete, nodal displacements:

$$K \cdot \vec{u} = \vec{P} \tag{2.37}$$

Following the index-notation previously used in this work, equation (2.37) was formulated with the u_g as

$$K_{gg} u_g = P_g \tag{2.38}$$

The main outcome of a finite element formulation for further studies in this thesis is given by the global stiffness matrix K_{gg}. It embodies the overall elastic information of a given system and enables the determination of an elastic displacement field from externally applied loads. In a post-processing step, strains and stresses can be calculated with the given mechanical equations.

In numerical applications, structures are discretised through structural elements as one-dimensional rods, bars or beams and two-dimensional shells, plates and membranes. Each of these elements comes with a proper finite element formulation. Mechanical system responses of compound materials can be determined with finite element solvers, as well.

It has to be pointed out, that results from linear, finite element analyses must be considered valid only for small deformations (see Bathe (1996)). Most structural problems in aircraft

design can accurately be handled with the assumption of linearity. This is especially true for the phase of conceptual design. As soon as high deformations occur in a structure, a geometrically non-linear formulation must, however, be applied. Basically, this means that the influence of the structural deformation is considered during the evaluation of the stiffness, i.e. the stiffness matrix depends on the deformation itself:

$$K(\vec{u}) \cdot \vec{u} = \vec{P} \tag{2.39}$$

To numerically solve this algebraic equation, an iterative approach must be used, as the system matrix K depends on the actual solution u, itself.

2.1.3 Interconnection of Aerodynamics and Structural Mechanics

The general, circular dependencies of static aeroelasticity was mentioned at the beginning of this chapter (compare Figure 2.1). Displacements and loads from the isolated disciplines of aerodynamics and structural mechanics must now be brought into interaction. Of central importance are the aerodynamic and the structural degrees of freedom given through u_k and u_g, as quantities like velocities, strains or stresses can be derived from these primary solution values.

Generally the aerodynamic DoFs are collected in the dependent set, whereas the structural DoFs are selected as the independent set. Postulating linear dependencies, this leads to the generic equation

$$u_k = G_{kg} u_g \tag{2.40}$$

where the entries G_{kg} of the matrix G contain the information of how aerodynamic degrees of freedom result from the structural ones.

Only in the rare case that an aerodynamic and a structural mesh coincide, the respective DoFs match each other. In that case, no translation between the DoF-sets is needed. From a modelling point of view, however, this is a highly inflexible solution to achieve a proper interconnection between u_k and u_g. Connecting the aerodynamic and the structural nodes with rigid elements is another approach, which was applied in the first days of aeroelastic projects in aircraft industries. Especially when aerodynamic forces shall be applied to structural stick models, the beam splining method was developed. It demands that all structural nodes are aligned on a geometrically straight line as it assumes that deflections pass through the deflection field resulting from an elastic beam (compare Rodden & Johnson (2004)). This requirement dramatically limits the applicability of beam splining and necessitates high modelling effort.

A more state of the art aerostructural interconnection is given by two-dimensional splining methods. The Infinite Plate Spline (IPS) method is based on the mechanical theory of plate

elements. It solves the deflections of an infinite plate that is supported at a set of discrete points with known displacement values. The geometrical points of the two sets are projected to a plane where the solution takes place. The main numerical effort comes from evaluating geometrical relations between all points as the distances are main contributors to G. The outcome of the spline method comes from the determination of the matrix components G_{kg} of the spline matrix G.

The main principle which should be fulfilled by all interconnection methods is the PvW, again. All aerodynamic loads F_k and the equivalent loads F_g acting on structural points must do the same virtual work along the virtual displacements δu_k and δu_g:

$$\delta u_k F_k = \delta u_g F_g \tag{2.41}$$

Bringing together equations (2.41) and (2.40) results in

$$\begin{aligned} F_g &= G_{gk} F_k \\ F_g &= G_{kg}^T F_k \end{aligned} \tag{2.42}$$

The spline matrix can thus not only be used to transform displacements from the structural domain to the aerodynamic one, but relates aerodynamic with structural forces as well. In the scope of aeroelasticity it further comes into use when aerodynamic matrices as the aerodynamic stiffness matrix shall be transferred from the aerodynamic to the structural field:

$$\left.\begin{matrix} G_{kg}^T \\ Q_{kk} \\ G_{kg} \end{matrix}\right\} \rightarrow Q_{gg}$$

A more detailed derivation of the mathematical and physical basics of the IPS is beyond the scope of this work. For this purpose it shall be referred to e.g. Harder & Desmarais (1972).

2.1.4 Governing Equations of Direct Aeroelasticity

With the basic equations of aerodynamics and structural mechanics being described and the mathematical interrelations being explained, all ingredients can be brought together now. This chapter formulates the governing equations of aeroelasticity, such that they can be used in the scope of aeroservoelastic analyses.

To describe the physical behaviour of an aircraft, the equations of motion are used. Following Newton's second law of motion, all forces and moments in a system must be collected and brought into an equilibrium. The work done on the structure through external forces must

balance the change of internal energy. The main components contributing to these governing equations result from aerodynamics and structural mechanics and were presented on the previous pages.

The internal elastic force of a given aeroelastic system consists of two summands. One part of the elastic displacement field emerges from the loads and over the stiffness matrix K, known from the discussion on structural elasticity in Chapter 2.1.2 (compare the main equation (2.38)):

$$K_{gg}u_g = P_g \tag{2.38 revisited}$$

$$\vec{P}^{(el,SM)} = K \cdot \vec{u} \tag{2.43}$$

$$P_g^{(el,SM)} = K_{gg}u_g \tag{2.44}$$

The second part of the elastic displacement field emerges analogically from the loads and over the splined, aerodynamic stiffness matrix Q. It embodies the elastic contribution of aerodynamic displacements u_k to the structural displacement field u_g and is formed using the spline matrix G to transform the aerodynamic to the structural field:

$$\vec{P}^{(el,AD)} = -p_{dyn}Q \cdot \vec{u} \tag{2.45}$$

$$P_g^{(el,AD)} = -p_{dyn}Q_{gg}u_g \tag{2.46}$$

$$Q_{gg} = G_{kg}^T S_{kj} A_{jj}^{-1} D_{jk} G_{kg} \tag{2.47}$$

Summing up the two load vectors leads to the vector of internal elastic loads. It is connected to the elastic deformation field by the aeroelastic stiffness matrix K^a:

$$\vec{P}^{(el)} = \vec{P}^{(el,SM)} + \vec{P}^{(el,AD)} = K^a \cdot \vec{u} \tag{2.48}$$

$$P_g^{(el)} = [K_{gg} - p_{dyn}Q_{gg}]u_g = K_{gg}^a u_g \tag{2.49}$$

$$K_{gg}^a = K_{gg} - p_{dyn}Q_{gg} \tag{2.50}$$

Another load component stems from the inertia of the structure. It results from the acceleration experienced by the structural mass, formulated through the structural mass matrix M:

$$\vec{P}^{(inert)} = M \cdot \ddot{\vec{u}} \tag{2.51}$$

$$P_g^{(inert)} = M_{gg}\ddot{u}_g \tag{2.52}$$

The externally applied loads consist of two summands. The control surfaces of an aircraft are

used to induce desired movements. Ailerons, elevator and rudder therefore provide control in the aircraft roll-, pitch- and yaw-movement, respectively. Their deflections apply external loads by actively changing the flow around a specific component. The same type of external loads results from overall rigid body modes, changing the main aerodynamic parameters like the angle of attack. Although not being physical displacements, control surface deflections and the overall rigid body mode parameters are grouped in a vector of so called "extra point displacements" u_x, by MSC Nastran. Following the proceeding for the splined, aerodynamic stiffness matrix occurring in equation (2.47), a respective extra point differentiation matrix with the entries D_{jx} is formed. It mainly selects all VLM boxes modelling e.g. a control surface, to contribute to an additional downwash induced by the respectively commanded control surface deflection contained in u_x:

$$\vec{P}^{(extra)} = p_{dyn} Q_x \cdot \vec{u}_x \tag{2.53}$$

$$P_g^{(extra)} = p_{dyn} Q_{gx} u_x \tag{2.54}$$

$$Q_{gx} = G_{kg}^T S_{kj} A_{jj}^{-1} D_{jx} \tag{2.55}$$

It has to be noted that the number of columns in the entries D_{jx} is considerably smaller than the number of columns given in D_{jk}. Usually only few extra points (corresponding to index x) need to be defined, whereas the number of aerodynamic boxes (corresponding to k) depends on the chosen spatial discretisation and will therefore be considerably higher.

The last component that needs to be comprised is given classically by all those additionally applied loads, that were not yet respected by any other component. It shall be denoted as $\vec{P}^{(appl)}$. A concentrated thrust force modelling an engine, or distributed gravity loads can be examples for the vector entries $P_g^{(appl)}$.

Bringing all internal and external loads to a state of equilibrium, results in

$$\vec{P}^{(el,SM)} + \vec{P}^{(el,AD)} + \vec{P}^{(inert)} = \vec{P}^{(extra)} + \vec{P}^{(appl)} \tag{2.56}$$

$$\vec{P}^{(el)} + \vec{P}^{(inert)} = \vec{P}^{(extra)} + \vec{P}^{(appl)} \tag{2.57}$$

or in the form of displacements and accelerations:

$$[K_{gg} - p_{dyn} Q_{gg}] u_g + M_{gg} \ddot{u}_g = p_{dyn} Q_{gx} u_x + P_g^{(appl)} \tag{2.58}$$

Care must be taken here, not to account for gravity loads twice. If e.g. the gravitational acceleration is applied to the structure by $P^{(appl)}$, a respective acceleration can not be interpreted in $\ddot{u}$ any more. It must further be pointed out, that (2.57) does not only describe a

static equilibrium but enables dynamic states without consideration of damping components in the form of (2.58), as well.

Equation (2.58) now helps to solve two main problems of steady aeroelasticity. On the one hand the aeroelastic displacement field resulting from an aerodynamic state (defined e.g. through control surface deflections and aerodynamic parameters as the pre-defined AoA) can be determined. For this purpose, mainly u_x and $\ddot{u}$ have to be specified. A more difficult problem arises when a trimmed flight state shall be found. In that case only the accelerations are pre-defined, which still leaves u_x unknown. This results in an under-determined equation system.

One way to approach the issue of an under-determined system is to introduce further equations by making use of more, physical knowledge of the respective problem. MSC Nastran suggests dependencies which mainly capture possibilities of inertia relief and the formulation of a mean axes coordinate system as discussed in Rodden & Love (1984) and Rodden & Johnson (2004). A mathematical technique is applied, that is based on selecting specific structural reference DoFs u_r and thus splitting the structural displacements u_g. The accelerations of the remaining, "left over" DoFs u_l are then brought into an elastic relationship with this selection:

$$\left.\begin{matrix} u_r \\ u_l \end{matrix}\right\} u_g \tag{2.59}$$

$$\ddot{u}_l \leftrightarrow \ddot{u}_r \tag{2.60}$$

Another dependency is found by transforming extra points u_x to the accelerations of the selected structural reference DoFs.

$$u_x \leftrightarrow \ddot{u}_r \tag{2.61}$$

The introduction of these additional conditions leads to a definite, linear equation system. After numerical re-organisations, it guarantees a unique aeroelastic solution. A deeper description of the system of equations can be found e.g. in Rodden & Love (1984) and Rodden & Johnson (2004).

To solve the aeroelastic equations, two main procedures come into use. The first possibility uses numerical optimisation to find a trimmed flight state. A special trimming constraint is introduced, which formulates the flight mechanical demand of an aircraft not to experience any unbalanced loads or moments in an aerostructural way. An initial guess provides a first solution for the displacement field. The resulting load situation represents the input for the

assessment of the trimming constraint, which is violated as long as the external loads are not balanced through respective aerodynamic angles of attack. The latter are varied numerically until both the displacement field and the aerodynamic angles do no vary from one iteration to the next, the constraints are fulfilled and the aircraft is thus considered to be trimmed. This iterative approach is common in structural optimisation considering aeroelastic effects (compare e.g. Deinert (2016), Daoud et al. (2012), Daoud et al. (2015)).

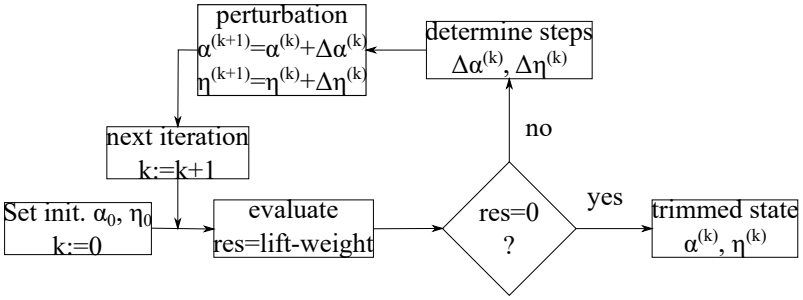

Figure 2.9: Process flow of optimisation based trimming

The main disadvantage of optimisation based trimming w.r.t. this work lies in the always remaining residuum. Especially when the obtained, not properly trimmed state is further used as initial condition in transient analyses, it can be noted that the residuum leads to an undesired movement (e.g. a loss in altitude or a pitch up according to the respective moment), even if it may be numerically rather small. An example for this is given in Chapter 4.2.1. In this work, equation (2.58) shall be solved directly, using the given suggestions (2.59) - (2.61). This results in a monolithic solution sequence, referred to as direct aeroelasticity. A great description of a numerical procedure realising this can be found in Rodden & Johnson (2004).

A further disadvantage of the optimisation approach compared to direct trimming comes with the necessity to declare additional design variables for a numerical optimiser. This can be a problem as the influence of the trimming design variables on the structural response may be considerably higher than that one of the structural design variables. As the mathematical optimiser doesn't differentiate between trimming and structural design variables, it is therefore possible that structural changes are exploited in order to reach a desired trim state, which is physically not sensible.

A positive side-effect of direct aeroelastic trimming is given by the fact that within the solution process stability derivatives are determined. Various force and moment quantities are reduced to aerodynamic angles. The angle of attack α and the elevator deflection η shall serve as an example, here. Their contribution to the resulting loads (e.g. z-force F_z or y-moment M_y) is given through selection matrices (e.g. sel_α and sel_η), that mainly select respective values out of all angles involved in the trim problem. $sel_{z,\alpha}$ can be interpreted as the component of sel_α, which represents the influence of α to a z-force. sel_α can be seen as a subcomponent

of a larger sel-matrix, again. Selected components shall serve as showcase derivations and demonstrate how the selection matrices are coupled to the stability derivative values:

$$\frac{\partial C_z}{\partial \alpha} = \frac{\partial \frac{F_z}{qS}}{\partial \alpha} = \frac{\partial \frac{sel_{z,\alpha}\alpha + sel_{z,\eta}\eta}{qS}}{\partial \alpha} = \frac{sel_{z,\alpha}}{qS}$$
$$\frac{\partial C_z}{\partial \eta} = \frac{\partial \frac{F_z}{qS}}{\partial \eta} = \frac{\partial \frac{sel_{z,\alpha}\alpha + sel_{z,\eta}\eta}{qS}}{\partial \eta} = \frac{sel_{z,\eta}}{qS}$$
$$\frac{\partial C_{my}}{\partial \alpha} = \frac{\partial \frac{M_y}{qSc}}{\partial \alpha} = \frac{\partial \frac{sel_{my,\alpha}\alpha + sel_{my,\eta}\eta}{qSc}}{\partial \alpha} = \frac{sel_{my,\alpha}}{qSc}$$
$$\frac{\partial C_{my}}{\partial \eta} = \frac{\partial \frac{M_y}{qSc}}{\partial \eta} = \frac{\partial \frac{sel_{my,\alpha}\alpha + sel_{my,\eta}\eta}{qSc}}{\partial \eta} = \frac{sel_{my,\eta}}{qSc}$$

The selection matrices are formulated such that they handle geometric properties like reference lengths or areas w.r.t. the derivatives, as well. More details on stability derivatives will be discussed later. Further information on the solution process to obtain $\frac{\partial C_z}{\partial \alpha}$, etc. can be found in Rodden & Johnson (2004).

2.2 Structural Dynamics

The previous formulations on aeroelasticity are all based on the assumption of steady states, where the system responses do not contain any time dependency. As soon as transient effects need to be studied, this representation must be extended by dynamic components. Control systems are always dealing with states that are varying in time. As the integrated airframe design process to be derived in this work desires an interaction with controllers, a transient solver instance is added to the governing equations, now.

With regard to modelling dynamic behaviour, it is especially necessary to capture damping effects. This is a highly complex task and involves practical testing and model adaptations (see Beards (1996)). Here, damping will be approached with a simple, mathematical model. Depending on the underlying, engineering problem, more advanced solutions might be necessary in a large scale aircraft program.

2.2.1 Governing Equations of Structural Dynamics

The governing equation for a static structural system, relating elastic deformation over the stiffness matrix with the external loads, was given as

$$K \cdot \vec{u} = \vec{P} \qquad \text{(2.37 revisited)}$$

The steady or static equilibrium described through this equation, is a special case of a mechanical equilibrium. If an external disturbance does not lead to a long term change of this state, it is further called stable. As soon as time-dependent effects act on the system, its gov-

erning equations must be enhanced to properly describe the resulting dynamic behaviour.

The static equilibrium assumes no velocities ($\dot{u} = 0$) and constant accelerations ($\ddot{u} = const$). Without these state characteristics, mass terms resulting in inertia effects and damping terms can not be neglected. The more general governing equation then contains a time dependency and states as

$$M \cdot \ddot{\vec{u}}(t) + D \cdot \dot{\vec{u}}(t) + K \cdot \vec{u}(t) = \vec{P}(t) \tag{2.62}$$

where the mass term $M \cdot \ddot{\vec{u}}(t)$ is known as an inertia load component from the static aeroelastic context:

$$\vec{P}^{(inert)} = M \cdot \ddot{\vec{u}} \tag{2.51 revisited}$$

With the assumption of steadiness, this component primarily is used to capture inertia effects. Transient behaviour is now contained in the governing equation (2.62) by respecting time-dependent accelerations $\ddot{u}(t)$.

The damping contribution $D \cdot \dot{\vec{u}}(t)$ is more difficult to handle. The coefficient of the velocity $\dot{u}(t)$ is the damping matrix D. Once excited, a system would oscillate endlessly, if no damping is considered in the model. The results obtained from such a description are useless for subsequent studies, which demand a proper dynamic modelling of the system. Thus, a sensible form of D is an absolute must for such applications. Properly estimating damping effects and generating respective models for a studied system is a science on its own. A system can be exposed to various forms of damping. Material damping, damping in structural joints and aerodynamic damping are well described in Beards (1996) and are of main interest for AC structures.

In this thesis the Rayleigh damping model is applied to capture damping behaviour in the analysed systems. The damping matrix D is assumed as a linear combination of the mass matrix M and the stiffness matrix K (compare Zienkiewicz et al. (2013) or Bathe (1996)):

$$D = \alpha_1 M + \alpha_2 K \tag{2.63}$$

With this formulation, the problem of determining D is reduced to the determination of two scalar parameters α_1 and α_2. α_1 can be denoted as the mass coefficient of the Rayleigh damping matrix, whereas α_2 is the stiffness coefficient of the Rayleigh damping matrix. In an AC project, they are best determined experimentally. A more analytic approach, applicable for early design phases as well, is possible over a modal decomposition. The angular eigenfrequency ω_m corresponding to the eigenvector $\vec{\Phi}_m$ for the structural mode m follows from equation (2.64) (compare Zienkiewicz & Taylor (2000)):

$$(K - \omega_m^2 M) \cdot \vec{\Phi}_m = 0 \tag{2.64}$$

Modal damping c_m of the mode m corresponding to the angular eigenfrequency ω_m is formulated as

$$c_m = 2\omega_m \xi_m \tag{2.65}$$

In this context the damping ratio ξ_m was introduced. It is the ratio of current damping to its critical value. $\xi = 1$ represents the critical damping case, which is the border between an over- and an underdamped system. Then, the damping is just high enough that no overshooting (change in direction w.r.t. the equilibrium state) occurs in the oscillation.

Figure 2.10 shows system responses of a mass-spring system damped with Rayleigh damping. The gravitational force acts as a step input, the steady state solution resulting for $t \to \infty$ thus means that the inertia force is in an equilibrium with the spring stiffness. In the upper case, only the mass term contributes to the resulting damping coefficient, while in the lower case, only the stiffness term does.

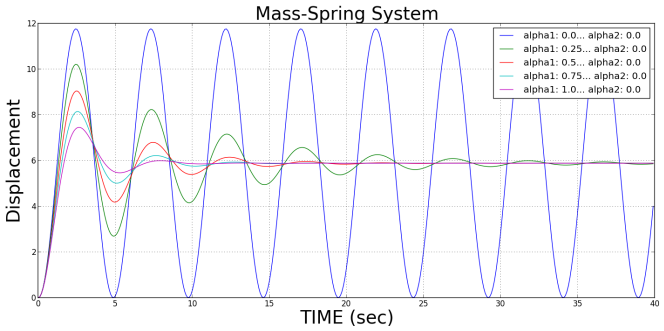

(a) Pure mass damping

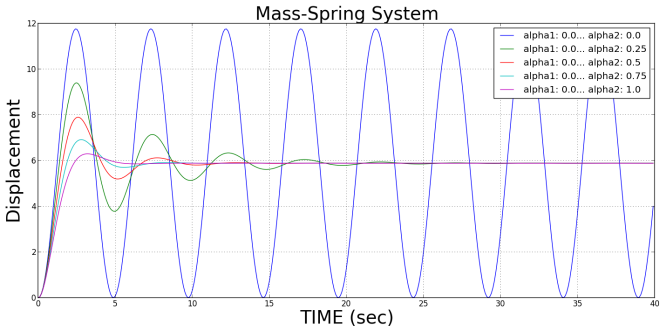

(b) Pure stiffness damping

Figure 2.10: Rayleigh damping considering only mass or stiffness terms

Equations (2.63), (2.64) and (2.65) help bringing together the damping ratio, the angular eigenfrequencies and the coefficients of the Rayleigh damping matrix:

$$\xi_m = \frac{1}{2}\left(\frac{\alpha_1}{\omega_m} + \alpha_2 \omega_m\right) \tag{2.66}$$

The two unknown parameters α_1 and α_2 can be determined from (2.66), now. Exactly two angular eigenfrequencies ω_1, ω_2 and damping ratios ξ_1, ξ_2 desired to damp the respective modes 1 and 2, must be provided to result in a unique solution for α_1 and α_2, therefore. In practice, usually a constant damping shall be reached for both modes, such that $\xi = \xi_1 = \xi_2$ and consequently

$$\begin{bmatrix} \frac{1}{2\omega_1} & \frac{\omega_1}{2} \\ \frac{1}{2\omega_2} & \frac{\omega_2}{2} \end{bmatrix} \cdot \begin{pmatrix} \alpha_1 \\ \alpha_2 \end{pmatrix} = \begin{pmatrix} \xi \\ \xi \end{pmatrix} \tag{2.67}$$

Equation (2.66) allows an interpretation of the meaning of the damping coefficients. The influence of mass damping through α_1 decreases for higher frequencies. Mass damping therefore mainly corresponds to damping of rigid body modes of a movement. Stiffness damping through α_2, however, increases linearly with the frequency (compare Figure 2.11). In the range between the selected frequencies f_1 and f_2 the damping can be considered as rather constant, depending on the range of selected eigenfrequencies.

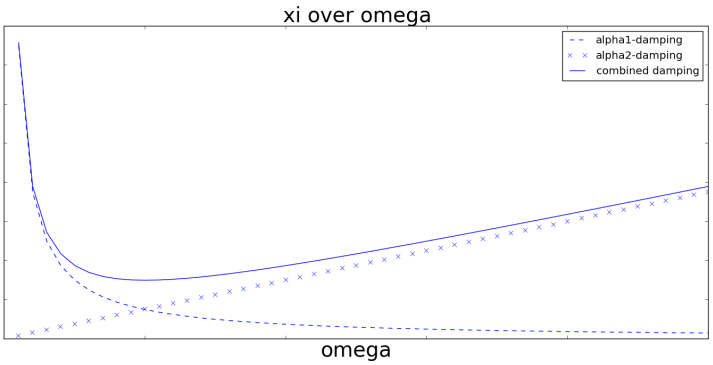

Figure 2.11: Damping ratio over frequencies

The determined Rayleigh damping coefficients α_1 and α_2 are selected in such a way that a constant damping of all frequencies in the range $[f1 = \frac{\omega_1}{2\pi}, f2 = \frac{\omega_2}{2\pi}]$ results. For oscillating structures ξ lies in a range of $1\% - 3\%$. This, however, depends on both materials and the overall construction itself (Beards (1996)). Various sources provide damping ratios valid for one or few studied or measured cases, only.

With all matrix coefficients of equation (2.62) being described, it is necessary to define a sensible Initial Condition (IC) of the transient problem to enable a unique solution of the linear equation system. In the static case this mathematically necessary step was given through the declaration of boundary conditions (DBC or NBC). Where in static analysis the boundary

conditions were given on the respective spatial boundary

$$\begin{aligned} &\text{DBC: } u_i = \hat{u_i} && \text{on } \Gamma_u, \forall\, i = 1,2,3 \\ &\text{NBC: } \sigma_{ij} n_i = \hat{t_j} && \text{on } \Gamma_\sigma, \forall\, i = 1,2,3 \end{aligned}$$

for dynamic problems, this must be valid with the additional time dimension for all time steps considered in the domain $[t_0, t_e]$:

$$\begin{aligned} &\text{DBC: } u_i = \hat{u_i} && \text{on } \Gamma_u \times [t_0, t_e], \forall\, i = 1,2,3 \\ &\text{NBC: } \sigma_{ij} n_i = \hat{t_j} && \text{on } \Gamma_\sigma \times [t_0, t_e], \forall\, i = 1,2,3 \\ &\text{IC: } u_i(t_0) = \hat{u}_{i,0} && \text{in } \Omega, \forall\, i = 1,2,3 \\ &\qquad \dot{u}_i(t_0) = \hat{\dot{u}}_{i,0} && \text{in } \Omega, \forall\, i = 1,2,3 \end{aligned}$$

In many applications, the initial condition for the displacement field $u(t_0) = u_0$ is obtained from a steady state and can thus result from a static structural or static aeroelastic analysis.

2.2.2 Numerical Solution of the Structural Dynamics Problem

The numerical solution of the equations from Chapter 2.2.1 demands a time discretisation. Temporal derivatives are approximated through forms of difference quotients. The time domain is divided in discrete intervals, of mostly uniform step size Δt.

With a given time discretisation, various solution approaches are possible (Faires & Burden (1994)). A basic time domain solver can be implemented through the forward Euler method. Based on the known values $u^{(i)} = u(t_i)$ and $\dot{u}^{(i)} = \dot{u}(t_i)$ of time step t_i, the solution for the next time steps $(t_{i+1}, t_{i+2}, ...)$ can be approximated through

$$\frac{u^{(i+1)} - u^{(i)}}{\Delta t} = \dot{u}^{(i)} \tag{2.68}$$

In equation (2.68) the unknown value $u^{(i+1)}$ appears on one side only, which enables a direct solution. Another approach is given when the unknown time step t_{i+1} appears on both sides:

$$\frac{u^{(i+1)} - u^{(i)}}{\Delta t} = \dot{u}^{(i+1)} \tag{2.69}$$

This is the backward Euler method, which represents an implicit solver. With backward Euler being an implicit solution method, its main advantage over forward Euler, lies within the solution stability even for a coarser time discretisation (Faires & Burden (1994))

A more advanced and state of the art solver for FEM applications is given by the implicit Newmark Beta Method , as described in Newmark (1959). The resulting numerical approximation

for the time step t_{i+1} contains two solver parameters β and γ:

$$\dot{u}^{(i+1)} = \dot{u}^{(i)} + (1-\gamma)\Delta t\ddot{u}^{(i)} + \gamma\Delta t\ddot{u}^{(i+1)} \tag{2.70}$$

$$u^{(i+1)} = u^{(i)} + \Delta t\dot{u}^{(i)} + (\frac{1}{2} - \beta)\Delta t^2\ddot{u}^{(i)} + \beta\Delta t^2\ddot{u}^{(i+1)} \tag{2.71}$$

β and γ can be used to control the approximation character of the accelerations: $\beta = \frac{1}{6}$ and $\gamma = \frac{1}{2}$ leads to a linear approximation of $\ddot{u}$. $\beta = \frac{1}{4}$ and $\gamma = \frac{1}{2}$ leads to a constant approximation of the mean $\ddot{u}$.

Newmark Beta can again be seen as a special case of the Generalized Alpha Method, which shall further be applied in this thesis. Along with β and γ, two additional parameters α_m and α_f are added to the numerical solution equations (compare Chung & Hulbert (1993)):

$$\beta = \frac{(1-\alpha_m+\alpha_f)^2}{4} \tag{2.72}$$

$$\gamma = \frac{1}{2} - \alpha_m + \alpha_f \tag{2.73}$$

$$\alpha_m = \frac{2\rho_\infty}{1+\rho_\infty} \tag{2.74}$$

$$\alpha_f = \frac{\rho_\infty}{1+\rho_\infty} \tag{2.75}$$

$\rho_\infty \in [0,1]$ controls numerical damping. The equations are intended to control the high frequency damping of the transient solution. With $\alpha_m = 0$ and $\alpha_f = 0$, the Newmark Beta method is obtained. Comparing the Newmark Beta Method with Generalized Alpha Method shows that both work with the same discrete, governing equations and that they only differ in the choice of β and γ.

2.2.3 Structural Dynamics in the Scope of Aeroservoelasticity

Flight mechanical calculations are often based on point masses. The mass property of the aircraft to study is condensed to a single point and its flight path is analysed and optimised in a spatial and temporal context. The structural dynamic equations in this work enable the same kind of studies if the DoF of the centre of gravity is considered. Thus, effects of changes in the AC dynamic behaviour through external loads can be studied. Further it enables the simultaneous evaluation of all structural properties as strains and stresses. This is crucial for a MDO based structural design, where working with the Global Finite Element Model (GFEM) rather than point masses and reduced models is a must.

In the scope of aeroelasticity, the responses obtained from a transient analysis and especially their changes from one time step to another can be interpreted as flight mechanical properties and changes in the aerodynamic flow conditions. A temporal change in a rotational DoF about

the y-axis can be seen as a change in the local angle of attack for an aerodynamic solver:

$$\Delta u_{rot,y} \hat{=} \Delta \alpha_{loc} \tag{2.76}$$

$$u_{rot}^{(i+1)} - u_{rot}^{(i)} \hat{=} \alpha_{loc}^{(i+1)} - \alpha_{loc}^{(i)} \tag{2.77}$$

The rotational DoF u_{rot} directly results from the dynamic-solver. A change in a local pitch angle Θ can as well be obtained as a change in the respective rotational DoF. The same applies for corresponding velocities (both translational $\dot{u}_{tra}$ and rotational $\dot{u}_{rot}$). The pitch rate (or pitch velocity) q, is the temporal derivative of Θ. Its change can thus be interpreted from a change in the rotational velocity $\dot{u}_{rot}$ of the AC for a given reference point (e.g. the Centre of Gravity (CoG)) resulting from the transient solver:

$$\dot{\Theta} = q \tag{2.78}$$

$$\Delta\Theta \hat{=} \Delta u_{rot,y} \tag{2.79}$$

$$\Delta\dot{\Theta} \hat{=} \Delta \dot{u}_{rot,y} \tag{2.80}$$

From a flight mechanical point of view, such assumptions pose a strong simplification of the often non-linear governing equations. A detailed description would cover a full representation in all axes (aerodynamic axes, body axes, wind axes, etc.). For airframe design they are still valid, as the focus lies on the loads resulting from the AoA and especially on their effect for the structural components.

To capture the behaviour of a mechanical system, where a controller is in the loop, time-dependent responses must be studied. Damping has a major influence on the dynamic response in such systems. Therefore a qualitative representation of transient effects can only be achieved by applying a damping model. Rayleigh damping is only one method to solve this problem. Accurate representations of aerodynamic damping in AC models is another important example in this context.

2.3 Control Theory

For a sensible treatment of control related tasks, a basic understanding of the mathematical description of engineering systems is indispensable. Especially when a controller shall be integrated into an airframe sizing loop, basic concepts of the engineering fields "control theory" and "flight mechanics and control" must be known. The following highlights those concepts, which can be considered as basic in controller design, but are not established in the context of integrated airframe designing with MDO. What shall not be described here, are fundamental

basics on topics like control system modelling, Laplace transformation, analyses of dynamic systems, stability and controllability or control system design. For such an introduction to control systems, basic engineering courses or literature like e.g. Ogata (2010) may be considered. If detailed information on flight control systems is desired, Brockhaus et al. (2011) shall be suggested.

2.3.1 Open Loop and Closed Loop Systems

The engineering discipline of controller design deals with dynamic systems. States x of such systems are often represented through a state space model (compare e.g. Ogata (2010), Brockhaus et al. (2011)). The mathematical representation of a state space model is given through the equation system

$$\dot{\vec{u}} = A \cdot \vec{x} + B \cdot \vec{u} \tag{2.81}$$

$$\vec{y} = C \cdot \vec{x} + D \cdot \vec{u} \tag{2.82}$$

with the state matrix A, the input matrix B, the output matrix C and the feedthrough matrix D.

The behaviour of transient signals is studied and manipulated w.r.t. a desired nominal value, or set point w. It is mainly analysed how changing the inputs u to a system affects its outputs y. Transferring the inputs and outputs into the Laplace domain results in U and Y. The concept of transfer functions G describes the connection between U and Y in the Laplace domain:

$$Y = G \cdot U \tag{2.83}$$

As long as the outputs are not used to influence the inputs for the purpose of manipulating the system state, the term open loop system applies (see Figure 2.12 (a)). The system to be controlled is referred to as the plant. Feeding back the outputs of the plant to its inputs helps to manipulate the system state. The result is a closed loop system (see Figure 2.12 (b)).

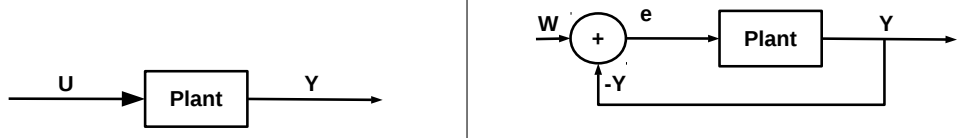

(a) Open loop system (generic input U) | (b) Closed loop system (set point input W)

Figure 2.12: Open and closed loop system

Closing an open loop system over a controller means selecting, measuring and pre-

processing proper signals as outputs, first. The selected outputs are then fed back to a controller, which generates a command u_c that aims to lead the system to a target state. Therefore, the plant output is subtracted from or summed to (negative or positive feedback) the input signal, which leads to the control error e. Closing the loop changes the Transfer Function (TF) of a given system, as can be seen in Figure 2.13.

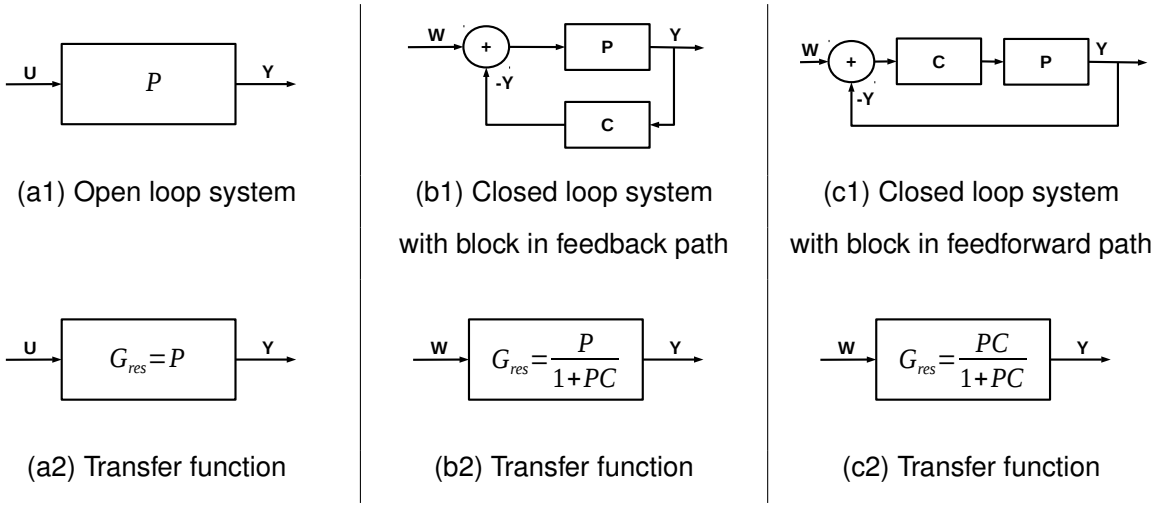

(a1) Open loop system | (b1) Closed loop system with block in feedback path | (c1) Closed loop system with block in feedforward path

(a2) Transfer function | (b2) Transfer function | (c2) Transfer function

Figure 2.13: Systems and respective transfer functions

In the scope of MDO and integrated airframe design, closing the loop over a given plant is a highly important step. Complex flight control systems possess a high number of inputs and outputs. If only one signal is not properly connected to the plant, the control system will not behave as intended. Further, numerical actuators need to be implemented to enable handling of time delays and to smooth digital signals. The generic form of a closed loop system with a controller in the loop is given in Figure 2.14 (a). The actuator appends the block diagram resulting in the representation of Figure 2.14 (b).

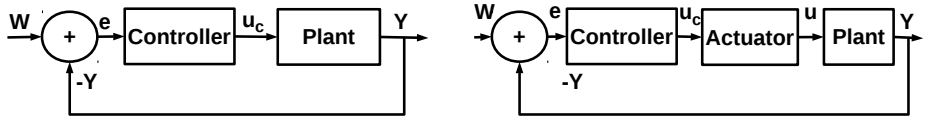

(a) Without actuator | (b) With actuator

Figure 2.14: Closed loop controlled system

Before a controller is applied to a plant, it is important to assess the quality of the resulting controlled system. There are various numerical properties that help to assure that a controller is working properly, i.e. as intended by the designer. The control error e of a dynamic system measures the distance between the current output y at a given time t and the respectively

desired nominal value w:

$$e(t) = w - y(t) \tag{2.84}$$

For $t \to \infty$ the output should reach a steady state. The resulting control error is the steady-state error. The control error varies strongly over time and the steady state error for a properly working closed loop system should finally be 0. To better express the performance of a control system, integral criteria are used. Integration of the control error over time leads to the integrated error IE:

$$IE = \int_0^\infty e(t)dt \tag{2.85}$$

To better handle error cancellation (where positive values of e cancel out negative values) the integrated absolute error IAE may be considered:

$$IAE = \int_0^\infty |e(t)|dt \tag{2.86}$$

Further integral criteria as integrated quadratic error or weighted quadratic error can be used as well, to evaluate the quality of a control system.

The previously mentioned concepts on open and closed loop systems are fundamental for a successful integration of flight control systems into an airframe sizing framework and shall therefore be highlighted, again:

- Mathematical state space representation
- Laplace transformation
- Understanding of open and closed loop systems
- Transfer functions
- Evaluation of control errors

2.3.2 Flight Control Systems

A modern aircraft FCS fulfils various control tasks (see Brockhaus et al. (2011)). Flight control functionalities can support the pilot in directly steering the AC or help him to follow a prescribed path, what is enabled by flight guidance modes of operation. Even fully automatic flight path guidance can be achieved through enhanced flight management capabilities. The range of subtopics from this field is huge and fills numerous books. Here, it shall be focussed on basic flight control related topics and their relevance for airframe sizing. To properly couple flight control and aerostructural airframe design, it is of high importance to describe common physical properties handled by both disciplines.

MDO-relevant quantities of a FCS

A mathematical model for the calculation of aerodynamic forces and moments was presented

in Chapter 2.1.1. Lift and drag forces (L and D), as well as resulting moments (M) represent the main load components P. In control system related analyses, governing loads are expressed through dimensionless force and moment coefficients:

$$L = \frac{\rho}{2} v^2 S_{ref} C_L \tag{2.87}$$

$$D = \frac{\rho}{2} v^2 S_{ref} C_D \tag{2.88}$$

$$M = \frac{\rho}{2} v^2 c_{ref} S_{ref} C_m \tag{2.89}$$

Aerodynamic forces and moments are normalised through a reference pressure (e.g. the dynamic pressure $p_{dyn} = \frac{\rho}{2} v^2$) and reference lengths and areas (e.g. c_{ref} and S_{ref}). Three main coefficients are the lift, drag and moment coefficients C_L, C_D and C_m, which again can be separated in different components:

- Lift coefficient:

$$C_L = C_{L(\alpha=0)} + C_{L\alpha}\alpha + C_{L\eta}\eta \tag{2.90}$$

- Drag coefficient:

$$C_D = C_{D_0} + C_{D_i} \tag{2.91}$$

- Moment coefficient:

$$C_m = C_{m(\alpha=0)} + C_{m\alpha}\alpha + C_{m\eta}\eta + C_{mq}\frac{c_{ref}}{v} q \tag{2.92}$$

The various components in these equations are the lift coefficient mainly due to wing camber $C_{L(\alpha=0)}$, the lift contribution due to angle of attack $C_{L\alpha}\alpha$, the lift contribution due to flap deflection $C_{L\eta}\eta$, the zero lift drag coefficient C_{D_0} (resulting from viscous and form drag), the induced drag coefficient C_{D_i} (induced by lift), the moment coefficient mainly due to wing camber$C_{m(\alpha=0)}$, the moment contribution due to angle of attack $C_{m\alpha}\alpha$, the moment contribution due to flap deflection $C_{m\eta}\eta$, and the moment contribution due to pitch rate $C_{mq}\frac{c_{ref}}{v}q$. A detailed description on all relevant coefficients and their components can be found e.g. in Brockhaus et al. (2011).

The load coefficients represent a common interface for physical properties and result e.g. from aerodynamic calculations, wind tunnel tests or flight test data. Further information on force and moment coefficients along with basic concepts as polar curves, zero lift coefficient, the quadratic dependence of the drag coefficient on the lift coefficient and more can be found in e.g. Raymer (2018) or Brockhaus et al. (2011).

The derivatives of the dimensionless coefficients are important values to evaluate aircraft

performance, stability and manoeuvrability. The lift slope $C_{L\alpha}$ may serve as a common introduction and is defined as the derivative of the lift coefficient C_L w.r.t. the angle of attack α:

$$C_{L\alpha} = \frac{\partial C_L}{\partial \alpha} \tag{2.93}$$

Among the numerous variables resulting from the equations of motion, handled in flight system dynamics, flight mechanics and flight control design, the following derivatives shall be especially highlighted w.r.t. the topics of this thesis:

- Pitch stiffness or pitch stability given through $C_{m\alpha}$:

$$C_{m\alpha} = \frac{\partial C_m}{\partial \alpha} \tag{2.94}$$

- Elevator effectiveness given through $C_{m\eta}$:

$$C_{m\eta} = \frac{\partial C_m}{\partial \eta} \tag{2.95}$$

- Pitch damping given through C_{mq}:

$$C_{mq} = \frac{\partial C_m}{\partial q} \tag{2.96}$$

Flight control systems work with the equations of motion describing the longitudinal, directional and lateral movement of an aircraft. The governing state equations are usually linearised around an operating point. In the process of linearisation a lot of equivalent variables are introduced for the purpose of simplification (compare Brockhaus et al. (2011)). Well known representatives of such equivalent variables are e.g.

$$M_\alpha = p_{dyn} \frac{S_{ref} c_{ref}}{I_y} C_{m\alpha}$$
$$M_\eta = p_{dyn} \frac{S_{ref} c_{ref}}{I_y} C_{m\eta}$$

For lateral movement further properties and derivatives like N_β containing $C_{n\beta}$ need to be considered. They are especially valuable for assessing the aircraft side-stability. The "Cnbeta-dynamic" or Weismann-criterion shall be named in this context, as well (compare e.g. Brockhaus et al. (2011), Osterhuber (2011), Osterhuber (2013)).

Despite their high value for the mathematical model of aircraft movement, equivalent variables like M_α, M_η or N_β are not directly considered in the following discussions. Rather their corresponding derivatives $C_{m\alpha}$, $C_{m\eta}$ and C_{mq} will be studied as primary variables and evaluated

during the overall airframe design.

Depending on how they are determined, the previously described properties and coefficients may contain information on the elasticity of the aircraft. Elasticity poses a problem to FCS designs. The equations of motion used in flight mechanics, and thus in flight control systems, often apply a Rigid Body Approximation (RBA) of the aircraft structure. The aircraft is assumed to behave as a rigid body without noteworthy elastification. This model is valid as long as the aircraft is stiff enough, which results in a wide separation of the lower frequencies of the rigid body modes and the higher frequencies of elastic modes. Sensors are feeding back both flight mechanic signals (like rigid body rates and accelerations) and structural signals (like higher frequencies resulting from elastification) to the FCS. Notch filters are applied to decouple this structural coupling for flight control primary tasks (compare Zeng et al. (2011), Ferreira et al. (2010), Calise et al. (2002)). They aim to filter out the undesired higher frequency elastic modes from the signals that are fed back to the controller (see Figure 2.15). A detailed study of the coupling between aeroelastic response and flight dynamics is given in Kitson et al. (2016), where non-linear strain-based FEM is brought together with CFD-based aerodynamics.

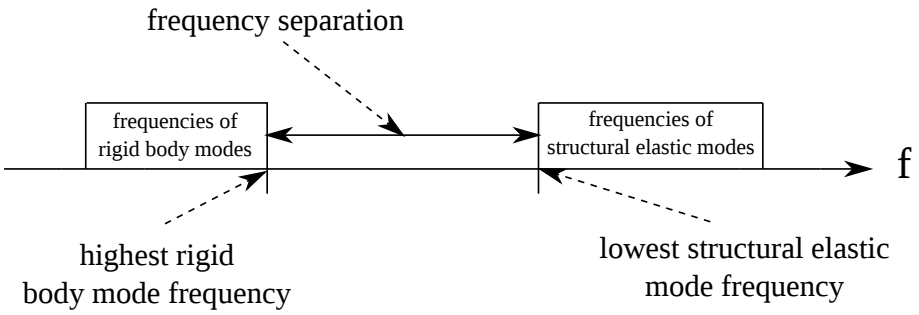

Figure 2.15: Separation of low frequency rigid body modes and high frequency elastic modes

For very elastic configurations (e.g. high aspect ratio configurations using low-density materials like composites), the separation of frequencies is not given any more. As a result, the higher frequencies of the rigid body modes overlap with the lower frequencies of the elastic modes and the notch filter is not working accurately any more. In that case, controllers can command outputs leading to dangerous instabilities as flutter or limit cycle oscillations.

The main output of a FCS is given by commanded control surface deflections, such as aileron, elevator and rudder commands ξ_c, η_c and ζ_c. They define the movement of the control surfaces and thus provide control of the AC about all three axes. The digital control command u_c of the respective control surface is fed through an actuator model, which results in a realistic behaviour of a desired control surface deflection ξ, η or ζ (see Figure 2.16). A first order lag element may serve as a basic model of a hydraulic actuation system:

$$G = \frac{1}{1 + \tau s} \tag{2.97}$$

The time constant τ models the dynamics and inertia of the actuation system and depends on the selected actuator. For a more accurate representation of the physical reality and inertia effects, higher order models for actuation systems must be applied. A good example for mathematical actuator modelling is given in Joshi (2012).

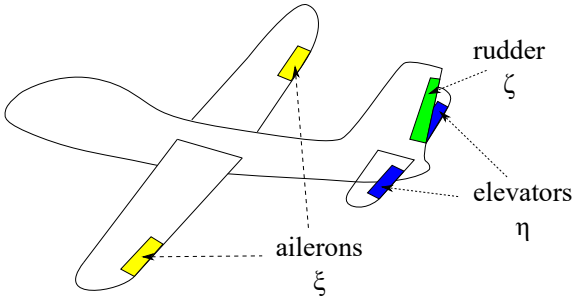

Figure 2.16: Primary control surfaces of an aircraft

The control laws, implemented in the controller concept, which provide the input for the actuator and thus for the actual control surface deflection, can be of arbitrary complexity. However, some basic controllers can be found in every FCS and shall be named here for the sake of completeness. Longitudinal control laws usually apply pitch dampers, pitch attitude and longitudinal trim controllers, whereas lateral control laws implement yaw dampers, turn and roll attitude controllers:

- Basic controllers for longitudinal movement:
  - Pitch damping controller
  - Pitch attitude controller
  - Longitudinal trim controller
- Basic controllers for lateral movement:
  - Yaw damping controller
  - Turn controller
  - Roll attitude controller

MDO-relevant aspects of controllers in the time domain

Controller design aims to find optimal control systems that manipulate a system to achieve a desired behaviour. Design activities are performed in the frequency and not the time domain, first. The implementation on a respective hardware is done later with controllers operating in the discrete time domain. Simulation of the aircraft system means calculation of the discrete responses on arbitrary input signals and is therefore performed in the discrete time domain, as well. Airframe design encountering such arbitrary inputs also means calculating discrete responses. A pre-known disturbance like a gust excitation could be transformed into the

frequency domain together with the respective plant. The frequency response resulting from a frequency-based solution process could then be transformed back to the time domain through inversion. An arbitrary, time-discrete command can not be represented with this approach, if it is not pre-known. Therefore, working with a time-discrete representation of control laws brings high flexibility for integrated design. An example where a pre-known control surface deflection is manipulated and transfered forth and back in an optimisation frame is given in Nussbächer & Petersson (2023).

A continuous time-dynamic system model can be transformed to a discrete form through discretisation. Different methods applying e.g. zero order hold or Tustin-transformation can be used for this purpose. The main methodical component coming with this discretisation is given through the sample time T. A signal is sampled for discrete time steps t_i, which means that only for these time steps system outputs are determined. With regard to integrated design, where multiple disciplines are interacting with each other, this poses a major requirement to the respective solution sequences, as it must be assured that the same sampling rates are used through all disciplines. For further reading on integrated airframe design and the topic of time domain simulation the works Karpel et al. (2004), Karpel et al. (2006), Hofstee et al. (2003) and Azoulay & Karpel (2006) are recommended.

Controllers and subcontrollers

The understanding of the difference between frequency and time domain controller analysis is important for handling a FCS in MDO tool-chains. Another crucial point, the MDO engineer must be aware of, lies in the fact that a high level flight control system (modelled in the frequency-, the continuous time or the discrete time domain) consists of submodels and subcontrollers. Usually, control laws are designed through multiple cascaded loops (Thümmel et al. (2005)). A high ranking controller is often contained within an even higher ranking unit and contains lower ranking control laws, itself (see Figure 2.17).

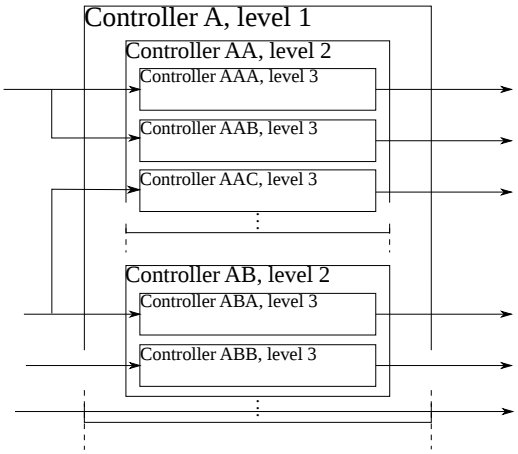

Figure 2.17: Lower ranking controller units as part of higher ranking controller units

Higher ranking units in a FCS are e.g. the longitudinal and lateral control laws, which among others support the pilot during flight in path and speed tracking. The control laws assure that lower order tasks as e.g. path stabilisation or improving damping of flight mechanical modes (e.g. short period or phugoid) can be carried out without active input of the pilot through respective subcontrollers. The subcontrollers thus relief the pilot workload. Pitch and yaw dampers can be named as common examples for such base controllers.

As a common subcomponent of a bigger longitudinal control law, only the pitch damper shall be highlighted, briefly. For reasons of safety, pitch control laws are formulated as uncomplex as possible (see Brockhaus et al. (2011)). The main output from the AC-plant is the pitch rate q, which is fed back to the elevator η (compare Figure 2.18).

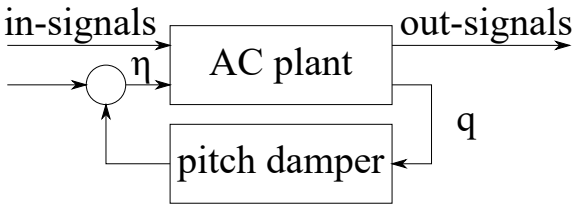

Figure 2.18: Pitch damper as basic flight control system given as a subcontroller

The desired pitch rate of a pitch controller is set to a value of $w = w^{(i)} = 0$ which means that it does not account for an actual set point. The resulting discrete control error for the time step t_i directly results from the sampled pitch rate $q^{(i)}$, at a given time step t_i:

$$e^{(i)} = w - q^{(i)}$$
$$e^{(i)} = -q^{(i)}$$

The design assures that the aircraft does not unintentionally pitch up or down. Respective undesired movements (induced e.g. through external disturbances) are damped through the pitch control system.

From the discrete control point of view, the pitch controller is given as a function, sampling the pitch rate for a given sample rate T, amplifying this signal through the gain factor $k_{\eta q}$ (resulting from the previous controller design) and feeding it back as an elevator command η_c:

$$\eta_c^{(i)} = -k_{q\eta} q^{(i)} \tag{2.98}$$

The sign of the gain factor $k_{q\eta}$ in equation (2.98) must match the desired implementation (positive or negative gain). The resulting command is then processed through a separate discrete actuator model, resulting in an actual elevator deflection η which can be used as an input for further (e.g. aeroelastic) studies.

MDO-relevant AC-assessment criteria

Along with the demand of good pitch damping, further flight mechanical demands may be posed to the aircraft system. Aircraft performance is often assessed by quantities like manoeuvrability or the thrust to weight ratio. Another important criterion is given when demanding that a specific bank to bank turn must be fulfilled within a respective time. As an example it may be assured that a bank to bank turn from $+30°$ to $-30°$ must be accomplished within $10s$. Such requirements apply to the overall aircraft system rather than to the FCS or the aerostructural design. Different resulting bank to bank slopes can be seen in Figure 2.19.

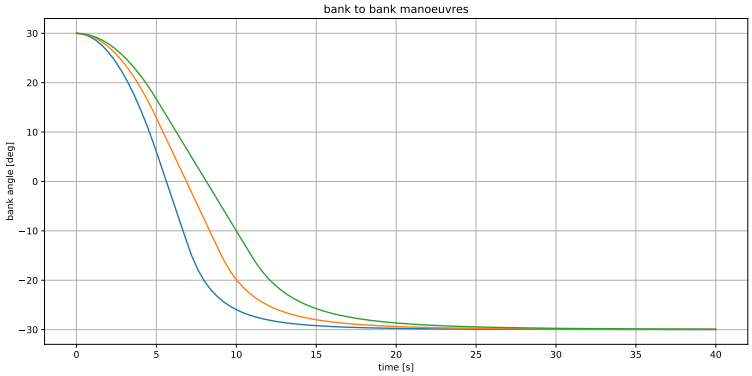

Figure 2.19: Bank to bank demand over time resulting from different roll rates

From the aeroservostructural design point of view this requirement can mainly be matched through the FCS design or the structural design. Either control surface deflections are commanded accordingly (within a feasible range) or the aircraft inertia is manipulated such that the desired degree of agility is reached.

Due to the high number of requirements posed to an aircraft system, the process of finding a design which fulfils all demands is highly complex. It is a process with a high potential for optimisation and automation. One mean which enables an optimal design while matching technical requirements in a multidisciplinary way is given through MDO.

2.4 Multidisciplinary Design Optimisation

The physical basics of aeroelasticity, structural dynamics and control theory were explained in the previous chapters. The missing ingredient enabling integrated design of airframe structures considering flight control demands is an algorithmic methodology of transferring and manipulating information between the different components. Numerical optimisation (or MDO in a wider sense) provides this capability. Its ideas, basic concepts and components are highlighted in this chapter.

When designing a new aircraft, the engineering fields described previously are commonly

treated separately and successively. The attempt to come up with a separate design from each discipline, necessitates one discipline to make assumptions concerning the respective other. Sometimes it is not possible to solve problems independently, which can best be seen at the example of aerostructural interaction, which motivates aeroelasticity as a proper discipline. If not a strong cooperation can be obtained between multiple design activities, it can not surprise that the best solutions from independently working subdisciplines have not much in common. This is not only valid for aeroelastic problems, but always when design engineers do not negotiate compromises between the dream designs of respective subdisciplines. In 1948 S.E. Sohler depicted this nicely in Sohler (1948), using drawings of C.W. Miller (compare Figure 2.20).

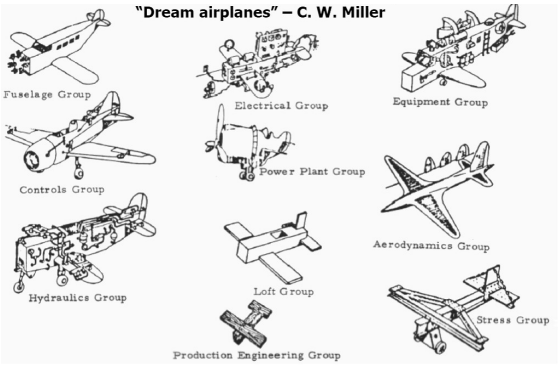

Figure 2.20: Dream airplanes collected and motivated from Sohler (1948)

The importance of integrated analyses for aeroelastic and aeroservoelastic problems enables the success of large aircraft projects. This could be shown at the example of the B-2 Bomber in Britt et al. (1999), Britt et al. (2000) and Winther et al. (1995).

The ultimate purpose of MDO is to find a good and feasible design, considering all disciplines involved in a given engineering problem. Thus, whenever multiple disciplines need to interact with each other, multidisciplinary designing should come into use. Such an integrated approach reliably leads to a solution incorporating a good tradeoff between all demands. For this purpose, modern automation and numerical optimisation methods are applied.

Numerical optimisers step through a given design space in an iterative way. For this purpose they use information available from previous steps, to make a decision for the next step. They can be categorised by the way they decide how to move through the design space:

- Stochastic optimisation algorithms:
  - Evolution strategies
  - Genetic algorithms
  - ...

- Deterministic optimisation algorithms:
  - 0^{th} order algorithms
  - 1^{st} order algorithms
  - 2^{nd} order algorithms

Stochastic algorithms use stochastic methods to examine the design space. Evolution algorithms (e.g. evolution strategies and genetic algorithms) are common representatives for this group. Their main advantages lie within the facts that they examine the whole design space, that they can easily handle discrete variables and that they need only few information of the underlying physical model. On the other hand they demand a relatively high number of evaluations of the system equations, which makes them very inefficient for large scale problems. Further, it is not guaranteed that they come up with the same optimal solution for two identical optimisation runs.

Deterministic algorithms always converge to the same final design from the same starting point. If only the system equations need to be evaluated, the method is of 0^{th} order. (Although not deterministic, stochastic algorithms can thus be considered as 0-order methods, as well.) Gradient based techniques demand further information on the given physical problem and are therefore higher order methods. If first order derivative expressions (Jacobi matrix) of the governing equations are considered during the optimisation, a 1^{st} order algorithm results. A 2^{nd} order algorithm is applied as soon as second order derivatives (Hessian matrix) of the governing equations come into effect.

With regard to large problems of industrial scale, which shall be treated within this thesis, deterministic and mainly gradient based algorithms shall come into use. Further discussions on optimisation shall therefore always be seen in the scope of applications with deterministic, gradient based methods.

2.4.1 Components and Process of Gradient Based Optimisation

A design optimisation task can be divided in three main components (see Eschenauer et al. (1990)). The **state model** evaluates the physical model. It considers physical inputs as cross sectional areas, angles of attack or control system gain values and provides system responses as displacements, stresses or aerodynamic loads (compare Chapters 2.1 - 2.3). The **optimisation algorithm** determines a new design based on gradient information, i.e. the information of how changes in certain inputs affect the desired outputs of the system to study. As an example, the optimisation algorithm "decides" if it is sensible to reinforce the aircraft wing through a thicker skin, based on the information that the wing root stresses would decrease, while the overall structural mass would increase. The decision must therefore be seen as rule-based. The interaction between the physical state model and the mathematical optimisation algorithm

is handled by the **optimisation model**. It considers physical responses from the state model and the mathematical representation for the optimiser. This step is performed in the evaluation model, consisting of the objective and criteria model, where responses are converted into objective and constraint function values. The optimisation model processes the physical information such that the optimiser can deal with it and transfers the current design from its mathematical representation, to enable system evaluations through the state model. This conversion between the physical and the mathematical representation is referred to as "transformation" and is covered in the design model. The three main components are represented as pillars in Figure 2.21. They can further be identified in the optimisation loop as depicted in Figure 2.22.

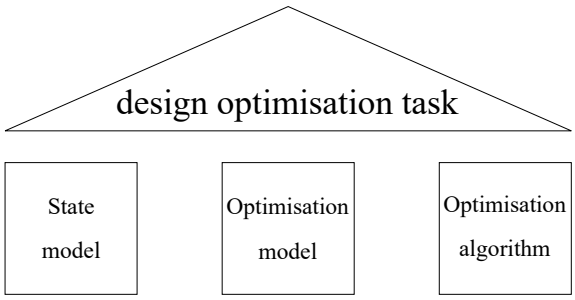

Figure 2.21: The three pillars applied in multidisciplinary design optimisation

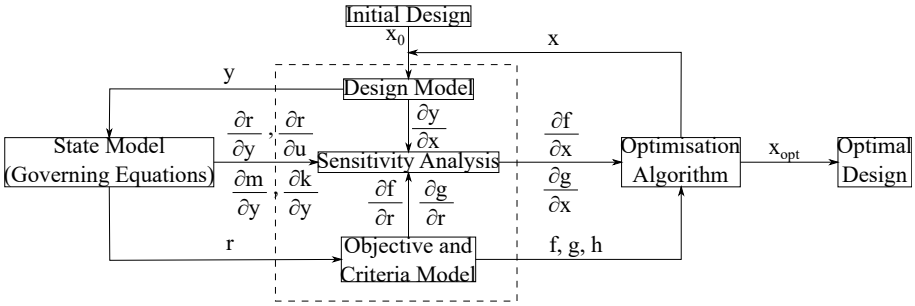

Figure 2.22: Classical design optimisation loop

2.4.2 Formulation of a Multidisciplinary Design Optimisation Problem

Modern optimisation tools make it possible to apply numerical optimisers without the need to understand what is actually happening behind the scenes. However, without good knowledge on the model and the underlying, physical equations, the results determined by an optimiser lose their engineering value. Therefore, the proper definition of the optimisation problem is a crucial, first step, whenever MDO is applied.

The main ingredients to describe an optimisation problem are the governing equations, the objective model, the design model and the criteria model.

The physical base of an optimisation problem is given by the analysis model. It describes the

physical problem to be studied through the governing equations in a mathematical form. A numerical optimisation algorithm uses these equations to evaluate a given design according to certain demands. The information of how the system outputs depend on respective inputs is therefore of high importance.

The governing equations provide the interface to the quantity which shall be optimised. In optimising AC structures, usually the GFEM primary mass is minimised. Range or performance characteristics can further be thought of in aircraft design. The mathematical formulation of this quantity is called the objective function f.

f shall be described through variables which represent the given design. It must therefore depend on a set of physical state variables s. In structural sizing problems s could be a set of cross sectional areas of beam elements or thickness values of thin plates, whose variation directly affect the structural mass. Such state variables are grouped as functions in the mathematical design variables x:

$$x = x(s) \tag{2.99}$$

Design variables are usually formulated in a normalised form. A common approach is to relate the current state variable s to its initial value s_0, i.e. the value of the initial design, leading to

$$x = \frac{s}{s_0} \tag{2.100}$$

The state variables must be restricted to a physically sensible range, by defining lower and upper allowable values s_l and s_u. An optimal solution is then searched in this definition domain. This restriction is known as design variable gage or side constraint.

$$s_l \leq s \leq s_u \tag{2.101}$$

$$x_l \leq x \leq x_u \tag{2.102}$$

The objective function then depends on the design variables:

$$f = f(x) \tag{2.103}$$

For purely linear problems, the objective function would result in a combination of lower and upper values for s. Usually further restrictions need to be considered in a multidisciplinary optimisation problem, however. Internal correlations, described through the governing equations are often taken into account to evaluate such restrictions. Structural components must be designed such that they are able to carry externally applied loads without failing, a wing must be able to provide a minimum amount of lift to carry a certain payload. An important value to quantify such demands is the reserve factor rf, which is defined as the fraction between an

allowable and an applied value:

$$rf = \frac{allowable}{applied} \tag{2.104}$$

As long as the reserve factor takes a value $rf > 1$, the applied value does not exceed the given allowable value and the underlying design can be considered as a feasible design.

Such demands are mathematically best formulated as numerical constraints g.

$$g = 1 - \frac{1}{rf} \tag{2.105}$$

With formulation (2.105), a design can be checked for feasibility by the numerical constraint function value itself:

$$g \geq 0 \leftrightarrow \text{feasible design} \tag{2.106}$$

$$g < 0 \leftrightarrow \text{infeasible design} \tag{2.107}$$

As the reserve factor explicitly or implicitly depends on the design variables ($rf = rf(x)$), changing the design affects the constraint functions over the governing equations.

An optimisation algorithm uses the constraint function g as an inequality constraint. A design is feasible as long as $g \geq 0$. However, constraints can be formulated as equality constraints h, as well. In that case the algorithm is forced to find a design which exactly fulfils a given demand. Finding a perfectly trimmed flight state without a resulting mathematical residuum could be one example. As equality constraints are numerically difficult to handle, they are often re-formulated through a narrow range of inequality constraints.

Putting all described ingredients together leads to the formulation of an optimisation problem:

> Find a design x, which results in an optimal (minimal or maximal) value of an objective function f, while a number of constraints g_i are fulfilled.

$$\underset{x}{opt}\{f(x)|g_i(x) \geq 0, i \in [1,p]\} \tag{2.108}$$

Here, f was considered as a scalar function. Then, the optimisation problem is called a "single objective problem". If more than one objective shall be optimised, one has to deal with a "multi-objective optimisation problem". One approach to tackle multi-objective optimisation problems is to re-formulate f as a weighted sum of the single objectives. A tradeoff between the various objectives is found as a solution, then. The result will, however, always depend on the selection on the weighting factors in the objective formulation.

2.4.3 Numerical Solvers and Optimisation Algorithms

The contribution of the optimisation algorithm in the optimisation loop lies in the determination and suggestion of new designs. Decisions are taken on the base of objective and constraint function evaluations. Gradient based methods further consider gradient information by means of the Jacobi matrix (first order derivatives) and/or the Hessian matrix (second order derivatives).

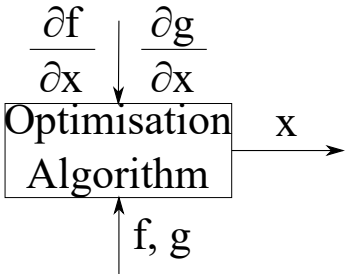

Figure 2.23: Inputs and outputs of the optimisation algorithms

A general optimisation run will start with the numerical assessment of an initial design x_0. The initial objective function value $f(x_0)$ helps to get an idea of the current design, the respective constraint functions $g(x_0)$ enable to decide if it is feasible or not. The gradients contain the information, how strong changes in the design variables affect the objective and constraint functions. They must therefore be considered as the primary decision drivers of gradient based algorithms. The outcomes of the optimisation model are then passed to the actual, numerical algorithm, which determines a new design. This step is followed by the re-assessment in the optimisation model and the re-calculation of objective, constraint and gradient values, which results in an iterative process as depicted in Figure 2.22.

The process is executed as long as the necessary stopping criteria are not fulfilled. Common criteria used to stop an optimisation algorithm formulate as follows:

- A predefined maximum number of iterations is reached.
- Design and objective function values do not change more than a predefined value between two iterations.
- Advanced criteria considering both objective and constraint gradients (e.g. Karush-Kuhn-Tucker) allow to break the iteration cycle.

The value of x after a stop criterion is reached is considered as an optimal design. It has to be kept in mind, that the optimal design x_{opt} is the output of the optimisation algorithm which must not necessarily be the overall global optimum of the problem. Optimisation results must always be interpreted within this context.

In structural aircraft design tasks usually a very high number of constraints needs to be re-

spected. The number of design variables may be of the moderate size of some 10^2 to 10^3 design variables. The criteria model, however, easily considers 10^5 or over 10^6 constraints, for overall airframe structural sizing activities, as it must be assured that all structural components resist the external loading with an accurate reserve factor. This is especially true with regard to modern composite materials, which are made of multiple layers, where each might be constrained individually (depending on the applied failure criteria). Although in practice by far not all of the available constraints will be violated in the optimisation iterations, high constraint-numbers pose a main issue for lots of applications dealing with optimisation. An optimiser must therefore be able to handle high numbers of constraints with a reasonable amount of computational effort. With algorithms that use active set strategies, it is possible to control and decide which constraints concretely influence the optimisation output. The explicit application of active set implementations can therefore reduce numerical costs. From the range of available algorithms three were pre-selected for usage in this work:

- Sequential Linear Programming (SLP): Sequential linear programming is an optimisation method, which works robust and converges in few iterations for common sizing problems. It is very efficient for high numbers of design variables and active constraints. In applications with non-linearities and where only few constraints need to be considered, SLP might struggle during the optimisation-finding process. Information and helpful examples on quadratic programming can be found e.g. in Rao (2009).
- Non-Linear Programming with Quadratic Line Search (NLPQL):

  NLPQL is based on recursive or sequential quadratic programming (SQP/RQP), which work well for problems of moderate size of hundreds of design variables. A high accuracy of the found optimum results from the second order convergence property within the algorithm. It integrates an active set strategy, by deciding which gradients shall be taken into account for large problems. NLPQL is a modern and efficient code, which enables internal restarts during the sizing process, as well. Further information can be found in Schittkowski (1986). For the sake of completeness, the NLPIP algorithm, which extends the NLPQL code by an interior point method, shall be mentioned. Detailed descriptions are given in Sachsenberg & Schittkowski (2013) or Sachsenberg & Schittkowski (2015).
- Method of Moving Asymptotes (MMA): The method of moving asymptotes approximates the inverse of the second order Hessian matrix of optimisation properties. Known from engineering experience, MMA provides good starting designs for further activities. Especially for small and moderate sized tasks, it is often the optimisation method of choice. Svanberg (1987) can be referred to for further insights in the algorithmic basics.

2.4.4 Gradients and Sensitivity Analysis

The main ingredient of gradient based algorithms is the sensitivity information determined from mainly the governing equations. Here, it shall not be differed between the terms "gradients" and "sensitivities". The gradient based optimisation algorithm needs the gradient of the objective function ∇f and the gradients of the constraint functions ∇g w.r.t. the mathematical design variables x (compare Figure 2.23).

Within the sensitivity analysis, the gradient information of the design model, the state model (governing equations) and the evaluation model must be brought together. Taking the constraint gradients $\frac{dg}{dx}$ as an example, from a programming point of view it is sensible to formulate the gradients as follows:

$$\frac{dg}{dx} = \frac{\partial g}{\partial x} + \frac{\partial g}{\partial u}\frac{du}{dx} \tag{2.109}$$

The first summand represents the explicit dependency of the constraint g w.r.t. the design variable x, whereas the second summand holds the remaining implicit dependency. The latter results from the fact that varying the design variables might not only change g directly but indirectly over a change in the displacement field u as well. This inconspicuous equation hides many nested dependencies, which must be properly resolved by the optimisation engineer and programmer to enable a correct solution sequence for the optimisation algorithm.

The complexity of this can be demonstrated at the example of the clamped cantilever beam with the initial cross sectional area A_0, the initial length l_0 and the elastic modulus E (see Figure 2.6 in Chapter 2.1.2 on structural mechanics). The displacement u under normal tension force N results analytically in the axial stress σ and contributes to a constraint function g (formulated with an allowable stress value σ_{all}) as

$$\sigma = E\epsilon = \frac{Eu}{l_0} \tag{2.110}$$

$$u = \frac{Nl_0}{EA} \tag{2.111}$$

$$\begin{aligned} g &= 1 - \frac{\sigma}{\sigma_{all}} = \\ &= 1 - \frac{E}{\sigma_{all} l_0} \cdot u \end{aligned} \tag{2.112}$$

The design variable x is selected such that it scales the cross sectional area A_0:

$$A = A_0 x \tag{2.113}$$

Equation (2.112) shows that in this case, no explicit dependency of the constraint g w.r.t. the

design variables x applies.

$$\frac{\partial g}{\partial x} = 0 \tag{2.114}$$

The displacement, however provides an implicit contribution of the design variable to the constraint gradient over the displacement:

$$\frac{\partial g}{\partial u} = -\frac{E}{\sigma_{all} l_0} \tag{2.115}$$

$$\frac{du}{dx} = -\frac{N l_0}{E A_0} \frac{1}{x^2} \tag{2.116}$$

Merging equations (2.114), (2.115) and (2.116) finally results in the desired analytical gradient of the constraint function for the given problem, as formulated in equation (2.109). The procedure to determine gradients analytically must be performed and subsequently implemented individually for every constraint.

Aside of this manual, analytic way to receive gradients for the optimisation algorithm, another possibility is given by finite differences. As soon as a purely numerical analysis provides system responses contributing directly to g, $\frac{dg}{dx}$ can easily be approximated using numerical gradients:

$$\frac{dg}{dx} \approx \frac{\Delta g}{\Delta x} \tag{2.117}$$

Commonly, the approximation is realised using a forward difference step

$$\frac{\Delta g}{\Delta x} = \frac{g(x+h) - g(x)}{\Delta x} \tag{2.118}$$

or a backward difference step

$$\frac{\Delta g}{\Delta x} = \frac{g(x) - g(x-h)}{\Delta x} \tag{2.119}$$

While numerical gradients can be realised easily, their application brings various problems. Their first, major problem is the determination of a proper step size Δx. A coarse discretisation through a large Δx results in a high truncation error. The desire to minimise this error by choosing a very small Δx, however, can lead to subtractive cancellation and machine round-off errors. This is called the "step size dilemma". Figure 2.24 shows the influence of the step size/perturbation step $\Delta x = h$ on the relative error, which results from using numerical gradients compared to the analytical solution of a given, analytical function. One common way to solve the step size problem is given through complex step differentiation:

$$\frac{dg}{dx} \approx \frac{Im[g(x+ih)]}{h} \tag{2.120}$$

Differentiation through complex step demands some programming effort as real-valued quantities need to be transferred into the complex regime (see Martins et al. (2003)). The numerical perturbation h takes place in the imaginary part of the complex plane.

The second main problem of numerical gradients is the fact that the full gradient information for "n" design variables demands "n+1" evaluations of the system equations. The resulting high computational effort can not be avoided and must necessarily be accepted if numerical gradients shall be used and analytical gradients are not available.

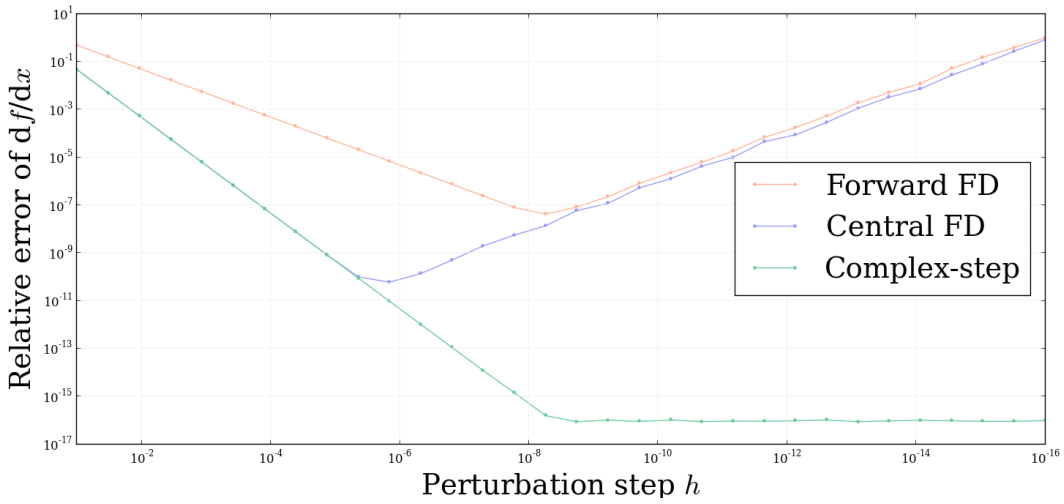

Figure 2.24: Step size dilemma of optimisation using numerical gradients

3 Modelling Components of Aeroservoelastic Airframe Design Optimisation

For solving aeroservoelastic design optimisation problems, it must be explained how models of the subdisciplines can be generated and how the models finally contribute in a coupled process. Here, aeroelastic approaches are applied to provide loads (Chapter 3.1), structural dynamic modelling is used to determine structural and flight mechanical system responses (Chapter 3.2), flight control systems calculate control surface deflections (Chapter 3.3) and optimisation algorithms are introduced, to automate the assessment of different designs and the process of finding better ones (Chapter 3.4). Proper modelling of the isolated, later embedded components defines the success of the overall process. The crucial point is to work with as much high-fidelity as necessary, and with as much low-fidelity as possible, in every subdiscipline. Limitations and possibilities of the respectively chosen methods shall be named in Chapter 3, as well. With the modelling basics introduced in this chapter, a method coupling the involved tools and processes can then be described.

The main numerical tool capturing the integrated design approach used in this thesis is the AIRBUS in-house multidisciplinary analysis and optimisation solver LAGRANGE. Originally designed as a structural optimisation code, its main strength is given through the implementation of fully analytical gradient information from various disciplines. Various external tools provide inputs for LAGRANGE, which handles the interactions between all tool-components. The tool was presented in various articles over the last decades. Representative works are e.g. Zotemantel (1992), Krammer (1992), Daoud et al. (2015) or Deinert et al. (2013*a*).

Targeting the development of an integrated design process considering flight control system demands, Chapter 2 formulated the physical basics, which shall be implemented through respective methods and tools now in Chapter 3. Later, in Chapter 4, the separate components are merged into a final process. This chapter contributes to the solution of the motivating problems and to reaching the objectives of the work at hands by

- describing the modelling components of the implemented direct method of aeroelasticity,
- describing the enhancement of the solver for structural dynamics through a damping model,
- explaining an implemented load enveloping capability,
- the identification of signal interfaces from the FCS.

3.1 Aeroelastic Modelling

For this work, both the iterative, optimisation based and the direct aeroelastic solution possibility (see discussion in Chapter 2.1.4) were available for studies on flexible, high aspect ratio configurations. They are very similar in the way of application, as the modelling bases

of the aerodynamic, the structural and the interconnection model are the same. These three components are presented, from an application oriented side in the following. The logic of their interaction is highlighted, what as well prepares their integration into an integrated framework. Special focus will be placed on the direct method. It must be noted, that the aeroelastic aspects presented in the following, are based on the approach of MSC Nastran. More information on the modelling side or the composition of respective matrices can be found in Rodden & Johnson (2004).

Aeroelastic modelling, as described in the following, is the key to enable designing with aeroservoelastic constraints.

3.1.1 Aerodynamic Modelling

The physical basics of aerodynamics were mathematically described in Chapter 2.1.1. The modelling components of a chosen VLM lead to the necessary matrices and vectors, now. Main component of the aero-model is the aerodynamic mesh, which discretises surfaces into panels. The panels are subdivided in boxes (see Figures 3.1 and 3.2). Each box hosts a horseshoe vortex, what enables predictions of resulting forces and moments.

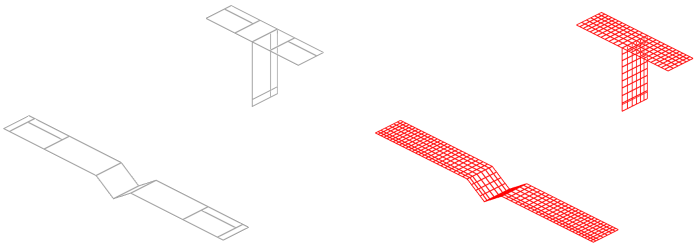

(a) Panels (b) Boxes

Figure 3.1: Aerodynamic panels and boxes of an AC model

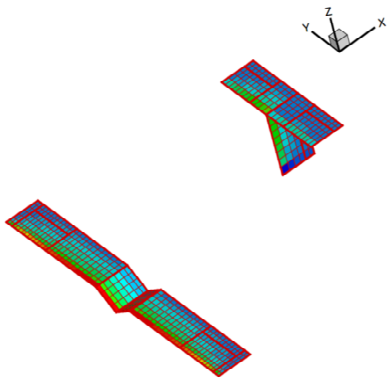

Figure 3.2: Lift coefficients of a generic model resulting from AIC matrix and local 1°-angle

The AIRBUS tool DESCARTES generates aerodynamic meshes, based on parametrised rep-

resentations of aircraft models. The CPACS, developed at the Deutsches Zentrum für Luft und Raumfahrt (DLR), is used in DESCARTES for that purpose. It provides both mesh inputs for LAGRANGE and for an external in-house aerodynamic solver tool, which numerically calculates the inverse of the AIC matrix A_{jj}^{-1}. The latter is an important component in the calculation of the lift coefficients. Figure 3.2 shows the lift coefficient distribution which results from the local lift coefficient derivative $C_{L\alpha} = \frac{\partial C_L}{\partial \alpha}$ multiplied with an angle of $\alpha_{loc} = 1^\circ$ for a generic model.

The solver imports the numerical A_{jj}^{-1} in order to process further intermediate matrices. The geometric information, contained in the aerodynamic mesh inputs are used to generate the integration and differentiation matrices S_{kj}, D_{jk} and D_{jx}. Numerically, the S_{kj} matrix is built as a sparse rectangular matrix with non-zero entries being the geometrical areas a_j of the aerodynamic boxes. D_{jk} and D_{jx} are rectangular selection matrices (i.e. their non-zero values are mainly 1). As the concrete matrices depend on the given problem, only examples to get an idea of their structures shall be given, here:

$$S_{kj} = \begin{bmatrix} a_1 & 0 & 0 & 0 & \dots & 0 \\ 0 & 0 & 0 & 0 & & 0 \\ 0 & a_2 & 0 & 0 & & 0 \\ 0 & 0 & 0 & 0 & & 0 \\ \vdots & & & & \ddots & \vdots \\ 0 & 0 & 0 & 0 & \dots & 0 \end{bmatrix} \qquad D_{jk} = \begin{bmatrix} 1 & 0 & 0 & 0 & \dots & 0 \\ 0 & 0 & 1 & 0 & & 0 \\ 0 & 0 & 0 & 0 & & 0 \\ 0 & 0 & 0 & 0 & & 0 \\ \vdots & & & & \ddots & \vdots \\ 0 & 0 & 0 & 0 & \dots & 0 \end{bmatrix} \qquad D_{jx} = \begin{bmatrix} 1 & 0 \\ 1 & 0 \\ \vdots & \vdots \\ 1 & 0 \\ 1 & 1 \\ 1 & 1 \\ \vdots & \vdots \\ 1 & 1 \end{bmatrix}$$

The index j iterates over the boxes of the aerodynamic mesh and ranges in $j \in [1, n_{boxes}]$. k on the other hand refers to both the quarter chord line and the collocation point of each box and therefore takes the values $k \in [1, 2 \cdot n_{boxes}]$. Multiplication according to equation (2.23) results in Q_{kk} (and Q_{kx}), for which sparsity representations can be found in the Appendix. Due to the given matrix structure, using sparse matrix algorithms is possible and can thus enable a very efficient numerical calculation.

The limitations and possibilities coming with VLM modelling shall be summarised in the following. In the case of VLM a main limit is given by the fact that it does not directly support the calculation of drag terms. As a result, those load parts can not be covered in a respective analysis for turbulent aircraft components like spoilers. Lattice methods are valid only for small angles of attack, what poses another limitation. This is a result of the assumption of linearity, represented mathematically through the linear equation system (2.16), as well. Lift distribu-

tions for high angles of attack will therefore not be accurate. Another key problem of the VLM is presented by the fact that it does not provide aerodynamic damping terms. This limitation is closely connected with the drag issue. Especially in this work, this is problematic as transient analyses must be carried out, due to the integration of time-discrete control laws. In transient analyses, a damping model is an essential component in order to model a physically sensible behaviour, however.

The capabilities of fast model generation and fast numerical result calculation must be named as important advantages. Particularly with a view on integrated designing, the possibility to work with parametrised models enables quick assessments of multiple use cases. This is of main interest for conceptual aircraft design studies. The aerodynamic modelling approach provides reliable results for quasi-steady flow regimes and small flow angles. While drag parts of aerodynamic loads can not be covered easily, the lift part is assessed accurately for the assumptions made in this thesis. Another main advantage of the presented method is given by the numerical formulation of the underlying equations of VLM. The applied tool can easily be substituted with similar tools providing AIC-matrices. That way, respective advantages of different codes can directly be exploited without bigger programming effort.

The main limits and possibilities of VLM-tools, with regard to this work, summarise as follows:

- − Only lift, no drag components (e.g. for roll spoilers) can be modelled.
- − Range of validity limited to small angles.
- − No aerodynamic damping coefficients.
- \+ Fast, parameter-based aerodynamic model generation and result calculation through integrated modelling.
- \+ Reliable lift results for slow manoeuvres with assumption of quasi-steadiness.
- \+ Easy substitution with similar tools.

To finish the presentation on aerodynamic modelling, a look back to the governing equations shall be taken. With regard to the aeroelastic equation (2.58), the aerodynamic model contributes by providing forces and moments P_k and P_{kx} for given translational and rotational structural deformations u_k and deflections u_x on the aerodynamic mesh. The physical in- and outputs of aerodynamics are visualised in Figure 3.3.

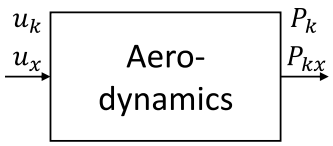

Figure 3.3: The aerodynamic component of an aeroelastic analysis

3.1.2 Structure Mechanical Modelling

To assess the elasticity of an aircraft design, advanced structural models must be developed and applied. The finite element method is state of the art in this context. Fundamentals were explained in a mathematical way in a proper section in Chapter 2.1.2. For its practical application some common modelling aspects must be known.

Focus shall be placed on linear finite element models, only. Structural non-linearity necessitated non-linear element formulations. With regard to the phase of early structural design, the application of such formulations is usually not sensible. As for the aerodynamic model, the mesh is of main importance and its creation is a time-consuming task.

Numerically the outcome of structural modelling is the global stiffness matrix K consisting of the respective matrix entries K_{gg} (sparsity representations can be found in the Appendix).

The selection of available finite elements depends on the physical effect that they shall represent. Not only the geometrical element formulation, but a sensible property and material model must be included accordingly, with the finite element model. Wing skins, ribs and spars or the outer layers of the fuselage of an aircraft are mostly analysed with isotropic or orthotropic shell elements (compare Figure 3.4). Stringers or spar caps, are examples of components that are usually modelled through finite bar or beam elements.

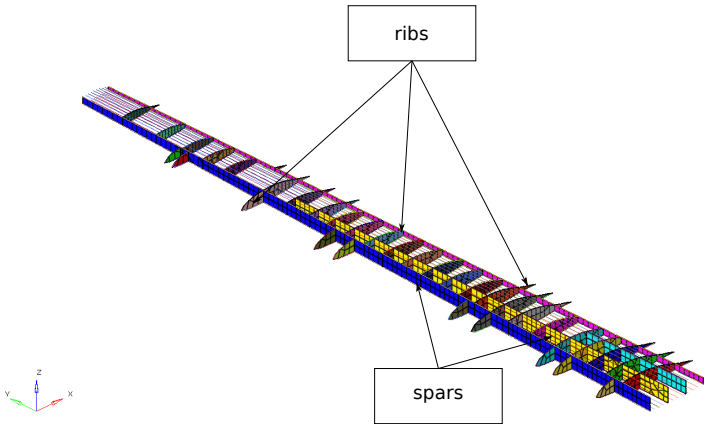

Figure 3.4: Common FEM modelling components in an AC wing

In practice, mainly one-dimensional elements with two nodes (rod-, bar- or beam-elements) and two-dimensional elements with three or four nodes (tria- or quad-elements) come into use. In some applications three-dimensional volume-elements are applied in structural modelling. Of major importance for a successful design are lightweight construction methods. For each component special methodologies were established resulting from the experienced load conditions. Wing spars experience concentrated shear loads, e.g. from engine supports or landing gear mounting. Further, their design respects the mechanical effects of fuel sloshing or a pressurised fuselage (in the centre wing area). Wing ribs are intended for the stabilisation

of wing surface panels. They redistribute loads and are as well sized from rib crushing loads or fuel sloshing. The fuselage skin mainly carries cabin pressure and transfers fuselage shear loads. Frames and bulkheads provide stiffness to guarantee the stability in the fuselage. The above is only a brief overview on some AC components and more details on construction methods can be found in Niu (2011).

The tool DESCARTES can be used as well to rapidly create FEM-models, which are especially valuable for early design phases. The generated model can be evaluated with LAGRANGE directly. For this purpose it parses the structural mesh exported by DESCARTES and calculates the relevant elastic matrices (K_{gg}), and the corresponding reduced matrices according to the respective boundary conditions. The structural design experiences forces and moments. Those can be applied directly within the solver through internal calculations (self-sufficient force and moment determination) or as pre-calculated loads from external sources (external loads process). The optimisation core of the tool needs to convert structural responses into engineering quantities evaluating the respective design. Therefore the code is designed such that reserve factors and constraint function values are directly available and no further post-processing calculations are necessary.

The following discussion on limitations and possibilities of structural modelling is restricted to the capabilities offered by DESCARTES and the realisation of the FEM in LAGRANGE. The finite element library in the structural solver offers a wide range of linear elements. This must be seen as a temporary, limiting factor of the finished design process, as physical effects resulting in very high deformations can not be evaluated, properly. The short time, which is needed to derive FEM-models, must be named as a strong benefit, offered through integrating DESCARTES and LAGRANGE into the structural design process to be derived in this work. The parametric base (CPACS) enables a fast model generation and bears the possibility to adapt quickly to changes, when necessary. Especially the mechanical analyses were tested and adapted countless times over the last decades. However, testing against commercial tools is unproblematic as the input is widely identical with the input for MSC Nastran. Therefore, most Nastran models can directly be evaluated with LAGRANGE and vice versa. In the past, the structural core of the solver was successively enhanced in various projects. The short development and integration time for new and advanced criteria based on mechanical calculations must be named as a key benefit, as well. This ongoing development process proved itself highly valuable for special demands arising in many aircraft projects.

Key limitations and possibilities from the described structural modelling component can be summarised as follows:

- $-$ Linear structural elements only; no possibility for non-linear structural analyses.
- $+$ Fast, parameter-based structural model generation and result calculation through inte-

grated modelling.

+ Frequently tested against other numerical tools.
+ High compatibility with commercial tools like MSC Nastran.
+ Ongoing enhancement of capabilities through constant development.

With regard to an integrated airframe design process, the structural model contributes to the aeroelastic equation (2.58) through providing translational and rotational deformations u_g for given structural loads P_g. This is indicated in Figure 3.5.

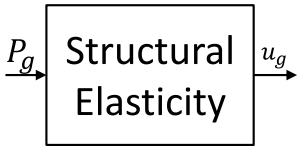

Figure 3.5: The structural component of an aeroelastic analysis

3.1.3 Modelling the Interconnection of Aerodynamics and Structural Mechanics

With an aerodynamic and a structural model being prepared, the corresponding aerodynamic loads and structural displacements must be brought together. Here, it is of high importance to transfer energy in a conservative way. Work is then dissipated only in an way that stems from actual, physical effects. Therefore the IPS method is used in this work, whose modelling aspects are highlighted below.

The main outcome of the spline model is the splining matrix G and its components (G_{kg} and G_{kg}^T, respectively). A spline always consists of a combination of structural nodes, which aerodynamic forces are applied to, and aerodynamic boxes, which structural displacements are transferred to. Usually, more aerodynamic boxes (referred to by the k-set) than structural nodes (referred over the DoFs in the g-set) should be selected for one spline. Otherwise the resulting spline shows oscillations and non-physical force distributions in order to match the requirements given by the underlying, elastic plate theory. The structural nodes and aerodynamic boxes must be selected both geometrically and physically sensible. When the aeroelastic interconnection in the wing shall be covered, mainly boxes and nodes of the wing must be used for the respective spline. Further, it is advised to select nodes from structural components which actually carry loads. Intersections of spars and ribs with the overlying wing skin are suggested, for example. As a result of this selection, the overall splining matrix is sparse. G_{kg} and G_{kg}^T come into use when the dense matrix Q_{kk} is transformed from the aerodynamic to the structural set: $Q_{gg} = G_{kg}^T \cdot Q_{kk} \cdot G_{kg}$. Sparsity representations of G_{kg}, G_{kg}^T and Q_{gg} can be found in the Appendix.

Depending on the way the aerodynamic mesh was created and the resulting boxes are numbered, aerodynamic boxes for the spline can be selected with comparatively low effort. With

a convenient numbering, only the first and the last index of the boxes must be specified from the aerodynamic side for a spline. The generation of sets grouping structural nodes is a more manual process. Although the selection can be automated through different approaches, it is still sensible to keep the engineer in the process, in order of keeping control over the modelled interconnection. The sets that group the boxes and nodes are parsed in LAGRANGE, which performs the actual calculation of the numerical matrices G_{kg} and G_{kg}^T, then. The IPS method converts both structural displacements u_g into aerodynamic displacements u_k and u_x and aerodynamic loads P_k and P_{kx} into structural loads P_g, as indicated in Figure 3.6.

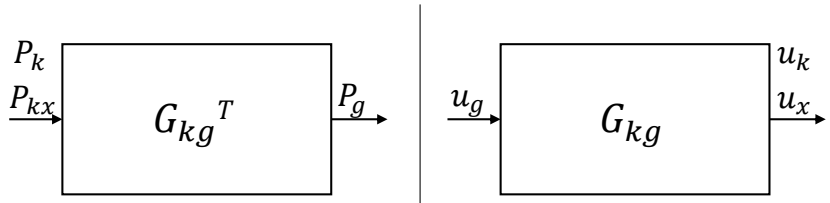

(a) G_{kg}^T - Converting aerodynamic to structural forces

(b) G_{kg} - Converting structural to aerodynamic displacements

Figure 3.6: The spline component of an aeroelastic analysis

For diagnostic purposes, information which allow the visualisation of the calculated spline are provided. As an example, the local AoA-distribution for both a rigid structure and an elastic structure can be visualised. Further, the resulting aerodynamic forces and moments can be studied with the LAGRANGE diagnostic output. Figures 3.7 - 3.9 give examples of a badly and a well modelled spline for a basic demonstrator model.

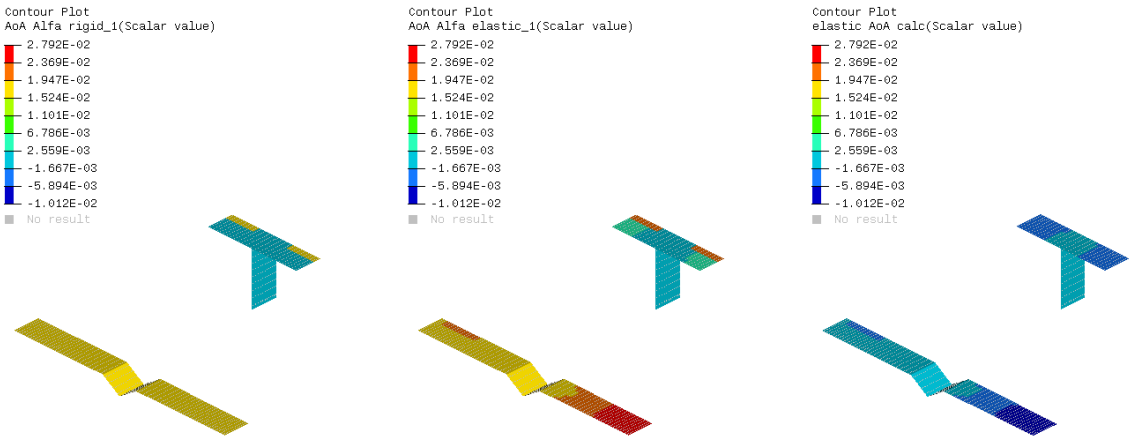

Figure 3.7: Angles of attack - Bad spline

In 3.7 and 3.9 (a) aerodynamic loads resulting from a unique AoA of $1°$ on the right wing are splined mainly on the two structural nodes showing the very high vertical forces ("bad spline"). A better spline is given for the left wing, where the aerodynamic loads are distributed to more

nodes attached to load carrying components. Figures 3.8 and 3.9 (b) show that the wing twist increases physically sensible in span-direction, when using a better spline model ("good spline").

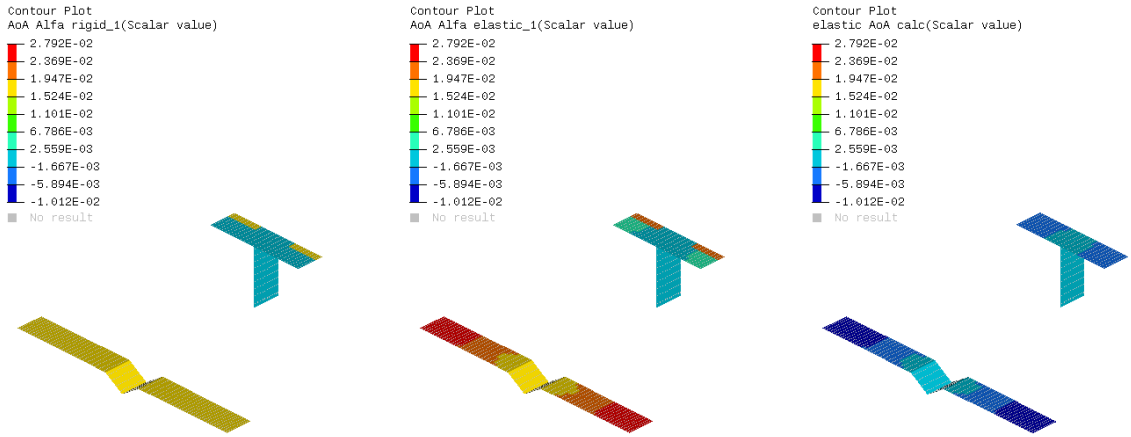

Figure 3.8: Angles of attack - Good spline

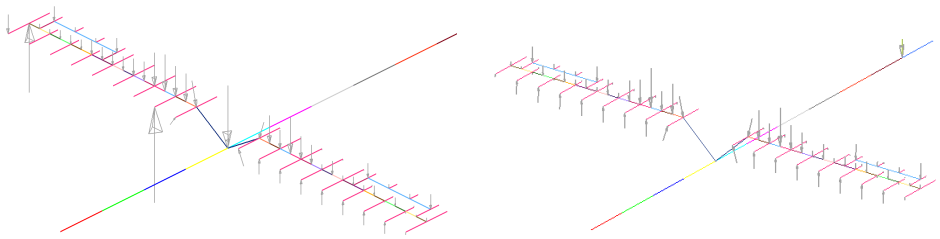

(a) Bad spline (b) Good spline

Figure 3.9: Splined forces

The integration of the selected splining method shows a number of possibilities and advantages, as well as limitations and disadvantages.

The method allows a conservative transition of aerodynamic loads and structural deformations. Energy remains in the system and is not dissipated through numerical effects. Further, the not automated step of choosing respective sets is supported through the parametric base of DESCARTES. The exported model contains valuable grouping information of structural components, which can be used during set-selection. The modelling effort is reduced through the method itself as the same model can be used for both forces and displacements. No difference needs to be made between an aerodynamic and a structural spline. It is highly applicable to design studies, where fast model generation is a must.

These points are summarised as follows:

- No fully automatic spline model generation.
- Danger of oscillating spline through bad nodes and boxes selection.

+ Physically sensible transition of both forces and displacements.
+ Spline modelling supported through parameter-base of integrated modelling.
+ Reduced modelling effort as the same spline can be used for forces and displacements.
+ High applicability as a fast method, both in generation and in computational time.

Figure 3.10 gives the schematic representation of the spline model to the aeroelastic component of the design process.

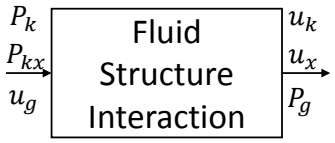

Figure 3.10: Fluid structure interaction in an aeroelastic analysis

3.1.4 Modelling Components of Direct Aeroelasticity

Besides the three main components (aerodynamic model, structural model and splining model) being available for a system evaluation, a clear formulation of the aeroelastic problem to be studied must be given. Appropriate DoFs contributing to the aerostructurally coupled problem must be defined, such that a unique solution is possible not only from a numerical, but from a physical point of view. The result of an aeroelastic analysis will always be a state of equilibrium, however, not necessarily in a steady way. Instead of claiming a given problem not to contain a solution, the numerical solver calculates load components that can not be brought into steady equilibrium and maintains them as resulting rigid body accelerations. The respective state is then considered aeroelastically trimmed by means of a dynamic equilibrium. It is the responsibility of the engineer to properly interpret the resulting outcome.

In this context, three main terms come into use. First a set of aeroelastic **trim DoFs** must be declared. The selection of respective DoFs depends on the problem to be studied. E.g., for a symmetric pitch up, at least the elevator is needed to properly adjust the angle of attack, such that the gravitational acceleration is trimmed out and no resulting pitch moment remains in the solution point. An asymmetric roll on the other hand will demand additional aileron deflection and if roll-yaw-coupling shall be considered, even the rudder deflection must be added to the set of trim DoFs. Pre-known components of the trim degrees of freedom are declared as **manoeuvre constraints**. When a steady, horizontally trimmed state shall be found, no acceleration and no resulting moment must remain. The respective accelerations can thus be pre-defined as manoeuvre constraints. The remaining DoFs shall be called the **trim variables** of the aeroelastic problem. The main target of the aeroelastic analysis is to determine their numerical values, such that the demands given through the manoeuvre constraints are met.

Numerically, the classification of trim variables and manoeuvre constraints define how the linear equation system must be solved. In other words, it re-orders the rows and columns of the underlying linear equation system. Where the declaration of trim DoFs and their classification into manoeuvre constraints and trim variables is intuitive for simple problems, it becomes more complex when more flight mechanical degrees of freedom are considered. Generally it must be assured that the physical problem is defined in such a way that trim variables are capable of balancing the manoeuvre constraints and no trim DoF remains unbalanced. If a rudder deflection was left over as a trim variable but no corresponding yaw acceleration was constrained, the respective trim problem must be considered as improperly defined. The resulting equation system does not contain a unique solution, then.

Besides the high importance of properly setting up the steady aeroelastic problem and its contributing degrees of freedom, an inertia relief model must be captured accordingly, as well. Therefore, representative structural DoFs need to be selected, which implicitly define the underlying mean axis coordinate system. Further, it is necessary to define hinge lines for respective control surfaces. While the orientation of the hinge line defines the sign of the resulting control surface deflection, its geometric position defines the amount of deflection applied for the given aerodynamic boxes, necessary to provide the desired loads. From an aeroelastic modelling point of view, it is of main importance, that the angular results for the control surfaces are interpreted according to the definition of the hinge line, only. With regard to an integration with flight controllers, it is advised to model hinge lines following a sensible standard. Following standards like DIN (1990) or ISO (1988) means that control surface deflections can be interpreted without the necessity to transfer them from one coordinate system into another. The flight mechanical convention for coordinate systems defines positive x from AC tail to nose, positive y from fuselage to the right wing and positive z downwards, accordingly. Control surface deflections and respective hinge lines can be modelled to match these definitions, resulting in the following relationships:

- A positive aileron deflection ξ means the right (starboard) aileron deflecting downwards, resulting in a negative roll moment. Right and left aileron are usually linked anti-symmetrically.
- A positive elevator deflection η means the elevator deflecting downwards, resulting in a negative pitch moment.
- A positive rudder deflection ζ means the rudder deflecting to the left side (port), resulting in a negative yaw moment.
- A spoiler deflection κ is always negative, resulting in a loss of lift force.

Keeping these conventions in mind helps with a consistent modelling of hinge lines. Usually the x-axis of a supplementary coordinate system is used to represent the hinge line.

Figure 3.11 gives an idea of control surface modelling according to a flight mechanical coordinate system orientation.

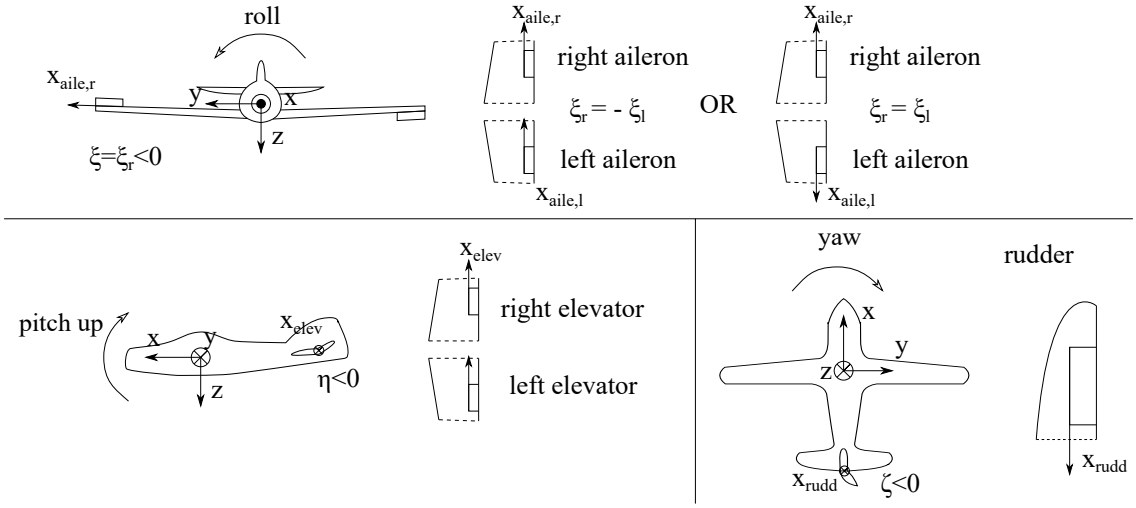

Figure 3.11: Control surface and hinge line definition

The properly modelled aeroelastic problem is read and processed with LAGRANGE. The input is converted into numerical matrices, which are brought together in a linear equation system. After the reduction of boundary conditions and condensation of the matrices to representative degrees of freedom, the equation system is re-ordered according to the problem formulation. The primary solution are the trim variables, which, together with the manoeuvre constraints, form the trim DoFs, which again are the base for further post-processing solution sequences. The resulting displacement field and both strains and stresses in the structural model can then be evaluated. These quantities are primary variables for assessing structural integrity through reserve factors rf and optimisation constraints g:

$$x \rightarrow u \rightarrow \epsilon, \sigma \rightarrow rf \rightarrow g$$

W.r.t. aeroservoelastic designing, the given analysis determines an initial state, on which further calculations can be based on, and provides forces and moments for given control surface deflections. Bringing together the three components aerodynamics, structural mechanics and fluid structure interaction leads to one aeroelastic block (Figure 3.12) contributing to the integrated solution of AC design.

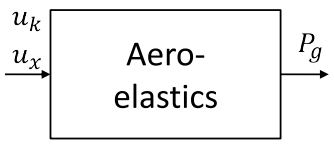

Figure 3.12: The aeroelastic component

3.2 Structure Dynamic Modelling

In order to realise designing with aeroservoelasticity in the loop, the results of an aeroelastic analysis must be processed to a flight control model. The dynamic behaviour of the mechanical structure must be captured, therefore. Which numerical components are needed for this purpose is described in this chapter.

The aeroelastic model provides forces and moments for given flight states, described through angles of attack, control surface deflections and rigid body accelerations. An explicit dynamic component is not given through this modelling approach.

The core of the transient solution is given through an appropriate dynamic solver. The Generalized Alpha Method used in this thesis can be seen as a generalisation of various numerical solution strategy approaches. The governing equation to solve in structural dynamics stated as

$$M \cdot \ddot{\vec{u}}(t) + D \cdot \dot{\vec{u}}(t) + K \cdot \vec{u}(t) = \vec{P}(t) \qquad \text{(2.62 revisited)}$$

The mass and stiffness matrices M and K are given through the structural model, the damping matrix D is derived as a linear combination of the two. The scaling factors α_1 and α_2 can be defined according to a desired damping behaviour.

An analytical solution of the system equations is only possible for academic problems. The practical approach to this problem is to numerically solve the equations for discrete time steps, only. Those time steps shall be defined such that they are distributed equidistantly over the time domain of interest. If an interaction with an external system (as a controller) applies, the temporal discretisation for the dynamic structural solver must match the sampling of the respective system. The sample frequency f and the sample time step T are linked through

$$f = \frac{1}{T} \qquad (3.1)$$

The solution sequence follows a pre-defined time slope of external excitations, which is processed during the LAGRANGE run. In this mode of operation all external influences must be known before the initiation of the solution process. The developed analyses in this work will use displacements, velocities and accelerations to deflect the structure at an initial time step, and will apply forces and moments in the following time steps. Three components are necessary to define a dynamic load case. First, the excitation must be distributed spatially. Loads must be applied to the relevant DoFs, therefore. Second, the time slope, which the loads shall follow over time, needs to be formulated. Third, delay times can be modelled, if necessary. Given loads are applied to the structure after the respective delay time, then. Further, a linear superposition of multiple dynamic load cases is possible. It can thus be studied how dynamic loads, which were first calculated individually, interact with each other when applied

simultaneously.

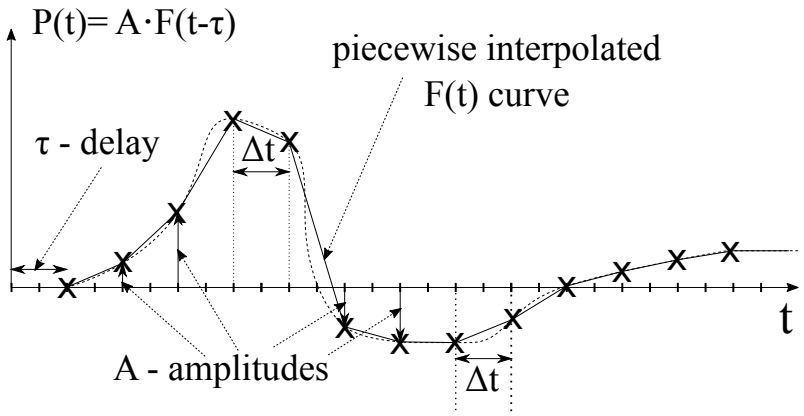

Figure 3.13: Dynamic load function modelling

The calculation of structural responses for a discrete time step depends on the preceding ones. Therefore, an initial state, where the transient solver can start from, must be given. For a purely structural analysis, all displacements, velocities and accelerations can be set to values of 0, first, such that the initial state is given through the unloaded FEM-model, itself. The initial condition, which is actually used by the dynamic solver, will result from an aeroelastic pre-analysis, then: All trim DoFs for the desired flight state are determined and the corresponding displacement field overwrites the initialised values of the unloaded FEM. The change in the displacement field describes the movement of the AC. In case no additional excitations and no external loading is applied, the solution calculated by the dynamic solver will result directly as keeping the given initial condition. As soon as this state is disturbed, respectively varying system responses will result.

Analyses of large models with millions of structural DoFs and a fine time discretisation, demanding to solve thousands of time steps, will produce huge amounts of data. The displacement u, velocity $\dot{u}$ and acceleration $\ddot{u}$ fields can be obtained for each structural DoF and for each time step. Further, strains ϵ and stresses σ, which are of main importance for mechanical evaluations, are available for each element and for each time step. Additionally, reserve factors rf and constraint function values g (usually based on stress and strain data), enabling an assessment of the design's integrity, are calculated for each time step. To handle this huge amount of data, it is sensible for both the engineer and the optimisation algorithm, to filter the quantities of interest. An enveloping capability is used for this purpose. For each time step t_j ($j = 1, ...m$), the n_{con} constraint function values are stored in the constraint vector g_j. Bringing together the vectors for all time steps, leads to the constraint matrix g_{ij}:

$$g_{ij} = [g_1, g_2, \dots g_m],\, i = 1, ...n_{con},\;\; j = 1, ...m \tag{3.2}$$

Of high interest are those time steps which lead to a violation of at least one of the n_{con} constraints by means of $g < 0$ (compare Figure 3.14). Based on the g value, the enveloping module detects these time steps, adds the respective constraint to the criteria model, saves the corresponding load and, in case, writes out the affected elements.

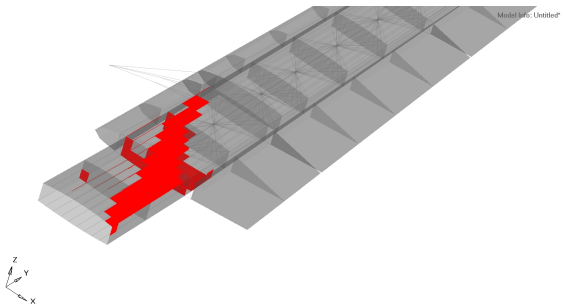

Figure 3.14: Critical elements detected through LAGRANGE enveloping

The settings of the enveloping module enable wider applications as described above. It is further possible to not only extract violated constraints, but to filter constraint values with minimal value or to enlarge the criteria model and the set of design driving loads by data from adjacent time steps.

The main technical problem of structure dynamic modelling currently lies in the damping model. In the current implementation, no separate damping elements are available and only the mathematical Rayleigh damping model can be used to represent the desired behaviour.

An advantage of the selected transient solver can be seen in the fact that it contains a state of the art structural dynamic solution algorithm. A wide range of problems can be solved with it and no methodically relevant restrictions have to be suffered. It enables robust computations of transient responses due to the various solution methods that are contained. W.r.t. design optimisation activities, the possibility to filter the calculated data for critical time steps must be named as a valuable capability. With a proper integration of this feature in the integrated design process, the computational time for a structural optimiser can be reduced dramatically. In this context, the benefit of detecting the elements and components, which are critically affected in a corresponding time step, shall be pointed out, as well. The described limits and possibilities can be given in a summarised form:

- − No separate damping elements but only mathematical Rayleigh model available.
- − Fully manual generation of time slope data.
- \+ State of the art algorithm to solve the problem of structural dynamics.
- \+ Filtering of huge amount of transient system data.
- \+ Detecting and visualising structurally critical elements and components.

The structural dynamics model contributes to the integrated airframe design process through

transient system responses. Figure 3.15 indicates the contributions of structure dynamics modelling to integrated airframe design.

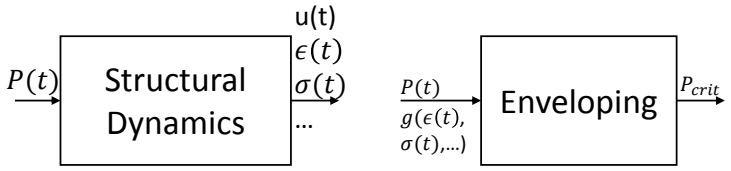

(a) Structural dynamics model (b) Load enveloping

Figure 3.15: The structural dynamics components

3.3 Flight Control System Modelling

Which modelling components are necessary to set up an aeroelastic model and to model a structure dynamic system was described above. The missing ingredient to enable an aeroservoelastic analysis is a control system. Descriptions in this chapter explain how to set up a controller model in a way that it can be used for integrated airframe design.

Mathematical models for control systems, giving the connections between physical properties in forms of equations, were introduced in Chapter 2.3. The simulation model covers those connections numerically through the implementation of respective functions, procedures, routines, etc.

The descriptions in this chapter are intended for the structural optimisation and not the control system design engineer. Focus will be laid on those control system modelling aspects that are necessary to couple the controller to other relevant disciplines. Modelling will be described for both, conceptual controller design (application in the conceptual design phase) and industrial control law implementation (application in later design phases). The provided modelling-guidelines shall be seen as a base for control related modelling activities in integrated airframe design.

3.3.1 Control System Modelling

When designing a control system, a respective numerical model needs to be set up. The main quantities from Chapter 2.3, which come into term during the integration of a FCS into an integrated design process and which embody the interfaces between the controller and its environment, are recapped in Table 3.1 and **highlighted in bold**. While system set points are prescribed externally from a higher level and shall remain at their given values, inputs and outputs are constantly changing. It is sensible to store the respective data for every evaluated time step in an appropriate, computational data type covering all time steps, to facilitate post-processing activities. Therefore, time discretisation parameters like the simulation start and end time t_0 and t_e or the number of discrete time steps n_t are defined globally as indicated

in Figure 3.16 (a). It might be necessary to define controller gain factors here, as well (see Figure 3.16 (b)).

Symbol of controller variable	Name of controller variable
x	Control system state
A	State matrix
B	Input matrix
C	Output matrix
D	Feedthrough matrix
u	**System input**
y	**System output**
w	**Control system set point, nominal value**
G	Transfer function
u_c	**Controller command**
e	**Control error**
IE / IAE	**Integrated error** / **Integrated absolute error**

Table 3.1: Important control system variables

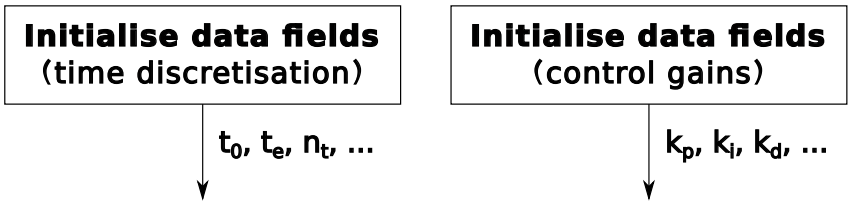

(a) Time discretisation properties (b) Exemplary controller properties

Figure 3.16: Initialise numerical properties

The controller can either be implemented in the integrated framework directly, what simplifies opening numerical interfaces, or it can be implemented externally, stemming from a different source. The latter case makes it more difficult to realise computational interfaces as the actual code may not be accessible. The controller selection workflow is depicted in Figure 3.17. Discrete controller commands need to be processed through an actuator before they are fed into a plant model. Actuator functions can be treated like controllers and can be implemented through transfer functions. The evaluations of the controller are carried out in a loop over discrete time steps, what is drafted in Figure 3.18. According to current plant-response values, controller outputs are calculated corresponding to the respective control task. A controlled plant provides outputs y, which are evaluated in the controller, where a respective control error e is computed. Based on e, controller outputs u_c are calculated and commanded (as e.g. commands for control surface deflections). To assess the quality of a control system, this error can be integrated to IE, IAE or similar quantities from one time step to the next one. They help to quickly evaluate how well a respective control task was met, after all time

steps are processed. Integration is realised through a numerical integration scheme (e.g. the trapezoidal rule).

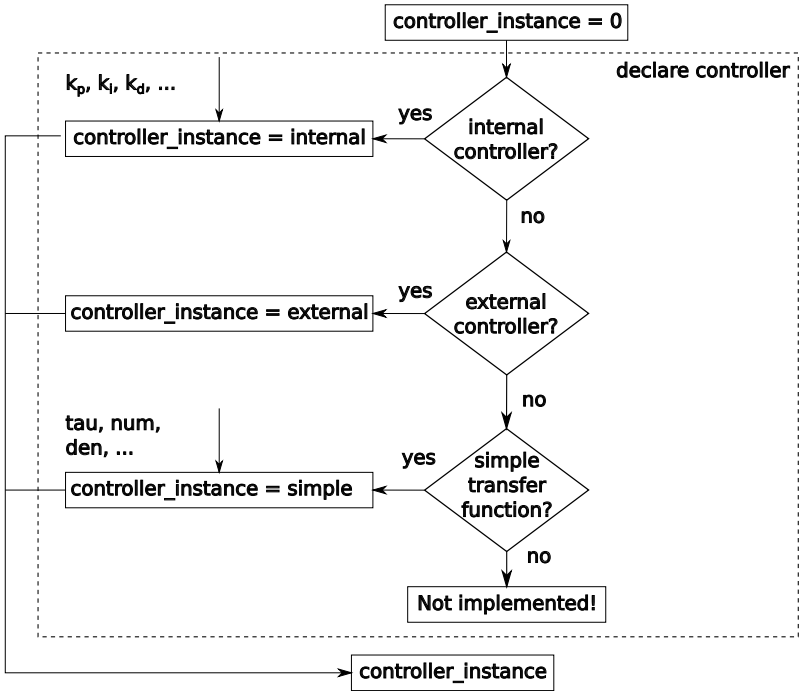

Figure 3.17: Declare controller instances

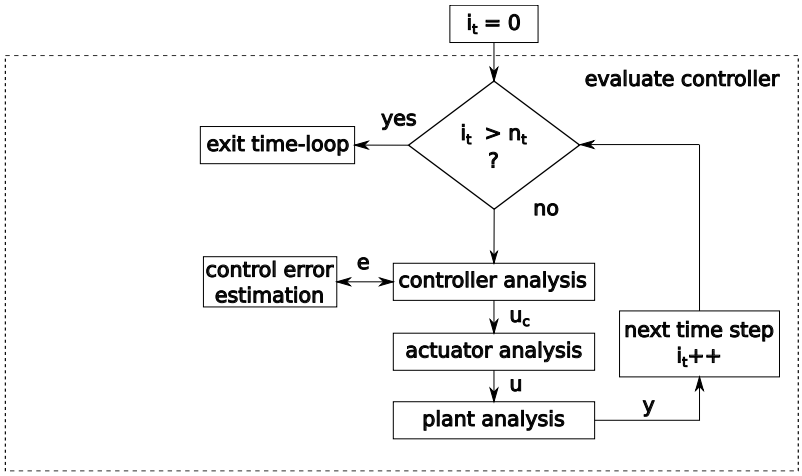

Figure 3.18: Controller in the time loop

As a real system suffers from delay times and inertia effects, the command should not be applied to a system analysis, directly. Such effects can be modelled through an actuator, which transfers a command value to a plant-input value. The actuator could be modelled as a transfer function and can be used like a separate control system component.

The generated plant-input leads to a change in the system behaviour, when it is applied to the plant. Plant-evaluation is performed separately, unrelated to the control system (embedded

in Figure 3.18). The resulting response is fed back in the next time step, which enables the controller to react accordingly. When embedding a control system in an integrated framework, this feeding back of signals is a critical modelling aspect. It strongly influences the technical requirements of the framework, which again depend on the architecture of the control system. A generic formulation of demands can therefore not be given. A recipe of the conceptual steps that have to be performed is given below. Each step is explained on the *example of a pitch damper*:

- Understand the applied controller. Which inputs do affect which outputs and how?
  $\rightarrow$ Identify the pitch rate as input and the elevator deflection as output of a pitch damper.
- Understand the applied plant to be controlled. Which quantities have to be adjustable through and which have to be fed to a controller? How can these values be processed or provided, respectively? (Implement numerical sensors)
  $\rightarrow$ Enable applying an elevator command onto and calculate the pitch rate within a AC-model.
- Connect the output of the numerical sensor from the plant with the input of the controller.
  $\rightarrow$ Feed the calculated pitch rate from the AC-model to the pitch damper.
- Connect the output of the controller with the input of the plant.
  $\rightarrow$ Feed the commanded elevator deflection to the AC-model.

This recipe follows from the closed loop character of control systems (see Figure 2.12 (b)). The identification of interfaces between the FCS and the plant becomes more complex with the FCS becoming more complex. Each input for the controller might need to be derived and calculated manually from the plant first and each output of the controller might need to be preprocessed before the plant model can work with it.

When integrating pre-designed control units and control systems into the airframe design process, it is not advised to treat a given controller as a black box. It is sensible to be familiar with some fundamentals for being able to independently model and understand the basic behaviour of control systems. The following explains generic aspects of control system modelling, necessary for upcoming studies. Even complex control laws can be reduced to recurring components. Proportional control is achieved when the control error is amplified through multiplication with a gain factor k_p. The output provided through proportional control is given as

$$u(t) = k_p e(t) \tag{3.3}$$

Depending on the sign in k_p, a control error can be reduced or increased in a comparatively uncomplicated way. One problem of proportional control is given by overshooting. Depending on k_p, more or less heavy oscillations occur until a stable output is reached. Further, the finally

stable output must not necessarily meet the control target.

To assure that the controlled plant will result in a steady state error of $e\,(t \to \infty) = 0$, an integrator element needs to be used. The control error is not only amplified through the integrator gain k_i, but is integrated over time as well:

$$u(t) = k_i \int_0^t e(\tau) d\tau \tag{3.4}$$

Although an integrator element enables meeting the control target ($e = 0$), it brings the problem of acting rather slowly. To increase the dynamics of a controller, a differentiator element is applied. It provides an output based on its derivative for the time step. A differentiator gain k_d again amplifies the respective output:

$$u(t) = k_d \dot{e}(t) \tag{3.5}$$

The derivative action of a differentiator element is thus concerned with the rate of change of the control error. A derivative control component can however lead to oscillations, again.

Bringing together these three basic control functionalities allows to benefit from their respective advantages and to compensate their disadvantages. Famous composed basic controllers are PD-, PI- and PID-controllers. The corresponding control outputs are given in equations (3.6) - (3.8):

$$\text{PD-control: } u(t) = k_p e(t) + k_d \dot{e}(t) \tag{3.6}$$

$$\text{PI-control: } u(t) = k_p e(t) + k_i \int_0^t e(\tau) d\tau \tag{3.7}$$

$$\text{PID-control: } (t) = k_p e(t) + k_i \int_0^t e(\tau) d\tau + k_d \dot{e}(t) \tag{3.8}$$

Such equations are implemented through control system modelling, what means choosing basic controller units and properly connecting respective signals in a cascaded system of systems. Figure 3.19 shows common representations of block diagrams for three basic controller functionalities in (a)-(c) and of block diagrams for composed controllers in (d)-(f), which can be found in every FCS. At this point, Hamann et al. (2014) shall be suggested, as it gives a great overview on how to design flight control functions for conceptual design. In the scope of FCS-integration into the airframe sizing process, not only the FCS itself, but basic con-

troller modelling and analysis techniques are challenging MDO tasks. Along with the arising possibilities, the simultaneously resulting limitations must be highlighted.

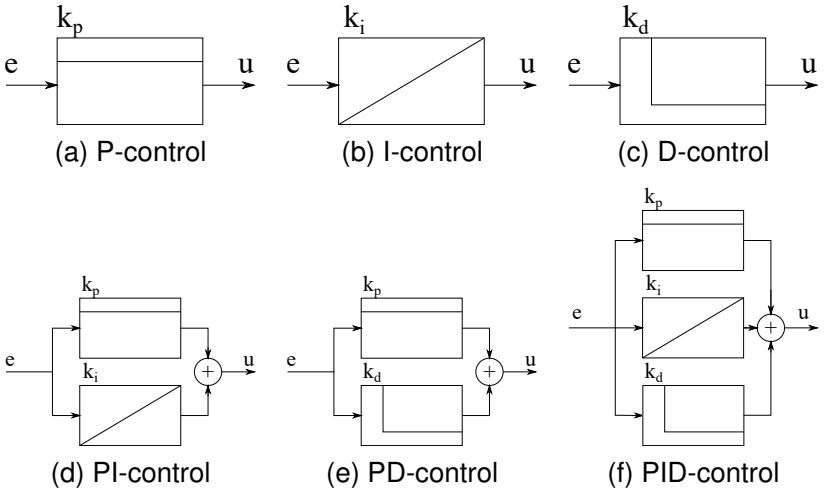

Figure 3.19: Basic controller components

To adress the need of understanding the basic functionality of a control system, it is not sensible to treat it as a black box. The plant to be controlled must be analysed in detail, to couple it with a respective controller. The physical variables serving as inputs for the control system need to be properly identified and numerically extracted as outputs from the plant. As a control system aims to manipulate time-dependent data, the respective plant must provide time-dependent signals. Even slow or quasi-steady plants must still result in temporal changes that can be evaluated in the controller. Therefore, a transient formulation of the governing equations is a mandatory requirement. Along the demand for a dynamic representation arises the question of numerical time discretisation. In the context of integrated design, it is not advised to treat respective sample frequencies as variables. Often controller components (as filters or actuator models) are designed for a specific sample frequency. Therefore, a further limitation for the overall design process, brought with a control system, is given by the fact that time discretisation of all involved components may be pre-defined by the controller design. If a finer discretisation is needed, major changes of the control system might be necessary. Control parameters such as basic gain variables are influential properties, which can have strong impact on the behaviour of a system. When the possibility is given to manipulate them externally (as shown for the basic controllers above), a high level of system understanding must be demanded of the respective modelling engineer.

The evaluation of control system blocks is realised through function calls. The interface to other numerical components is designed on a low, basic level. Therefore, no tool- or program-specific procedures must be met to work with control systems. This poses a high potential for all design activities as no specific definitions of numerical interfaces must be respected. Fur-

ther, this generic interface formulation enables working with both preliminary control system designs and with detailed controller implementations. Topics from the classical control system design phase (e.g. stability, robustness, controllability, etc.), using state space models, can be handled and studies with the final control laws, represented through discrete, embedded controllers, can be performed. The presented way of working fits to both control system design and detailed controller implementation. Limits and possibilities of the basic control system modelling used in this thesis state as follows:

- − Control systems demand physical inputs of the plant and thus fundamental understanding of the plant itself.
- − Familiarisation with controller components is necessary.
- − Evaluations for the controller necessitates plant signals from the time domain.
- − Sampling rates and frequencies are predefined and should not be varied independently.
- − Influential control parameters can accidentally be overwritten.
- \+ Simple formulation of interfaces enables high flexibility for design activities.
- \+ Way of working fits to large scale, industrial control system design.

3.3.2 Large Scale Flight Control System Modelling

The general concepts, components and variables for control systems, described previously, can be found in all engineering activities related to laying out control systems. Keeping that in mind, the MDO-engineer can and must be aware of some general aspects concerning flight control system procedures in the overall airframe design process.

In a large scale project, the mathematical control laws and their numerical implementation will be provided from different control system engineers. The initial controller design will deal with the definition of FCS laws and the appropriate tuning of gain factors. The resulting flight control system will be analysed in the continuous time domain. Such activities are mostly performed in respective commercial tools like MATLAB-Simulink. In a later phase, it is brought into a generic code form, which allows dealing with discrete time signals, as is necessary for the integration to hardware.

From the integrated design point of view, this code-conversion and implementation has primary meaning, as it enables using the final controller layout. However, the benefit, of being able to work with the FCS in a form as it is mounted to the final product, brings some problems. It demands the capability of handling control law formulations in the discrete time domain, which is an uncommon requirement for the field of optimisation. As the employed filters are often designed for specific sample frequencies, it further pre-defines the discrete time steps, a multi-disciplinary plant-analysis must be performed for. Changing the temporal discretisation of the plant-analysis might in the worst case mean that the underlying FCS-code needs to be

adapted and re-generated.

The process of creating controller source code for the purpose of integration into an integrated framework shall be demonstrated with the software SCADE from Esterel Technologies. It enables model-based software-development and code generation. The different components explained below are not bound to a specific software, must be enabled, however, if integrated designing is aspired. Figure 3.20 shows the working environment of SCADE.

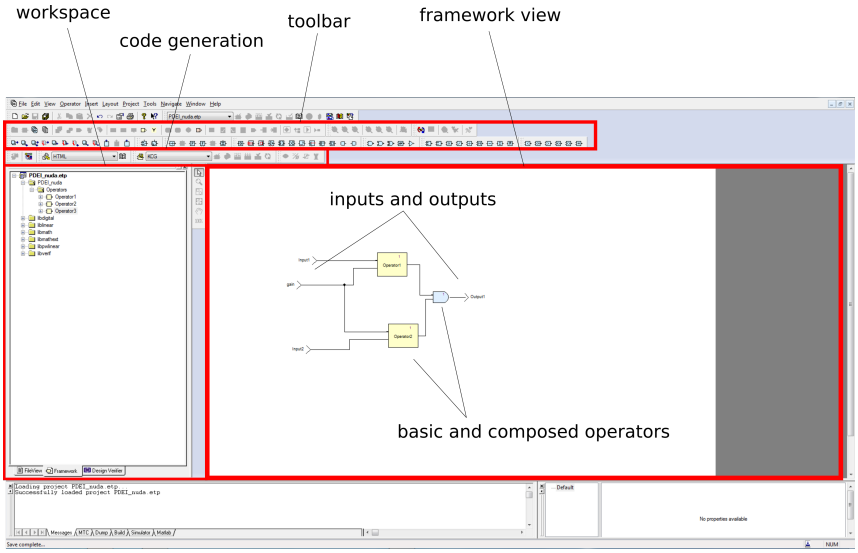

Figure 3.20: SCADE environment for control system modelling

The software package supports controller design through various automated model checks. The generated code for the previously modelled controller is compiled for an integration in a simulation and analysis framework. For an interaction of the flight control system with a structural sizing process, these codes were compiled as a dynamic library such that they can be used in a tool-independent framework. Creating the FCS in the desired form follows the process depicted in Figure 3.21.

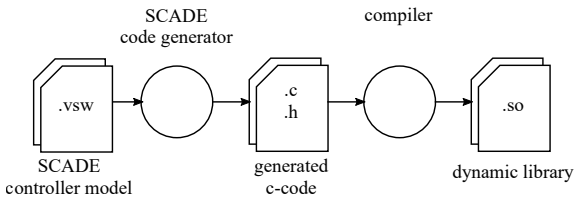

Figure 3.21: Generation of controller code

There are some basic functionalities which can be found in most flight control systems. Some selected FCS components shall be highlighted to illustrate the main modelling procedure, followed in this thesis.

Integrators are one example for a reoccurring unit in a FCS. They determine a signal based

on its temporal derivative. As a subcomponent in a cascaded design they integrate various signals in higher level control laws as a longitudinal or lateral control law. One main purpose of a longitudinal controller is to calculate an elevator command according to a respectively given control task. In longitudinal control, subcontrollers take over subtasks like damping the aircraft pitch rate q or integrating control surface deflections like η. An important input for the elevator integration to deliver a respective η-command is a trimmed elevator deflection. A pitch damper implementation primarily works with pitch rate, the angle of attack and the current air speed. Both components can be modelled through basic signal blocks and shall represent the lowest modelling level, here. Functionalities like pitch damping and the η-integration can be grouped into one subcontroller, together with further components like according rate limiters and feedback operators. Figure 3.22 visualises the idea of linking subcontrollers to realise a desired compound functionality. Mainly based on the AoA, respective gain factors and flight mechanical states, an elevator deflection command is calculated.

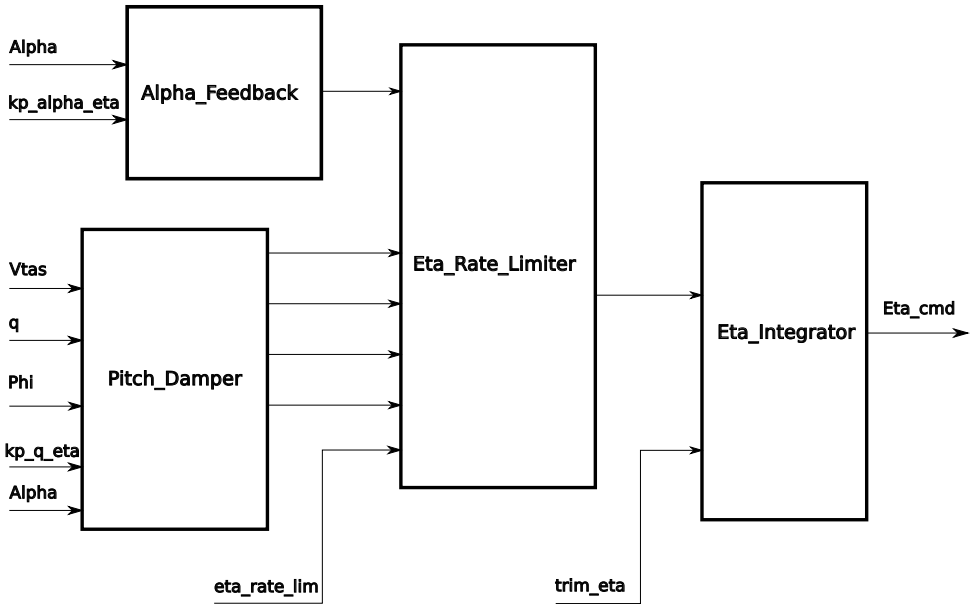

Figure 3.22: Pitch damping and elevator integration

The concrete design of elemental control blocks contributing to subcontrollers (which again contribute to the final control law) and the design and optimisation of control law gains is done by the flight control engineer. Physical properties that are invariant during flight like e.g. I_{yy}, CoG, b, c are brought together for the respective AC. Variable quantities like velocities, rates, altitude, Mach number, etc. are monitored for the purpose of fulfilling different control tasks. Gain factors are amplifying the corresponding signals. Amplification of the aileron ξ to the rudder ζ or to the spoiler κ is given through gains like $k_{\zeta\xi}$ or $k_{\kappa\xi}$.

In addition to these gains, more sophisticated, composed parameters can be found in industrial aircraft programs, as well. The ratio between control surface deflections of spoiler and

aileron could be defined explicitly. The idea of splitting loads between aileron and spoiler in an asymmetric manoeuvre will be studied later, in more detail.

Integrator functionalities like those, briefly described for longitudinal AC-control, occur in lateral control laws as well. As an example, integrators could be grouped into a lateral integrator module and help to provide commands for control surfaces, which are primarily used for rolling and yawing the aircraft (ailerons, rudder, roll spoilers). Based on trimmed values of ξ, ζ and on rate values like $\dot{\xi}, \dot{\zeta}, \dot{\kappa}$, and under consideration of respectively relevant rate limits, corresponding commands ξ_c, ζ_c, κ_c are calculated.

This approach of FCS modelling through a modularised control law layout enables both, reusing code or subcontroller designs and splitting design activities in the team of control law designers. From the depicted points on industrial FCS design in an integrated design process with SCADE, a number of limits and possibilities can be identified.

It shall be noted that main limitations presented in the following stem from the fact that SCADE was not specifically developed to contribute to an MDO-process. System modelling and simulation, conducted through discrete signals in SCADE, is relatively complex compared to other software. Detailed knowledge on the methodology of control system modelling is indispensable, simulation and visualisation of respective data is not intuitive. This makes SCADE difficult to use for engineers without specific training. A further limitation can be seen when addressing the capability in fast controller model generation. The library of available controller-components and subcomponents is small, basic controller prototypes must often be designed manually. The functionalities that support the design of control parameters are comparatively limited. These points restrict the range of applicability w.r.t. fast, tool-supported FCS-model generation for usage in an integrated process.

A big advantage in the presented modelling approach can be seen in the fact that the created FCS design can be used both in conceptual and in detailed numerical studies. The main outcome is the automatically generated code, which can be used for further simulation in a respective software environment (conceptual and preliminary design) or testing with hardware in the loop (detail design). The step of bringing the design model to a form which can finally be implemented in the aircraft system is thus not necessary, or at least strongly facilitated. Further, the capability to model arbitrary control systems must be highlighted as a possibility for the overall process. Complex control structures can thus be created, based on respectively underlying basic components. The FCS designer is not limited to a tool-given controller type. Through the possibility of automatic code-generation, coupling the final control system to external sources does not pose a considerable problem. The design is therefore not limited by a tool-specific modelling process, which gives further freedom. The generation of both internal and external signal interfaces is not a complex task. All interfaces can be defined graphically.

Internal signals are connecting controller blocks of a common model. Communication with external sources can be realised through manually connecting the respective signals with the plant in-/outputs on the code-side. Especially w.r.t. a functionality in a MDO-process, where such connections are indispensable, this is of high value. Pros and cons of the chosen large scale modelling approach can be listed as follows:

- − Complex modelling and simulation of controllers through discrete signals.
- − Fewer capabilities concerning fast controller design compared to other software.
- + Direct usage of final, detailed FCS design.
- + Possibility to model arbitrary control systems.
- + Uncomplex generation of both internal and external signal interfaces.

The flight control system model takes transient data as an input to mainly determine control surface commands. These commands are processed in an actuator model to result in actual control surface deflections which can be used for further calculations. The two aspects are visualised in Figure 3.23.

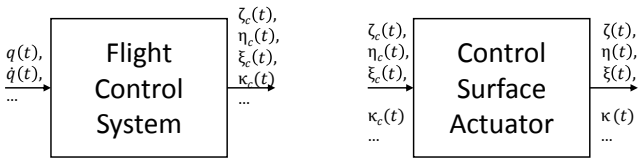

(a) Flight control system model (b) Actuator model

Figure 3.23: The flight control system components

The control laws used in this work stem from controllers which are well suited for full, numerical manoeuvre simulations. Still, only subfunctionalities, focussing on the possibilities for integrated designing through MDO, shall be used and studied in the following.

3.4 Design Optimisation Modelling

Bringing together the previously described modelling components (aeroelastic model, structural dynamic model, the flight control system model), an aeroservoelastic model can be set up and aeroservoelastic *analyses* can be performed. Containing the governing equations and thus providing system responses, it represents the MDO-state model. With a proper optimisation model, these responses can be used by a numerical optimisation algorithm to find an improved design. A missing ingredient for an aeroservoelastic *optimisation*, therefore is the optimisation model. It defines how responses from an aeroservoelastic analysis must be reformulated as constraints for an optimisation algorithm and which variables shall be used to minimise or maximise a certain physical property. The three numerical core ingredients are given by the objective function, the set of design variables and the set of constraint func-

tions.

Design optimisation modelling is the final component which is necessary to create an integrated design framework, that is capable of respecting FCS demands for an airframe layout. Its elements are described in this chapter.

3.4.1 Objective Model and Objective Function

To assess a given design, a proper assessment-value must be found. In MDO the objective function is the main quantity of interest, as it evaluates the quality of a given design by its numerical value. It formulates the key demand in an engineering task in a quantifiable way.

Basically the objective function implements the scalar value f and the vectorial quantity $\frac{df}{dx}$ according to a design model x. Classically, the structural mass of an AC is used in the definition of an objective function. The mass value m in the current optimisation iteration is mostly related to its initial value m_0. The current mass value is determined from the FEM-model by summing mass related information m_i of all structural components i:

$$m = \sum_i m_i \tag{3.9}$$

Both concentrated masses (e.g. used to model fuel capacities) and distributed masses (defined through material densities given in the model) are taken into account. As geometric properties like cross section areas of 1D-elements (rods, bars, beams, etc.) or thickness values of 2D-elements (shells, plates, membranes, layer thicknesses of composite elements etc.) are varied by the optimiser, the corresponding mass changes with the volume ($m = \rho V$). The respective gradient information $\frac{df}{dx}$ is implemented analytically, based on the particular elements in LAGRANGE. From the modelling point of view, no effort is needed for structural mass optimisation as it is the default in the MDO tool.

Besides the possibility to improve a given design through reduction of structural mass, further objective functions can be used, as well. Minimising the structural compliance is known from topology optimisation (see Bendsoe & Sigmund (2003)). Compliance c can be seen as a measure of stiffness in a given system. While it relates to an energetic term in the PvW formulation, its calculation is performed easily over the external loads and the respective displacement field from the FEM-model ($c = \sum_i P_i u_i$). For flight performance optimisation, fuel capacity could be maximised by choosing and summing only selected concentrated masses for the objective function. Further criteria to improve performance are given through AC-range or through the induced drag from aerodynamic data. While range evaluations are still an open topic of developments in the selected MDO-solver, respecting the induced drag in the scope of shape optimisation was successfully demonstrated in Deinert (2016).

The objective model provides an objective function value f and contributes to the calculation

of respective gradient information ∇f for a given design variable x (compare Figure 3.24).

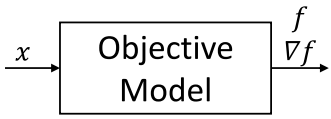

Figure 3.24: The objective model component of an optimisation model

3.4.2 Design Model and Design Variables

The objective model defines which quantity is to be optimised. The design model now contains the information which parameters (state variables) shall be varied to achieve this.

The design variables represented through x must be chosen carefully. They embody the flexibility which is given to a certain design. Describing a given model through many design variables means to grant a high design-flexibility to the numerical optimisation algorithm, which finally works with it. The dimension of x strongly impacts the computational time of an optimisation run. Therefore, sensible grouping of physical properties into x is a must. The challenge is to select as many design variables as possible for maximum design-flexibility but as few as necessary for computationally reasonable effort.

From a modelling point of view, a design variable can be seen as a set of state variables. While the abstract, conceptual grouping itself must be sensibly thought of by the engineer, the manual creation of respective inputs for LAGRANGE can be done with different helper tools. The Airbus internal program DEFOPT was implemented specifically to create design model inputs, based on a given Finite Element (FE)-model. Sets of elements containing structural variables like beam cross section areas, shell thickness or composite layer thickness values and angles serve as input. Design variables are then created according to geometric boundaries, which can be given on a purely elemental base or through selected aircraft substructures like stringers, spars, ribs, etc. Figures 3.25 - 3.27 visualise three example design models for a generic FEM model of a right AC wing.

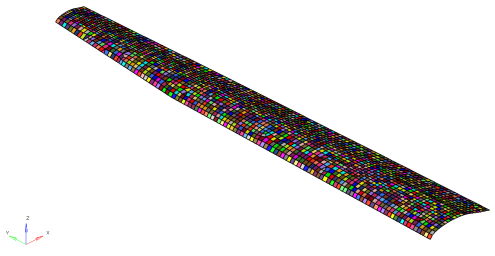

Figure 3.25: Design variables when using one design variable per element

Focus is placed on the wing skin elements, here. With Figure 3.25 an unnecessary high computational effort for the optimiser is provoked as each element embodies at least one design

variable. In case the wing skin is made from composite material, where one finite element can contain multiple composite layers, the number of resulting design variables can increase further, as multiple layer thickness parameters or layer angles can be grouped into separate design variables. It was even possible to create one design variable for each separate layer.

Figure 3.26 represents another grouping of elements into a design model. Specific ribs were used to geometrically separate the resulting three design variables.

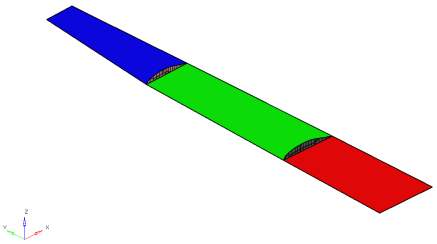

Figure 3.26: Design variables when using specific ribs as spatial separators

Intersections between ribs and spars can be used as boundaries of design variable patches. This is shown in Figure 3.27 which depicts a more sensible grouping.

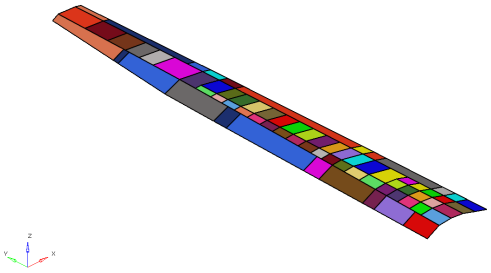

Figure 3.27: Design variables when using all ribs and spars as spatial separators

Strongly connected to the design model is the definition of gages for the design variables. As the gages are often referred to as "side constraints", they could be classified in the criteria model, as well. The gages define the range in which a state variable is allowed to vary for the purpose of optimising the objective function. It is possible to use an absolute range by hardly defining a lower and an upper limit, or to allow a relative change with respect to e.g. the initial value of a given state variable, in LAGRANGE. The gage-selection can have a major influence on the finally optimised design. Narrow ranges of gages, not only reduce the design-flexibility, but can even pose an unnecessary limit to the numerical optimisation algorithm. As a result, the design variables are driven to values corresponding to gages of the state variables, instead of searching in a sensible range of designs. However, wide ranges, especially in combination with a high dimension of x, bear more risk of leading the deterministic optimiser into local

optima and thus not exploiting the full range of the given design-flexibility. It is usually a good start to allow a variation of physical properties based on criteria as manufacturability or availability. Here again, engineering mind is needed when formulating the side constraints.

The design model provides design variables x for sets of state variables s (Figure 3.28).

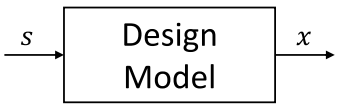

Figure 3.28: The design model component of an optimisation model

3.4.3 Criteria Model and Constraint Functions

With the objective model, defining which quantity shall be optimised, and the design model, defining the parameters which shall be varied and how strong their variation may be, an optimisation was already possible. An engineering system will, however, always demand side conditions which have to be met. Maximum displacements of the wing tip, mechanical strains and stresses, which shall not exceed a certain level, or eigenfrequencies which have to be kept in a pre-defined range are examples for such side conditions. They are modelled by assigning FE-nodes, elements, DoFs, etc. into a criteria model. For a design to be feasible by means of these criteria, constraint functions are evaluated for respective loading situations.

In flight, an AC experiences various excitations, which are modelled through forces and moments. Those loads can emerge intentionally e.g. from manoeuvres, induced by the pilot, but also from environmental influences as in the case of gusts. In the scope of MDO, the collection of all parameters describing a loading situation of interest, resulting in a set of forces and moments (see Figure 3.29), is referred to as a load case. From transient analyses, each discrete time step is evaluated for a respective loading state. Thus, each time step can be interpreted as a separate load case.

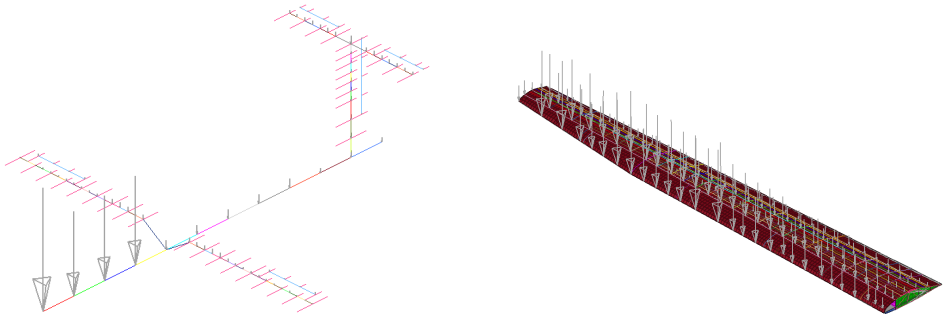

(a) Gravity load component

(b) Aerodynamic load component from equation (2.56) (left hand side)

Figure 3.29: Example load cases for structural design

AC are always certified for numerous load cases and for numerous criteria. In aircraft industry, it is the sovereignty and responsibility of loads departments to provide respective sets of relevant loads. Multi-fidelity aerodynamic data (low-fidelity from vortex- and doublet lattice methods, medium-fidelity from Euler- and RANS-methods or high-fidelity from wind tunnel or flight testing) come into use for this purpose. The outcome is a loads model, consisting of forces and moments, that can be used in a numerical program by a structural designer.

During optimisation, each loadcase must evaluate all optimisation constraints, in the first place. The following list gives an incomplete insight in constraints, which can be contained in a classical criteria model:

- **Displacement constraints:**
  Displacement constraints are restrictions on deformations and a very common stiffness constraint. Lower and Upper limits for a desired displacement can be defined node-wise. Both translational and rotational DoFs can be constrained. A classical application for displacement constraints is given when studying passive aeroelastic tailoring. A range of desired or allowed displacements, which must be met or must not be exceeded through structural optimisation, can be defined. Usually, only few nodes and DoFs will be constrained. With a proper model, stiffness then assures that the transition of displacements between neighbouring nodes remains in a sensible range. Figure 3.30 shows the evaluation of a displacement constraint for the wing tip of a generic transport aircraft in level flight, where an absolute allowable value of $100mm$ is exceeded through an applied value of $181.07mm$, what results in a violated, i.e. negative constraint function value.

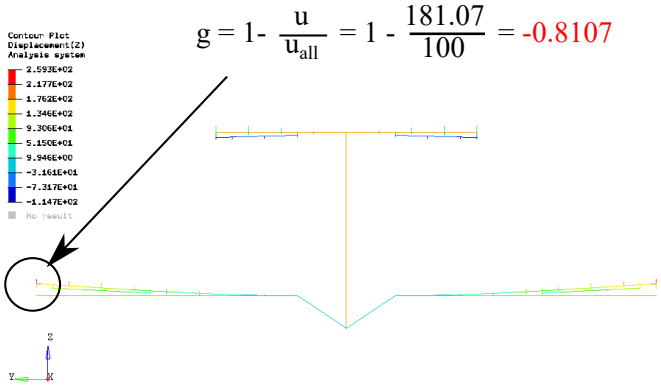

Figure 3.30: Displacement constraint for wing tip

- **Strength constraints:**
  Strength constraints in LAGRANGE optimisations are evaluating stresses and strains in the structural elements of a FEM-model. Isotropic materials are usually assessed with von Mises formulations, but can use tensorial components of the respective stresses

and strains, as well. Composite structures demand more complex criteria models. LAGRANGE offers various composite failure criteria, originally described by Hill, Hoffmann or Tsai (see Jones (1998)). A commonly applied constraint formulates the maximum strain criterion, which mainly considers the maximum strain in a composite (see Hart-Smith (1998)). From the computational side, LAGRANGE reduces all strength constraints to a reserve factor, formulated as ratio of allowable and applied loads. To assure a higher structural reserve, a scaling factor can be used to increase the actually applied load, if desired.

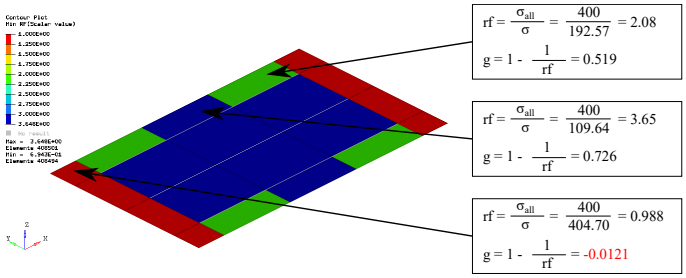

Figure 3.31: Reserve factors and strength constraint values for a structural skin panel under external load

- **Structural stability constraints:**
  Assuring mechanical stability of aerospace structures means evaluating its capability of carrying compressive loads. From a FEM point of view, it has to be differed between plate buckling of 2D isotropic and orthotropic elements and 1D stiffener elements. Partial differential equations are solved resulting in critical values of compressive stresses or strains. The analysed structure must be considered to fail as soon as these are exceeded, although these may by significantly lower than those considered in the material or structural allowables. Mathematical details of methods for isotropic materials can be found in e.g. Timoshenko & Gere (1963) and for orthotropic materials in e.g. Jones (1998), ESDU (1994), Hörnlein (1988), Hörnlein (2006), Weaver (2004), Weaver (2005), Weaver (2006). For works with a focus on mathematical algorithms for shape optimisations considering structural stability Daoud (2005) shall be suggested.
- **Aeroelastic stability derivative constraints:**
  During the work on this thesis a new constraint, intended for aeroelastic applications was formulated (compare Nussbächer et al. (2016)). Depending on the design model, structural optimisation can change the position of the CoG. As a result, stability derivatives can change in an undesired way. Such changes are not monitored in classical optimisation tasks with considered aeroelasticity. Evaluating respective stability derivative properties and controlling them by means of appropriate constraints means assuring that a desired flight stability level is maintained or reached. Especially in applications,

where shape optimisation comes into use, this will be an important tool to reach better AC designs. From the modelling side, it is sensible to first evaluate the level of flight stability of a given design, to then define the stability derivative constraint by means of a relative change of the obtained stability property and to successively increase the range from one optimisation to another, hereafter. It is suggested to allow relative changes of only $1 - 5\%$, first, in order not to heavily change the flying characteristics of the given configuration through structural optimisation. As long as structural changes do not violate the demand for the stability derivative, the constraint remains inactive, becomes very dominant, however, as soon as this is not the case anymore.

Various other, modern constraints can be introduced in a criteria model of LAGRANGE. Aeroelastic trimming constraints, damage tolerance criteria, limits for flutter frequencies, or restrictions given through manufacturability can be named, here. It shall be noted, that all constraints can arbitrarily be combined in one criteria model. This means that within one optimisation run all constraints can be evaluated simultaneously.

The total number of constraints to be respected during a numerical optimisation depends on the number of restrictions formulated for nodes, elements, etc. and on the number of load cases (and/or time steps) to be studied. Especially for transient analyses, the number of time steps can be very high and thus bring many loads into the evaluations for an optimisation run. Reducing this number of loads to a set of structurally critical loads is done through the enveloping feature in LAGRANGE as described earlier in Chapter 3.2.

Numerically, the constraint functions implement the vectorial quantities g and the matrix $\frac{dg}{dx}$, according to a design model x. For the optimisation algorithm, a distinction between the different types of constraints is not possible and not intended. An optimisation algorithm does only use the numerical values in g and $\frac{dg}{dx}$ and should never need the information where these originate. Their dimensions, however, are of importance concerning the computational time, the algorithm needs to provide a better design. Reducing these to a sensible size demands both, engineering mind (e.g. selection of critical areas of a structure into the criteria model and neglecting uncritical areas) and the proper choice of optimisation control settings like the number of time steps to be considered or acceptable scaling of reserve factors.

W.r.t. integrated design, the presented ingredients for design optimisation modelling bring both, limitations and possibilities. The following summarises advantages and disadvantages.

Manual action is necessary during the generation of the optimisation model. Grouping of structural elements or separately defining feasible ranges for state variables must be carried out by hand and can not be fully automated, yet. Design tasks often demand the simultaneous optimisation of various quantities. Often the single tasks can be reformulated such that

finally one primary target remains in the final formulation. If this reduction to one objective is not possible or does not meet a good tradeoff between the single objectives, the presented optimisation methodology does not offer approaches to solve multi-objective problems. The majority of objective and constraint functions and of design variables, which can be handled with the presented method, are of structural nature, only. The consideration of demands from other disciplines are not as strongly established as those from structural mechanics.

The wide range of already available structural objectives, criteria and design variables can, however, be named as an advantage of the depicted optimisation modelling, as well. It enables multidisciplinary assessments of the overall AC and leaves the underlying programming code with an inherent claim for integrated design. The capability of respecting requirements of multiple disciplines simultaneously, opens a wide range of applications, which could not be analysed with other processes. High numbers of *interdisciplinary* constraints can be evaluated, what demonstrates the flexibility w.r.t. analysing problems from different engineering disciplines. Another advantage of the described optimisation method lies within the fact that there is no dependency between an optimisation model and a respective optimisation algorithm. In case the current task can not be solved in a satisfying way with one algorithm, another can directly be applied without any changes to the original model. The different components contributing to the optimisation model are clearly separated from each other. This modularity enables short implementation times for adding new criteria to the given process. The sovereignty over optimisation model generation and the independence of third party tools opens the possibility to quickly study and test complex design ideas without the need to account for time- and cost-consuming developments.

Limitations and possibilities of the optimisation model generation summarise as follows:

- − Moderate modelling effort still necessary for some optimisation model components.
- − No innovative multi-objective optimisation.
- − Criteria models mainly formulated for structures.
- \+ Wide range of objective, criteria and design models.
- \+ All optimisation algorithms use the same optimisation model.
- \+ Fast implementation of new optimisation demands through in-house code-access.

The constraint model provides constraint function values g and contributes to the calculation of gradient information ∇g for a given design variable x (compare Figure 3.32).

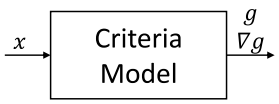

Figure 3.32: The criteria model component of an optimisation model

4 Method of Aeroservoelastic Airframe Design Optimisation

The previously described ingredients need to be coupled methodically, now. Step by step the final aeroservoelastic design process is assembled. Successively, its components are added to the process developed in the respective previous step. First, data transmission between the three main disciplines (aerodynamics, structural mechanics and flight control system) has to be realised. Enabling the exchange of information results in the possibility to run aeroservoelastic *analyses*, then. Based on the so derived capability to run integrated studies, *optimisations* can be performed, hereafter. This enables running aeroservoelastic design studies in an integrated way, what solves the main issue of this work. The evolution of the design process up to its final version can be seen when Figures 4.11, 4.13 with 4.14, 4.15 and 4.17 (all of whom are explained in the following) are put next to each other.

The physical basics for the development of an integrated design process considering flight control system demands, were formulated in Chapter 2, while their implementation through respective methods and tools was described in Chapter 3. In Chapter 4 the separate components are merged into a final process. For the solution of the motivating problems and for reaching the objectives of the work at hands this chapter contributes by

- creating a numerical evaluation process by combining aeroelastic and structural dynamic analyses
- enhancing the workflow through a FCS component
- integrating the resulting analysis in an optimisation frame

4.1 Data Exchange Between the Disciplines

The time for data exchange between numerical models can be reduced drastically through automation. A dynamic way of working is given when all data are centrally available in one framework. The framework assembled in this work offers a computational interface, which is capable of exchanging data from various sources and brings them together for the purpose of multidisciplinary optimisation. The LAGRANGE-python-Application Programming Interface (API) gives full control over the program flow. The previously described methods (Chapter 2) can be brought into interaction through coupling their implementations (Chapter 3).

Before an optimisation model is composed, an important point concerning automation-based, integrated design must be accentuated. The quality of an optimisation result depends on two main components. First, the solution of a MDO problem is only as good as the underlying equation system in each contributing discipline and second, a MDO can only work if the governing equations of all disciplines are properly interacting with each other. Deep knowledge and understanding of a system are fundamentally important for a successful optimisation.

To enable data exchange between different disciplines, an instance based way of working

must be followed. This means that the information in each discipline has to be organised in the same way, such that data can be exchanged similarly on a common level. Computationally, each model then works in a separate programming instance and shares information with other instances. Figure 4.1 shows an example of an abstract instance. It contains the data processing steps, well known from most engineering codes.

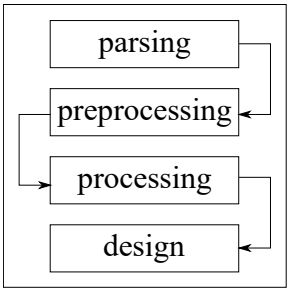

Figure 4.1: Classical workflow of a LAGRANGE optimisation task

The parser reads the information from the numerical model, like e.g. for finite elements or for aerodynamic panels, one by one. In the preprocessing step, the data behind it is organized in respective structures, like e.g. in collections of finite element IDs together with their nodes and thicknesses or aerodynamic IDs together with their chord and span lengths. Processing means to prepare information, such that it can be used for evaluation in a next step. Here, e.g. finite element sizes or aerodynamic panel areas are calculated. In the design the data is finally used in an analysis, what provides desired engineering quantities, like e.g. mechanical strains or stresses or aerodynamic pressures and loads.

The framework implemented in this work enables controlling these steps for all defined instances (and thus disciplines) during runtime. This gives the possibility to exchange data between one discipline and the other. How the different instances are set up depends on the definition of the engineering problem and is a main task of the MDO-engineer. Figure 4.2 gives an example of how three disciplines can share information and manipulate each other.

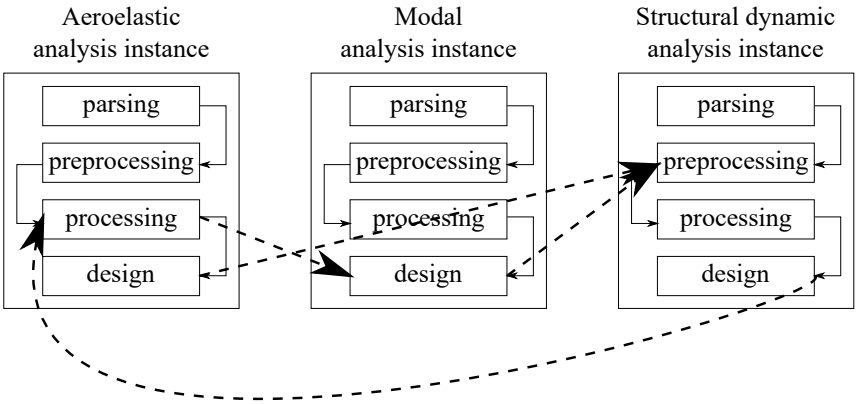

Figure 4.2: Example of multiple LAGRANGE instances working together

Every analysis, optimisation or general mode of operation enables a separate API instance. The following gives an overview on instances, which are used to address the topics of this work:

- Mathematical optimisation instance:
  Use only the numerical optimisers, without any connection to a physical, engineering model. (E.g. find the minimum of a mathematical function.)
- Static structural analysis instance:
  Run a pure, structure mechanical analysis. (E.g. determine structural responses like displacements, strains, stresses, etc. for a given structural model and load case.)
- Modal instance:
  Run a modal analysis of a structural system. (E.g. determine eigenfrequencies or eigenmodes of a structural model.)
- Aeroelastic analysis instance:
  Couple structural and aerodynamic models for interdisciplinary analyses. (E.g. make use of aeroelastic constraints for the solution of an MDO-problem.)
- Dynamic structural analysis instance:
  Calculate transient responses of structure mechanical systems. (E.g. calculate structural responses for various time steps of a dynamic analysis.)
- Enveloping instance:
  Find structurally critical events from a respective analysis. (E.g. filter critical loads or time steps from a respective range for an optimisation run.)
- ...

Interfacing respective instances is like setting up a problem in the weak form as used in the FEM (compare Chapter 2.1.2). Unlike a monolithic, strong coupling, a loose, partitioned coupling does not solve the system equations of all disciplines in a closed form. Interchanging data between disciplines and passing data from one discipline to another is a basic characteristic of this interconnection method. The necessary procedures in the framework of this work are represented through **getter**- and **setter**-functionalities (Figure 4.3 and Figure 4.4).

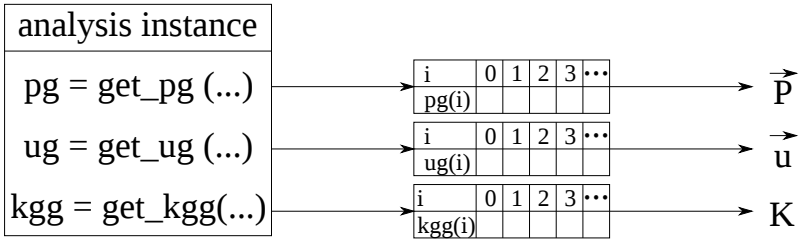

Figure 4.3: Getter functions of the LAGRANGE-python-interface

While a getter-function **gets**, i.e. extracts arbitrary data like displacements, strains, stresses, pressures, etc. from an analysis run, a setter-function **sets**, i.e. writes such information or overwrites respective, already available information.

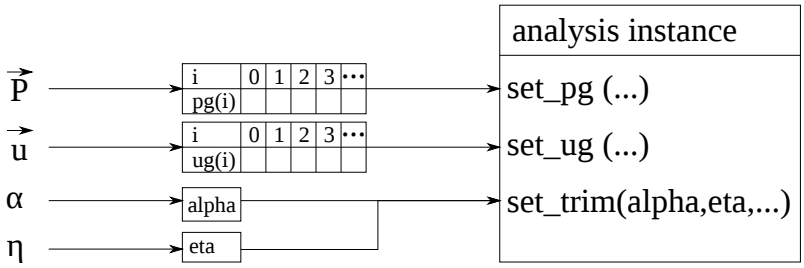

Figure 4.4: Setter functions of the LAGRANGE-python-interface

Which capabilities are needed in detail, depends on the problem to be solved and they need to be implemented accordingly. Load-, displacement-vectors or stiffness-matrices can be extracted as depicted in Figure 4.3, while loads and displacements or properties of an aeroelastic trim problem can be overwritten as displayed in Figure 4.4.

4.2 Aeroservoelastic Design Analysis

With the capabilities evolving through the generic coupling approach briefly described in 4.1, it is now possible to set up the coupled analysis and optimisation models necessary for aeroservoelastic studies. First, an aeroelastic instance will be connected to a structure dynamic instance. The resulting transient aeroelastic analysis shall be extended by coupling a flight control system instance. Activating the enveloping functionality in the structural dynamic solver part already allows to filter critical loads and properties in the design of the airframe. The information of this aeroservoelastic analysis can then be used in an optimisation instance, which only deals with the task of finding better designs.

4.2.1 Coupling the Aeroelastic with the Structural Dynamics Model

The modelling basics of aeroelastic analyses and structural dynamics were explained in Chapters 3.1 and 3.2. This chapter describes how an aerostructural analysis can be coupled with a transient analysis. Both, the aeroelastic and the structural dynamic solver used in this thesis are implemented directly in the framework. The LAGRANGE-python-API enables data exchange between the two. Loads extracted from a steady aeroelastic analysis can be applied as NBCs on a transient analysis. Structural responses resulting from a time step of the dynamic solver (as e.g. rotations in the CoG) can be fed back and interpreted as changes in the flow conditions. They thus alter the loading condition for the subsequent time step. To automatically tune the damping model, used in the time-dependent analysis, a one-time determination of eigenfrequencies by a modal solver instance is implemented. Alternatively, damping coefficients like α_1 and α_2 can be supplied externally, as well.

A necessary demand for the multidisciplinary analysis framework, which is build up from various instances, is that all underlying numerical AC-models must use the same modelling base. Although a structural dynamic instance does not need an aerodynamic model, and the steady aeroelastic instance can not deal with transient modelling components, the underlying structural FEM-model must not differ in a single DoF. This is assured through a shared, central GFEM (Figure 4.5).

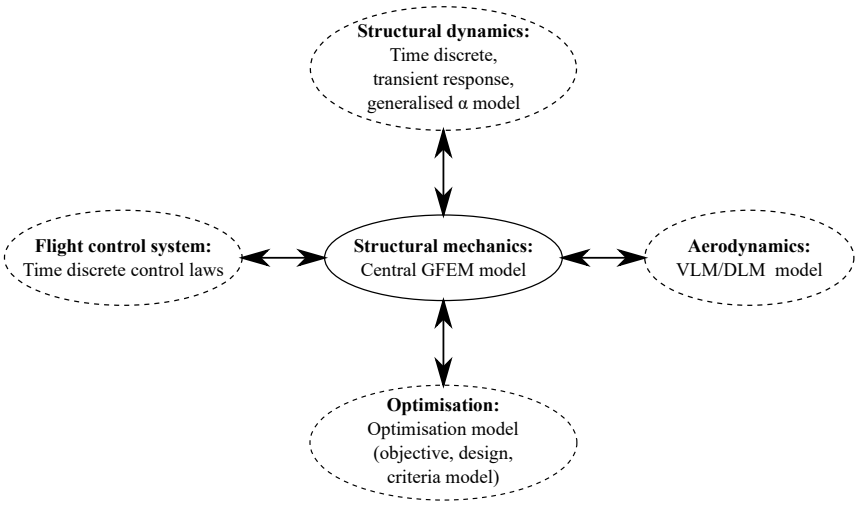

Figure 4.5: Shared GFEM as common basis for instance based numerical simulation

A transient aeroelastic calculation shall always start from an aeroelastically trimmed state. Therefore, an initial trimming calculation for the respective flight state must be performed, first. The results are control surface deflections and aerodynamic angles, which serve as starting values for the aeroelastic evaluation instance. The aeroelastic analysis is mainly fed with aerodynamic angles and provides resulting rigid and/or elastic forces acting on the structure. An external command, like a pilot stick input or a control system command, may change the control surface deflections (compare Figure 4.6). From a modelling point of view, this alters the boundary conditions of the aerodynamic model. The respective input can be given through a progression of signals at discrete time steps.

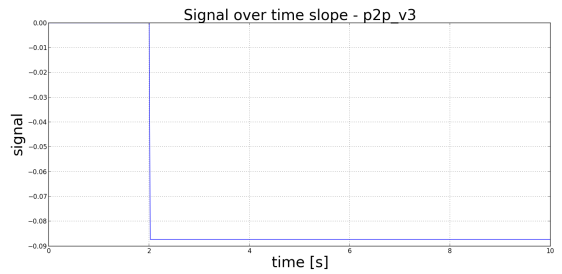

(a) Step input

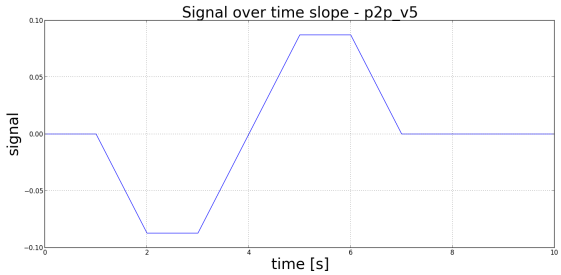

(b) Input through section-wise linear slopes

Figure 4.6: Modelling exemplary stick inputs

The transformation of load data from one instance to another is of high importance for the methodical coupling. From a computational point of view, load vectors of numerical aircraft models can easily be kept in memory of modern computers. Therefore, transferring load components is usually not a resource problem, but demands attentiveness in properly matching degrees of freedom data between the numerical models. It must be assured that forces of translational DoFs are transferred to the corresponding translational ones and that moments of rotational DoFs are transferred to the corresponding rotational ones. Further it is necessary to always be aware of the components a load vector is made of. E.g. rigid body accelerations stemming from multiple sources must not be considered multiple times (compare Chapter 2.1.4). If, for example, a gravitational acceleration is applied in both a structure dynamic and in an aeroelastic instance, its contribution to the forces and moments will result in the load vectors of both instances. If loads from the aeroelastic shall now be transferred to the dynamic instance, the doubled effect of the acceleration can be removed, when the resulting forces are subtracted from the resulting load vector *before* they are transferred. In this example (aeroelastic and dynamic instance), the same applies for the elastic forces $K \cdot u$ in the system, as they are contained in both analyses. This can be seen when comparing equation (2.56) for aeroelastic modelling with equation (2.62) for dynamic modelling. The components, which are relevant for coupling aeroelastic with transient analyses, occur in the governing equations of direct aeroelasticity (compare Chapter 2.1.4).

$$\vec{P}^{(el,SM)} + \vec{P}^{(el,AD)} + \vec{P}^{(inert)} = \vec{P}^{(extra)} + \vec{P}^{(appl)} \qquad \text{(2.56 revisited)}$$

Elastic and inertia related load components ($\vec{P}^{(el,SM)}$ and $\vec{P}^{(inert)}$) can be determined from a structural dynamic solver, if the three remaining load components are available:

- Pure aerodynamic forces and moments: $\vec{P}^{(el,AD)}$
- Forces and moments resulting from extra point displacements u_x: $\vec{P}^{(extra)}$
- Further, externally applied load: $\vec{P}^{(appl)}$

$\vec{P}^{(el,AD)}$ occurs on the left hand side in equation (2.56), while $\vec{P}^{(extra)}$ and $\vec{P}^{(appl)}$ occur on the right hand side. Therefore, to properly consider the aeroelastic effects during a transient analysis, the vector

$$\vec{P} = -\vec{P}^{(el,AD)} + \vec{P}^{(extra)} + \vec{P}^{(appl)} \qquad (4.1)$$

needs to be assembled from the aeroelastic instance and applied as external excitation to the structural dynamic one according to equation (2.62)

$$M \cdot \ddot{\vec{u}}(t) + D \cdot \dot{\vec{u}}(t) + K \cdot \vec{u}(t) = \vec{P}(t) \qquad \text{(2.62 revisited)}$$

resulting in

$$M \cdot \ddot{\vec{u}}(t) + D \cdot \dot{\vec{u}}(t) + K \cdot \vec{u}(t) = -\vec{P}^{(el,AD)} + \vec{P}^{(extra)} + \vec{P}^{(appl)} \tag{4.2}$$

This equation system couples the structural dynamic calculation with aeroelastic evaluations. Solved with e.g. the Generalized Alpha Method it provides displacement, velocity and acceleration fields for discrete time steps t_i. For this purpose, respective data fields must computationally be prepared and an appropriate amount of space needs to be reserved in memory (indicated in Figure 4.7).

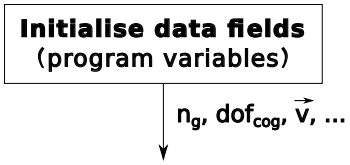

Figure 4.7: Initialise task specific program variables

With available control surface deflection data, the aeroelastic solver input can be replaced in each time step. Control surface deflections might result from an initial trimming calculation first, and as an explicit input (like a stick input) or from a control system in later time steps. The manipulated aeroelastic solver evaluates the load state and provides aeroelastic moments and forces. The load components necessary for the dynamic instance are then assembled according to e.g. equation (4.2), what is depicted in Figure 4.8 (a). The resulting data is applied as external excitation in the current time step. After the solver step, displacements, velocities or accelerations can be extracted from the transient instance and serve for follow-up studies, what can be seen in Figure 4.8 (b).

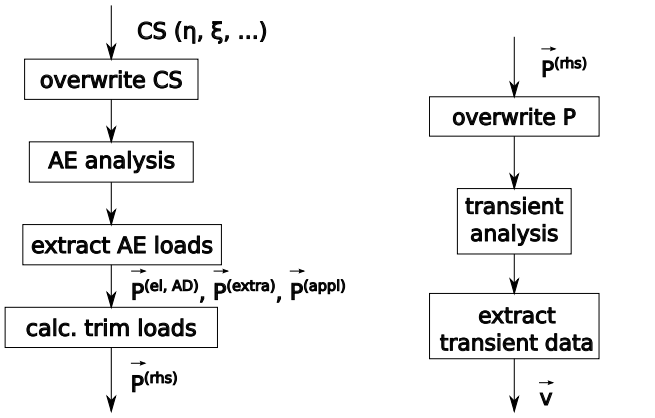

(a) Trim loads (b) Transient response

Figure 4.8: Determine and extract loads and responses

The velocity field contains the information of rates (like the pitch rate). The displacement field

can be used to evaluate the change in the AC position from one time step to another. From a structure mechanical point of view, especially its rotational DoFs are of interest, as they are the interface to flight mechanical quantities. The pitch movement shall serve as an illustrative example. Neglecting wind influences, the pitch angle Θ flight mechanically consists of the climb angle γ and the aerodynamic angle of attack α:

$$\Theta = \gamma + \alpha \tag{4.3}$$

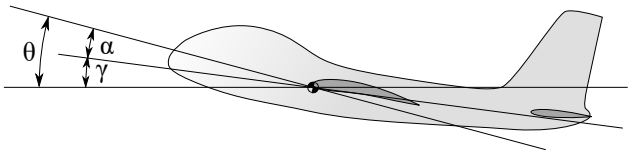

Figure 4.9: Pitch angle, angle of attack and climb angle

Assuming that changes in γ occur as a result of a changing load situation, represented by α, a perturbed Θ can be interpreted as a change in α, first:

$$\Delta\alpha \approx \Delta\Theta \tag{4.4}$$

The change in the aerodynamic load situation results in a new climb angle, which can be determined through the transient instance, for the next time step.

The accuracy of the aeroelastic solver is a critical element in this process chain. Providing the external loads, every inaccuracy passes through to the transient solver and leads to inaccurate transient data. This can be seen when comparing the altitude change over time, resulting from the trimmed loads of the two aeroelastic solvers (optimisation based solution and direct solution), as done in Figure 4.10.

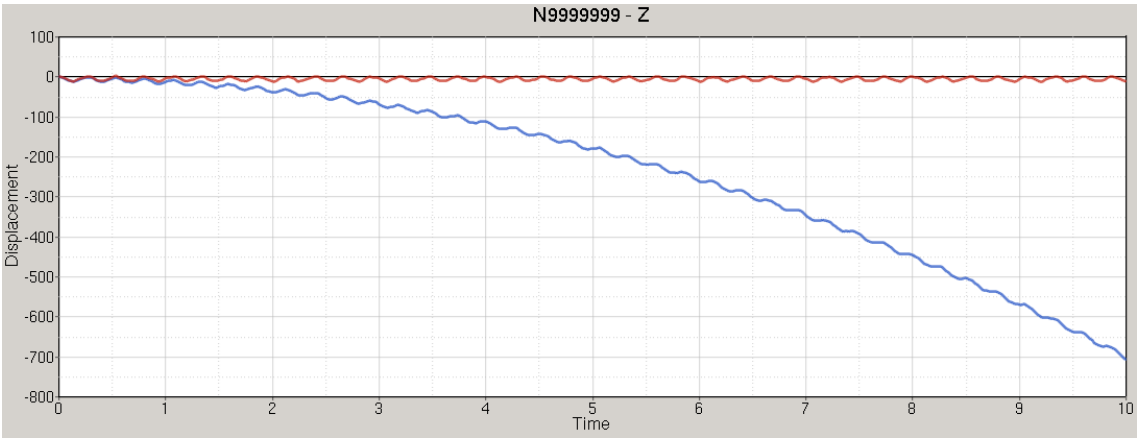

Figure 4.10: Direct and optimisation based aeroelastic solver in transient aeroelastic analyses

The forces and moments determined with standard settings of the optimisation based approach naturally show a load residuum F_{res}, which does not come from bad modelling but from the method itself. Over time this residuum leads to a noticeable loss in altitude.

The graphical progression matches the parabolic trajectory resulting from the acceleration, which occurs due to the remaining, not perfectly trimmed loads of the AC ($h(t) = \frac{a_{res}}{2}t^2$). The numerically remaining acceleration ($a_{res} = \frac{F_{res}}{m_{AC}}$) is considered as appropriate level of trimming inaccuracy in most steady aeroelastic applications. The monolithic solver does not lead to comparable inaccuracies, as its residuum is a result of the algorithm solving the mathematical equation system, and not of the aeroelastic method. It must be considered as the superior solver for applications with unsteady character, where higher inaccuracies lead to physically insensible behaviour.

Using the monolithic aeroelastic solver, control surface deflections can be varied as free input variables, when they are defined as respective trim DoFs of the aeroelastic problem. It is then possible to apply a pre-defined time-dependent control surface slope in an analysis and thus to study the aeroelastic responses of the system through the dynamic instance. The respective control surface values are overwritten through the LAGRANGE-python-API, again. Applying a pilot command, like the generic stick input from Figure 4.6 as control surface slope for the ailerons, leads to a roll movement. Aerostructurally relevant data can be determined. For the MDO-engineer, resulting structural response progressions must be highlighted as very valuable outcomes of such analyses. The slopes of stresses and strains over time help directly to understand structurally critical effects.

The abstract relationships between the components participating in a transient aeroelastic analysis are visualised in Figure 4.11.

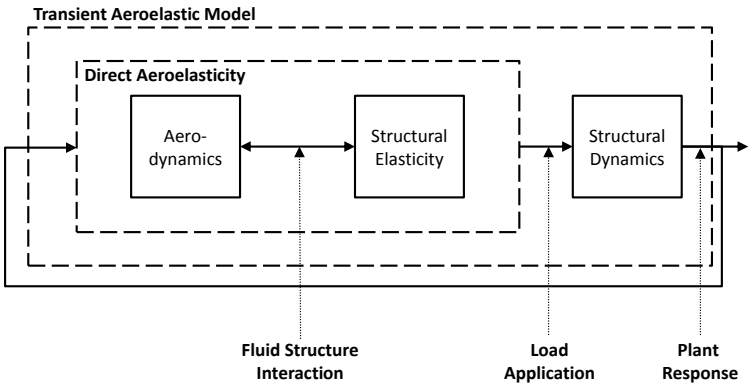

Figure 4.11: Transient aeroelastic analysis process

4.2.2 Closing the Loop by Flight Control Laws

The capability of using aeroelastic loads in a structure dynamic analysis as described in Chapter 4.2.1 shall now be extended by a flight control system model (compare Chapter 3.3). This empowers the control system to actively monitor and manipulate the loads extracted from the aeroelastic instance, which are then applied in the transient one.

So far, control surface deflections were used as variable parameters in the aeroelastic solution step of a coupled transient-aerostructural analysis. Studies evaluating structural responses to pre-defined control surface deflections or load situations can thus be performed. A FCS, however, determines the deflections *during* the AC-manoeuvre. Therefore, instead of applying pre-defined deflections, signals calculated by the FCS in each time step are considered. These signals then lead to plant responses. To evaluate a quantity for the respective engineering task, a resulting plant response must be selected, first. The FCS-command is generated according to the control laws and monitored through the plant response. The control architecture and complexity depend on the level of fidelity, which is contained in the system to be studied. If only scalar responses shall be controlled, a low-fidelity SISO-controller might be modelled internally in the framework-script while more complex controllers, often given as Multiple Input Multiple Output (MIMO)-systems might be accessible through external source code, only. The so determined, commanded signal can either be processed through an actuator or directly replace the data in an aeroelastic instance. It thus influences the transient behaviour in the following time steps. How a controller command is determined from an available plant response value is drafted in Figure 4.12.

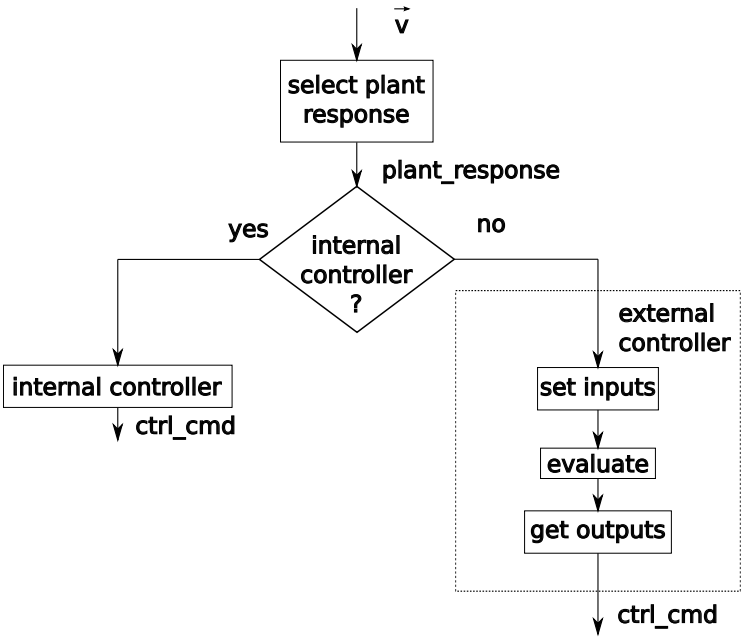

Figure 4.12: Determine controller command

To close the open loop system, the steps

- extracting a plant response to be controlled
- processing the corresponding signal
- calculating a resulting command
- applying it to the plant

must be performed. Data can now be exchanged between a controller and an aeroelastic model, what extends the integrated analysis process by a FCS. Numerical applications can be brought into interaction through physical quantities (load components, control surface deflections, etc.). Multi-fidelity w.r.t. FCS design is given by the fact that both, preliminary control laws or more detailed controllers can be respected in coupled analyses. A flowchart indicating information flows is given in Figure 4.13.

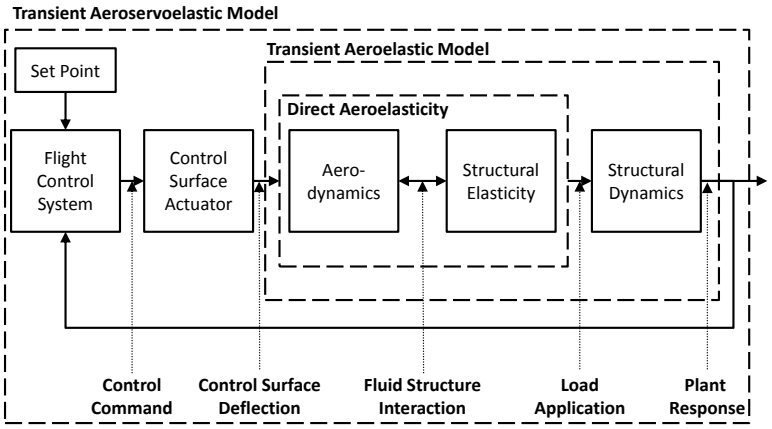

Figure 4.13: Transient aeroservoelastic analysis process

4.3 Aeroservoelastic Design Optimisation

As indicated in the beginning of Chapter 4.2, the results from the coupled analysis can now be used for the purpose of optimisation in order to find better designs. The main task for enabling this capability is the step of embedding the coupled analysis in an optimisation framework. Although the concrete embedding does always and strongly depend on the engineering task to be studied, some hints with general character can be given. The final implementation of the aeroservoelastic analysis within an optimisation frame results in a process chain, which captures all the couplings, described in the chapters before.

4.3.1 Optimisation Model Components

The capability resulting from using the governing equations of aeroservoelastic analyses in an optimisation model is aeroservoelastic optimisation. The main outcome of the governing equations are the forces and moments filtered through the possibility of enveloping within the

framework. This information is used to especially optimise for only critical loading situations, which are formulated through the constraint model for the optimiser.

To methodically realise the step from pure analysis to optimisation, a properly formulated optimisation model must be set up. As known from Chapter 3.4, main ingredients for an optimisation model are the objective model, the design model and the criteria model. The components were already described as isolated elements, while they shall now be brought into interaction with each other as indicated in Figure 4.14. The optimiser, which finally handles the outputs of the optimisation model, is visualised, as well.

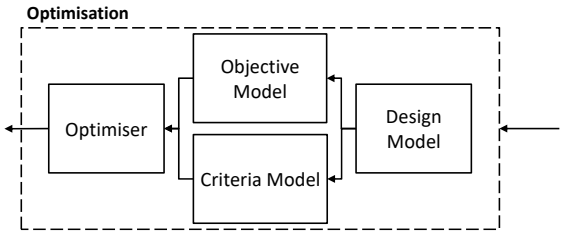

Figure 4.14: Servostructural Optimisation

The objective function shall be discussed as the first component of the optimisation model to be created. Although a variety of objective functions can be handled in the developed framework, it is focussed on the reduction of structural mass, here. A very important point concerning mass variations in the scope of ASE, is given by the fact that the CoG may be displaced and structural responses may change over the optimisation iterations. In the context of servostructural analyses, this alters the system responses calculated by the FCS. How strong such quantities are allowed to be changed through the optimisation, depends on the permitted design flexibility and thus on the design model.

As a second component of the optimisation model, the design variables must be highlighted. If only small changes in the state variables are allowed, the change in the system response will be rather small. The amount of acceptable variation defines the dimension of the feasible design space. However, not the absolute range of the design variables alone, but the geometric region in the AC structure, which is affected by the permitted flexibility, controls the response of the overall system. Examples for the effect of design variables on the aeroservoelastic system can be found, when thinking of flight stability. A relatively small change of the mass distribution at the aircraft tip or tail may lead to more flight instability than stronger mass-variations in the wing sections. While such relationships between design model and flight mechanical effects are described from a theoretical point of view, here, they are used in practical applications, as well. The controlled transfer of fuel between tanks can be named as example technology to actively manipulate the CoG in modern AC.

The third component of the optimisation model is the criteria model. The design and the

optimisation model define which parameters are to be varied to achieve an optimal value of a physical quantity through integrated designing. The criteria model, on the other side, decides which loading situations must be respected, therefore. The interdisciplinarily determined forces and moments lead to system responses, which are numerically assessed by the criteria model. Returning to the example of flight stability, a proper criteria model would detect infeasible mass and loading states through evaluation of e.g. a stability derivative constraint (see Nussbächer et al. (2016)). In this work, such loads could result from aggressive control commands. Based on the assessment of the criteria model, load enveloping highlights loading states which are critical for the AC structure.

The previous paragraphs pointed out what thoughts must be made, when implementing the components of an optimisation problem for applications with FCS in the loop. With that and the importance of the governing equations in the scope of MDO in mind, solution sequences for aeroservoelastic optimisation can be derived. The analysis model must always be brought into interaction with the optimisation model. Two approaches, one based on the other, realising such a data exchange shall be explained in the following.

4.3.2 Process Chains Coupling the Analysis into an Optimisation

The loads from a closed aeroservoelastic analysis process, evaluated by a criteria model and extracted through enveloping, can directly serve as input for a numerical optimisation algorithm (see Figure 4.15).

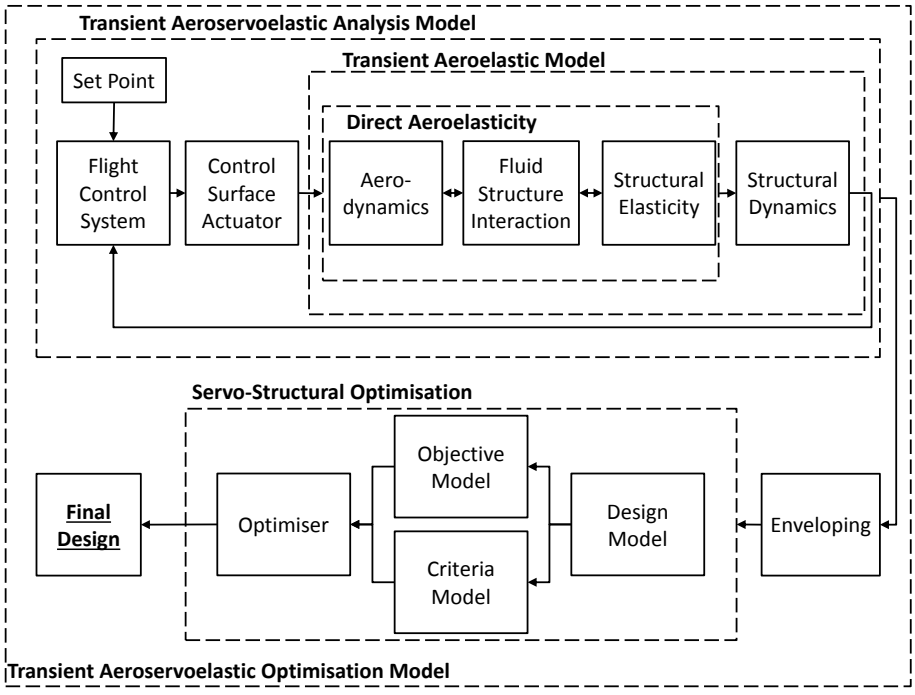

Figure 4.15: Aeroservoelastic optimisation process without feedback between optimisation and control system

Linking the analysis (Figure 4.13) with the optimisation step (Figure 4.14) over an enveloping feature leads to a process as depicted in Figure 4.15. The resulting process shall be described in more detail, now. Common system evaluations will start with an AC in a trimmed flight state, where no control activity should appear. A disturbance or a control surface input might change the loading situation at a certain, discrete time step in the transient aeroelastic analysis. This alteration leads to a new state of flight. As the FCS monitors the aircraft flight behaviour in the aeroservoelastic evaluation, it will react according to its control laws. After being processed through an actuator, its commanded output is applied as input to the aerostructural system. During all time steps, a criteria model evaluates the resulting structural responses and enables highlighting of critical time steps through enveloping. The associated manoeuvre forces and moments are considered in the subsequent optimisation step, then.

The result of this subsequent optimisation will be a design optimal for those loading situations, detected by the enveloping which accompanies the aeroservoelastic analysis. However, forces and moments change with an altering structural design, what is not respected with the process in Figure 4.15. Neither a re-analysis of the determined structural layout, nor a re-assessment of the resulting plant with the FCS is performed. Without this feedback, the resulting solution can not be seen as integrated in the scope of structural design optimisation. The integration of the analysis into the optimisation is implemented like an open loop system. Therefore, an approach iterating between analysis and optimisation is developed in the following.

Respecting an update of the structural model shall be possible in an integrated way, i.e. the model update must be applied for all contributing instances. In order to realise this, the already available optimised FEM-model needs to be embedded in the framework. As the framework was set up such that all instances work with the same FEM-model, the update must be applied only at one central point (compare Figure 4.5 and 4.16). Then, model-consistency is inherently respected through the architecture, a manual supervision is not necessary.

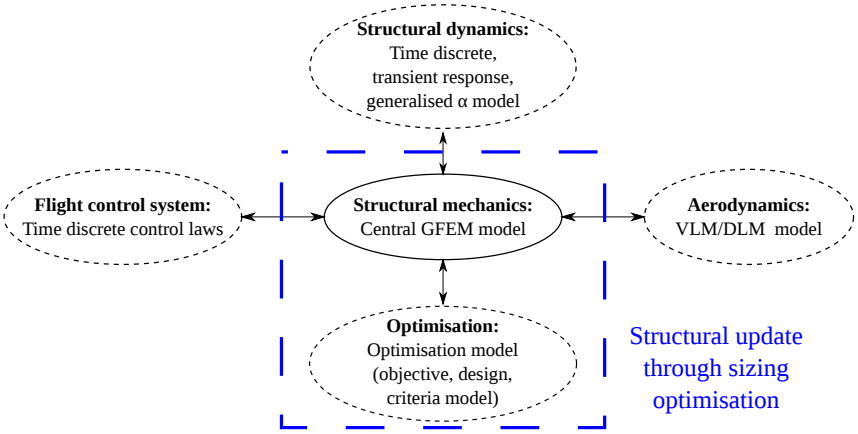

Figure 4.16: Updating the shared GFEM after optimisation

As soon as one optimisation run finishes, the resulting model is updated and a new iteration can start, automatically. The new design is evaluated aeroservoelastically and the enveloped forces and moments are used to find the next model update. This process is executed as long as changes in the structure occur from one optimisation to another. Bringing together all the points discussed above leads to the process visualised in Figure 4.17.

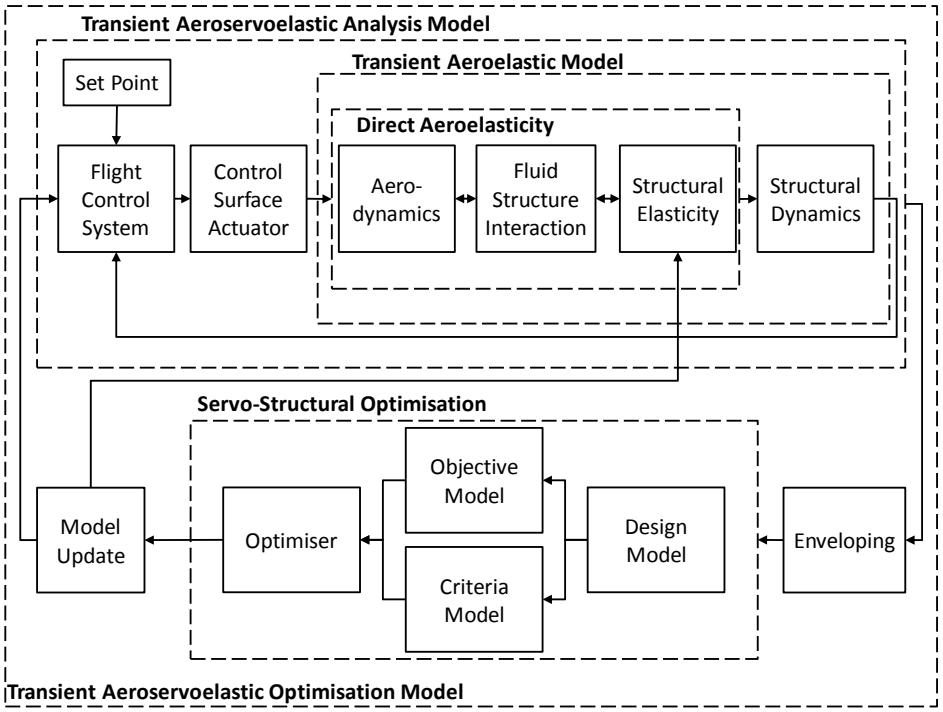

Figure 4.17: Aeroservoelastic optimisation process with feedback between optimisation and control system

As the primary design variables consider structural state variables in this work, some aspects on changing the structure w.r.t. the overall optimisation process shall be pointed out. The responses, and thus the loads resulting from an optimised structural model, must not necessarily vary strongly from one optimisation to the next. The amount of respective variability depends on how much design flexibility is granted to the optimiser. For only small structural variations, the controller inputs might be similar between two optimisations, what applies for its outputs, as well. The adaptation of the criteria model to FCS responses is new ground in MDO studies and demands further research. A highly critical point in this regard is the necessity to derive the analytical relations between FCS outputs and the respective aeroelastic responses of the system, which first demands to realise a strong coupling in the governing equations. For structural sizing with small amount of flexibility, the strongest model change will usually occur from the initial to the first optimised design. As forces and moments can be traced back to the controller, the load update between two runs depends on the impact of structural variations on the FCS. If e.g. the main FEM information used by the respective controller connects to

the CoG, the change in the control command should as well be small, as long as the sizing alters the FEM information only slightly. In case of structural shape or topology optimisation, where the structure varies more dramatically, a different behaviour can be expected. A higher number of enveloped loads results, then.

Thoughts on further extending the aeroservoelastic design process

With the overall design process considering aeroservoelastic effects being described now, still some open issues remain in the scope of integrated structural airframe design. The generated process can be used as a base for adding further design components. Enabling to study the interaction of configurational changes like shape variations with given control laws was a sensible next step to extend the process. The work in Deinert (2016) could be brought together with the here presented approach, what still does not solve the issue of a weak coupling of the various disciplines, however.

The process described so far is set up for changes of the internal airframe structure, only. Variations in the control system itself and the resulting effects on the aeroelastic plant might be sensible to study, as well. To use gradient based strategies for controller optimisation, respective sensitivity information is necessary. Such gradients depend strongly on the FCS design itself. A general formulation and implementation is expected to be very time-consuming and therefore usually not sensible. If available, automated model generation tools may support the modelling activities. Another possibility is given, when working with the underlying source code directly. If differentiation shall be approximated numerically, problems coming with the step size dilemma must be kept in mind. If control laws are implemented using computational variables of the complex data type, complex step differentiation can bring some big advantages. It must, however, be pointed out that the otherwise necessary step of re-implementing or at least revising an already existing, highly complex controller, can be a time-consuming task. In that scope, certification of the final result may become a further issue, that needs to be properly thought of.

If the issue of controller sensitivities was solved, a wide range of aircraft engineering tasks could be studied. FCS-gain parameters could be optimised with a GFEM in the loop. The controller gains have a very strong impact on the responses obtained by the system. Therefore, such analyses and optimisations, bear a high potential for design improvements. Further, combined studies, taking both, structural state variables and controller gain parameters, into account in the optimisation step, were possible. Even analyses simultaneously varying the aerostructural shape and sizing the servostructural design (both structural sizing and controller gain adaptation) can be thought of with the given process and framework, then.

4.4 Flight control system in the overall aircraft design process

As the FCS is a complex component within the MDO-supported design process, its integration is commented separately in this chapter.

The three phases of aircraft design according to Raymer (2018) are

- conceptual design
- preliminary design
- detail design

which can be seen as subcomponents in the sequential overall process, as depicted in Figure 4.18.

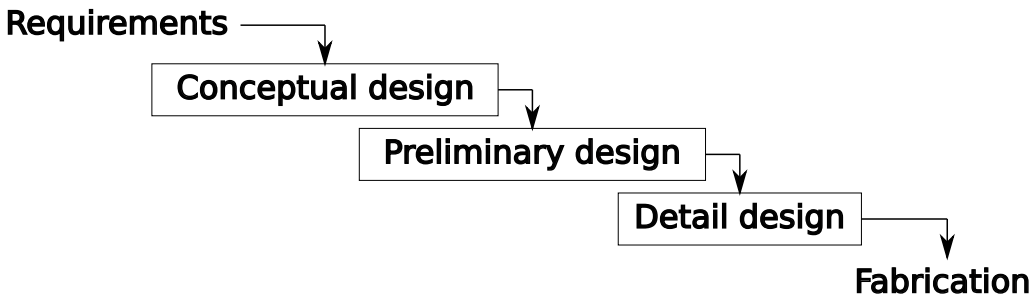

Figure 4.18: The three phases of aircraft design

Major work in the main disciplines aerodynamics and structures is first conducted in the preliminary phase ("design major items" in Raymer (2018)). However, in modern AC design the respective centres of competence support the aircraft development throughout all conceptual activities. The same applies for the MDO engineer, who supports the conceptual designer with the numerical model generation (Chapter 3) and their integration into respective numerical processes (like depicted for aeroservoelastic analyses and optimisations in Chapters 4.2 and 4.3). The main outcomes when following MDO-methodologies for the final conceptual design (which serves as input for the preliminary phase) are improved mass-estimations and better assessments of aircraft performance. The field of flight control system on the other hand is addressed not at all or only vaguely in the conceptual phase. This can again be seen in Raymer (2018), where two main design iterations are described, what is visualised in Figure 4.19 (a). Both the initial and the revised layout are altered through design iterations. While aero, weight, propulsion and structures can be found here, flight control is not mentioned. Applied methods in e.g. aero, weight or structure were developed further and further over the last decades. Numerical methods like FEM or CFD (with the VLM or the DLM as low-fidelity representatives) found entry in state of the art designing processes. With this work, flight control laws are put into the design iteration, which leads to a revised layout, as the created processes from Chapter 4.2 and Chapter 4.3 enable the intergrated evaluation of aeroservoelasticity in

early design phases. While the FCS designer previously was consulted during preliminary design, only, he can start with first (supporting) analyses in the iterations for the conceptual layout, as marked in green in Figure 4.19 (b). The insights of these activities do not only improve the input for preliminary design but also provide valuable information when it comes to designing the actual FCS, later. Aerodynamic lattice models or finite element models being created for conceptual studies are not used in preliminary or detail design. Of course, the same applies for the (simplified) numerical control laws. Still, times for model development are reduced, what gives more time to improve the developed systems, compared to the conventional process, later. This becomes clear, when considering that the configuration is frozen before preliminary design. When laying out the flight control system is only initiated then, the available design space is limited, compared to performing first studies within an MDO frame during conceptual design.

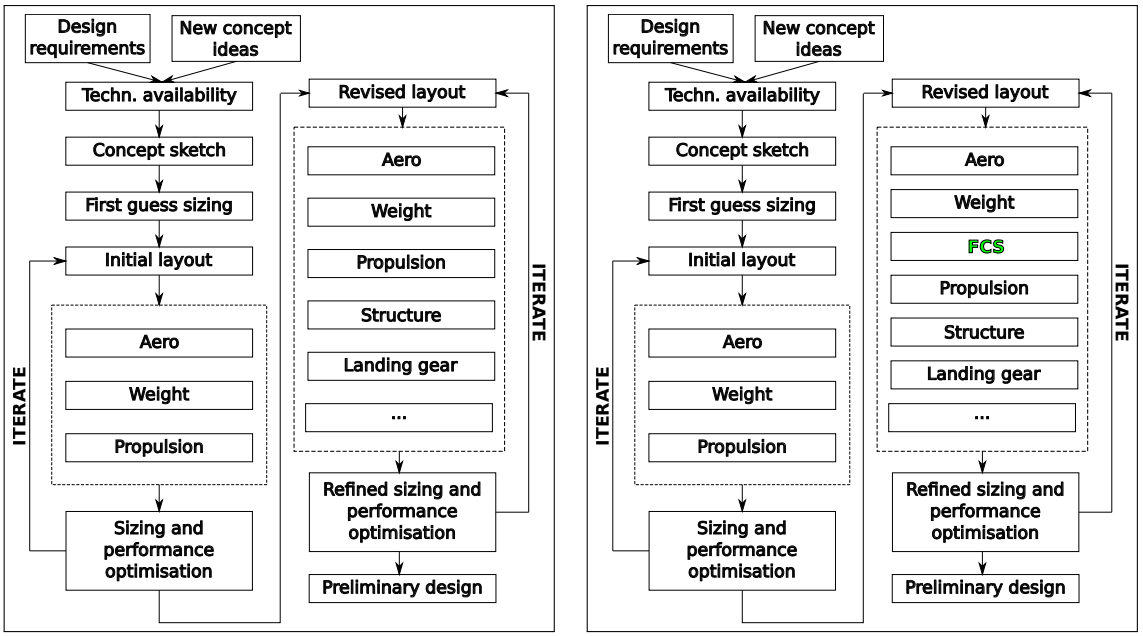

(a) Conventional process according to Raymer

(b) FCS-extended process

Figure 4.19: Iterations in aircraft conceptual design

5 Applications of Aeroservoelastic Airframe Design Optimisation

The methods described in the previous chapters shall be applied now on a set of selected use cases. For this purpose a generic MALE UAV, the OptiMALE is presented in Chapter 5.1. To get an insight in the practical side of multidisciplinary design optimisation, in Chapter 5.2 structural components of the OptiMALE are sized considering aeroelastic constraints within the numerical analyses as described in Chapter 2.1 and in Chapter 3.1. Hereafter, it is demonstrated how flight mechanical stability can and must be respected in the optimisation process in Chapter 5.3. To analyse with an actual FCS in the loop, a time-discrete pitch controller is used to actively manipulate different loading states and manoeuvres in Chapter 5.4. The capabilities of the framework for studying load alleviation topics are presented in this context, as well.

The focus of all analyses will lie clearly on finding a structural layout, that is able to carry the demanded loads. While the primary target of MDO is to determine a weight optimal design, an optimised design can be heavier than the corresponding initial one, if the latter is not feasible w.r.t. a desired loading. In the design process described in this work, models created with DESCARTES contain generic mechanical properties like rib or spar thicknesses or generic composite layups. The applied values stem from engineering experience and are a first guess of an AC layout. If the resulting design is infeasible, LAGRANGE aims to find a feasible one and if the initial layout is feasible, it helps to reduce mass by structurally sizing it.

5.1 The OptiMALE UAV Optimisation Demonstrator

The OptiMALE demonstrator is a numerical MALE UAV model, used for the purpose of demonstrating optimisation capabilities on an aircraft model of industrial size. Due to its high wing aspect ratio, aeroelastic effects have a strong influence on its structural integrity. Various examples on optimisation studies with aeroelastic constraints for the OptiMALE are available and can be found e.g. in Daoud et al. (2015) or Nussbächer et al. (2018). This work extends the OptiMALE model by a pitch controller and studies different load alleviation tasks.

Aeroservoelastic model of the OptiMALE

The OptiMALE is a T-tail configuration aircraft with two engines, mounted at the tail. Its fuselage has a length of $15m$ and is made of aluminium. The model of the initial design in use has a Maximum Takeoff Weight (MTOW) of $8.45t$. The wing has a span of $28m$ and contains ribs, spars, stringers and skin elements, which are mainly made of composite materials. (The rear spar and some ribs in the centre wing region are made of aluminium.) To provide maximum roll moment, ailerons are installed at the wing tip region. Inboard and outboard roll spoilers are modelled on the upper skin to support banking. Elevators and rudder, used for pitching

and yawing are integrated in the T-tail.

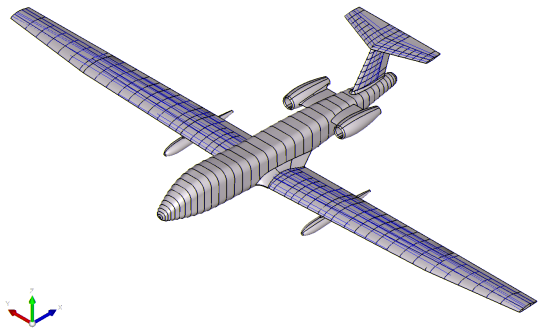

Figure 5.1: OptiMALE aircraft model

The first 10 eigenfrequencies corresponding to elastic deformations are listed in Table 5.1. They are of special interest for the Rayleigh damping model. The coefficients α_1 and α_2 are determined on the base of a modal analysis of the respective, current structural model. As the structure changes through optimisation, the modal responses change as well. Therefore the structural model is re-analysed after numerical sizing. The resulting frequencies of the first two elastic modes contribute to the Rayleigh damping matrix, then.

Mode number	Eigenfrequency [Hz]
1	2.2787
2	3.8367
3	5.0052
4	6.4312
5	6.9709
6	8.0387
7	8.1501
8	8.3330
9	8.4803
10	9.3815

Table 5.1: Elastic eigenfrequencies of the OptiMALE aircraft model

The structural model uses a discretisation of approximately 31.000 finite elements and 186.000 numerical DoFs. The aerodynamic doublet lattice model consists of 2.800 boxes.

Time-discrete control systems are modelled with external software and are linked to the aeroelastic model as a dynamic library. Figure 5.2 represents the feedback pitch controller as exemplarily used in Chapter 3.3.2 (compare Figure 3.22) already. It is designed to monitor the pitch rate q, to accordingly provide an elevator command η_c counteracting unintended pitching and is applied for the OptiMALE demonstrator, now. The experienced AoA is processed both

through the subcontroller-components "pitch damper" and "alpha-feedback". The output signals are controlled by an "eta-rate-limiter", which assures that calculated elevator deflections do not surpass a pre-defined limit value (which e.g. an actuator might not be able to realise). Hereafter, an "eta-integrator" is determining the elevator command using its externally calculated trim value. Which physical quantities are handled within a particular subcomponent depends on the respective FCS design. In Figure 5.2 for example it can be seen that gain factors are externally fed into the "pitch damper" and the "alpha-feedback" but not in the "eta-integrator", where a necessary gain might be hard-coded within the component itself.

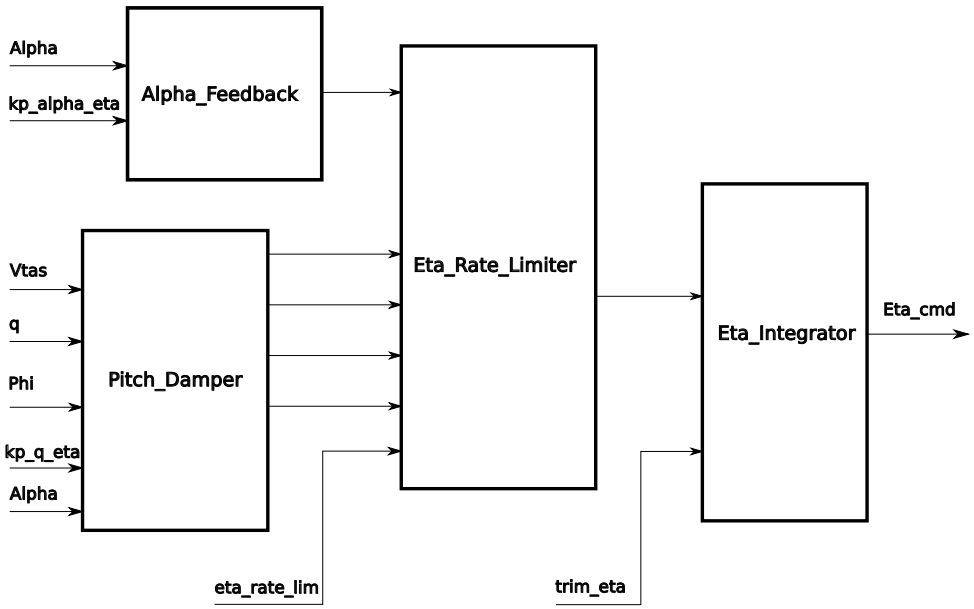

Figure 5.2: Pitch damper and elevator integrator applied for the OptiMALE

Optimisation models

The main task of the following studies will be the optimisation of structural mass m in the wing, while assuring structural integrity by means of strength and buckling.

- Objective Model: The mass optimisation as primary target is achieved through variation of structural properties. The resulting changes in the geometric volume leads to changes in the respective mass values.

  The initially variable mass for the calculations in Chapter 5.2 and 5.4 sums up to $489.1kg$, which is distributed over a high number of design variables. This means that 5.8% of the MTOW of the AC shall be varied numerically.

  Chapter 5.3 will use the wing sized in 5.2 and optimises the tail, then. Therefore 40.6% of the mass from the lightweight tail is made variable for the optimiser.

- Design Model: Not only the thickness of isotropic rib- and spar-webs but the layer thickness values in composite rib- and spar-webs and in the wing-skin are varied in the sizing

studies. Variables on the left and the right side of a component (wing or tail) are linked, assuring a symmetric configuration after the optimisation. For the wing sizing analyses, especially the centre wing is of interest as main loading acts in the wing root region. Figure 5.3 visualises design variables in the centre wing by different colours. Each of the in total 615 design variables links different numbers of structural elements.

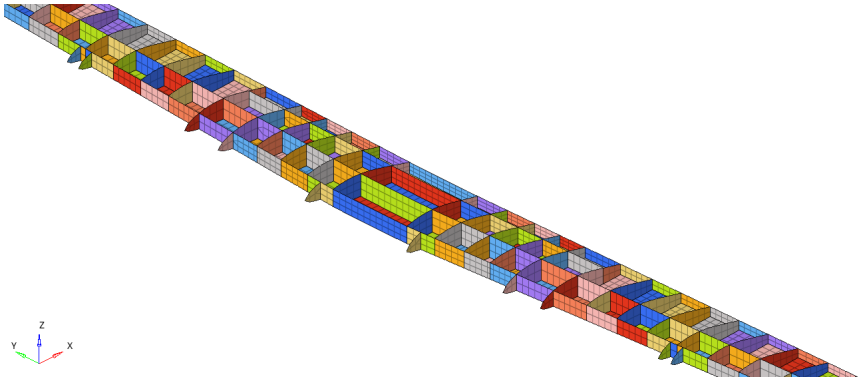

Figure 5.3: Design variables for the centre wing

- Criteria Model: The criteria model is set up to assure structural integrity by the classical maximum strain criterion for composite materials. Mechanical strains in the wing skin layers and in the layers of composite spars and ribs are therefore monitored and converted into reserve factors and constraint function values. For conventional aluminium spars and ribs the experienced stresses are compared with allowed stress quantities, accordingly. Further local buckling of the structural elements is considered as an important part of the constraints. Special criteria for both aluminium and composite material are computed.

  Of high importance for the criteria model are the selected load cases, which the structure is evaluated for. While each of the following analyses differ in some special loading situations, a set of representative load cases, common for all studies, is described in the following chapter on classical sizing optimisation.

This optimisation model setup used for classical sizing is sufficient to demonstrate the interaction of control system and structural design, here. In design projects for modern aircraft structures, maximum strain and structural buckling are not necessarily the crucial design drivers. More advanced criteria would additionally be applied. Damage tolerance, like impact constraints or constraints observing joints between structural components, can be named as examples.

Numerical optimisation algorithm

The selection of a suitable optimisation algorithm has an important effect on both the quality of the final design and the quantity of system evaluations, necessary to reach it. For the linear

aerostructural problems to be studied, mathematical functions are expected to be smooth and continuous. Therefore gradient calculation is possible. Due to the high number of constraints and due to the numerical nature of the problem, the modern NLPQL optimiser is selected (see Schittkowski (1986)).

5.2 Classical Structural Sizing

To get an idea of a classical sizing task, the OptiMALE wing shall be sized using the previously described optimisation model for selected load cases. It will be seen that the initial design for the OptiMALE is evaluated as infeasible by the optimiser. So, not only a basic mass reduction will be performed, but the problem to find a feasible design is solved in parallel, as well. This chapter gives a practical insight in the state of the art design process with numerical optimisation considering aeroelastic constraints. It does not aim to describe all details of the overall sizing process, as established in aircraft industries. Rather it wants to give a rough overview on its most important outcomes, such that not only structural and MDO engineers can follow the upcoming explanations. Respecting control related and transient demands will be covered in the following chapters. Due to the briefness of the overview on the design process as presented below, hints on literature with further insights shall be given. Various studies approaching the classical aircraft sizing problem with MDO-approaches similar to this work were published: Examples for finding proper designs with a focus on the structural side are given by Daoud et al. (2012) or Schuhmacher (1995). An example for shape variation using aeroelastic constraints is Deinert (2016). In Petersson & Daoud (2012) both static and dynamic requirements are considered. Teufel et al. (1999), Teufel (2003), Petersson (2009), Petersson, Leitner & Stroscher (2010), Petersson, Stroscher & Baier (2010) approach flutter and gust demands. For more details on the aircraft structural optimisation process Daoud et al. (2015) and Schuhmacher et al. (2012) shall be suggested.

Classical load cases for structural sizing

The AC shall be sized for flight conditions at $Ma = 0.2$. The three flight altitudes of interest are $h = 0m$, $h = 5000m$ and $h = 10000m$. Eight load factors (ratio of lift over weight) ranging from $n = -1.0$ to $n = 2.5$ will be studied. This results in 24 loading situations (Table 5.2).

The OptiMALE is trimmed aeroelastically for these load cases as described in Chapter 2.1.4. The forces and moments experienced by the structure result from the determination of the necessary angle of attack α and elevator deflection η such that the OptiMALE is in a state of equilibrium.

Analysis

Aeroelastic analyses of the 24 load cases provide results like plots of the displacement-fields, distributions of stresses and strains, contours of reserve factors in the structural components

Load case description	Push-over	Push-over	Push-over	Push-over	Cruise	Pull-up	Pull-up	Pull-up
$Ma[-]$	0.2	0.2	0.2	0.2	0.2	0.2	0.2	0.2
Altitude $[m]$	0	0	0	0	0	0	0	0
Load factor $[-]$	-1.0	-0.5	0.0	0.5	1.0	1.5	2.0	2.5
$Ma[-]$	0.2	0.2	0.2	0.2	0.2	0.2	0.2	0.2
Altitude $[m]$	5000	5000	5000	5000	5000	5000	5000	5000
Load factor $[-]$	-1.0	-0.5	0.0	0.5	1.0	1.5	2.0	2.5
$Ma[-]$	0.2	0.2	0.2	0.2	0.2	0.2	0.2	0.2
Altitude $[m]$	10000	10000	10000	10000	10000	10000	10000	10000
Load factor $[-]$	-1.0	-0.5	0.0	0.5	1.0	1.5	2.0	2.5

Table 5.2: Basic load cases for sizing of the OptiMALE aircraft model

and information on critical load cases and the critical criteria. As an example, the minimum reserve factors of the centre wing region over all load cases are displayed in Figure 5.4.

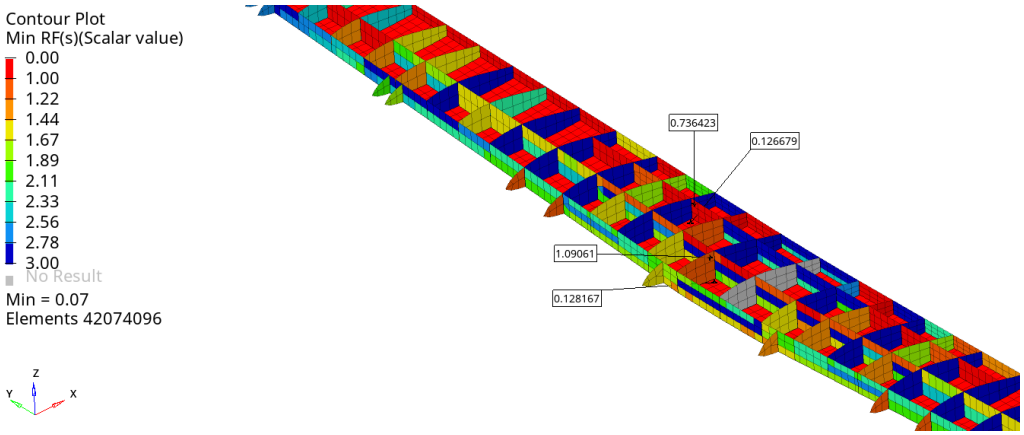

Figure 5.4: Minimum structural reserve factors for the 24 sizing load cases of the initial design

The wide areas of red elements together with the minimum value in the model being below 1.0 (see legend) mark the structurally critical regions for the given load cases by means of strength or buckling. The closer the experienced strains or stresses in the structure are to the respectively allowed strains or allowed stresses, the closer the reserve factors are to a value of 1.0. The criteria $rf > 1.0$ identifies areas with a feasible design and $rf < 1.0$ highlights regions, which violate the constraints and thus mark the design there as infeasible. The wing root sections are especially critical as high bending moments act here. Composite structures (like e.g. the wing skins) are evaluated using the maximum strain criterion as briefly discussed in Chapter 3.4.3. For isotropic materials the von Mises criterion is applied to detect structural failure. Different buckling formulas are used for isotropic or orthotropic materials. Especially the lower wing skin and parts of the spars seem to carry more load than they are able to, with this initial design. Figure 5.5 shows whether strength (numerical value 2) or stability (numerical

value 1) criteria deliver more critical reserve factors for a given component. The smaller the rf value, the more critical is the respective design.

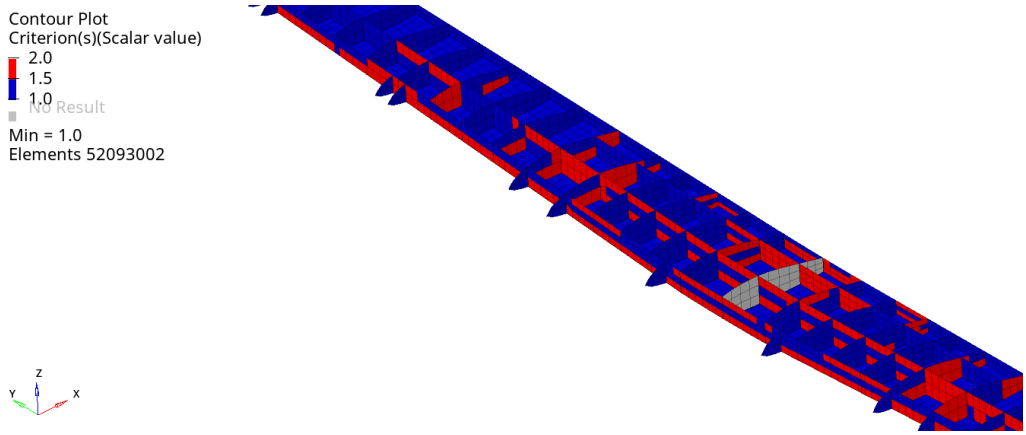

Figure 5.5: Critical criteria for the 24 sizing load cases of the initial design

An overview on the thickness distribution of ribs, spars and skin elements of the initial design is presented in Figure 5.6. The composite front spars are designed thicker than the isotropic rear spars. Especially in the centre wing region, where high bending moments are expected, element thickness values are intentionally increased. Comparing the thickness distribution of the initial design with the optimised design, helps to get an idea of *what* the numerical optimiser does. Controlling the reserve factor plot explains then *why* the algorithm locally reduces or adds material.

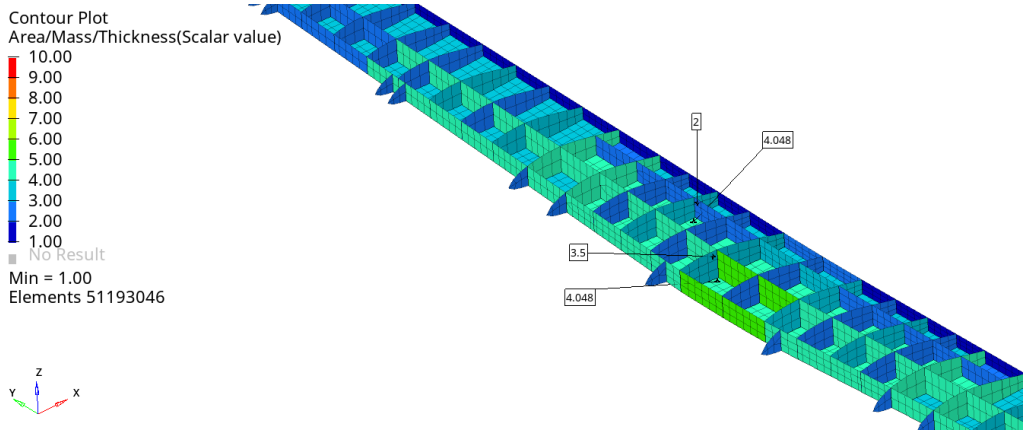

Figure 5.6: Thickness distribution of ribs, spars and skin elements of the initial design

Optimisation and re-analysis

The main target of the numerical sizing optimisation is to reduce structural mass. The optimiser will make use of unnecessary high reserve factors to reduce thicknesses in the wing components. The optimisation problem here formulates as follows:

Find a wing design with an optimal mass distribution of the AC, while assuring structural integrity by means of respective failure criteria for all given load cases.

Figure 5.4 showed that the initial design does not fulfil the structural requirements of the 24 given load cases. Therefore, both strength and buckling constraints shall force the optimiser to find a design with reserve factors ≥ 1.0. After the problem is defined properly and the respective components of the optimisation model are modelled completely, the algorithm can be started. Main quantities to be monitored over the numerical iterations are

- the objective function value
- the maximum value of the constraint violations
- the absolute number of the active constraints
- the design variable values

While ideally the objective function should decrease for an initially valid design, the maximum constraint violation and the number of active constraints should reach a value of 0, when convergence is reached. Design variable slopes help to see if state variables reach their defined boundaries.

The optimisation curves in Figure 5.7 show that the structural sizing process converges after 8 iterations for the given problem. Approximately 6.0% of the overall AC mass or 103.7% of the variable wing mass is increased using the variable mass in the wings. The maximum constraint violation as well as the number of active constraints are led to a value of 0 smoothly over the iterations.

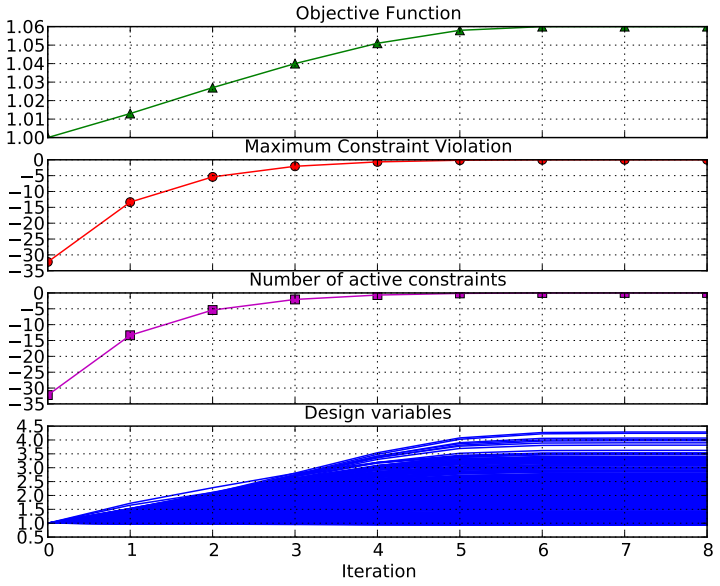

Figure 5.7: Optimisation curves for classical load cases

The minimum reserve factor is pushed above the desired value of 1.0, what is shown through the reserve factors of the final design in Figure 5.8. As expected, the root section is still the critical region of the design. While ribs and spars are strongly relieved from high loading, the skin still remains with a low but feasible reserve factor of 1.0. By comparing Figure 5.6 with Figure 5.9 it can be seen that the components in the most critical regions are stiffened and that thicknesses are reduced in less loaded areas. The necessity to stiffen wide areas mainly stems from the most critical load case in Table 5.2. A comparatively high angle of attack is necessary to produce enough lift in an altitude of $10000m$ for flying with $Ma = 0.2$ and a load factor of 2.5. This demand can still be fulfilled with the structural layout found by the numerical optimiser.

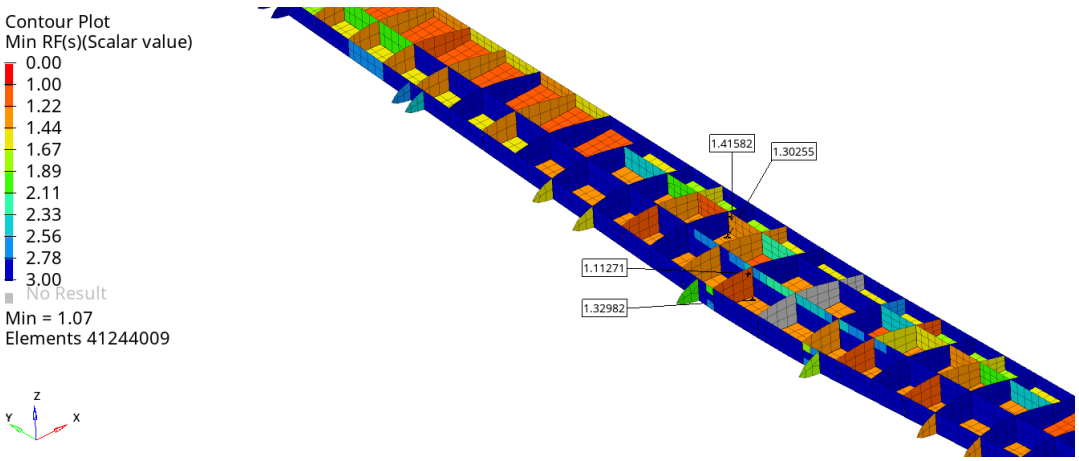

Figure 5.8: Minimum structural reserve factors for the 24 sizing load cases of the optimised design

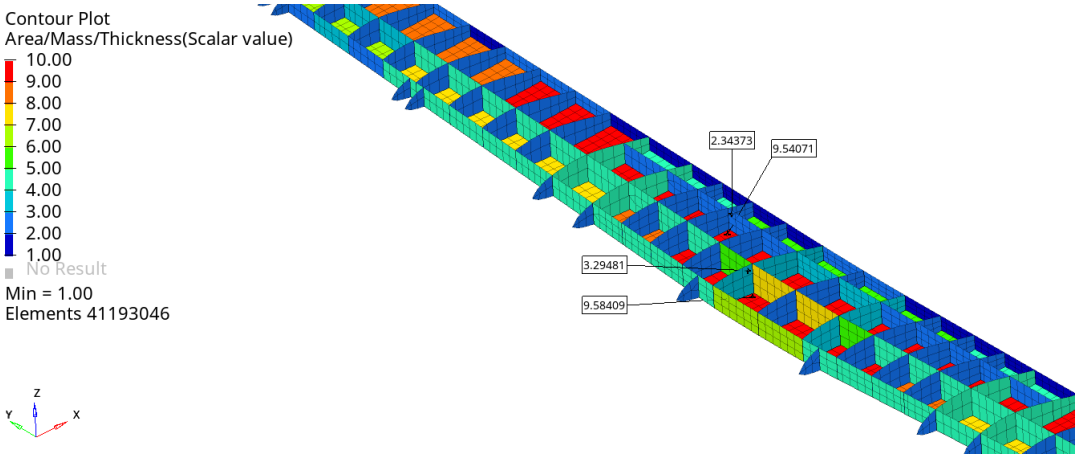

Figure 5.9: Thickness distribution of ribs, spars and skin elements of the optimised design

Summary

This study was taken out to give a basic idea of how structural components are sized through the application of computational optimisation. Classical load cases were considered, main components of the wing were varied numerically. A feasible design could be found based on an infeasible start layout. As a result, reserve factors were driven to their critical values as defined through the criteria model. Overall AC weight needed to be increased slightly, through sensibly shifting material within the wing. With the brief overview on classical sizing optimisation, a better understanding of the following studies is now given.

5.3 Structural Sizing with Aeroelastic Stability Derivatives

Stability derivatives resulting from the pitching moment due to incidence and the pitching moment due to pitch rate, given through equivalent variables M_α and M_q, are important values for the assessment of an AC design. M_α and M_q are key parameters in flight control system design. In MDO-based sizing optimisation processes of structures they are not well established, yet. While the pitch rate q, which mainly influences M_q, will actively be controlled in Chapter 5.4.1, this chapter deals with the pitch moment M_α due to incidence α. The dimensionless pitch moment coefficient C_m and its derivative, the pitch stability $C_{m\alpha}$ are defined as

$$C_m = \frac{M}{p_{dyn} S_{ref} c_{ref}} \tag{5.1}$$

$$C_{m\alpha} = \frac{\partial C_m}{\partial \alpha} \tag{5.2}$$

with the pitch moment M, the dynamic pressure p_{dyn}, the reference area S_{ref} and the reference chord length c_{ref}. The following study demonstrates the difference between optimising with and without respective constraints. Further studies analysing stability derivatives are e.g. Raney et al. (2001), Grafton & Libbey (1971) or D'Vari & Baker (1999).

Analysis and Methodology

Changes in mass and stiffness through structural sizing do affect aeroelastic stability derivatives. In detail design, when usually only single components are sized, these changes might not be crucial with regard to the overall aircraft. In phases where the design freedom is still comparatively high, the size of the optimisation model still has strong impact on the mass distribution over the airframe. Then, structural optimisation can lead to an undesired worsening of stability parameters and may even result in a flight mechanically unstable design.

A value of $C_{m\alpha} < 0$ is a key demand for static stability (compare e.g. Brockhaus et al. (2011) or Yechout (2003)). Aeroelastic stability derivatives are calculated as side quantities during the solution sequence of the aeroelastic solver applied in this work. As an available system

response, they can therefore be formulated and implemented as numerical constraints and can be used in the criteria model of an optimisation. For this purpose, a lower and an upper limit ($C_{m\alpha,l}$ and $C_{m\alpha,u}$) for a desired stability value have to be defined. For first studies, these limits can be set such that a given design is not allowed to deviate strongly in terms of its pitch stability. A design with a $C_{m\alpha}$ not within these boundaries is considered to be infeasible. A sensible constraint function formulation is given by equation (5.3). The demands posed to a physical and to a numerically normalised $C_{m\alpha}$ are represented in equation (5.4).

$$g(C_{m\alpha}) = 1 - (\frac{2(C_{m\alpha} - C_{m\alpha,u})}{C_{m\alpha,u} - C_{m\alpha,l}} + 1)^2 \tag{5.3}$$

$$C_{m\alpha} \in [C_{m\alpha,l}, C_{m\alpha,u}] \rightarrow \bar{C}_{m\alpha} \in [-1, 1] \tag{5.4}$$

It is sensible to normalise physical values for numerical analyses. A normalised form of equation (5.3) is given through equation (5.5), which allows to detect a flight mechanically infeasible design through a negative constraint function value, and is represented in Figure 5.10. A structural layout not fulfilling the demands of the new constraint is detected through $g(C_{m\alpha}) < 0$ as a result of $\bar{C}_{m\alpha}$ not being in $[-1, 1]$.

$$g(\bar{C}_{m\alpha}) = 1 - \bar{C}^2_{m\alpha} \tag{5.5}$$

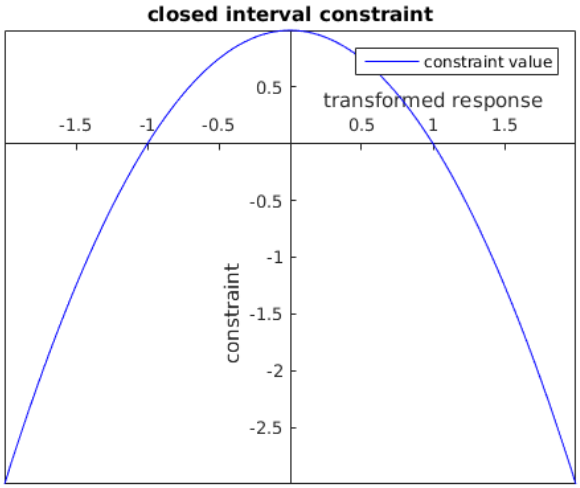

Figure 5.10: Aeroelastic stability derivative constraint

Later, different optimal designs are compared to the initial OptiMALE model by means of their stability derivative constraint values. The trimmed state of the starting design provides a numerical base for further studies. A change in a numerical value z through optimisation w.r.t.

the initial design is presented by a relative difference Δ_r. The pitch stability $C_{m\alpha}$ serves as an example.

$$\Delta_r z = \frac{\Delta z}{z^{(init)}} = \frac{z^{(opt)} - z^{(init)}}{z^{(init)}} \tag{5.6}$$

$$\Delta_r C_{m\alpha} = \frac{\Delta C_{m\alpha}}{C_{m\alpha}^{(init)}} = \frac{C_{m\alpha}^{(opt)} - C_{m\alpha}^{(init)}}{C_{m\alpha}^{(init)}} \tag{5.7}$$

Optimisation and re-analysis

The final design from Chapter 5.2 with its sized wings is used as initial design for this study. The impact of the structural mass distribution on the stability of the aircraft will be seen during the optimisation run. Different tail designs of the OptiMALE AC model are generated numerically by the optimiser. The thickness values of ribs, spars and the skin of the fin, the rudder and the elevator are grouped in sensible sets. The results of this grouping are 24 design variables representing 40.6% of the initial tail-mass, which are varied by the optimisation algorithm. Structural integrity of these elements is assured again through strength and buckling constraints evaluated for all components (ribs, spars, skins). The same load cases as in Chapter 5.2 are used to size the model. Although it is a relatively light structure, changing the tail has a particular impact on the pitch stability coefficient, due to its large lever w.r.t. the aircraft CoG. As a side effect, the trim-state and the resulting load situation are altered following the changes in the mass distribution. The elements to be varied numerically are shown in Figure 5.11.

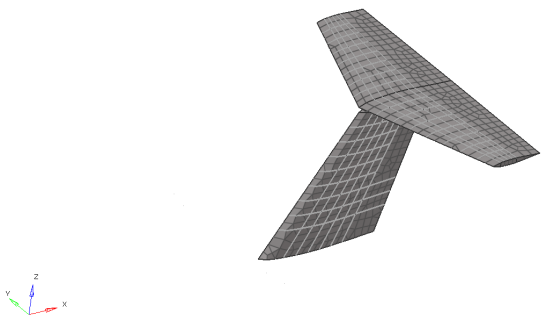

Figure 5.11: Finite elements of the tail, considered for structural sizing

The optimisation problem formulates as follows:

> Find a tail design with an optimal mass distribution of the AC, while assuring its structural integrity by means of respective failure criteria **and** simultaneously assuring that the pitch stability of the configuration remains close to its initial value for all given load cases.

To compare the influence of the stability derivative constraint on the optimisation run, first an optimisation without $C_{m\alpha}$-constraint will be performed. The resulting curves are shown in Figure 5.12.

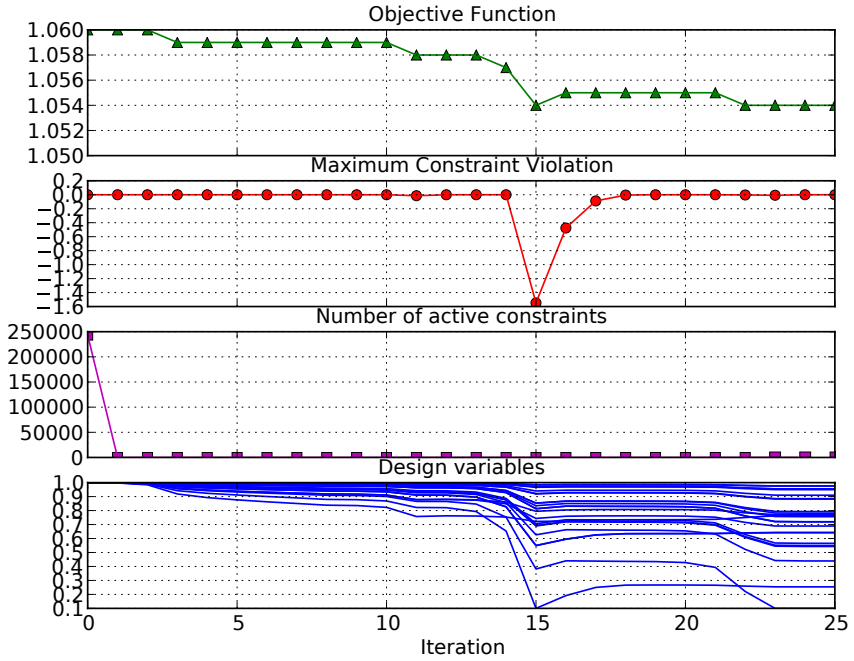

Figure 5.12: Structural sizing with structural integrity and without stability derivative constraint

W.r.t. the initial design of the optimisation, the overall AC mass is reduced by approximately 0.57% within few iterations. This corresponds to a reduction of 85.7% of the variable tail mass. The strong loss in mass explains with the fact that some design variables are able to decrease up to values of $0.1 - 0.4$. For these variables, the selected load cases do not pose critical boundaries in terms of structural strength and stability. During the optimisation, the trimming conditions are constantly changing, as the tail designs are changing. This effect is captured in the given problem. Flight mechanical stability, however, is not assessed at all.

The selected tail elements account for a rather small part of the aircraft total mass. Even this small contribution can already affect $C_{m\alpha}$ in an undesired way. This can be seen when a stability derivative constraint $g(C_{m\alpha})$ is included in the criteria model. To assure that no bigger changes in $C_{m\alpha}$ are obtained through the structural variations, its lower and upper boundaries $C_{m\alpha,l}$ and $C_{m\alpha,u}$ are set to $0.1-1.0\%$ of the initial $C_{m\alpha}$. Thus, the classical sizing optimisation with pure strength constraints is extended by the stability derivative constraints, now.

Compared to the previous case, the mass is not reduced as heavily, as the additional constraint adds a very strict boundary to the optimiser. It smoothes the behaviour over the iterations, what can be seen in both the slope of the design variables and the number of iterations.

The given variable mass in the tail is now reduced by only 28.6% (corresponding to a 0.19% reduction of the overall mass). The resulting optimisation curves are given in Figure 5.13.

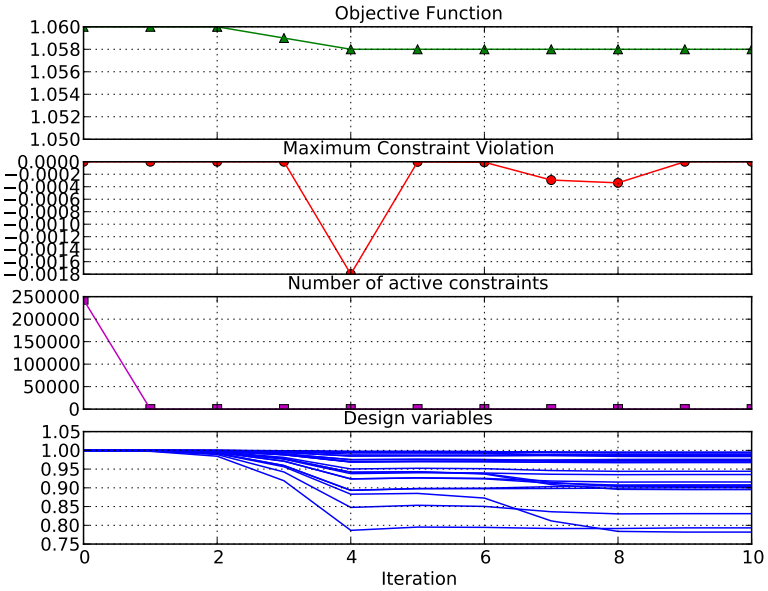

Figure 5.13: Structural sizing with structural integrity and with stability derivative constraint

When comparing Figures 5.12 and 5.13, it becomes clear how strongly the additional flight mechanical constraints influence the path of the design variables x over the iterations. The tail thicknesses are driven by fulfilling the flight mechanical constraint, now. Structural strength and stability are still contributing to the search direction through their respective gradients. Another side-effect concerning the gradients is given by the changing load situation over the optimisation. The trim states and the resulting AoAs are re-determined in every iteration. This is noticed by the algorithm and modifies the search direction accordingly.

A re-analysis of the two optimised designs shows that the classically sized tail is infeasible by means of the stability derivative constraint. The model obtained with the activated $g(C_{m\alpha})$ is a valid one. (Compare the g-values in Table 5.3.) For common optimisation studies the classical result was sufficient, as problems w.r.t. aircraft stability would not be detected, yet. Only in later design phases this issue had to be handled, usually for the price of high costs and engineering effort.

Design	$g(C_{m\alpha})$	$\Delta_r f[\%]$
Initial	$+0.039$	0.0
Pure sizing opti.	-0.580	-0.566
Derivat. & sizing opti.	$+0.0$	-0.189

Table 5.3: Stability derivative constraints and objective function values of the designs

Summary

Using the example of the pitch stability $C_{m\alpha}$, this study demonstrated how aircraft parameters, relevant for flight control system design, can be considered in a multidisciplinary optimisation approach. Large scale applications would come with a high number of load cases and would add further constraints (e.g. damage tolerance or manufacturability) in order to respect all possible effects experienced during design, manufacturing and in service. Still, the given study proofs that flight mechanical stability can unintentionally be modified, when applying numerical optimisation. This effect can, however, be controlled through respective criteria models. A list of outcomes of the stability derivative analyses states as follows:

- Structural changes of the tail can modify the flight mechanical aircraft stability through numerical optimisation in an unintended way.
- Assuring a more or less constant pitch stability during structural optimisation leads to a tail layout with higher thickness variables, compared to studies not controlling $C_{m\alpha}$.
- Following an integrated airframe design approach, flight mechanical demands as pitch stability must necessarily be respected during structural sizing, to save costs in later design phases.

5.4 Structural Sizing Respecting Load Alleviation Demands

Taking the pitch stability $C_{m\alpha}$ into account in structural sizing problems is a first step into control topics. Next, an actual FCS shall contribute to the load determination in the sizing loop. When the FCS reacts to external influences in order to compensate an undesired behaviour, its coupling to the load determination subprocess is a mean of active load control. In the context of sizing airframe structures, this means designing with controlled loads and enables respecting load alleviation demands.

It has to be highlighted that working with structural dynamics is an unconventional, new step when sizing airframes through MDO. Especially when approaching active load alleviation topics, it becomes a necessary step that must be developed further, however. Therefore, after a brief description on the topic of load alleviation, three different studies dealing with structural dynamics in an algorithm-driven design process are performed. They intend to demonstrate how manoeuvre-loads and loads from a disturbance (e.g. a gust) can be modelled, simulated and finally used in a MDO-framework.

Load Alleviation

LAF is of high interest in modern aircraft design. While the term Passive Load Alleviation Functionality (PLAF) mostly focusses on purely aeroelastic design methodologies, Active Load Alleviation Functionality (ALAF) uses the FCS to actively deflect control surfaces in order to manipulate loads experienced by the structure. Many studies on passive load alleviation fol-

low the idea of aeroelastic tailoring (e.g. Roessler et al. (2019), Deinert (2016), Deinert et al. (2013*a*)). Directional stiffness in orthotropic composites is used to form the load carrying structures of aircraft components. An overview on the state of the art in aeroelastic tailoring is given in Jutte & Stanford (2014). Active load alleviation topics have been studied for decades already (see Urie (1979)). They can be grouped into Manoeuvre Load Alleviation (MLA) and Gust Load Alleviation (GLA). Designing with MLA aims to reduce forces and moments experienced during a specific flight manoeuvre, while using a GLA approach targets to alleviate undesired behaviour resulting from atmospheric disturbances like gust load excitations. Example studies, where active control for gust alleviation is approached, are given in e.g. Binder et al. (2021), Regan & Jutte (2012), Soreide (1996), Pusch et al. (2019), Wildschek et al. (2009), Wildschek (2009), Wildschek et al. (2010). Flutter control is applied and studied in Roessler et al. (2019) or Andreas Hermanutz (2019). The special topic of fin-buffet load alleviation is analysed in Breitsamter (2001) and Breitsamter (2005).

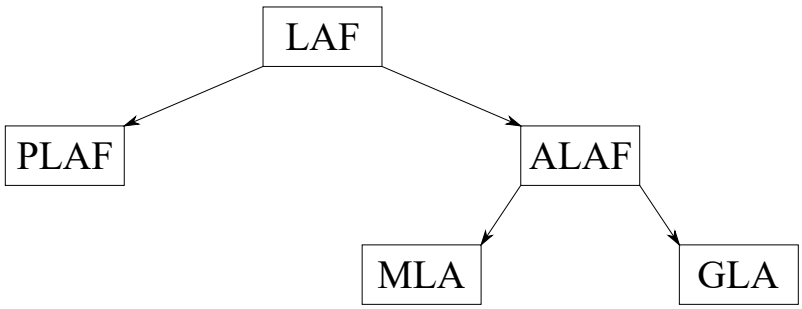

Figure 5.14: Load alleviation

While methods using passive LAF are strongly in use in state of the art structural sizing, MLA and GLA strategies are not established to a similar extent. In the following, two applications for designing with load control will be given. It must be pointed out that the control system used here is not explicitly designed for load alleviation. This is due to the fact that this work demonstrates the generic capability of sizing structures with controlled loads and did not want to be restricted to the application of explicit LAF controllers.

5.4.1 Structural Sizing with Loads of a Controlled Disturbance

As a first example for a structural optimisation with actively controlled loads and to test the implemented methodology, the short period oscillation induced by an external excitation of the OptiMALE shall be studied. While the frequency of this mode mainly depends on $C_{m\alpha}$, it is damped by the pitch damping C_{mq}, which again is influenced by the Horizontal Tail Plane (HTP) design (see Brockhaus et al. (2011)). A pitch damper provides additional damping by commanding respective elevator deflections η inducing a pitch rate q, which results in additional pitch moment through C_{mq}.

Again, the components of the wing shall be sized. Active load alleviation is captured as a

control system reacts actively on an external pitch-down disturbance. This study does not primarily focus on the control system or the optimisation procedure but on the interaction of all involved disciplines, methods and processes.

Disturbance

The OptiMALE is trimmed in level flight in an altitude of $h = 1000m$ with Mach number $Ma = 0.2$ through an angle of attack of $6.67°$ and an elevator deflection of $-5.84°$. It is now disturbed by a discrete force applied to its nose section. The disturbance force acts for 1 second, corresponds to an inertia load of approximately 25% of the MTOW and intends to change the pitch rate q from its implicit set-point value of 0 deg/s.

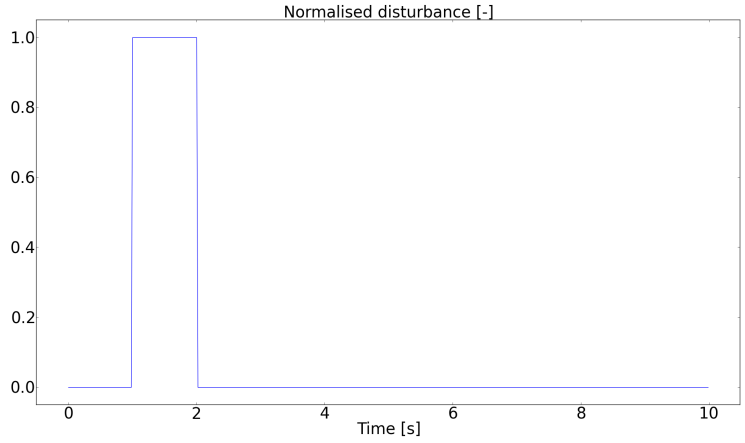

Figure 5.15: Signal of normalised disturbance

The disturbance leads to an undesired external loading. The criteria model is set up to assess the influence of the loading on the structural integrity of the design. Load states, which the structure cannot carry and must therefore be considered as critical, can thus be detected by numerical values of reserve factors and constraint functions. Here, the latter are used to track critical time steps in the dynamic, disturbed manoeuvre by LAGRANGE enveloping. The resulting critical loads are added to the classical sizing load cases from Chapter 5.2. This criteria model is then used to size the structure with numerical optimisation.

Pitch controller

In order to counteract the applied disturbance actively, the pitch damper subcomponent of a large FCS is integrated into the design and sizing process. The pre-designed discrete pitch damping controller monitors the pitch rate and commands an elevator deflection η in such a way that q returns to an implicit set-point value of 0. Its generic layout and components were given in Figure 5.2. The FCS-calculated elevator command is passed to an actuator, modelled

as a first order lag element with a typical time constant of $\tau = 0.06s$:

$$G = \frac{1}{1 + \tau s} \tag{5.8}$$

The actuator transfers the time-discrete control command into a physical elevator deflection, which is applied to the aeroelastic model of the OptiMALE. It thus induces aerodynamic forces on the elevator control surface changing the resulting pitch rate. A similar study can be found in Nussbächer et al. (2018), with a more academic pitch controller. The result of the controller output to reduce q is shown in Figure 5.16.

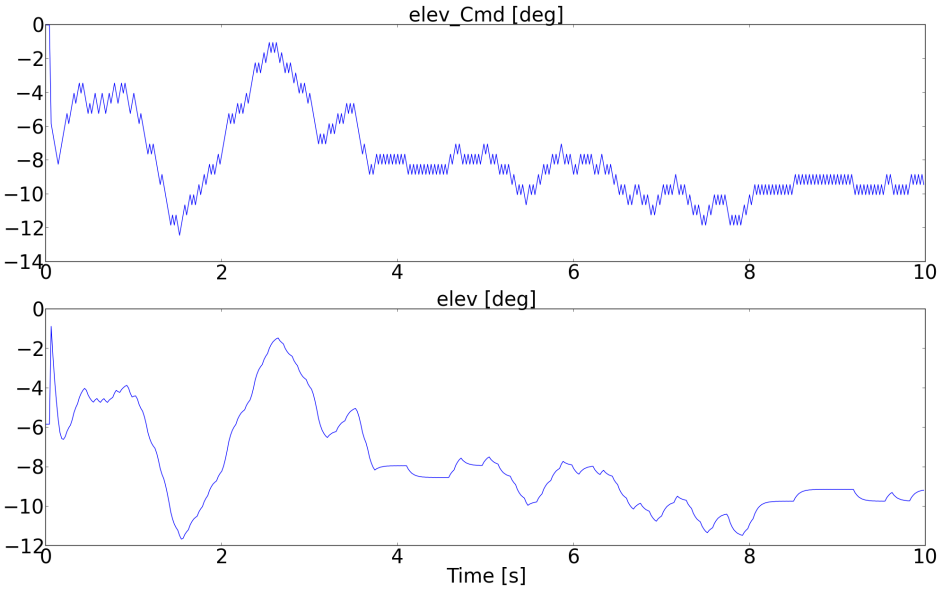

Figure 5.16: Discrete elevator command and actuator output

Analysis

The effect of the disturbance can best be seen at the pitch rate and at the change of the angle of attack. While the elevator deflection remains unchanged at its trim value of approximately $-6.0°$ in the uncontrolled case, it is strongly changed with the pitch rate through the pitch controller in the controlled case in a range of $[-2°, -12°]$ over time (compare Figure 5.16).

From Figure 5.17 (a) it can be seen that in the controlled case (solid green line), the pitch rate is reduced faster than in the uncontrolled case (solid blue line). The disturbed pitch rate can be kept in a range of $\frac{\pm 5°}{s}$ starting from $t = 3.3s$ using the controller, while it is kept in the same range starting from $t = 4.4s$ without active control activity.

The angle of attack and thus the main loading changes, as well. Figure 5.17 (b) shows the difference between the current AoA and its initially trimmed value. The validity of aerodynamic

lattice methods (small angles) is violated for a small time frame ($t \in [1.5s, 2.5s]$). As the resulting amount of lift is overestimated, the following sizing process can be seen as conservative. The controller indirectly reduces the acting loads, which can be seen at the structural reserve factors of the design. The reserves are generally higher in the controlled case, compared to the uncontrolled case. The design is infeasible in both cases, which can be seen from the rf-values of the skin, which would fail under the given loading.

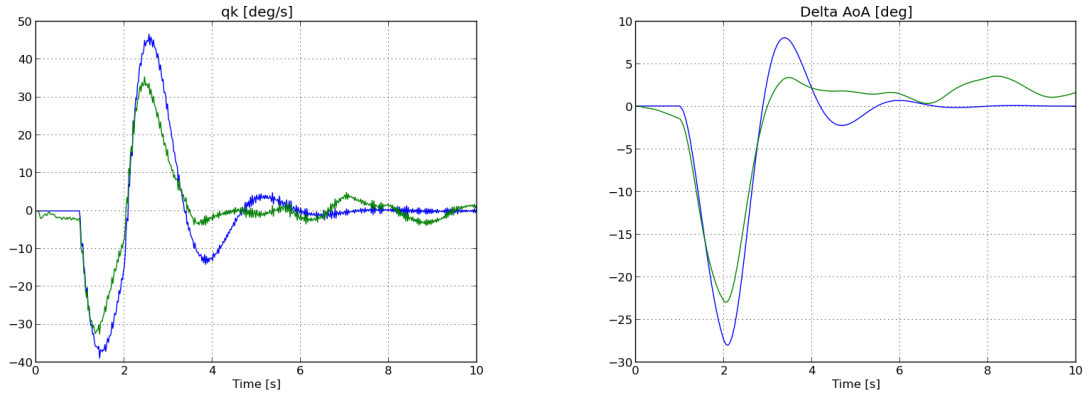

(a) Pitch rate (b) Difference from initial angle of attack

Figure 5.17: System response - uncontrolled (blue) and controlled (green) case - initial design

The lower reserve factors in the uncontrolled case result from the higher angle of attack, which the design experiences during the disturbance (see Figure 5.18). These reserves will be exploited in the subsequent structural sizing loop by the numerical optimiser for both the controlled and the uncontrolled design.

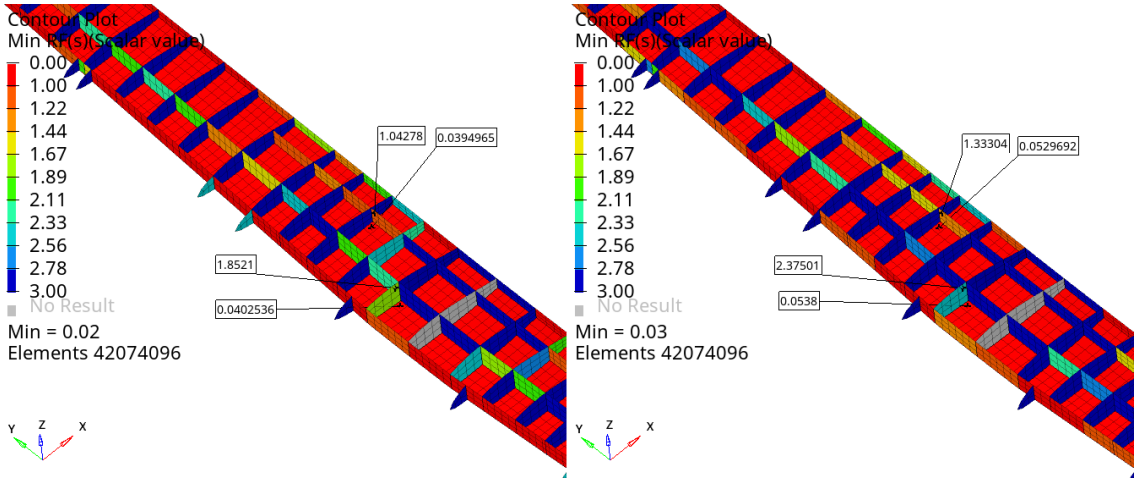

Figure 5.18: Reserve factors - uncontrolled (left) and controlled (right) case - initial design

Optimisation and re-analysis

The enveloped loads resulting from the disturbance load case and the previously discussed basic loads (compare Table 5.2) are now forwarded to the structural optimisation step. Using a controller means altering the experienced forces and moments, compared to not using one. Therefore the optimised designs will naturally differ.

Without control interaction the overall structural mass of the initially infeasible design is increased by 7.38% (see Figure 5.19). This corresponds to more than doubling the available variable mass (additional 127.5%). A high number of 52 numerical iterations is necessary to find this design. The start design contained physically sensible thicknesses for spars, ribs and skins for the wing. Only few design variables reached a relatively high value of approximately 6.5, which means that they needed to be drastically increased for the design to become feasible.

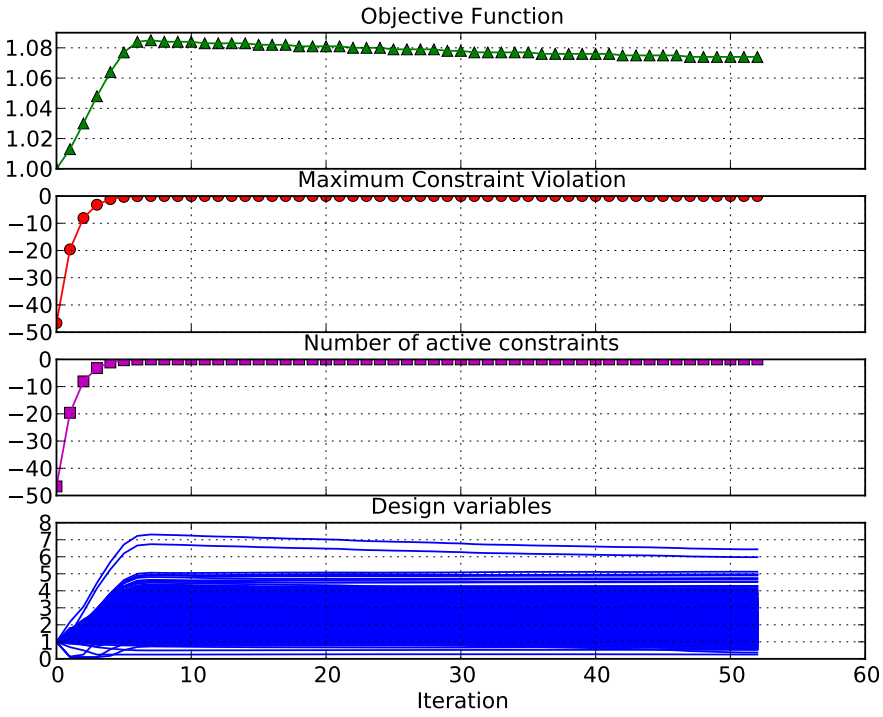

Figure 5.19: Optimisation using critical loads from disturbed state w/o controller interaction

Figure 5.21 shows that the skin thickness was tripled locally, while a selected spar was thickened only slightly, whereas a selected rib thickness could even be reduced. However, no gages of the state variables where reached, what indicates that mechanical properties for a feasible design could be found in a range of physically sensible values. The infeasibility of the initial design and the success of the optimiser in finding a feasible one can be seen in

Figure 5.20. The maximum constraint violation and the number of active constraints are both close to 0 after view iterations. At this point, there are still constraints rating the design as invalid, however. The optimiser has difficulties to converge, therefore.

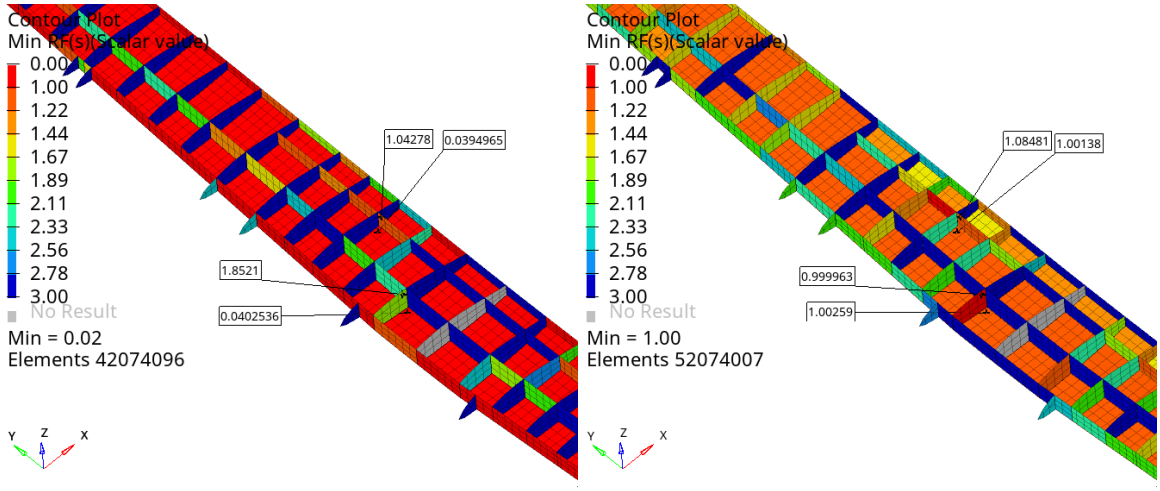

Figure 5.20: Reserve factors - uncontrolled case - initial (left) and optimised (right) design

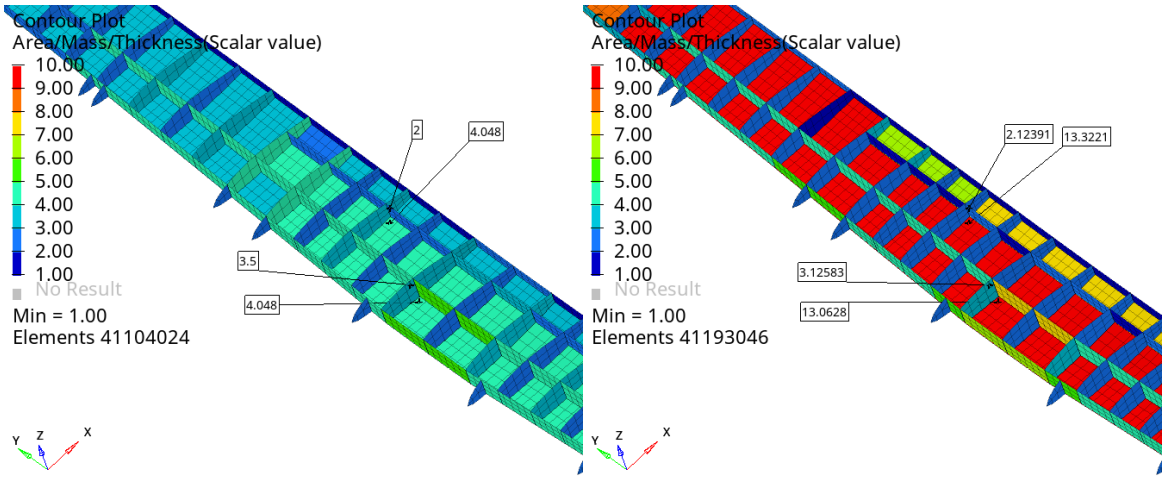

Figure 5.21: Thickness distribution - uncontrolled case - initial (left) and optimised (right) design

This effect can not be seen with the interaction of the controller (see Figure 5.22). Maximum constraint violation and the number of active constraints reach their desired values of 0 and indicate a feasible design after 8 iterations, only. The overall mass can be reduced, compared to the design without controller activation. An increase of 3.64% overall mass (corresponding to 63.0% of the variable mass) is necessary to fulfil the demands of the criteria model, i.e. of the mechanical failure criteria. Both, without and with controller application, the numerical optimiser assures that especially initially infeasible spar- and the skin-components are designed such that they can carry the loads as demanded. Many rib-components were initially over-

sized for the given load cases, where the gain in mass of the spar- and skin-components can be compensated.

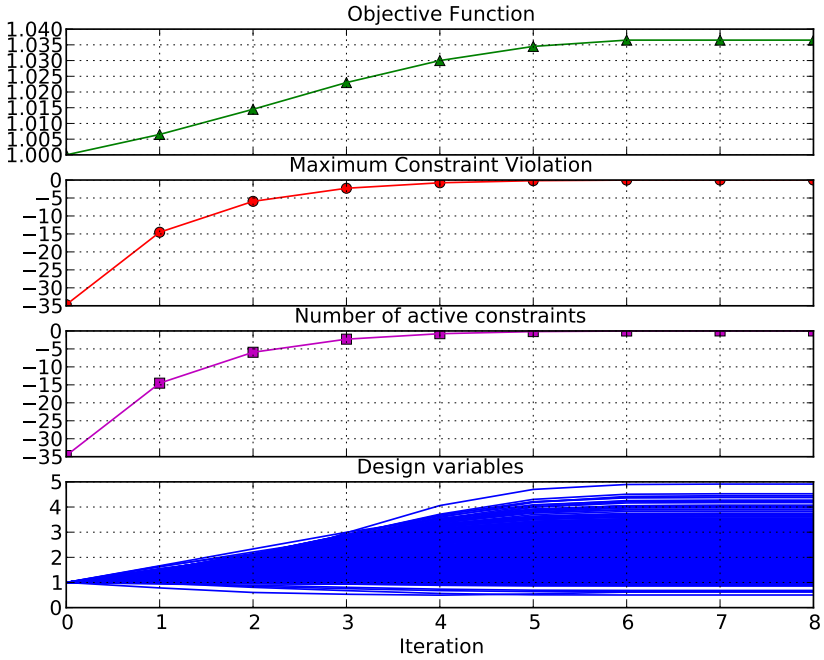

Figure 5.22: Optimisation using critical loads from disturbed state with controller interaction

Figure 5.23 shows the relaxation and fitting of the reserve factors due to optimisation. The selected regions are brought to feasible domains. Strong changes in the rf can be observed in the skin and the spar segments.

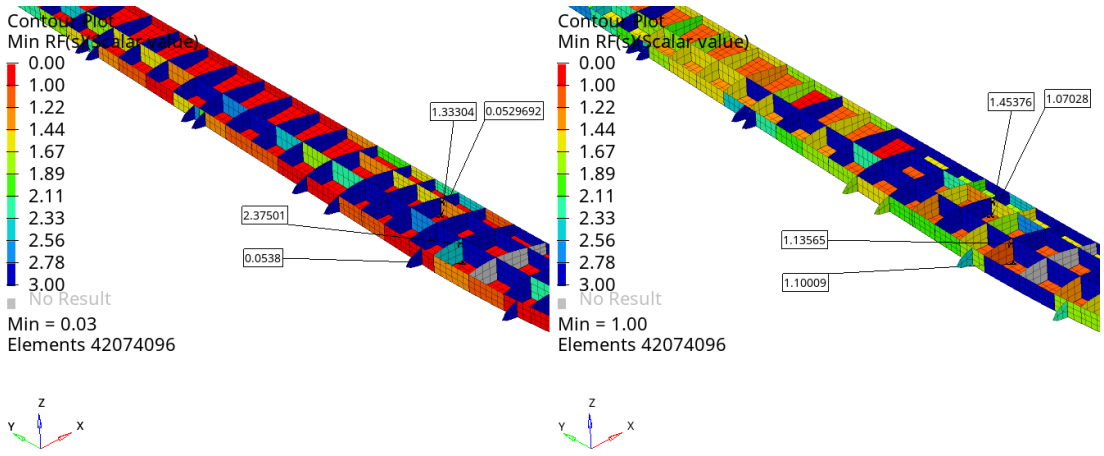

Figure 5.23: Reserve factors - controlled case - initial (left) and optimised (right) design

The respective thickness adaptations are expected and are visualised in Figure 5.24. Both, the increase in skin-thickness and reductions in rib-thicknesses can be seen. What may be

highlighted are the minor changes in the spar-design, which can be interprated as a load transition from the spars to the (now thicker) skin.

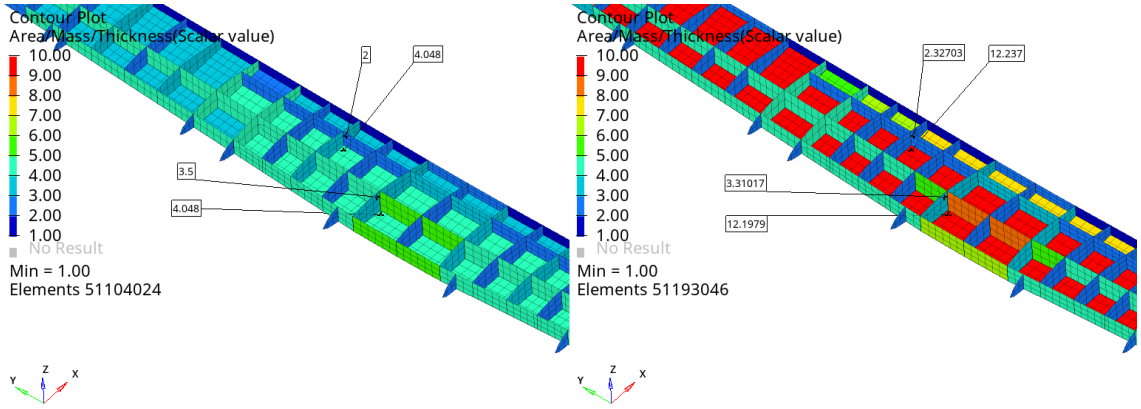

Figure 5.24: Thickness distribution - controlled case - initial (left) and optimised (right) design

The differences in the two optimised designs (uncontrolled and controlled) can be seen at the spatial thickness distributions and the reserve factor plots in the wing. Comparing the two designs, shows that the reserve factors are close to 1.0 as expected (Figure 5.25).

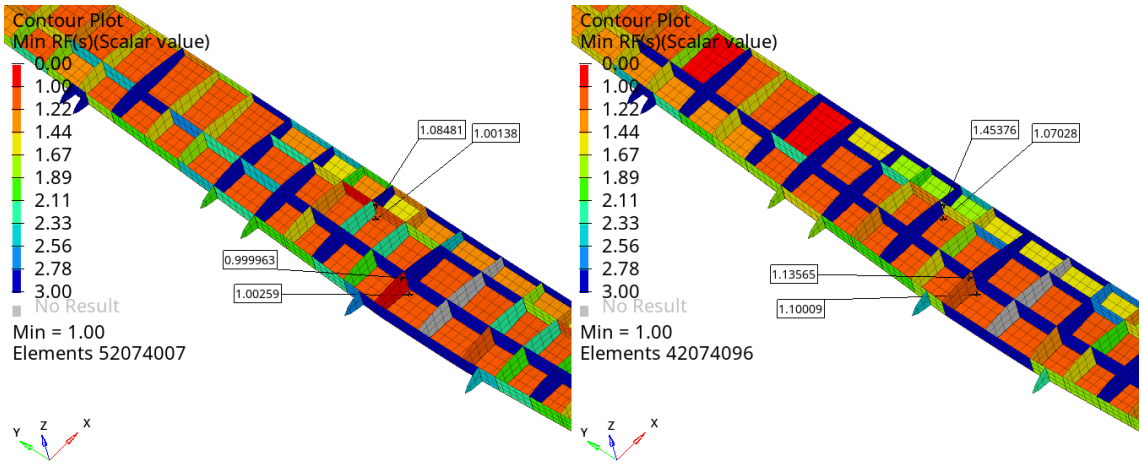

Figure 5.25: Reserve factors - uncontrolled (left) and controlled (right) case - optimised design

The thickness values, however, differ by approximately 10.0% for exemplarily selected elements. This comes on the one hand from a different optimisation behaviour, and on the other from a different loading situation, induced through the control system. As the root-area experiences higher loads in the uncontrolled case, more material is needed there to support the external forces and moments, accordingly. In the controlled case, the root-area is relieved from the loading. This can be seen when comparing the resulting composite skin thickness

of the optimised designs for the uncontrolled with the controlled case (Figure 5.26). Naturally, the optimiser changes the load path, what explains why thickness values are increased or decreased locally.

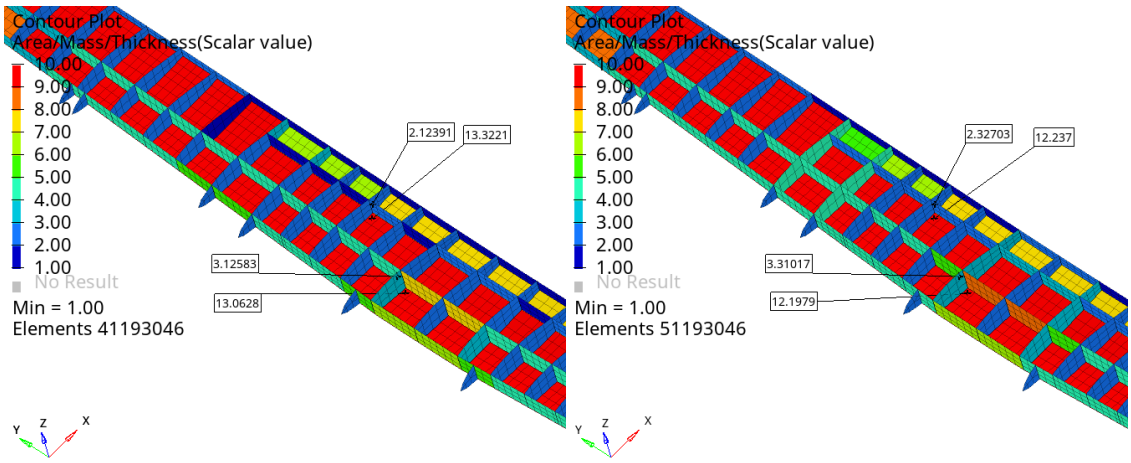

Figure 5.26: Thickness distribution - uncontrolled (left) and controlled (right) case - optimised design

This study shall be concluded with a remark on how the control system reacts to the changes in the structural design. With a new design being controlled, the system responses will change. In this case the commanded and the actuated elevator deflections applied to the optimised structure will differ from those applied to the initial layout (Figure 5.27).

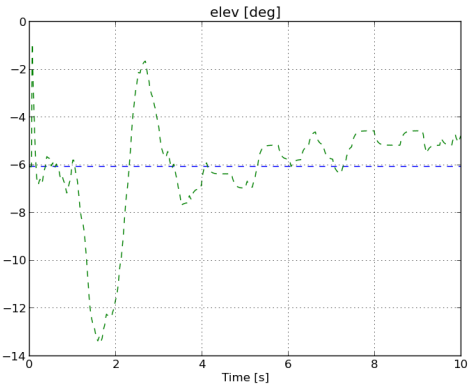

(a) Uncontrolled (dashed blue) and controlled (dashed green) case for the optimised designs

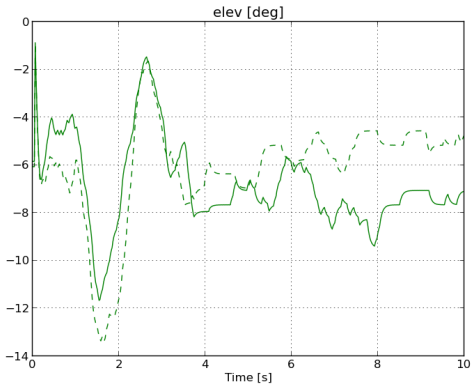

(b) Controlled case for the initial (solid green) and the optimised (dashed green) design

Figure 5.27: Elevator deflections

An alteration of the commanded η-deflection results in a different, actuated η, which again leads to a new pitch rate q:

$$\Delta\eta_c \rightarrow \Delta\eta \rightarrow \Delta q$$

A change in η does not only reflect in the pitch rate curves. It strongly affects the overall AoA of the aeroelastic loading state what expresses in the resulting forces F and moments M:

$$\Delta\eta \rightarrow \Delta\alpha \rightarrow \Delta F, \Delta M$$

Especially the new wing root bending moments lead to differing stress and strain values, which again changes the reserve factors:

$$\Delta M \rightarrow \Delta\sigma, \Delta\epsilon \rightarrow \Delta rf$$

The effects can be seen in Figure 5.25 for the reserve factors and in Figure 5.28 for the pitch rates.

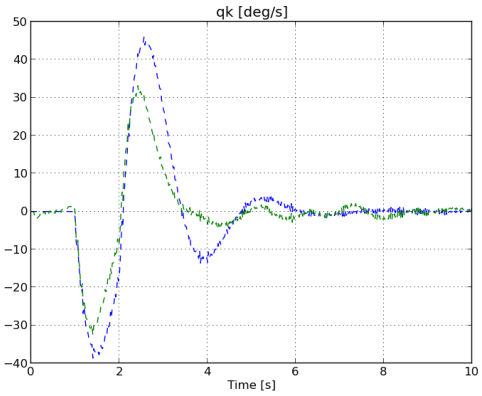

(a) Uncontrolled (dashed blue) and controlled (dashed green) case for the optimised designs

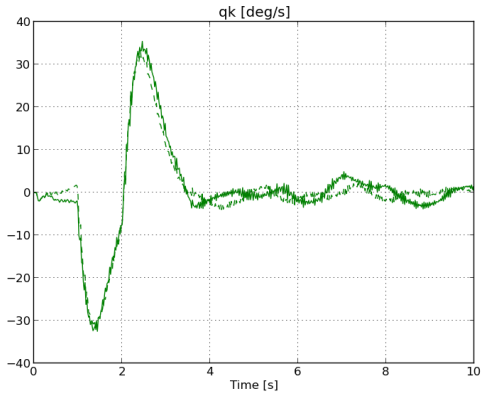

(b) Controlled case for the initial (solid green) and the optimised (dashed green) design

Figure 5.28: Pitch rates

An open issue that remains from these studies is given by the missing feedback of structural changes to the controller layout. Automatically altering FCS gains through algorithms is a complex topic and belongs to the discipline of controller design. Still, a subsequent study can use this work as a base and implement a further computational layer in the process such that a modified structure is respected through adaptations in the control laws. As the structural changes are kept rather small, this effect is not taken into consideration, in this work. Depending on the control system and the external loading, it must, however, not be neglected in general.

5.4.2 Structural Sizing for an Asymmetric Manoeuvre

As an enhancement to optimising with structural dynamics and control system in the loop, an asymmetric manoeuvre, resulting from a pre-defined pilot input, will now be assessed. The

pitch controller from previous analyses remains active here, as well. Although the pitch rate is actively controlled during the roll manoeuvre, it does not take a major role in the analysis, however. Main focus is placed on identifying critical states according to the given criteria model during the roll movement. The study demonstrates that the implementation of a flight mechanical loop in the presented MDO process and the extension of the process through a FCS can be adapted to different use cases in a flexible way. Setting up this analysis can be seen as the base for an integration of a roll-controller in a next step.

Analysis

The manoeuvre to be analysed consists of multiple phases. Starting from a trimmed horizontal flight, banking is initiated by deflecting the ailerons. Lift is increased on one side and reduced on the other, which induces a roll movement. While banking, the lift vector is rotated, what results in a loss in altitude, if the AoA is not adjusted accordingly. Further the side component of the lift vector leads to a side movement. After maintaining the aileron deflection for few seconds, the ailerons are brought back to their initial position. To recover from the bank, the complete stick input needs to be performed in reverse, hereafter. The ailerons are thus deflected the other way round, initiating recovery from the bank. After the roll-command, a trimmed state is re-gained, as no further change in flight parameters occurs any more. Again, physical quantities are mainly calculated in an aeroelastic coordinate system. A positive right aileron command means a downward deflection, resulting in a positive roll around the aeroelastic x-axis, i.e. to the left wing. The aileron command input is depicted in Figure 5.29 a).

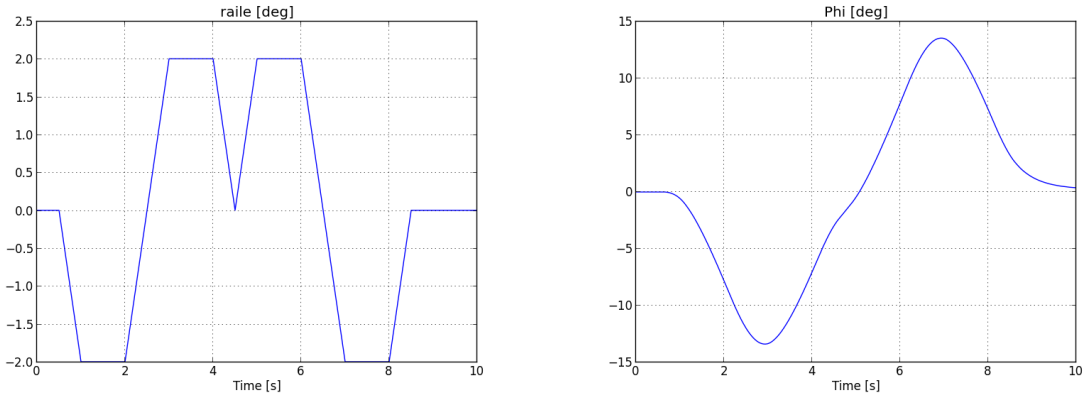

(a) Right aileron command as system input (b) Bank angle as system output

Figure 5.29: Manoeuvre input and output

To realise the coupled analysis, the model from Chapter 5.4.1 can be re-used. First, the simplified disturbance load has to be removed. The ailerons have to be added as control surfaces to the aeroelastic model. The aileron deflection of the pre-defined command can then be applied for each time step. The developed framework is fed with the manoeuvre input

and the resulting system response can be studied. Of main interest is the bank angle response Φ, given in Figure 5.29 b). It follows the description above and varies between approximately $-13.0°$ and $13.0°$. During the bank movement, an adverse yaw, in which the increased drag on the outer wing pulls the aircraft nose away from the flight path, would be encountered. The rudder needed to be engaged, to counteract the movement. In the following analysis, this flight mechanical effect will be neglected. Focus will be placed on the loading resulting from the roll-movement, only.

Optimisation and re-analysis

The critical loads resulting from the banking manoeuvre are automatically used to size the OptiMALE. While in a usual sizing process further design driving loads were applied, here only the effect of the banking loads is evaluated. The reserve factor plots represent the structural information which are used by the numerical optimiser. Figure 5.30 highlights that upper skin and rear spar components are badly designed in the initial layout for the given manoeuvre. These under-reserves are removed by the optimiser. The overall minimum reserve factor of 0.11 for the basic design is changed to a value of 1.00 for the optimised one, indicating that the layout is able to carry the given loads as desired, now.

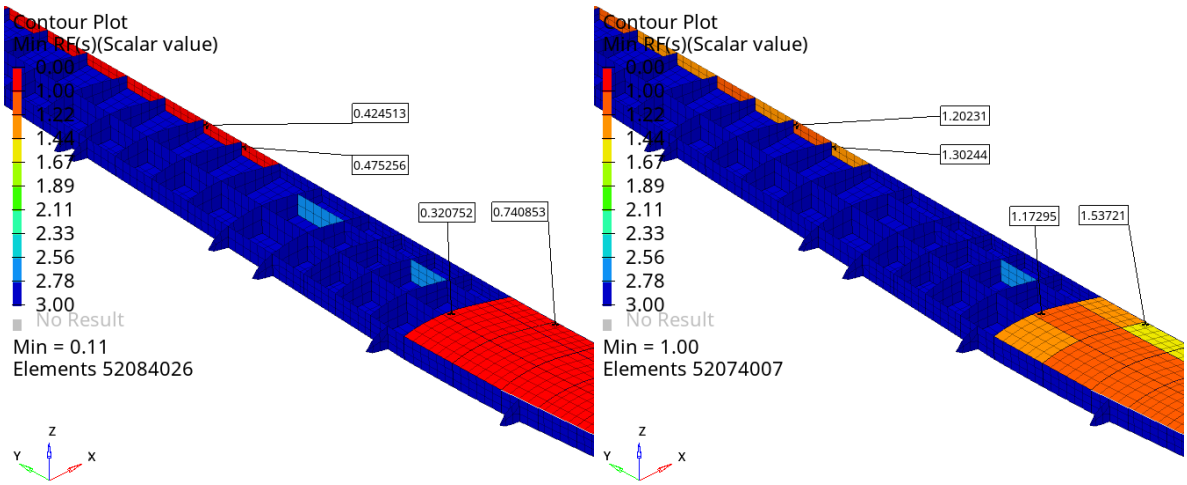

Figure 5.30: Reserve factors - initial (left) and optimised (right) design

As can be seen in Figure 5.31, the spar elements had to increase only slightly in thickness, whereas the composite skin needed stronger modifications. The upper skin naturally experiences compression loads when the wing is bent upwards, what may lead to skin-buckling and eventually a collapse of the structure. The respective reserve factors are increased to feasible values by adding resistance against this instability through a thicker skin. The numerical optimiser converges to a solution in 6 iterations. Through sizing optimisation, the overall structural mass was increased by 1.7%, as can be seen in Figure 5.32. This means

an additional variable mass of 29.4%, which comes from the fact that wide areas of the upper skin (not visualised in Figure 5.31) had to be thickened to resist the danger of skin-buckling. Some design variables take values in the range of 2.0 to 2.6 for the final layout. This means that the corresponding physical thicknesses of the model need to be at least doubled, as well.

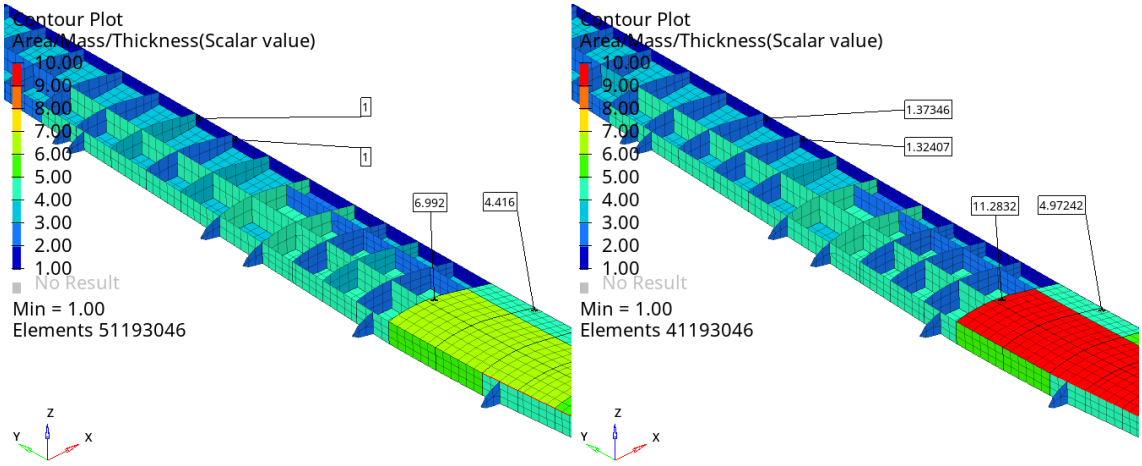

Figure 5.31: Thickness distribution - initial (left) and optimised (right) design

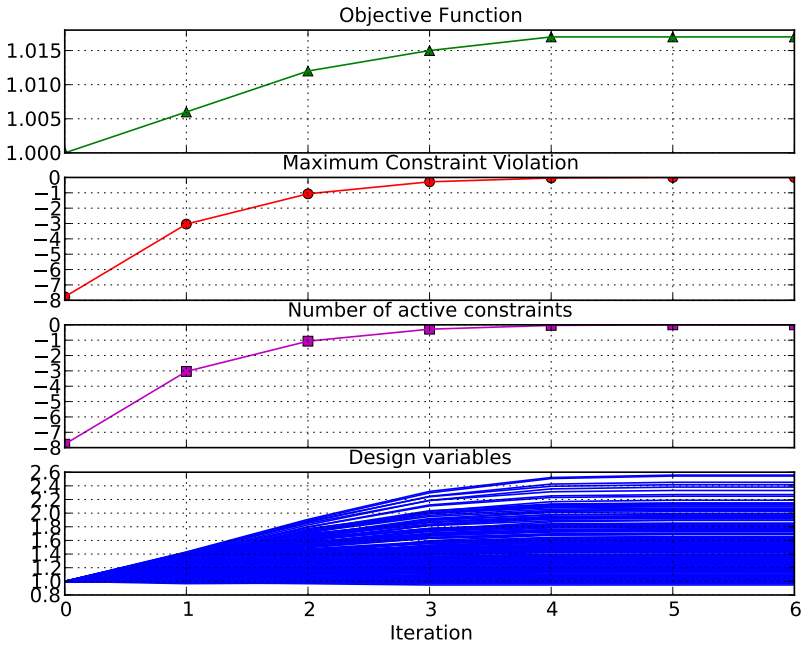

Figure 5.32: Optimisation using critical loads from aileron command

Comparing the initial and the optimised design shows that the bank angle as a system response slightly increases. This is displayed in Figure 5.33. The small change in maximum

Φ explains as a slightly different inertia counteracts the banking movement in the optimised case.

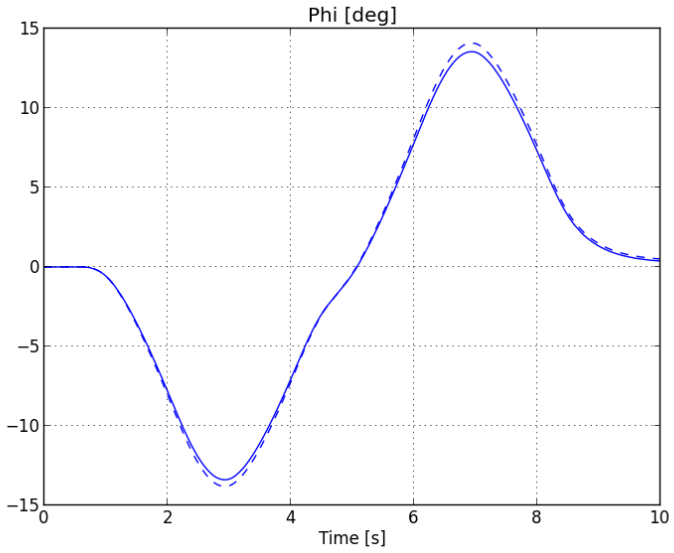

Figure 5.33: Bank angle resulting for the initial (solid) and the optimised (dashed) design

This study demonstrated the flexibility of the developed framework. With few changes to the input and some simplifying assumptions, an asymmetric manoeuvre could be simulated and structural responses could be extracted to support sizing optimisations. The manoeuvre simulation will now be extended by a further control surface, such that a desired flight mechanical system response can be met with reduced structural loading.

5.4.3 Load Alleviation by Optimising the Linking of Control Surfaces

Ailerons are not the only devices used to roll an aircraft in flight. Spoilers can support ailerons in turning as they deliberately reduce lift. In that case roll spoilers are deflected on the side of turn direction in conjunction with the ailerons. The drag effect coming with spoilers can not be captured directly with low-fidelity vortex lattice methods. A change in lift can, however, be modelled. In this chapter an optimal ratio between aileron and additional spoiler deflection is found such that a specific maximum bank angle of a desired bank manoeuvre is met. Insights from such studies can help in designing flight control and flight guidance systems, especially when banking agility must be assessed and improved. The pitch controller used in the last chapters will again be deployed in this use case to control the pitch rate. The primary control surfaces are the anti-symmetrically coupled ailerons ξ and the respectively linked spoiler deflection κ on the right or left upper wing surface.

Methodology

To mathematically describe roll spoilers supporting the ailerons during a bank manoeuvre, a spoiler-aileron-deflection ratio λ can be defined. In a flight control system representation it can be formulated as

$$\lambda = \frac{\kappa}{\xi} \tag{5.9}$$

A value of $\lambda = 0$ means that no roll spoiler is used to support the desired banking. In that case, the bank angle is solely built up by the ailerons. $\lambda = 1$ signifies that as much spoiler as aileron deflection is applied. To achieve the same bank angle, less aileron deflection (and consequently less root wing bending moment) is needed, as rolling is supported by the spoiler, then. The primary variable is ξ. κ follows as result of ξ according to the respective λ.

The aim of the following study is to determine a spoiler-aileron-deflection ratio λ through numerical optimisation, such that a desired movement is achieved. Therefore, λ shall be varied as design variable. With a pre-defined aileron command, a maximum bank angle Φ_{max} shall be met using additional spoiler deflection κ. From the structural design point of view, it seems sensible to use as much spoiler as possible instead of commanding more aileron deflection, as this reduces the root strains. This is due to the fact that the roll spoilers are located more at the inboard side of the wing, compared to the ailerons and therefore show a shorter lever arm for the external aerodynamic forces. This represents a load alleviating affect for the λ-optimal design. However, too much additional κ leads to a bank angle higher than the desired one ($\Phi > \Phi_{max}$). In that case the λ-design is considered to be infeasible. The spoiler-aileron ratio will therefore be increased iteratively as long as the bank angle stays under the desired maximum value ($\Phi \leq \Phi_{max}$). The λ-refinement shall be stopped only if the change from one design to the next one is lower than 5%. The optimisation problem is thus formulated without an actual objective function, with one design variable λ and with a binary constraint ("Φ_{max} overshot, or not.") and evaluates the global aircraft model using the coupled analysis as already described.

The design variable is iteratively varied using the golden section algorithm (compare e.g. Kiefer (1953)). The design space is split multiple times into two regions by a ratio of $\tau = \frac{1+\sqrt{5}}{2}$. The ratio stems from the demand that the splitting point C^i divides the current search interval $[A^i, B^i]$ of length $\overline{A^iB^i}$ in two subintervals $[A^i, C^i]$ and $[C^i, B^i]$ with the lengths $\overline{A^iC^i}$ and $\overline{C^iB^i}$ such that

$$\tau = \frac{\overline{A^iB^i}}{\overline{A^iC^i}} = \frac{\overline{A^iC^i}}{\overline{C^iB^i}} \tag{5.10}$$

The design space is reduced successively using this ratio until the convergence criterion is met. A minimum change of the search interval from one iteration to the next can be used, for example.

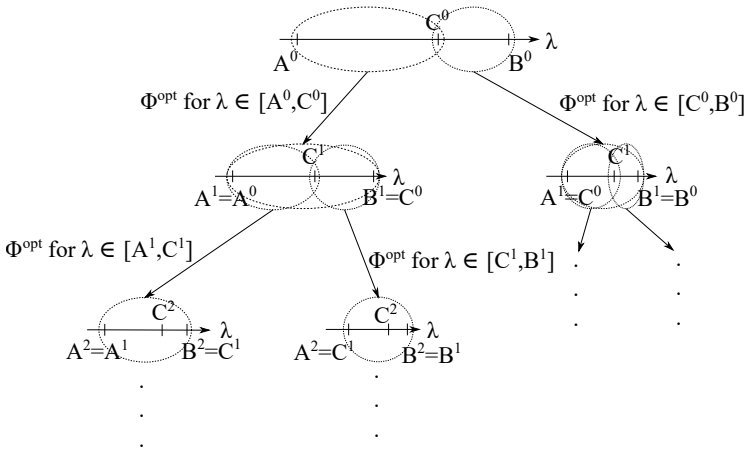

Figure 5.34: Golden section algorithm

The result from the golden section algorithm is the maximum allowable spoiler-aileron ratio, such that the desired bank angle is reached but not overshot through the bank-supporting spoiler engagement.

Analysis and optimisation

In the aeroelastic analysis, the spoiler deflection is treated as a dependent variable of the aileron. The amount of spoiler deflection is given through a scaling factor, resulting from the respective λ value. Thus, there is only a minor change in the aeroelastic equation to be solved, coming with the introduction of the spoiler. To get an idea of the effect of different control surface command inputs, both maximal ξ command and λ values are studied, first. The spoilers are not deflected yet, i.e. $\lambda = 0$. Higher aileron deflections lead to more bank angle. Figure 5.35 shows the bank angle response for two different aileron command inputs.

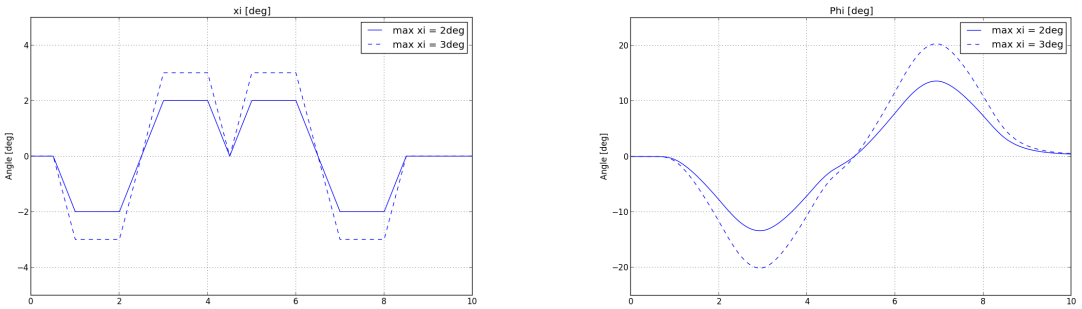

(a) Variable aileron input

(b) Resulting bank angle output

Figure 5.35: Variable bank angle from varying maximal aileron command

The resulting bank angle, when using one pre-defined aileron command slope with a fixed, maximum value of 2° but varying the amount of spoiler deflection linked to it, is shown in Figures 5.36 - 5.38 (the fixed aileron slope for all cases can be identified through the solid blue line for ξ). Exclusively applying the aileron, without an additional spoiler deflection can be seen in Figure 5.36.

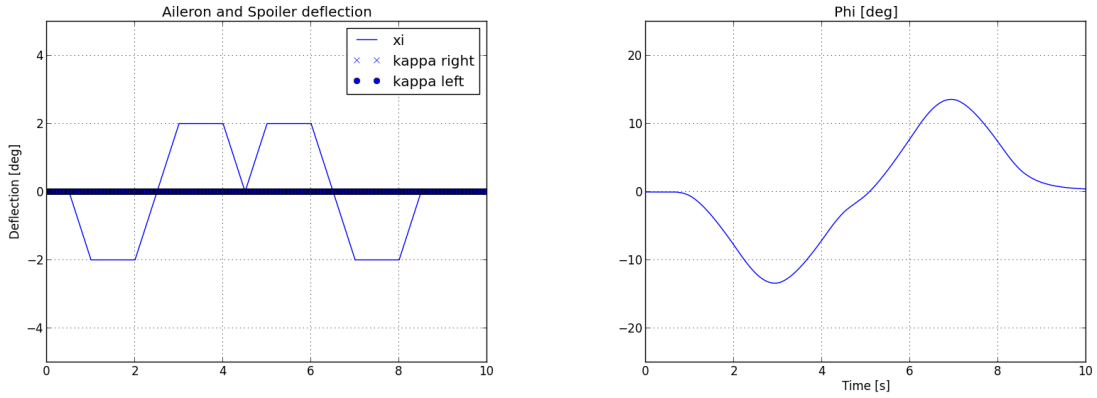

(a) Inputs ξ and κ (b) Output Φ

Figure 5.36: Roll manoeuvre with spoiler-aileron ratio $\lambda = 0$

In case a κ deflection is applied (Figure 5.37 and Figure 5.38), it is commanded such that it supports the aileron in rolling the aircraft. The case $\lambda = 1$ can be seen in Figure 5.37.

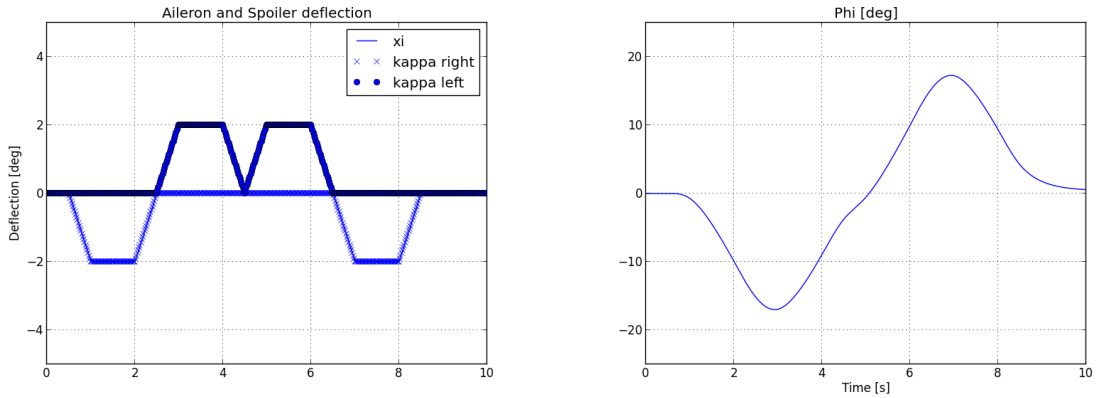

(a) Inputs ξ and κ (b) Output Φ

Figure 5.37: Roll manoeuvre with spoiler-aileron ratio $\lambda = 1$

A more aggressive spoiler engagement through $\lambda = 2$ is visualised in Figure 5.38. In all cases, initially neither aileron nor spoiler is deflected. As soon as roll to starboard is initiated (negative Φ according to aeroelastic coordinate system), the right spoiler is engaged to additionally reduce lift in the right wing. After a short time of rolling, an inverse deflection of the ailerons

aims to bring back the aircraft into horizontal flight ($\Phi = 0$). This phase is supported by the left spoiler. To bank further to the other side, over the initial bank angle, another phase where the left spoiler supports the ailerons in rolling to the port side follows. Hereafter, the right spoiler and the ailerons are commanded to regain horizontal flight. As a result of the pre-defined ξ and κ curves, levelled flight is recaptured. According to the selected λ the plant responses vary as expected.

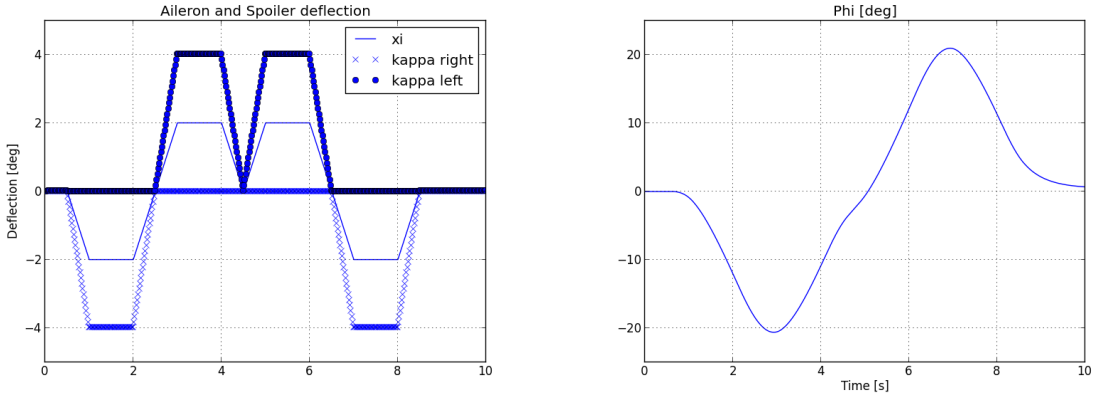

(a) Inputs ξ and κ (b) Output Φ

Figure 5.38: Roll manoeuvre with spoiler-aileron ratio $\lambda = 2$

Changing λ in separate studies and recording the resulting maximum Φ for $\xi_{max} = 2°$ gives Figure 5.39. Thus, running multiple analyses of the problem enables the estimation of an optimum through linear interpolation.

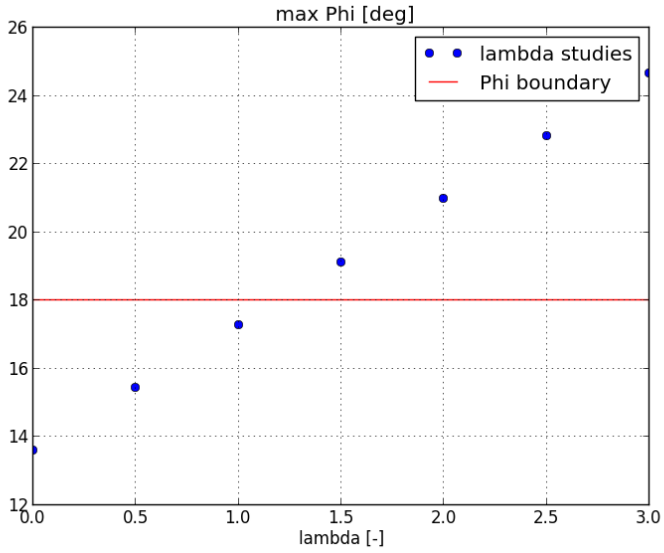

Figure 5.39: Maximal bank angle for different spoiler-aileron ratios

The solution for λ to meet the Φ demand of $18°$ can be estimated in the interval $[1, 1.5]$. For lower ratios the desired bank angle is not achieved, for higher ratios it is overshot. However, instead of running numerous analyses, the solution shall be found numerically through automation. The golden section algorithm runs as shown in Figure 5.40. An optimal λ of 1.276 is determined after 8 iterations, what fits the estimation from Figure 5.39. It embodies the highest additional spoiler deflection to support the banking movement in order to meet the desired maximum bank angle.

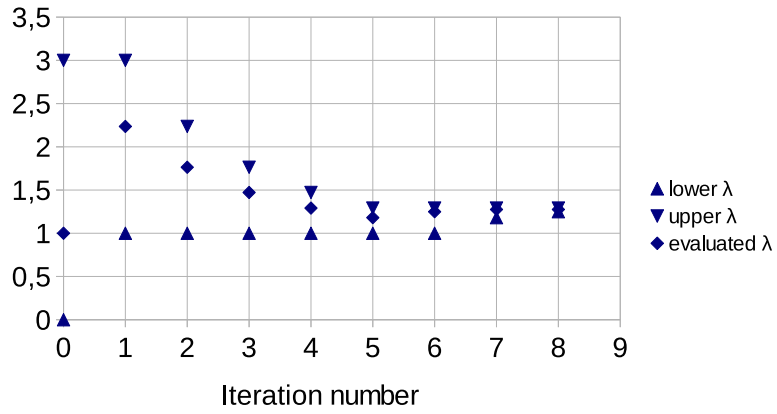

Figure 5.40: Optimisation run for spoiler-aileron ratio

The LAGRANGE enveloping capabilities could be applied again to scan the manoeuvre for structurally critical load steps and to subsequently optimise the structural design. A sensible follow-up study of the combined spoiler-aileron optimisation was to couple the multidisciplinary analysis to a lateral control law, which directly implements the idea behind λ. A fully coupled sizing optimisation using both the structural layout and the control system parameter λ in the design model would result. The necessary, interdisciplinary connections are highly complex. Their realisation, however, promises the possibility to find further optimal aircraft designs and is possible using the developed process as a basis.

Summary

New capabilities and findings from Chapter 5.4 shall be summarised, briefly.

The study in Chapter 5.4.1 demonstrated a direct coupling of a discrete flight control system into the MDO design loop for a symmetric manoeuvre. It could be shown that using controlled loads brings load reducing effects, which enables exploiting more available structural reserves and thus leads to lighter designs. The presented use case showed how applying a flight controller changes the design obtained through integrated optimisation, compared to not applying one. In both cases, the variable mass had to be increased to find a feasible design. Thickness variables of the internal wing structure distributed differently, what lead to different

load paths the optimiser can benefit of to change the variable mass by 63.0% in the controlled case compared to 127.5% in the uncontrolled case.

A first step into optimising structures for asymmetric manoeuvres with control system interaction was made in Chapters 5.4.2 and 5.4.3. The pre-defined banking input in 5.4.2 lead to a set of forces and moments, which were used to size the wing skin structure for the limits defined through the requested movement. 29.4% of the variable wing mass needed to be changed, to find a feasible design. Then, in Chapter 5.4.3, the lift reducing effect of roll spoilers was used to alleviate aileron-loads especially to match a desired aircraft behaviour. An optimal ratio of 1.276 between spoiler and aileron deployment was found through numerical optimisation. Both asymmetric studies were supported by the action of a pitch damper, designed for actions in the longitudinal axis. Additionally coupling a lateral control law into the design process can be realised with reasonable effort, within the scope of an industrial project, now.

6 Conclusion

This thesis realised the extension of the multidisciplinary airframe design process by respecting flight control systems. As a main outcome this enables optimising aircraft structures in consideration of controlled loads in an automated and integrated way. Physical basics relevant to approach the topics of this thesis were summarised in Chapter 2. A fundamental understanding for the methods and tools that came into use is therefore given. Full FEM and aerodynamic modelling were described together with time-discrete flight control system designing and aspects of structural dynamics in Chapter 3. Chapter 4 presented in detail which load components must be extracted from an aeroelastic analysis such that they can be manipulated actively through a FCS. Coupling all ingredients numerically resulted in an analysis which is capable of evaluating structural design, aerodynamic forces and moments and the influence of concrete control laws for a respective aircraft model. In an additional step, the computational process was embedded in an automated optimisation framework, targeting the sizing of airframe structures. The resulting design process was applied to various AC engineering problems in Chapter 5. Aeroelastic stability derivatives were used in a first step for sizing airframe components with control system demands. Different LAF ideas were then analysed and solved.

6.1 Summary

It was explained how discrete flight control systems can be respected in the state of the art integrated, structural airframe design and optimisation process. A FCS, monitoring flight mechanical properties, commanded control surface deflections to actively reach a desired behaviour. The quasi-steady equations of motions, formulated in a mean axis coordinate system and using an inertia relief approach, were numerically implemented and provided aeroelastic forces and moments. Unreduced FEM and low-fidelity VLM modelling came into use. A structural dynamics solver was engaged to calculate displacements, strains and stresses, used to evaluate structural reserve factors. Resulting constraint functions for MDO were determined and used to directly optimise internal airframe structure components like wing skins, ribs and spars.

From a conceptual AC design point of view, the presented methodology and framework extend the integrated design philosophy. Not only aeroelastic, but control system capabilities can be addressed in early stages of aircraft development, now. The flexibility of MDO, currently given through parametrised aeroelastic model generation and automated design optimisation, is therefore further increased.

These points were demonstrated in structural sizing studies, performed on a high aspect ratio MALE UAV. State of the art optimisation was carried out to show the benefit of finding a feasible design, with the aid of automated designing. The initially infeasible layout (which

resulted from a first guess and was created with the CPACS-based conceptual design tool DESCARTES) could successfully be transferred into a valid one by adding 103.7% mass for elements especially chosen to be variable.

Then, a special aeroelastic stability derivative constraint was formulated and additionally respected during optimisation. It could be shown that structural sizing can change stability derivatives, which are of high interest for flight mechanical and control system design activities, in an undesired way. It could further be presented, that integrated, automation based designing through MDO can handle such problems computationally. Without the demand to maintain a given level of stability, the optimised design of the tail could be reduced by 85.7% mass of its initial layout, although classical sizing constraints were activated. Adding the stability demand still resulted in a decrease to a value of 28.6% initial mass, however, kept the design in a flight mechanically more reasonable range.

To demonstrate how an active control system affects the structure resulting from MDO application, the UAV was disturbed through external loading, next. The pitch controller subsystem of a discrete FCS layout was extracted and added to a transient aeroelastic analysis process. It commanded control surface deflections, targeting to counteract the undesired disturbance. It could be demonstrated that the FCS implicitly brings a load reducing effect, which positively affects the optimisation runs, through its consideration in the optimisation loop. Where the variable weight had to be increased by 127.5% without FCS-consideration, only 63.0% were necessary when respecting a controller in the MDO-loop.

In a further study it was analysed how subcontrollers must be attached to an integrated manoeuvre simulation and how this affects the airframe sizing optimisation. For this purpose a simplified, asymmetric roll manoeuvre was set up to monitor the structural responses with activity of the already available pitch controller. The bank movement was defined through a pre-described slope of aileron deflection, pitch moment control was achieved by commanding elevator deflections. As an outcome it was shown that the loads determined through the integrated structural simulation necessitated an increase of 29.4% variable mass for the given optimisation problem.

In modern flight control laws, aircraft rolling is not only achieved through ailerons, but supported through roll spoilers, as well. How such a coupling of load control surfaces can be respected in numerical AC optimisation, was presented in another study. Target was the determination of an optimal ratio between roll spoiler and aileron deflection to perform a desired bank to bank manoeuvre. It was assumed that a low aileron deflection and a resulting higher spoiler engagement must be most suitable w.r.t. structural strains and stresses in the wing root. In the present case a spoiler-aileron ratio of 1.276 to fulfil a desired banking movement was found through golden section optimisation. This study wanted to demonstrate how engi-

neering problems, that conventionally demand high effort of numerous specialists and centres of competence, can be solved quickly, with basic methods of integrated, MDO based design.

The results of the mass optimisations from Chapters 5.2, 5.3, 5.4.1 and 5.4.2 are summarised in Table 6.1. In the study of Chapter 5.4.3 no mass data was manipulated.

Chapter	Brief description: Optimisation of ...	Mass change **relative to variable mass** of respective initial design
5.2	wing skin, ribs, spars	$+103.7\%$
5.3	tail skin, ribs, spars without stability constraint	-85.7%
5.3	tail skin, ribs, spars with stability constraint	-28.6%
5.4.1	wing skin, ribs, spars without controller	$+127.5\%$
5.4.1	wing skin, ribs, spars with controller	$+63.0\%$
5.4.2	wing skin, ribs, spars	$+29.4\%$

Table 6.1: Summary of mass variation studies

6.2 Outlook

As the applied controllers were developed in large scale development processes, no simplified control designs came into use, here. However, only relatively small subcontroller components were extracted. Although the general steps, necessary to respect a FCS in today's integrated airframe design process could successfully be described, coupling more and especially more advanced control laws are next steps that must be carried out. As an example, the studies considering the λ parameter can be named. This ratio realised a basic connection between roll spoiler and aileron deflection. A FCS component, actually respecting this ratio within the implementation of its lateral control law, might be coupled to the resulting design process, next. The respective source code could be integrated into the developed process, to study the influence of such a deeply nested parameter to the overall airframe design.

A proper FCS-consideration demands the presence of aerostructural responses and controller signals in the time domain. On the structural side, this necessity was met through the application of a Rayleigh damping model used in the governing equations of structural dynamics. This kind of damping, has a strong mathematical character and should be replaced by advanced models in future research activities. Although it is applied in various research activities, using it to represent physical effects demands high testing effort. Discrete, numerical damper elements could come into use in the global FEM model, for example.

The aerodynamic models were based on the quasi-steady equations of motion, often applied in studies dealing with aeroelasticity and also integrated in various commercial modelling and simulation software packages. This was acceptable for the slow manoeuvres analysed here. For the design of fighter aircraft and high aspect ratio configurations exposed to faster motions,

unsteady aerodynamic modelling can not be avoided. In applications where more complex aerodynamic effects become more dominant (e.g. necessity to respect the boundary layer), higher fidelity methods must be used. If the aeroelastic approach used here shall be extended through the consideration of advanced aeroelastic methods, Hodges & Pierce (2002) and Bisplinghoff et al. (2013) may be suggested.

Full FEM models provided structural responses that were handled by numerical optimisation algorithms. No condensation or model reduction had to be carried out. Still, the restriction to linear finite elements allows small deformations, only. As soon as manoeuvres or load cases which lead to larger deformations shall be studied, the range of validity of the presented methods must be challenged. In that case, the structural models must be extended by non-linear finite elements.

Main focus was laid on structural sizing of airframe components, i.e. the variation of thicknesses and cross section areas. Respecting shape or topology variations in a fully *integrated* design process are research topics on their own. As the work at hands established a working MDO-chain, it can be used as a base to further extend the developed process, targeting shape and topology optimisations in simultaneous consideration of flight control systems.

Analytical gradients are a must for gradient based optimisation algorithms. Sensitivities of various objective and constraint functions, frequently used in AC optimisation projects, w.r.t. structural design variables were derived mathematically and implemented in the LAGRANGE program. While aeroelastic subgradients were successfully integrated in the code over the last few decades, control system related sensitivities were so far never addressed. This work can serve as a starting point for the formulation of analytical gradients, when considering aeroservoelastic effects. The developing engineer must be aware of the complexity of this task, which results from the necessity of a time domain formulation and the very high dependency of the concrete control law in use. In the scope of fast gradient determination, automatic differentiation using the capabilities of modern program languages may be a game changer.

Bibliography

Albano, E. & Rodden, W. P. (1969), 'A doublet-lattice method for calculating lift distributions on oscillating surfaces in subsonic flows.', *AIAA Journal* **7**(2), 279–285.

Andreas Hermanutz, M. H. (2019), Influence on the flutter behavior of pre-stressed wing structures under aerodynamic loading, *in* 'IFASD 2019 - International Forum on Aeroelasticity and Structural Dynamics'.

Azoulay, D. & Karpel, M. (2006), Characterization of methods for computation of aeroservoelastic systems response to gust excitation, *in* '47th AIAA/ASME/ASCE/AHS/ASC Structures, Structural Dynamics, and Materials Conference'.

Bathe, K.-J. (1996), *Finite element procedures*, Upper Saddle River, NJ, Prentice Hall.

Beards, C. F. (1996), *Structural vibration analysis and damping* , Butterworth-Heinemann.

Becker, J., Caldwell, B. & Vaccaro, V. (1999), The interaction of flight control system and aircraft structure, *in* 'RTO AVT Specialists' Meeting on 'Structural Aspects of Flexible Aircraft Control".

Bendsoe, M. & Sigmund, O. (2003), *Topology Optimization: Theory, Methods and Applications*, Engineering online library, Springer.

Binder, S., Wildschek, A. & Breuker, R. D. (2018), Aeroelastic Stability Analysis of the FLEXOP Demonstrator using the Continuous Time Unsteady Vortex Lattice Method, *in* '2018 AIAA/ASCE/AHS/ASC Structures, Structural Dynamics, and Materials Conference'.

Binder, S., Wildschek, A. & De Breuker, R. (2021), 'The interaction between active aeroelastic control and structural tailoring in aeroservoelastic wing design', *Aerospace Science and Technology* **110**, 106516.

Bisplinghoff, R. L., Ashley, H. & Halfman, R. L. (2013), *Principles of Aeroelasticity*, Dover books on engineering, Dover Publications, Inc.

Breitsamter, C. (2001), Aerodynamic active vibration alleviation for buffet excited vertical tails, *in* 'RTO/AVT Symposium on Advanced Flow Management, Part A: Vortex Flows and High Angle of Attack', Loen, Norway.

Breitsamter, C. (2005), 'Aerodynamic active control for fin-buffet load alleviation', *Journal of Aircraft* **42**(5), 1252–1263.

Britt, R., Jacobson, S. & Arthurs, T. (2000), 'Aero-servo-elastic analysis of the b-2 bomber', *Journal of Aircraft* **37**(5).

Britt, R., Volk, J., Dreim, D. R. & Applewhite, K. A. (1999), Aeroservoelastic characteristics of the b-2 bomber and implications for future large aircraft, Technical report, National Aeronautics and Space Administration.

Brockhaus, R., Alles, W. & Luckner, R. (2011), *Flugregelung*, Springer Berlin Heidelberg.

Calise, A., Kim, N. & Buffington, J. (2002), Adaptive compensation for flexible dynamics, *in* 'AIAA Guidance, Navigation, and Control Conference and Exhibit'.

Chung, J. & Hulbert, G. M. (1993), 'A Time Integration Algorithm for Structural Dynamics With Improved Numerical Dissipation: The Generalized-α Method', *Journal of Applied Mechanics* **60**(2), 371–375.

Daoud, F. (2005), Formoptimierung von Freiformschalen - Mathematische Algorithmen und Filtertechniken, Dissertation, Technische Universität München, München.

Daoud, F., Deinert, S., Maierl, R. & Petersson, Ö. (2015), Integrated multidisciplinary aircraft design process supported by a decentral mdo framework, *in* '16th AIAA/ISSMO Multidisciplinary Analysis and Optimization Conference'.

Daoud, F., Petersson, Ö., Deinert, S. & Bronny, P. (2012), Multidisciplinary airframe design process: Incorporation of steady and unsteady aeroelastic loads, *in* '12th AIAA Aviation Technology, Integration, and Operation (ATIO) Conference'.

Davies, C., Stelmack, M., Zink, P., Garza, A. & Flick, P. (2012), High fidelity mdo process development and application to fighter strike conceptual design, *in* '12th AIAA Aviation Technology, Integration, and Operation (ATIO) Conference'.

Deinert, S. (2016), Shape and Sizing Optimization of Aircraft Structures with Aeroelastic and Induced Drag Requirements, Dissertation, Technische Universität München, München.

Deinert, S., Petersson, Ö., Daoud, F. & Baier, H. (2013*a*), Aeroelastic tailoring through combined sizing and shape optimization considering induced drag, *in* '4th CEAS Air and Space Conference'.

Deinert, S., Petersson, Ö., Daoud, F. & Baier, H. (2013*b*), Aircraft loft optimization with re-

spect to aeroelastic lift and induced drag loads, *in* '10th World Congress on Structural and Multidisciplinary Optimization'.

Dillinger, J., Abdalla, M. M., Meddaikar, M. Y. & Klimmek, T. (2019), 'Static aeroelastic stiffness optimization of a forward swept composite wing with cfd-corrected aero loads', *CEAS Aeronautical Journal* .

DIN (1990), *Begriffe, Größen und Formelzeichen der Flugmechanik – Bewegung des Luftfahrzeugs gegenüber der Luft*, number DIN 9300-1, Beuth Verlag, Berlin. DIN.

D'Vari, R. & Baker, M. (1999), 'Aeroelastic loads and sensitivity analysis for structural loads optimization', *Journal of Aircraft* **36**(1), 156–166.

Eschenauer, H. A., Osyczka, A. & Schäfer, E. (1990), Interactive multicriteria optimization in design process, *in* 'Multicriteria Design Optimization: Procedures and Applications', Springer Berlin Heidelberg, Berlin, Heidelberg, pp. 71–114.

ESDU (1994), Esdu 81047 - buckling of flat rectangular plates - amendment (c), Technical report, Engineering Science Data Unit.

Faires, J. D. & Burden, R. L. (1994), *Numerische Methoden*, Spektrum Akademischer Verlag.

Ferreira, D. P., Paglione, P. & da Silva, C. P. S. (2010), Design of flight control systems considering the measurement and control of structural modes, *in* '27th International Congress of the Aeronautical Sciences'.

Grafton, S. B. & Libbey, C. E. (1971), Dynamic stability derivatives of a twin-jet fighter model at angles of attack from -10 to 110, Technical report, National Aeronautics and Space Administration.

Haghighat, S., Martins, J. R. R. A. & Liu, H. H. T. (2012), 'Aeroservoelastic design optimization of a flexible wing', *Journal of Aircraft* **49**(2), 432–443.

Hamann, A., Köthe, A. & Luckner, R. (2014), Automatische Auslegung von Flugregelungsfunktionen für den Flugzeugvorentwurf, *in* 'Deutscher Luft- und Raumfahrtkongress, Augsburg'.

Handojo, V. (2021), Contribution to load alleviation in aircraft pre-design and its influence on structural mass and fatigue, Technical report, Technische Universität Berlin.

Harder, R. L. & Desmarais, R. N. (1972), 'Interpolation using surface splines.', *Journal of Aircraft* pp. 189–191.

Hart-Smith, L. (1998), 'Predictions of the original and truncated maximum-strain failure models for certain fibrous composite laminates', *Composites Science and Technology* **58**(7), 1151–1178.

Hermanutz, A. & Hornung, M. (2017), High fidelity trim calculation under consideration of aeroelastic effects of a high aspect ratio swept wing, *in* 'IFASD 2017 - International Forum on Aeroelasticity and Structural Dynamics', Como, Italy.

Hodges, D. & Pierce, G. (2002), *Introduction to Structural Dynamics and Aeroelasticity*, Cambridge Aerospace Series, Cambridge University Press.

Hofstee, J., Kier, T., Cerulli, C. & Looye, G. (2003), A variable, fully flexible dynamic response tool for special investigations (varloads), *in* 'Proceedings International Forum on Aeroelasticity and Structural Dynamics 2003, June 4-6, 2003'. LIDO-Berichtsjahr=2004,.

Hörnlein, H. R. (1988), Lokales beulen für membranelemente. Internal technical report MBB.

Hörnlein, H. R. (2006), Update der analytischen stabilität von einfach gelagerten rechteckplatten. Internal Technical Report EADS.

ISO (1988), *Flight dynamics — Concepts, quantities and symbols — Part 1: Aircraft motion relative to the air*, number ISO 1151-1, Beuth Verlag, Berlin. ISO.

Itskov, M. (2007), *Tensor Algebra and Tensor Analysis for Engineers*, Springer.

Jones, R. (1998), *Mechanics Of Composite Materials*, Materials Science and Engineering Series, Taylor & Francis.

Joshi, A. (2012), Modelling of flight control hydraulic actuators considering real system effects, *in* 'AIAA Modeling and Simulation Technologies Conference and Exhibit'.

Jutte, C. V. & Stanford, B. (2014), Aeroelastic tailoring of transport aircraft wings: State-of-the-art and potential enabling technologies, Technical report, NASA technical memorandum.

Karpel, M., Chen, P. & Moulin, B. (2005), 'Dynamic response of aeroservoelastic systems to gust excitation', *Journal of Aircraft* **42**, 1264–1272.

Karpel, M., Moulin, B., Anguita, L., Maderuelo, C. & Climent, H. (2004), Aeroservoelastic gust response analysis for the design of transport aircrafts, *in* 'Collection of Technical Papers - AIAA/ASME/ASCE/AHS/ASC Structures, Structural Dynamics and Materials Conference', Vol. 2.

Karpel, M., Moulin, B., Feldgun, V., Anguita, L., Rosich, F. & Climent, H. (2006), Active alleviation of gust loads using special control surfaces, *in* '47th AIAA/ASME/ASCE/AHS/ASC Structures, Structural Dynamics, and Materials Conference'.

Katz, J. & Plotkin, A. (2010), *Low-Speed Aerodynamics*, Cambridge Aerospace Series, Cambridge University Press.

Kiefer, J. (1953), 'Sequential minimax search for a maximum', *Proceedings of the American Mathematical Society* **4**, 502–506.

Kier, T. (2005), Comparison of unsteady aerodynamic modelling methodologies with respect to flight loads analysis, *in* 'Proc. of AIAA Atmospheric Flight Mechanics Conference'.

Kier, T. (2018), An integrated modelling approach for flight dynamics, manoeuvre- and gust-loads analysis, *in* '2018 AIAA/ASCE/AHS/ASC Structures, Structural Dynamics, and Materials Conference'.

Kier, T. & Hofstee, J. (2004), VarLoads - Eine Simulationsumgebung zur Lastenberechnung eines voll flexiblen, freifliegenden Flugzeugs, *in* 'Deutscher Luft- und Raumfahrtkongress'.

Kier, T. & Looye, G. (2009), Unifying manoeuvre and gust loads analysis models, *in* 'International Forum on Aeroelasticity and Structural Dynamics'.

Kier, T. M. (2011), An integrated loads analysis model including unsteady aerodynamic effects for position and attitude dependent gust fields, *in* 'IFASD 2011 - International Forum on Aeroelasticity and Structural Dynamics'.

Kitson, R. C., Lupp, C. & Cesnik, C. E. (2016), Modeling and simulation of flexible jet transport aircraft with high-aspect-ratio wings, *in* '15th Dynamics Specialists Conference'.

Klimmek, T., Schulze, M., Abu-Zurayk, M., Ilic, C. & Merle, A. (2019), cpacs-mona – an independent and in high fidelity based mdo tasks integrated process for the structural and aeroelastic design for aircraft configurations, *in* 'International Forum on Aeroelasticity and Structural Dynamics 2019, IFASD 2019'.

Krammer, J. (1992), ‘Practical architecture of design optimisation software for aircraft structures taking the MBB-lagrange code as an example’, *AGARD-Lecture Series No. 186* .

Kuchar, R. (2012), An integrated data generation process for flight dynamics modeling in aircraft design, *in* ‘Deutscher Luft- und Raumfahrtkongress 2012’.

Liersch, C. & Hepperle, M. (2011), A distributed toolbox for multidisciplinary preliminary aircraft design, *in* ‘CEAS Aeronautical Journal 2’, pp. 57–68.

Livne, E. (2018), ‘Aircraft active flutter suppression: State of the art and technology maturation needs’, *Journal of Aircraft* **55**(1), 410–452.

Luber, W. (2012), Aeroservoelastic flight control design for a military combat aircraft weapon system, *in* ‘28th International Congress of the aeronautical sciences’.

Martins, J., Sturdza, P. & Alonso, J. (2003), ‘The complex-step derivative approximation’, *ACM Transactions on Mathematical Software* **29**, 245–262.

Newmark, N. M. (1959), ‘A Method of Computation for Structural Dynamics’, *Journal of the Engineering Mechanics Division* **85**, 67—-94.

Niu, M. C. (2011), *Airframe Structural Design: Practical Design Information and Data on Aircraft Structures*, Conmilit Press Hong Kong.

Nussbächer, D., Daoud, F., Petersson, Ö. & Hornung, M. (2016), Aeroelastic optimisation respecting stability derivatives from unrestrained trimming, *in* ‘5th Aircraft Structural Design Conference’.

Nussbächer, D., Daoud, F., Petersson, Ö. & Hornung, M. (2018), Multidisciplinary optimisation of flexible aircraft structures in consideration of flight control system demands in the time domain, *in* ‘6th International Conference on Engineering Optimization’.

Nussbächer, D. & Petersson, Ö. (2023), Integrated design of airframe structures in consideration of passive and semi-active gust load alleviation, *in* ‘DLRK 2023’.

Ogata, K. (2010), *Modern Control Engineering*, Instrumentation and controls series, Prentice Hall.

Osterhuber, R. (2011), Fcs-requirements for combat aircraft - lessons learned for future designs, *in* ‘STO-AVT-201 Edinburgh’.

Osterhuber, R. (2013), Fcs-requirements for future lo combat aircraft, *in* 'STO-AVT-215 Stockholm'.

Petersson, Ö. (2009), Optimization of aircraft wings including dynamic aeroelasticity and manufacturing aspects, *in* '5th AIAA Multidisciplinary Design Optimization Specialist Conference (4.-7.5.) 2009, Palm Springs CA'.

Petersson, Ö. & Daoud, F. (2012), Multidisciplinary Optimization of Aircraft Structures with Respect to Static and Dynamic Aeroelastic Requirements, *in* 'Deutscher Luft- und Raumfahrtkongress, Berlin'.

Petersson, Ö., Leitner, M. & Stroscher, F. (2010), Structural optimization framework for aircraft subject to transient maneuver and gust loads, *in* '13th AIAA/ISSMO Multidisciplinary Analysis Optimization Conference'.

Petersson, Ö., Stroscher, F. & Baier, H. (2010), Multidisciplinary optimisation of aircraft wings including gust loads, *in* '2nd RAeS Aircraft Structural Design Conference 2010, London'.

Pusch, M., Knoblach, A. & Kier, T. (2019), 'Integrated optimization of control surface layout for gust load alleviation', *CEAS Aeronautical Journal* **10**.

Raney, D. L., Jackson, E. B., Buttrill, C. S. & Adams, W. M. (2001), The impact of structural vibration on flying qualities of a supersonic transport, *in* 'AIAA Atmospheric Flight Mechanics Conference'.

Rao, S. (2009), *Engineering Optimization: Theory and Practice*, John Wiley and Sons, inc.

Raymer, D. (2018), *Aircraft Design: A Conceptual Approach, Sixth Edition*, American Institute of Aeronautics and Astronautics.

Regan, C. & Jutte, C. (2012), Survey of applications of active control technology for gust alleviation and new challenges for lighter-weight aircraft, Technical report, National Aeronautics and Space Administration, Dryden Flight Research Center.

Rodden, W. & Johnson, E. (2004), *MSC.Nastran Aeroelastic Analysis User's Guide*, MSC Software Corporation, MSC.Software Corporation 2 MacArthur Place Santa Ana, CA 92707 USA.

Rodden, W. P. & Love, J. R. (1984), 'Equations of motion of a quasisteady flight vehicle utilizing restrained static aeroelastic characteristics', *Journal of Aircraft* **22**(9), 802–809.

Roessler, C., Stahl, P., Sendner, F., Hermanutz, A., Koeberle, S., Bartasevicius, J., Rozov, V., Breitsamter, C., Hornung, M., Meddaikar, Y. M., Dillinger, J., Sodja, J., De Breuker, R., Koimtzoglou, C., Kotinis, D. & Georgopoulos, P. (2019), Aircraft design and testing of flexop unmanned flying demonstrator to test load alleviation and flutter suppression of high aspect ratio flexible wings, *in* 'AIAA Scitech 2019 Forum', American Institute of Aeronautics and Astronautics.

Rozov, V., Volmering, A., Hermanutz, A., Hornung, M. & Breitsamter, C. (2019), 'Cfd-based aeroelastic sensitivity study of a low-speed flutter demonstrator', *Aerospace* **6**(3), 30.

Sachsenberg, B. & Schittkowski, K. (2013), Nlpip: A fortran implementation of an sqp-ipm algorithm for solving large-scale nonlinear optimization problems - user's guide, version 2.0, Technical report, Department of Computer Science, University of Bayreuth.

Sachsenberg, B. & Schittkowski, K. (2015), 'A combined sqp–ipm algorithm for solving large-scale nonlinear optimization problems', *Optimization Letters* **9**.

Schittkowski, K. (1986), 'Nlpql: A fortran subroutine solving constrained nonlinear programming problems', *Annals of Operations Research* **5**(2), 485–500.

Schuhmacher, G. (1995), Multidisziplinäre, fertigungsgerechte Optimierung von Faserverbund-Flächentragwerken, Dissertation, Forschungszentrum für Multidisziplinäre Analysen und Angewandte Strukturoptimierung - Inst. für Mechanik und Regelungstechnik.

Schuhmacher, G., Daoud, F., Petersson, Ö. & Wagner, M. (2012), Multidisciplinary airframe design optimisation, *in* '28th International Congress of the Aeronautical Sciences', Vol. 1, pp. 44–56.

Seywald, K. (2016), Impact of Aeroelasticity on Flight Dynamics and Handling Qualities of Novel Aircraft Configurations, Dissertation, Technische Universität München, München.

Shearer, C. & Cesnik, C. (2006), Modified generalized-α method for integrating governing equations of very flexible aircraft, *in* '47th AIAA/ASME/ASCE/AHS/ASC Structures, Structural Dynamics, and Materials Conference', Vol. 3, pp. 1877–1897.

Shearer, C. & Cesnik, C. (2007), 'Nonlinear flight dynamics of very flexible aircraft', *Journal of Aircraft* **44**(5), 1528–1545.

Shearer, C. & Cesnik, C. (2008), 'Trajectory control for very flexible aircraft', *Journal of Guidance, Control, and Dynamics* **31**(2), 340–357.

Sohler, S. S. (1948), 'An airplane is not a rabbit', *Engineering and Science* **11**(4), 3–9.

Soreide, D. (1996), Coherent lidar turbulence measurement for gust load alleviation, Technical report, National Aeronautics and Space Administration.

Svanberg, K. (1987), 'The method of moving asymptotes—a new method for structural optimization', *International Journal for Numerical Methods in Engineering* **24**(2), 359–373.

Teufel, P. (2003), Böenmodellierung und Lastabminderung für ein flexibles Flugzeug, Dissertation, Universität Stuttgart.

Teufel, P., Hanel, M. & Well, K. (1999), Integrated flight mechanic and aeroelastic modelling and control of a flexible aircraft considering multidimensional gust input, *in* 'RTO AVT Specialists' Meeting on 'Structural Aspects of Flexible Aircraft Control".

Tewari, A. (2015), *Aeroservoelasticity - Modeling and Control*, Springer-Verlag New York.

Thümmel, M., Looye, G., Kurze, M., Otter, M. & Bals, J. (2005), Nonlinear inverse models for control, *in* '4th International Modelica Conference', pp. 267–279.

Timoshenko, S. P. & Gere, J. M. (1963), *Theory of elastic stability*, McGraw-Hill International Editions.

Urie, D. (1979), Accelerated development and flight evaluation of active controls concepts for subsonic transport aircraft. volume 2: Aft c.g. simulation and analysis, Technical report, National Aeronautics and Space Administration.

Voss, A. & Klimmek, T. (2022), Aeroelastic modeling, loads analysis and structural design of a fighter aircraft, *in* '33rd Congress of the International Council of the Aeronautical Sciences, ICAS 2022'.

Weaver, P. M. (2004), On optimisation of long anisotropic flat plate subject to shear buckling loads, *in* '45th AIAA/ASME/ASCE/AHS/ASC Structures, Structural Dynamics & Materials Conference'.

Weaver, P. M. (2005), Design formulae for buckling of biaxially loaded laminated rectangular plate with flexural/twist anisotropy, *in* '46th AIAA/ASME/ASCE/AHS/ASC Structures, Structural Dynamics & Materials Conference', American Institute of Aeronautics and Astronautics.

Weaver, P. M. (2006), Approximate analysis for buckling of compression loaded long rectangular plate with flexural/twist anisotropy, *in* 'Proceedings of the Royal Society of London A: Mathematical, Physical and Engineering Sciences', Vol. 462, pp. 59–73.

Weigold, W., Stickan, B., Travieso-Alvarez, I., Kaiser, C. & Teufel, P. (2017), Linearized unsteady cfd for gust loads with tau, *in* 'IFASD 2017 - International Forum on Aeroelasticity and Structural Dynamics'.

Wildschek, A. (2009), An Adaptive Feed-Forward Controller for Active Wing Bending Vibration Alleviation on Large Transport Aircraft, Dissertation, Technische Universität München, München.

Wildschek, A., Maier, R., Hahn, K.-U., Leissling, D., Press, M. & Zach, A. (2009), Flight test with an adaptive feed-forward controller for alleviation of turbulence excited wing bending vibrations, *in* 'AIAA Guidance, Navigation, and Control Conference'.

Wildschek, A., Prananta, B., Kanakis, T., van Tongeren, H. & Huls, R. (2015), Concurrent optimization of a feed-forward gust loads controller and minimization of wing box structural mass on an aircraft with active winglets, *in* 'AIAA Aviation', American Institute of Aeronautics and Astronautics.

Wildschek, A., Stroscher, F. & Klimmek, T. (2010), Gust load alleviation on a large blended wing body airliner, *in* '27th International Congress of the Aeronautical Sciences 2010'.

Winther, B. A., Hagemeyer, D. A., Britt, R. T. & Roden, W. P. (1995), 'Aeroelastic effects on the b-2 maneuver response', *Journal of Aircraft* **32**(4), 862–867.

Yechout, T. (2003), *Introduction to Aircraft Flight Mechanics*, AIAA Education Series, American Institute of Aeronautics & Astronautics.

Zeng, J., Wang, J., de Callafon, R. & Brenner, M. (2011), Suppression of the aeroelastic/aeroservoelastic interaction using adaptive feedback control instead of notching filters, *in* 'AIAA Atmospheric Flight Mechanics Conference'.

Zienkiewicz, O. & Taylor, R. (2000), *The Finite Element Method: Solid mechanics*, Butterworth-Heinemann.

Zienkiewicz, O., Taylor, R. & Zhu, J. (2013), *The Finite Element Method: Its Basis and Fundamentals*, Butterworth-Heinemann.

Zimmer, M., Feldwisch, J. M. & Ritter, M. R. (2022), Coupled cfd-csm analyses of a highly flexible transport aircraft by means of geometrically nonlinear methods, *in* '19th International Forum on Aeroelasticity and Structural Dynamics, IFASD 2022'.

Zotemantel, R. (1992), MBB-LAGRANGE: A General Structural Reliability and Optimization Structural System, *in* R. Rackwitz & P. Thoft-Christensen, eds, 'Reliability and Optimization of Structural Systems '91', Springer Berlin Heidelberg, Berlin, Heidelberg, pp. 427–442.

A Appendix

The following figures show the densities/sparsities of various matrices mentioned in Chapter 3.1.1. The respective matrices contain a numerical value which differs from zero, where a blue entry is present. They were created for a model with 210 structural nodes, 1260 structural degrees of freedom and 624 aerodynamic boxes ($j \in [1, 624]$ and $k \in [1, 1248]$).

Figure A.1 and Figure A.2 visualise the extreme sparsities of the numerical matrices S_{kj} and D_{jk}.

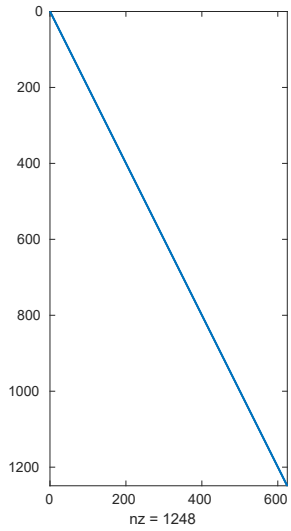

Figure A.1: Sparsity of the Integration Matrix S_{kj}

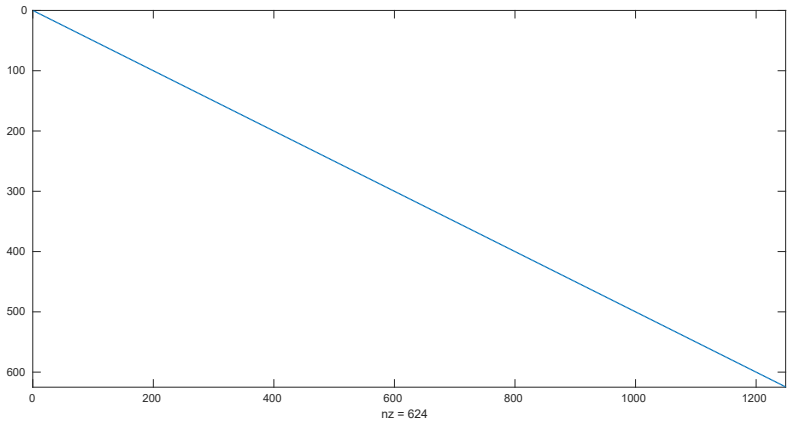

Figure A.2: Sparsity of the Differentiation matrix D_{jk}

Figure A.3 visualises the sparsity of a common numerical stiffness matrix K_{gg} in aeronautical applications.

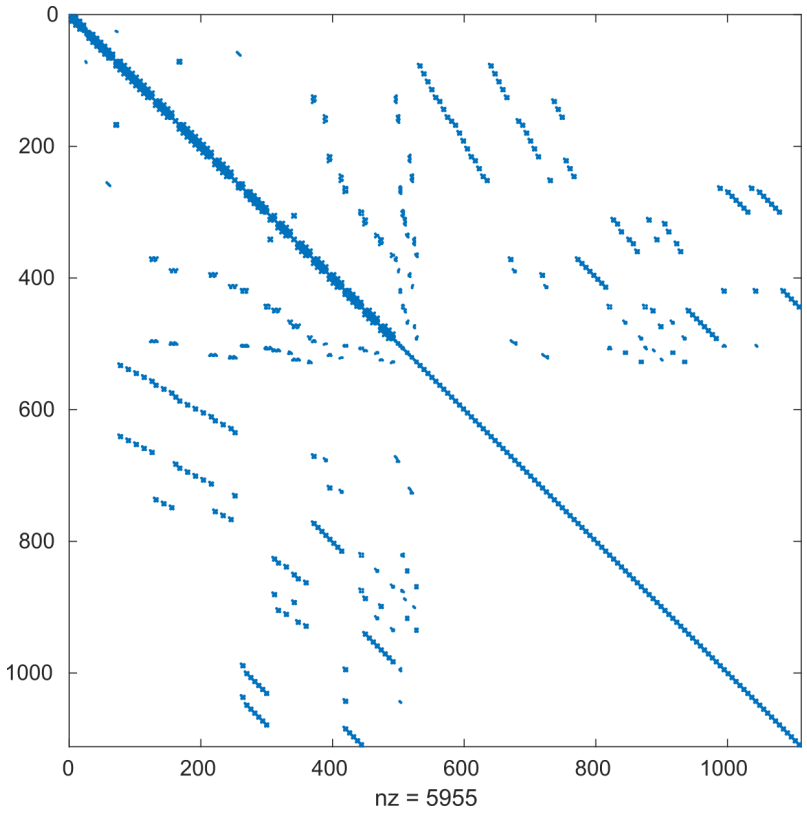

Figure A.3: Sparsity of a structural stiffness matrix

Figure A.4 visualises the sparsity of the spline matrices G_{kg}^T and G_{kg}.

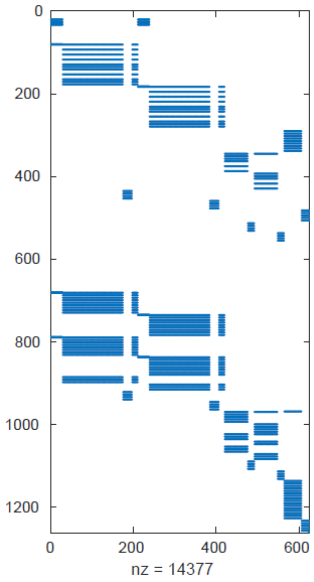

(a) G_{kg}^T - Converting aerodynamic to structural forces

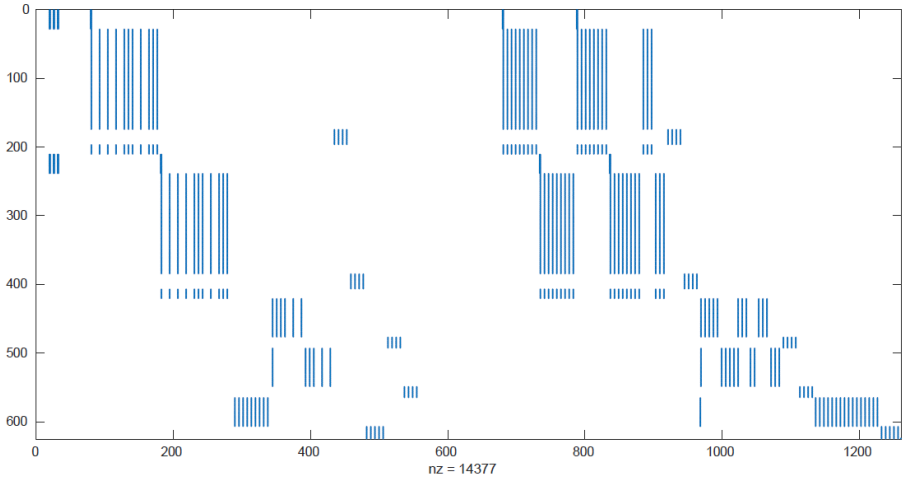

(b) G_{kg} - Converting structural to aerodynamic displacements

Figure A.4: Sparsity of spline matrices

The sparsity of the splined aerodynamic stiffness matrix Q_{gg} is displayed in Figure A.5

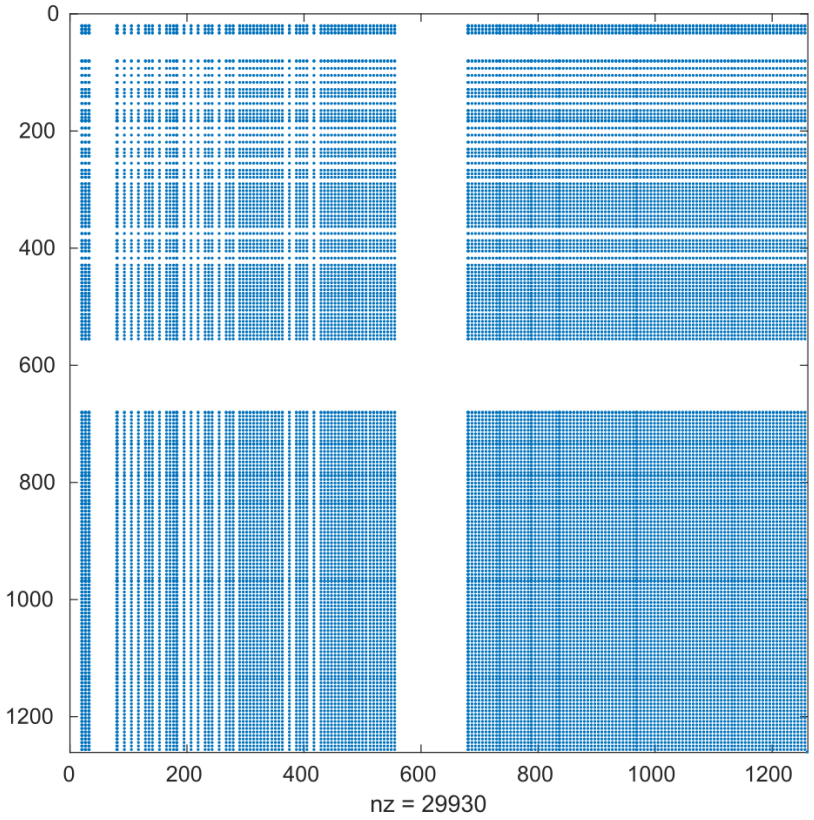

Figure A.5: Sparsity of a splined aerodynamic stiffness matrix Q_{gg}